ADVANCES IN PHYSICS

A QUARTERLY SUPPLEMENT of the PHILOSOPHICAL MAGAZINE

VOLUME 7 JANUARY 1958 NUMBER 25

PRICE per part £1
PRICE per annum £3 15*s.* 0*d.* post free

PRINTED AND PUBLISHED BY TAYLOR & FRANCIS LTD
RED LION COURT, FLEET ST., LONDON E.C.4

A new International Journal

ERGONOMICS

HUMAN FACTORS IN WORK, MACHINE CONTROL AND EQUIPMENT DESIGN

Contents of November, 1957

Editorial

Human Limitations and Vehicle Design. By Ross A. McFarland, Harvard School of Public Health, Boston, Massachusetts

Effects of Noises of High and Low Frequency on Behaviour. By D. E. Broadbent, Medical Research Council Applied Psychology Unit, Cambridge, England

Changing Physical Demands of Foundry Workers in the Production of Medium Weight Castings. By H. Scholz, Max-Planck-Institut für Arbeitsphysiologie, Dortmund

A Comparison Between the Results of Three Different Methods of Operator Training. By Eunice Belbin, Medical Research Council, R. M. Belbin and Frank Hill, The Wool (and Allied) Textile Employers Council, Bradford, England

The Effects of Increasing Skill on Cycle Time and its Consequences for Time Standards. By J. R. De Jong, Bilthoven, Holland

Intermittent Light Stimulation and Flicker Sensation. By J. B. Collins and R. G. Hopkinson, Department of Scientific and Industrial Research, Building Research Station

Consideration of the User in Telephone Research. By J. E. Karlin, Bell Telephone Laboratories, Inc.

Factors in Fatigue and Stress in the Operation of High-Speed Diesel Passenger Railway Cars with Only One Driver Present. By Robert S. Schwab, Harvard Medical School, Boston

Price £1 5s. 0d. per part, plus postage
Subscription price per volume £4 15s. 0d. post free, payable in advance

Printed and Published by

TAYLOR & FRANCIS LTD

RED LION COURT, FLEET STREET, LONDON, E.C.4

Orders originating in U.S.A., and Canada should be sent to the Academic Press Inc., 111 Fifth Avenue, New York, 3, N.Y., U.S.A.

Journal of Electronics and Control

A Philosophical Magazine Associated Journal

Editor:
J. THOMSON, M.A., D.Sc., M.I.E.E., F.Inst.P.

Assistant Editor:
J. R. DAY, B.Sc.

Consultant Editor:
Professor N. F. MOTT, F.R.S.

Editorial Board:
Professor P. AIGRAIN (France)
Professor H. B. G. CASIMIR (Holland)
Dr. W. KLEIN (Germany)
Dr. R. KOMPFNER (U.S.A.)
J. F. COALES (U.K.)

Contents of January, 1958

Electronics Section

Developments in Transistor Electronics. By L. B. Valdes, Microwave Laboratory, General Electric Company, Palo Alto, California

On Carrier Accumulation, and the Properties of Certain Semiconductor Junctions. By J. B. Gunn, Royal Radar Establishment, Great Malvern

The Effect of Small Additions of Magnesia on some High-Permittivity Ceramics Based on Barium Titanate. By K. W. Plessner and R. West, British Dielectric Research Ltd., 38 Wood Lane, London, W.12

Avalanche Breakdown Voltage in Hemispherical (p–n) Junctions. By J. Shields, Research Laboratory, The British Thomson-Houston Co. Ltd., Rugby

Radial Variation of Minority Carrier Lifetime in Vacuum-grown Germanium Single Crystals. By C. A. Hogarth and P. J. Hoyland, Royal Radar Establishment, Great Malvern, Worcs.

Control Section

B.S.I.R.A. Open Days Address. Three Dimensional Microscopy. By S. Tolansky, Royal Holloway College, University of London

Price per part £1 5s. plus postage
Price per volume £7 post free, payable in advance
6 monthly issues per volume

Printed and Published by

TAYLOR & FRANCIS LTD
RED LION COURT, FLEET STREET, LONDON, E.C.4

Orders originating in U.S.A. and Canada should be sent to the Academic Press Inc., 111 Fifth Avenue, New York, 3, N.Y., U.S.A.

The Philosophical Magazine

First Published in 1798

Editor :

PROFESSOR N. F. MOTT, M.A., D.Sc., F.R.S.

Editorial Board :

SIR LAWRENCE BRAGG, O.B.E., M.C., M.A., D.Sc., F.R.S.
SIR GEORGE THOMSON, M.A., D.Sc., F.R.S.
PROFESSOR A. M. TYNDALL, C.B.E., D.Sc., F.R.S.

Contents of February, 1958

The Interaction Rates of Stopped Negative Muons in Iron and Copper. By A. M. Hillas, W. B. Gilboy and R. M. Tennent, Physics Department, University of Leeds

A Variational Calculation of the Equilibrium Properties of a Classical Plasma. By S. F. Edwards, Department of Mathematical Physics, University of Birmingham

On the Origin of Dislocations. By Doris Kuhlmann-Wilsdorf, School of Metallurgical Engineering, University of Pennsylvania

The Calculation of the Drag in Problems Solved by the Hodograph Method. By A. G. Mackie, St. Salvator's College, St. Andrews

The Protons Emitted from Iron-54 and Iron-56 on Bombardment with 13·5 MEV Neutrons. By P. V. March and W. T. Morton, Department of Natural Philosophy, University of Glasgow

Boundary Layer Growth on a Spinning Body : Accelerated Motion. By Y. D. Wadhwa, Department of Applied Mathematics, Indian Institute of Technology, Khargpur, India

The Ultimate Distribution of Impurity in the Zone-Melting Process. By L. W. Davies, Division of Radiophysics, C.S.I.R.O., Sydney, Australia

The Positron Decay of the Ground State of Aluminium-26. By P. S. Fisher and D. W. Hadley, Department of Physics, University of Birmingham, and G. Speers, The Radiochemical Centre, Amersham

The Remanent Magnetism of Some Lavas in the Deccan Traps. By E. R. Deutsch, Department of Physics, Imperial College of Science and Technology, and C. Radakrishnamurty and P. W. Sahasrabudhe, Tata Institute of Fundamental Research, Bombay

The Electronic Structure of the Metals of the First Transition Period. By W. M. Lomer and W. Marshall, Atomic Energy Research Establishment, Harwell, Berkshire

Correspondence :

Parity Conservation in Strong Interactions: The $^{7}Be(n, \alpha)^{4}He$ Reaction. By R. E. Segel, Aeronautical Research Laboratory, WADC, J. V. Kane, Brookhaven National Laboratory, Upton, N.Y., U.S.A., and D. H. Wilkinson, Brookhaven National Laboratory, Upton, N.Y., U.S.A., and Clarendon Laboratory, Oxford

On the Fermi Surface of Copper. By F. Garcia Moliner, Cavendish Laboratory, Cambridge

Electromagnetic Stirring in Zone Refining. By I. Braun, F. C. Frank, S. Marshall and G. Meyrick, University of Bristol, H. H. Wills Physics Laboratory

Price per part £1 5s. plus postage

Price per annum £13 10s. post free, payable in advance

Printed and Published by

TAYLOR & FRANCIS LTD

RED LION COURT, FLEET STREET, LONDON, E.C.4

Physics in Medicine and Biology

A Taylor & Francis International Journal published in association with the Hospital Physicists' Association

Contents of October, 1957

Exposure of Man to Ionizing Radiation arising from Medical Procedures. An Enquiry Into Methods of Evaluation. A Report of the International Commission on Radiological Protection and International Commission on Radiological Units and Measurements.

Measurement of the Gonadal Dose in the Medical Use of X-Rays: A Preliminary Report on a Survey being made in the United Kingdom. By F. W. Spiers, D.Sc., Department of Medical Physics, The University of Leeds.

The Dosimetry and Lethal Effects of Maternally Administered Phosphorus-32 after 14 and 17 Days of Gestation in the Rat. By Melvin R. Sikov, Ph.D. and James E. Lofstrom, M.D., Division of Radiology, Wayne State University College of Medicine, Detroit, Michigan, U.S.A.

Some Physical Measurements with 30 Mev X-Rays. By R. Braams, Ph.D., Department of Radiotherapeutics, University of Cambridge, England.

Oscillatory Flow in Arteries: the Constrained Elastic Tube as a Model of Arterial Flow and Pulse Transmission. By J. R. Womersley, Aeronautical Research Laboratory, Wright Air Development Center, Dayton, Ohio, U.S.A.

Subscription price per volume £3 10s. post free, payable in advance

4 parts per volume—£1 per part plus postage

Printed and Published by

TAYLOR & FRANCIS, LTD

RED LION COURT, FLEET STREET, LONDON, E.C.4

Orders originating in U.S.A. and Canada should be sent to the Academic Press Inc., 111 Fifth Avenue, New York, 3, N.Y., U.S.A.

CONTENTS

The Scattering of Nucleons by Alpha-Particles. By P. E. Hodgson, University of Reading 1

Spin-Disorder Effects in the Electrical Resistivities of Metals and Alloys. By B. R. Coles, Department of Physics, Imperial College, London, S.W.7 40

Metal Fatigue. By N. Thompson, H. H. Wills Physical Laboratory, University of Bristol and N. J. Wadsworth, Royal Aircraft Establishment, Farnborough, Hants. 72

ADVANCES IN PHYSICS

A QUARTERLY SUPPLEMENT
of the
PHILOSOPHICAL MAGAZINE

VOLUME 7 JANUARY 1958 NUMBER 25

The Scattering of Nucleons by Alpha-Particles

By P. E. HODGSON
University of Reading

CONTENTS

§ 1. INTRODUCTION
§ 2. THE TOTAL CROSS SECTION.
§ 3. THE DIFFERENTIAL CROSS SECTION FOR ELASTIC COLLISIONS
§ 4. INELASTIC COLLISIONS.
§ 5. MESON PRODUCTION.
§ 6. POLARIZATION.
§ 7. COULOMB SCATTERING.
§ 8. RESONANCE THEORY.
§ 9. PHASE-SHIFT ANALYSIS.
§ 10. PHENOMENOLOGICAL THEORIES.
REFERENCES.

§ 1. INTRODUCTION

SINCE the early experiments of Lord Rutherford, alpha-particles have been extensively used in investigations of the interactions between nucleons and aggregates of nucleons. There are several reasons why alpha-particles are convenient both for the design of experiments and for their elegant interpretation. If we wish to use alpha-particles as the projectiles, then convenient monoenergetic sources are readily available; radioactive preparations for the lower energies and accelerators for the higher. They can as easily be the target either in the form of gaseous helium contained in a thin vessel at high pressure, or, with rather more difficulty, cooled to form the liquid. Scattered or recoil alpha-particles, being doubly charged, may easily be detected by counters, ionization or cloud chambers, or by photographic emulsions.

Alpha-particles have many properties that facilitate the interpretation of experiments made with them. The alpha-particle is a highly stable and symmetric structure, so that its deformation by the oncoming nucleon in a collision may usually be neglected as a first approximation and many terms in the equations either add or cancel. Its spin is zero, so that coupled equations do not arise in the analysis of the collision, and polarization

phenomena are confined to the nucleon. It has no excited states below at least 20 MeV so that at lower energies there can be no inelastic scattering to complicate the analysis of the collision phenomena.

In the last decade there have been many experimental studies of nucleon–alpha collisions, so that now their main features in the MeV region are well known. At the same time attempts have been made, with some success, to provide a theoretical interpretation of these measurements. The behaviour of the waves of lowest angular momenta, the S and P waves, is now understood qualitatively in terms of nuclear interactions that are also able to account for other scattering phenomena.

It is the purpose of this review to collect together both the essential experimental results and the main lines of theoretical explanation and to present them as an integrated whole. Only nuclear collisions are considered; atomic collisions lie outside the scope of this review.

§ 2. The Total Cross Section

The total cross section for collisions of neutrons with alpha-particles is most conveniently measured by finding the attenuation of a neutron beam in gaseous or liquid helium. If n is the number of helium nuclei per cm^3 of

Fig. 1

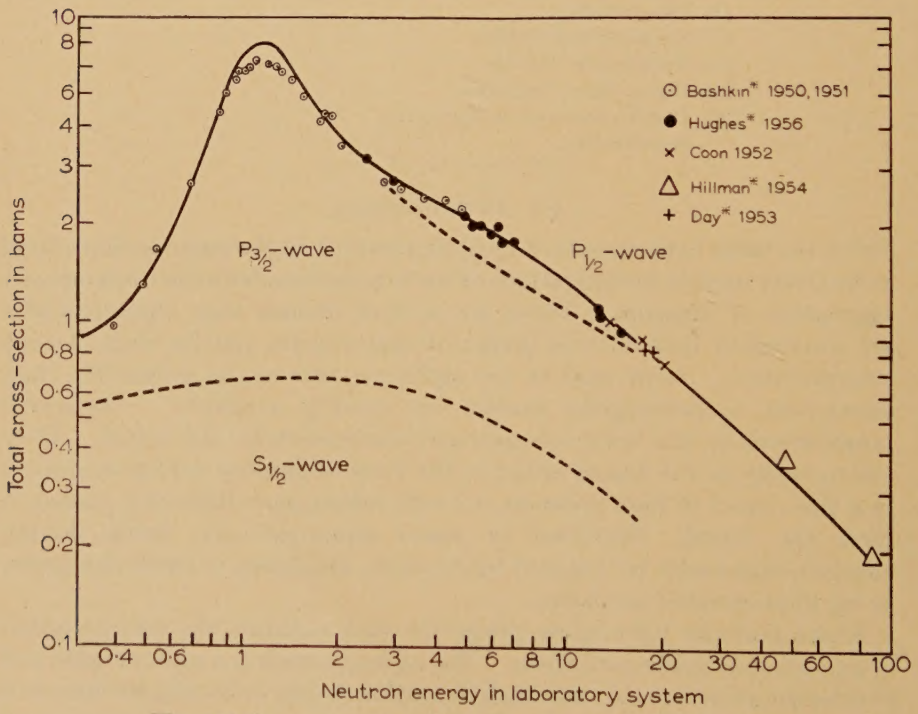

The total cross section for neutron–alpha collisions.

target, and σ their total cross section, then the proportion of an incident beam to traverse a distance d is given by $\exp(-n\sigma d)$. A subtraction procedure enables the container of the helium to be allowed for,

The results of several such investigations of neutron-alpha scattering are plotted in fig. 1 and summarized in table 1. Bashkin, Mooring and Petree (1951) used the ^{7}Li (p, n) ^{7}Be reaction as a source of neutrons for energies less than 2·1 MeV, and hence their results should be corrected for the low energy neutrons from the excited state of ^{7}Be. The proportion of these low-energy neutrons is not well known, but the correction would tend to increase the cross section between 0·65 and 1·45 MeV, and to decrease it between 1·45 and 2·1 MeV. The amount of this correction can be found from an analysis of measurements of the differential cross section.

The total elastic cross sections can also be found by integration of the differential cross sections found in the investigations summarized in § 3. This may be done even if the measurements of differential cross section extend over only part of the total angular range, provided it is assumed that the phase shifts determined from the range measured apply to the whole range. The total elastic cross-sections determined in this way as a function of energy from the differential elastic cross-section measurements using the best phase-shifts from § 9 are included in fig. 1, and agree well with the directly determined total cross sections at energies

Table 1. Total Cross Section for Neutron–Alpha Collisions

Author	Method†	Energy (Lab)	Notes
Carroll* 1938, 1941	I.C.	Thermal	σ=1·25b (Cf. Schwinger 1940, footnote 3).
Bashkin* 1950, 1951	P.C.	0·4–6·4	Extrapolated thermal σ=0·8 b.
Harris 1950	P.C.	Thermal	σ=1·4 b
Hibson* 1951	—	Thermal	σ=0·78 b
Coon* 1952 a	S.C.	14	σ=1·02 $\pm$0·02 b
Coon* 1952 b	S.C.	6.5, 17·6, 20·6	σ=1·7, 0·90, 0·78 b
Day* 1953	S.C.	17·97, 19, 20·07	σ=0·848, 0·816, 0·770 b
Tannenwald 1952	C.C.	~40–120	Total elastic cross section =110 $\pm$23 mb
Coon 1953	S.C.	2·49, 2·99	3·16 $\pm$0·06; 2·79 $\pm$0·06 b
Hillman* 1954	S.C.	4·75, 88·0	377 $\pm$12, 199 $\pm$6 mb
Henkel* 1955	—	5–14	Los Alamos data
Hughes* 1956	—	—	Summary of previous work including unpublished Los Alamos data.

* Here and elsewhere an asterisk indicates multiple authorship; only the first author is named. This is followed by the year of publication.

† The following abbreviations will be used throughout for the various experimental techniques: C, Geiger–Müller Counters; P.C., Proportional Counter; S.C., Scintillation Counters; I.C., Ionization Chamber; C.C., Wilson Cloud Chamber; D.C.C., Diffusion Cloud Chamber; P.P., photographic plates. All energies are in MeV, and angles in degrees. The energies of the nucleons in the centre-of-mass (CM) system are 0·8 times the corresponding energies in the laboratory system.

below the inelastic scattering region. The contributions from the poorly-known D-phases are omitted from this figure, and the correction for low energy neutrons has been made.

The scattering of protons by alpha-particles is due not only to the nuclear forces, but also to the Coulomb inverse-square forces. The differential cross section for scattering by Coulomb forces tends to infinity at small angles in such a way that the total cross section is very large, so the methods used to investigate the total cross section for neutron–alpha scattering are not applicable to proton-alpha scattering. Instead, the differential cross section is measured by the means described in § 3, and the contribution of the nuclear forces found by subtracting the Coulomb part in the way described in § 9.

The total cross section for neutron–alpha scattering may also be estimated with good accuracy at energies beyond the resonance region by interpolating the results of similar measurements on neighbouring elements, such as those of Cook *et al.* (1949).

§ 3. The Differential Cross Section for Elastic Collisions

At low energies, the differential cross section for neutron–alpha collisions may be measured by passing a beam of neutrons into a helium-filled ionization chamber. If an incident neutron of energy E is deflected through an angle θ by collision with an alpha-particle application of the conservation laws shows that the recoiling alpha-particle is given an energy $\frac{16}{25} E \cos^2\theta$. Providing that the alpha-particle is brought to rest within the chamber this energy may be found directly from the corresponding pulse-height. If E is known, then θ may be found also. Thus if the incident neutrons are monoenergetic and of known energy, measurement of the pulse-height distribution gives directly the angular distribution of the recoiling alpha-particles in the laboratory coordinate system.

Additional information can be obtained by the use of a helium-filled cloud chamber. The direction of the recoiling alpha-particles can be measured for each event, and hence the energy of the incident neutron found. The angular distribution can thus be obtained at any energy even if the incident neutrons have a broad energy spectrum. Absolute values of the differential and total cross section can only be found if the intensity and energy distribution of the incident neutrons is known.

At higher energies these methods become impracticable as more and more alpha-particles pass out of the counter or cloud-chamber before coming to rest. The differential cross section can then be measured by directing a nucleon beam on to a helium target and detecting the scattered nucleons or recoil alpha-particles by photographic emulsions or counters arranged radially around it. Measurement of both the scattered and the recoil particles enables the differential cross section to be measured over a wider range than is possible using either separately, since at angles where it is easy to measure one it is difficult to measure the other, and *vice versa*.

Table 2. Differential Cross Section for Elastic Neutron–Alpha Collisions

Author	Method	Energy (Lab)	Angles (CM)	Notes
Staub* 1939 a, b	C.C.	0·5–6	171–180	Relative σ for H and He
Gaerttner* 1939	P.C.	~1	–	Confirms anomalous scattering at 1 MeV
Hudspeth* 1940	C.C.	0·6–2·5	160–180	Relative σ for H and He. Anomaly at 1 MeV.
Staub* 1940	C.C.	0·4–3	171–180	Double peak indicated
Barschall* 1940	I.C.	2·5–3·1	50–180	Absolute σ found
Bonner* 1940	I.C.	0·5–1·3	0–180	Relative total σ for H and He
Hall* 1947	P.C.	0·6–1·6	50–180	Could not fit results with close P doublet
Adair 1951, 1952	P.C.	0·4–2·73	50–180	
Huber* 1952	I.C.	3–4·14	50–180	
Swartz 1952	C.C.	140–230	0–180	Angular distribution increasingly peaked forward at higher energies. Analysed by Squires (1957)
Tannenwald 1952, 1953	C.C.	~40–120	0–180	
Seagrave 1953	P.C.	2·6–14·3	70–145	Relative σ
Smith 1954	C.C.	14·1	0–180	
Alston* 1954	D.C.C.	15·7	0–180	
Shaw 1955	C.C.	14·3	0–180	
Striebel* 1957	I.C.	2·61–4·09	60–140	

Fig. 2

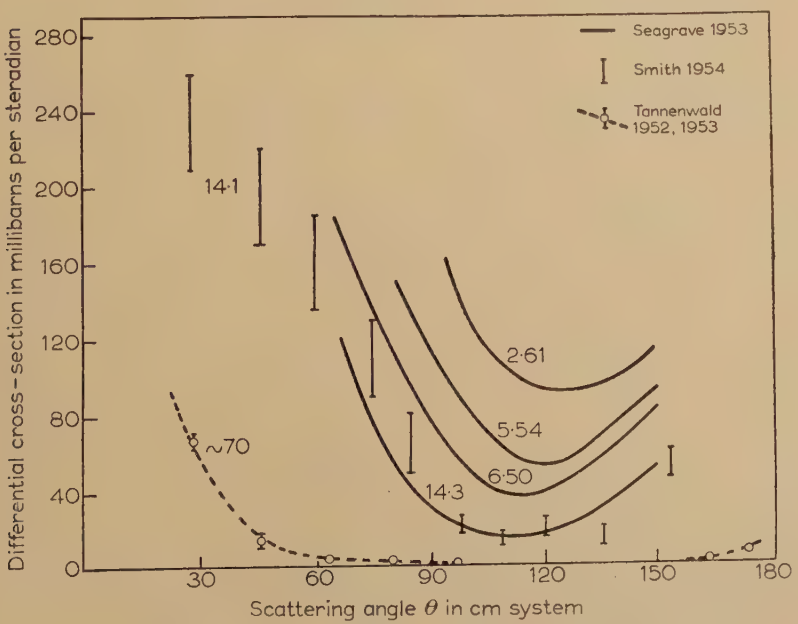

The differential cross section for neutron–alpha collisions.

Usually there is some overlap between these regions, and this provides a useful check on the measurements.

The main features of the experimental determinations of nucleon–alpha differential scattering cross sections are given in tables 2 and 3, and the cross sections themselves are plotted in figs. 2 and 3.

Fig. 3

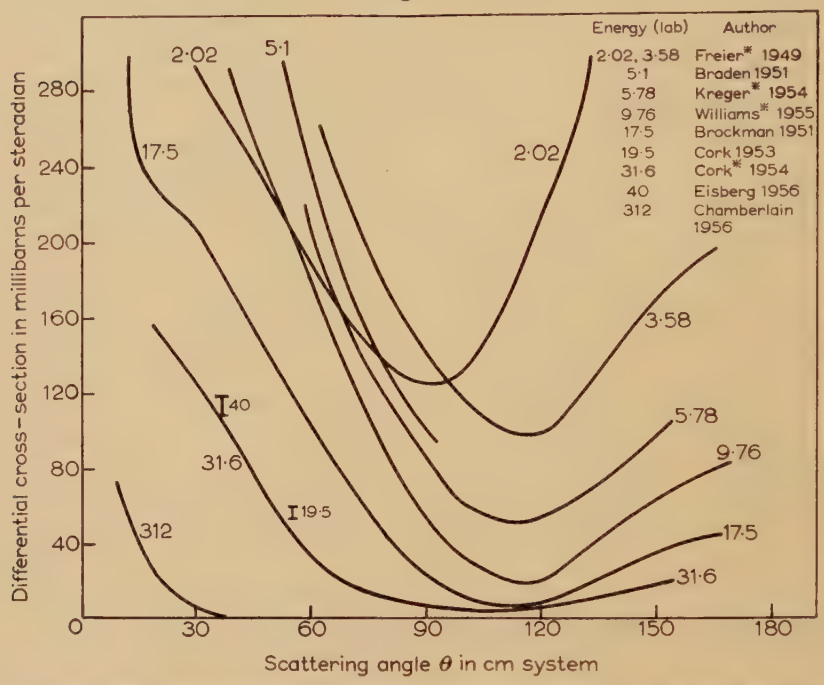

The differential cross section for proton–alpha collisions. To avoid confusion only a representative selection of all the published results are plotted.

§ 4. Inelastic Collisions

At higher energies nucleon–alpha collisions are no longer completely elastic, and as the energy increases it is necessary to consider in turn the possibility of scattering through an excited state of ^{4}He, and of collisions leading to the partial or complete break-up of the alpha-particle, perhaps with meson production.

An early experiment on the disintegration of lithium by protons (Lauritsen and Crane 1934, Crane *et al.* 1935) indicated the presence of several states of the alpha-particle with energies less than 20 Mev. These states were in accord with current theoretical ideas (Feenberg 1936, Bethe and Bacher 1936), but later work on the reaction of deuterons with helium 3 (Allred 1950, Hatton and Preston 1949) set lower limits of 20·9 Mev and 18·3 Mev respectively on the lowest excited state of the alpha-particle. Further investigations of the reactions of neutrons and protons with tritium (Taschek *et al.* 1949, Argo *et al.* 1950), however, provided evidence for an excited state at 21·6 Mev.

Table 3. Differential Cross Section for Elastic Proton–Alpha Collisions

Author	Method	Energy (Lab)	Angles (CM)	Notes
Rutherford 1919	S.C.		~180	More protons projected forward than expected from inverse square law.
Chadwick* 1921	S.C.	0–2·1	~180	
Mohr* 1937	I.C.	0–2·1	~180	Ratio of observed to classical scattering large.
Heydenburg* 1939	I.C.	0·994	20–45	Agrees with Rutherford–Darwin formula
Heydenburg* 1941	I.C.	1–3	37–149	Relative σ
Heitler* 1947	P.P.	4·2	18–119	Relative σ
Freier* 1949	P.C.	0·95–3·58	12·5–168	Broad resonance at 2 MeV for backward scattering.
Braden 1951	P.C.	4·8, 5·1	36–157	Relative σ ; calibrated by p–p scattering.
Cork 1951, 1953	S.C.	31·8	17–62	
Putnam 1952	P.P.	9·48	10–172·5	
Kreger* 1952,	P.P.	5·78	16–154	
Atkins 1952	P.C.	5·78	–	
Cork 1953	S.C.	19·5	55	$d\sigma = 59{\cdot}1 \pm 1{\cdot}6$ mb/Ω.
Wickersham 1954, 1957	C.C.	28	0–180	
Cork* 1954	S.C.	9·73, 31·6	17–154	Agrees with Putnam (1952) for forward angles, but is 25% lower at backward angles.
Freemantle* 1954	P.P.	9·55	22–168	Results 15% low (cf. Williams 1955).
Williams* 1955	P.P.	9·76	43–174	Agrees with Putnam, but not with Cork above 90°.
Teem* 1955	S.C.	95	–	
Eisberg 1956	S.C.	40	37	$d\sigma = 110 \pm 10$ mb/Ω.
Brockman 1956	S.C.	17·5	6–168	Derives phase shifts.
Putnam* 1956a, b	P.P.	7·5	10–172·5	
Vanecian 1956	S.C.	19·4	20–164	Minimum $d\sigma$ of $7{\cdot}78 \pm 0{\cdot}2$ mb/Ω at 110°.
Chamberlain* 1956	C.	312	10–42	
Miller* 1957	—	2·2–5·8	–	
Brussel* 1957	S.C.	40	5–146	
Tyren* 1957	—	181	13–29	Accuracy $\pm 3\frac{1}{2}$%. Relative σ.

This work was not confirmed by later studies of proton–helium scattering in which the scattered protons were analysed to see if any of them had less energy than would be expected from an elastic collision. This experiment was performed by Benveniste and Cork (1953) using incident protons of energy 32 MeV, and they found no evidence for an excited state of energy less than 23·3 MeV. This was confirmed by Wickersham (1954). A later investigation by Eisberg (1956) using

40 MeV incident protons raised this upper limit to 28 MeV. He points out that since the width of a virtual state usually increases with increasing excitation energy, and broad states are difficult to detect, it is unlikely that such a state will be found at higher excitation energy.

In their experiment described above, Benveniste and Cork found secondary deuterons formed in the reaction ^{4}He(p, d)^{3}He. The angular distribution of these deuterons agreed qualitatively with the pick-up theory of Butler (1951).

Collisions leading to the break-up of the alpha-particle are most conveniently studied in a cloud chamber. Tracy and Powell (1950) used a cloud chamber containing a mixture of helium and oxygen and bombarded it with 90 MeV neutrons. They observed a number of stars due to nuclear disintegrations, and were in many cases able to identify the reaction concerned by measurements on the tracks of the emitted charged particles. This work was repeated by Tannenwald (1952, 1953) using a helium-filled cloud chamber. The observed frequencies of the possible break-up reactions are given in table 4 ; corrections for geometric loss have been made. A semi-theoretical argument was used to estimate the frequency of the last reaction in this table and in table 6.

Table 4

Reaction	Tracey and Powell	Tannenwald	
	Observed	Observed	Corrected
$n+\alpha \rightarrow d+t$	2	33	66·5
$n+\alpha \rightarrow 2d+n$	1	17	35·2
$n+\alpha \rightarrow p+t+n$	2	88	209·1
$n+\alpha \rightarrow p+d+2n$	1	31	76·3
$n+\alpha \rightarrow p+p+3n$	0	2	3·8
$n+\alpha \rightarrow {}^3He+2n$	0	—	80·8

A further study was made by Teem *et al.* (1955), who bombarded helium with 95 MeV protons, and measured the energy spectrum of the emitted protons and deuterons using a scintillation counter. The angular distribution of the deuterons was analysed using the pick-up theory of Chew and Goldberger (1950).

Tyren *et al.* (1957) measured the energy distribution of 181 MeV protons scattered through several small angles by helium and found a broad peak

corresponding to protons that had lost around $22{\cdot}7 \pm 0{\cdot}4$ MeV in the collision. They consider that this peak is too broad to be due to an ordinary level but too narrow to be due to the break-up of the helium nucleus.

§ 5. Meson Production

At high energies meson production occurs in nucleon–alpha collisions. So far only one paper has been published on this process (Moulthrop 1955). Protons of 340 MeV were incident on a lithium deuteride target,

Table 5

Reaction	Number Observed	Weighted number	Frequency (%)	Q value (MeV)	Threshold (MeV)
(1) $n+\alpha \rightarrow \alpha+p+\pi^-$	17	18·5	$5{\cdot}7 \pm 1{\cdot}4$	−138·2	175·5
(2) $n+\alpha \rightarrow$ $^3He+d+\pi^-$	91	98·9	$30{\cdot}4 \pm 3{\cdot}2$	−156·6	199·0
(3) $n+\alpha \rightarrow$ $^3He+p+n+\pi^-$	93	104·0	$32{\cdot}0 \pm 3{\cdot}3$	−158·8	201·9
(1) or (3)	14	14·9	$4{\cdot}6 \pm 1{\cdot}2$	—	—
(4) $n+\alpha \rightarrow t+2p+\pi^-$	9	10·8	$3{\cdot}3 \pm 1{\cdot}1$	−158·0	200·3
(5) $n+\alpha \rightarrow 2d+p+\pi^-$	18	20·3	$6{\cdot}2 \pm 1{\cdot}5$	−162·0	205·8
(6) $n+\alpha \rightarrow$ $d+2p+n+\pi^-$	46	50·1	$15{\cdot}4 \pm 2{\cdot}3$	−164·3	208·8
(7) $n+\alpha \rightarrow 3p+2n+\pi^-$	5	5·8	$1{\cdot}8 \pm 0{\cdot}8$	−166·5	211·9
Unclassified	2	2·3	$0{\cdot}6 \pm 0{\cdot}5$	—	—

Table 6. Comparison of Relative Reaction Cross Sections with and without Meson Production

$n+\alpha \rightarrow \pi^-$ at 300 MeV		$n+\alpha$ at 90 MeV	
Reaction	Frequency (%)	Reaction	Frequency (%)
$n+\alpha \rightarrow {}^3He+p+n+\pi^-$	34 ± 3	$n+\alpha \rightarrow t+p+n$	45 ± 6
$n+\alpha \rightarrow {}^3He+d+\pi^-$	32 ± 3	$n+\alpha \rightarrow t+d$	14 ± 3
$n+\alpha \rightarrow d+2p+n+\pi^-$	16 ± 1	$n+\alpha \rightarrow d+p+2n$	16 ± 3
$n+\alpha \rightarrow 2d+p+\pi^-$	7 ± 1	$n+\alpha \rightarrow 2d+n$	8 ± 2
$n+\alpha \rightarrow 3p+2n+\pi^-$	2 ± 1	$n+\alpha \rightarrow 2p+3n$	1 ± 1
$n+\alpha \rightarrow t+2p+\pi^-$	4 ± 1	$n+\alpha \rightarrow {}^3He+2n$	17

and the resulting neutrons, having a broad energy distribution around 300 MeV, entered a helium-filled diffusion cloud chamber situated in a magnetic field. About three hundred events were found in which a pion was produced in the neutron–alpha collision. The great majority of these pions were found to be negatively charged.

Measurements of the curvature and ionization of the tracks of the emitted particles enabled the complete reaction to be identified in most cases. The reactions found, together with their relative frequencies, values and threshold energies, are given in table 5.

Fig. 4

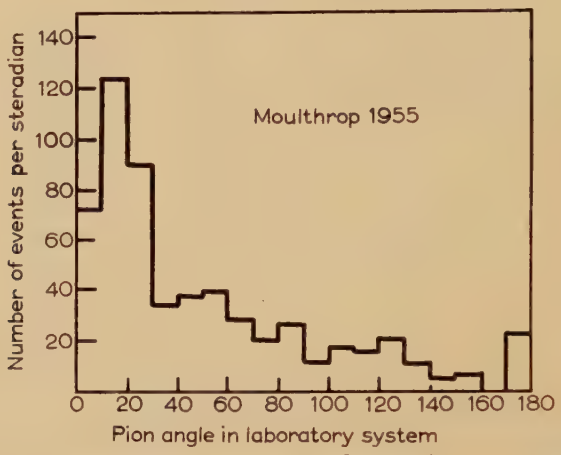

Relative differential cross section for pion production in neutron–alpha collisions.

Fig. 5

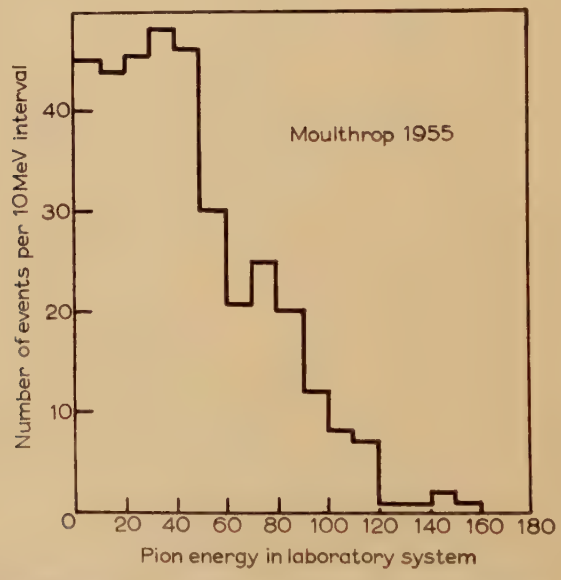

Energy distribution of pions produced in neutron–alpha collisions.

These results are compared with those of Tannenwald (1953) on neutron–alpha inelastic collisions at 90 Mev in table 6. The reaction $\alpha(n, p\pi)\alpha$ is not included as it is the analogue of the elastic $\alpha(n, n)\alpha$ process. This comparison shows that the relative inelastic cross sections for the different energetically possible reactions are hardly altered by

meson production. There is also a correlation between pion production and the emission of fast deuterons; these are more numerous than could be accounted for by the pick-up process.

The energy and angular distributions of the emitted mesons are shown in figs. 4 and 5. They agree closely with the corresponding distributions for mesons produced in neutron–oxygen collisions at 300 Mev (Ford 1953). The total cross section for pion production in neutron–alpha collisions at 300 Mev was found to be $0{\cdot}6\pm0{\cdot}3$ mb.

§ 6. Polarization

The interpretation of the anomalous nucleon–alpha scattering in the region of 1 Mev in terms of a P-wave resonance associated with the formation of an unstable nucleus of helium 5 (see § 8) indicates that the scattered nucleon is subjected to strong spin–orbit forces during the collision (Schwinger 1946). This causes the incident nucleons to be scattered differently according to their initial spin orientations, so that the emergent beams are polarized, that is, the particles composing them have their spins preferentially orientated. If the polarized beam now undergoes a second scattering, the scattered intensity is not axially symmetric, and the amount of the asymmetry gives a measure of the polarization at each collision.

Lepore (1950) has shown that the polarization is determined by the phase-shifts that are found from the cross sections in the way described in § 9 according to the relation

$$\mathbf{P}=\frac{2\,\mathrm{Im}\,A^*B}{|A|^2+|B|^2}\mathbf{n} \qquad \ldots\ldots\ldots \quad (1)$$

where A and B are defined by (15), and $\mathbf{n}$ is the normal to the plane of the scattering; it is defined by $\mathbf{k}\times\mathbf{k}'=\mathbf{n}\sin\theta$, where $\mathbf{k}$ and $\mathbf{k}'$ are unit vectors in the directions of the incident and scattered waves respectively. This relation applies when the initial beam is unpolarized; a more complicated relation can be derived for the case when it is not. All these formulae are special cases of the general relations given by Simon and Welton (1953).

If, therefore, all the phase-shifts are known, the polarization can be deduced from them and the only justification for an experimental determination of the polarization would be to provide a check on these phase-shifts. But it so happens that the cross section data do not quite determine the phase-shifts. Two sets of phase-shifts are found that are equally consistent with the observed cross sections; they correspond to a normal and an inverted P doublet respectively. These two sets of phase-shifts predict quite different polarizations, and so a polarization experiment may be used to decide between them (Dodder 1949).

This experiment was performed by Heusinkveld and Freier (1952). They designed a scattering chamber so that protons entered photographic

emulsions after two successive collisions with helium nuclei. The first scatterings were the same, and served to polarize the protons, while the second was either to the left or to the right through an angle of about 90°. They calculated that the ratio of the intensities in these two directions should be about 2·2 for one set of phase-shifts and about 0·05 for the other. These are so widely different that it was necessary to measure only a small number of tracks to show that the P doublet is inverted. This is the case for both neutron–alpha and proton–alpha scattering.

Once this ambiguity is resolved, the polarization phenomena in nucleon–alpha scattering are substantially understood, and can therefore be used to measure the direction of polarization of high energy nucleon beams, which is left undetermined by double scattering experiments. This method has the advantage over other methods that there are no narrow, isolated resonances to complicate the analysis (Lasinio and Monetti 1957).

A point of particular interest is whether the sign of the spin–orbit interaction that has been postulated (Fermi 1954) to account for the observed polarization in high-energy collisions is the same as that of the spin–orbit interaction used to explain the properties of heavy nuclei on the shell theory. This has been studied (Marshall and Marshall 1955, Brinkworth and Rose 1956, Bradner and Isbell 1957) by slowing down the protons that have undergone a high-energy collision, and then analysing their polarization by a second scattering in helium. These experiments showed that the signs of the two spin–orbit interactions are the same.

Several authors (Marshall and Marshall 1955, Heusinkveld and Freier 1952, Brinkworth and Rose 1956, Juveland and Jentschke 1956, Levintov Miller and Shamshev 1957, Johnston 1957, Bradner and Isbell 1957) have calculated the expected values of the polarization as a function of energy and angle from the phase-shifts determined from the experimental differential cross sections. These calculations are summarized in figs. 6 and 7 for neutron–alpha and proton–alpha collisions respectively.

Two direct experimental determinations of the polarization in neutron–alpha collisions (White and Farley 1957, Levintov, Miller and Shamshev 1957) and two of polarization in proton–alpha collisions (Scott and Segel 1955, Juveland and Jentschke 1956), have been made and the results agree well with those derived from the phase shifts. It would be desirable to extend this work to higher energies, because the polarization is more sensitive to the higher phase shifts than is the differential cross section (Juveland and Jentschke 1956).

In addition to these measurements at low energies, Chamberlain *et al.* (1956) have determined the polarization produced in collisions of 312 Mev protons with alpha-particles. At this energy most of the collisions are inelastic, so the experiment was designed so that only the protons from elastic collisions were recorded. Their results are given in fig. 8 and show that the polarization changes sign at the larger scattering angles.

Fig. 6

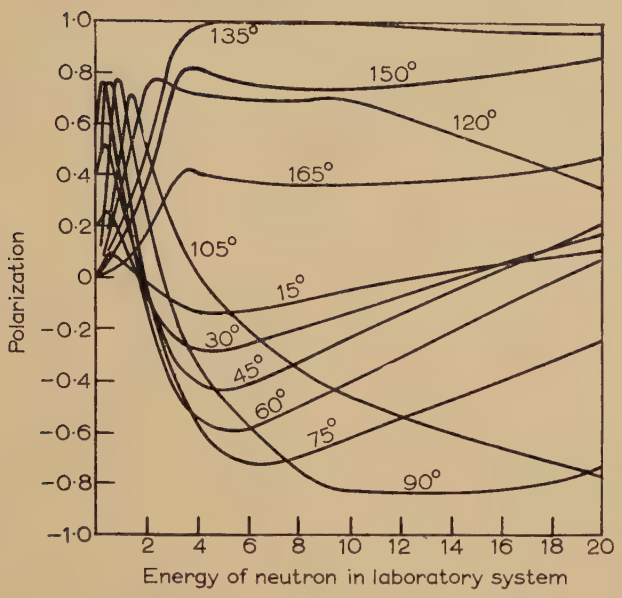

Polarization in neutron–alpha scattering.
(Levintov, Miller and Shamshev 1957.)

Fig. 7

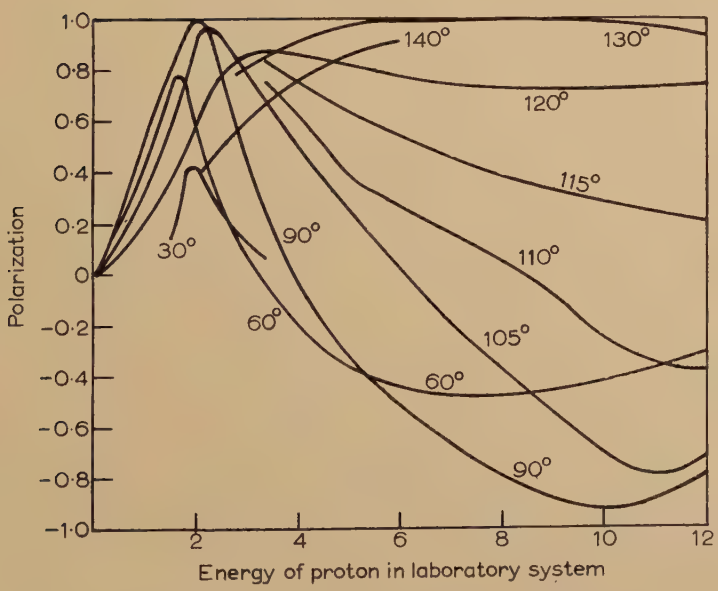

Polarization in proton–alpha scattering.

Some calculations of the polarization in high-energy proton–alpha scattering have been made by Tamor (1954, 1955). He used the impulse approximation and showed that for nuclei like alpha-particles, with a high degree of symmetry, the polarization does not depend on the nuclear wave function. Then, using phase shifts derived from nucleon–nucleon interactions, he found that the expected proton–alpha polarization rises

Fig. 8

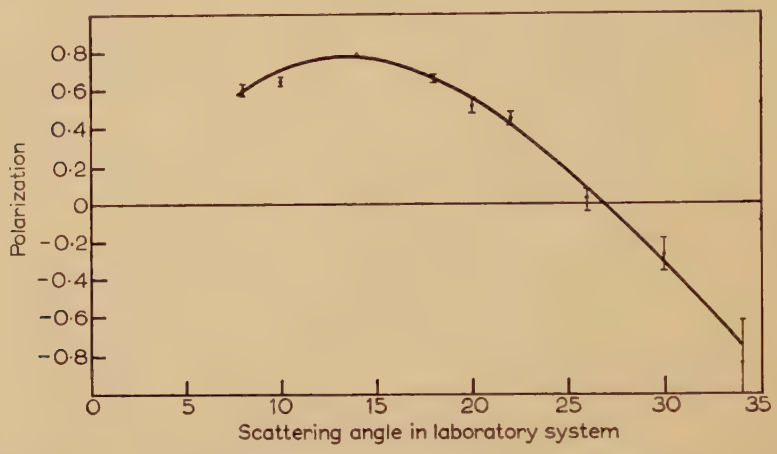

Polarization in proton–alpha collisions at 312 MeV. (Chamberlain *et al.* 1956.)

Table 7. Experiments on Polarization in Proton–Alpha Collisions

Author	Method	Energy (Lab)	Angles (CM)	Notes
Heusinkveld* 1952	P.P.	~3·3	~90	Showed $P_{1/2}$–$P_{3/2}$ doublet inverted
Marshall* 1955	P.P.	0–20		Showed that sign of spin–orbit coupling is the same as that used in the shell model of nucleus.
Brinkworth* 1956	P.P.	~7	120	
Bradner* 1957	P.P.	3·5–14	90±22·5	
Scott* 1955	P.P.	3	90	Results agree with those calculated from phase shifts.
Juveland* 1956	P.P.	5·3	55, 90	
Chamberlain* 1954, 1956	C.	315	10–42	
Scott 1957	P.P.	1·38–3·58	73–104	
Rosen* 1957	P.P.	10	32–147	

monotonically from zero at small angles to a maximum of nearly unity in the region of 30°, and thereafter declines. He did not, however, find the change of sign of the polarization observed by Chamberlain *et al.*

The main characteristics of the investigations of the polarization produced in proton–alpha collisions are shown in table 7.

§ 7. Coulomb Scattering

The early experiments of Rutherford (1911) on the scattering of alpha-particles by thin metallic foils led him to put forward his nuclear model of the atom. Assuming a Coulomb interaction between the interacting particles he was able, using classical dynamics, to derive his well-known expression for the differential cross section

$$I(\theta)=\left(\frac{ZZ'\epsilon^2}{2mv^2}\right)^2 \operatorname{cosec}^4 \tfrac{1}{2}\theta \qquad \ldots\ldots (2)$$

in which the symbols have their usual meanings. It is applicable to the scattering of any two charged particles, and has been experimentally verified, particularly for the collisions of low-energy alpha-particles with heavier nuclei.

For higher energies and lighter nuclei, however, Rutherford's law no longer holds. Thus, for example, Chadwick and Bieler (1921) found that when alpha-particles were passed into hydrogen, many more protons were knocked on in the forward direction than would be expected from Rutherford's law. This may be understood if there is a new type of interaction between the particles whenever they approach each other closely. This is called the nuclear interaction ; it is very strong in the immediate vicinity of the nucleus but negligible compared with the Coulomb at greater distances from it.

Thus if two charged particles collide at an energy and angle such that their distance of closest approach is greater than the combined range of their nuclear forces the interaction is entirely Coulomb, and the differential cross section is given by Rutherford's formula. If, however, they approach closer than this, the scattering is determined by both the Coulomb and the nuclear interaction. This is the case for most of the proton–alpha collisions considered here.

Studies of proton–alpha collisions by Marsden (1914), Rutherford (1919) and many others quoted in § 3 have shown that in the Coulomb region Rutherford's law is accurately obeyed but that outside it there are divergences due to the nuclear interaction. It is therefore necessary in studies of the nuclear interaction to disentangle the known Coulomb contribution from the observed scattering in the Coulomb–nuclear region. This can only be done using a quantum-mechanical treatment of the scattering process. In this way it has been shown that the observed differential cross section at any angle is the sum of three terms : the pure Coulomb term, the pure nuclear term and the Coulomb–nuclear interference term. This analysis enables the Coulomb scattering to be disentangled from the nuclear (see § 9).

In the quantum-mechanical treatment of the Coulomb scattering a solution of Schrödinger's wave equation that is the sum of incident and scattered waves is sought. Owing to the slow fall-off with distance of the Coulomb field the incident wave is distorted even at an infinite

distance from the scattering centre. The scattering amplitude $f(\theta)$ for pure Coulomb scattering is given by (Mott and Massey 1949)

$$f(\theta)=\frac{ZZ'\epsilon^2}{2\mathrm{m}\,v^2}\,\mathrm{cosec}^2\,\tfrac{1}{2}\theta\,\exp\left[-i\alpha\,\log\,(1-\cos\theta)+i\pi+2i\eta_0\right] \quad . \quad (3)$$

where $$\exp 2i\eta_0=\frac{\Gamma(1+i\alpha)}{\Gamma(1-i\alpha)}\,; \qquad \alpha=\frac{ZZ'\epsilon^2}{\hbar v}\,.$$

The scattered intensity is given by $I(\theta)=f|(\theta)|^2$, which reduces to Rutherford's formula.

§ 8. Resonance Theory

Much of the early work on nucleon–alpha scattering was devoted to an examination of the resonance in the region of 1 Mev. Its presence was indicated by a study by Williams *et al.* (1937) of the alpha-particle spectrum from the reaction

$$^7_3\mathrm{Li}+^2_1\mathrm{D}\rightarrow{}^8_4\mathrm{Be}+^1_0\mathrm{n}\rightarrow 2^4_2\mathrm{He}+^1_0\mathrm{n}.$$

They found a continuous distribution with a superposed peak which they ascribed to the reaction

$$^7_3\mathrm{Li}+^2_1\mathrm{D}\rightarrow{}^5_2\mathrm{He}+^4_2\mathrm{He}.$$

The position of the peak indicated that the ^{5}He is left in a state unstable by 0·84 Mev against disintegration into an alpha-particle and a neutron. Resonance effects are therefore expected in neutron–alpha scattering when the centre-of-mass energy is in the region of 0·84 Mev. These were found by Staub and Stephens (1939), who also showed from the magnitude of the resonance peak in the differential cross section in the backward direction that the resonance could be ascribed to a P level. Later Staub and Tatel (1940 a, b) found evidence of a doublet structure in the resonance peak, and suggested that this could be due to the P level being split into $P_{1/2}$ and $P_{3/2}$ levels with a separation of about 0·4 Mev. They were not able to say whether the doublet was normal or inverted : calculations based on either hypothesis agreed equally well with the experimental data.

Similar investigations, however (Bonner and Hudspeth 1940, Hudspeth and Dunlop 1940, Bashkin, Mooring and Petree 1951) did not provide any confirmation of this double peak, although slight indications of it were found by Gaertner *et al.* (1939) and by Hall and Koontz (1947). Furthermore, Wheeler and Barschall's (1940) analysis of Barschall and Kanner's (1940) data required a much larger level separation than Staub and Tatel had estimated.

Meanwhile, Primakoff and Goldsmith (1939) had suggested that owing to the symmetry between the nuclei ^{5}He and ^{5}Li similar resonance phenomena might be expected in proton–alpha scattering at about 1 Mev higher than in the neutron–alpha case, corresponding to the Coulomb energy difference between the two nuclei. This predicted resonance was found by Heydenburg and Ramsey (1941) and by Freier *et al.* (1949). Critchfield and Dodder (1949) made a phase-shift analysis

(cf. § 9) of the latter work and found that it was best interpreted by a combination of $S_{1/2}$, $P_{1/2}$, $P_{3/2}$ waves, with a small admixture of D waves. They were not able to say whether the P doublet was normal with a separation of about 1·1 Mev or inverted with a separation of about 2–5 Mev. Both these separations are larger than that previously used by Staub and Tatel to explain the indications of a doublet splitting in neutron–alpha scattering (Landau and Smorodinsky 1944).

Several observers (Frank 1934, Pose and Diebner 1934, Volland 1937, Tsien 1940) found a series of low-energy resonances in proton–alpha scattering in addition to the one at 1·8 Mev. but these were not confirmed by later work (Pollard and Margenan 1935 a, b, Ruhla 1954).

Goldstein (1950) used this work on proton–alpha scattering to reinterpret that on neutron–alpha scattering by making use of the symmetry between ^{5}He and ^{5}Li. He suggested that the levels are as widely separated in the neutron case as in the proton case. Then, since the normal doublet separation of 1·1 Mev is incompatible with the neutron–alpha data, he suggested that the doublet is inverted in both cases (this was later confirmed by the double scattering experiment of Heusinkveld and Freier 1952). In this case the level separation is so large that, although the level widths are considerable, the $P_{1/2}$ level has little influence on the $P_{3/2}$ level. The low energy resonance in neutron–alpha scattering is then ascribed to the $P_{3/2}$ level alone. The best parameters of this level are $E_r \sim 1{\cdot}2$ Mev, $\Gamma \sim 1{\cdot}4$ Mev ; the $P_{1/2}$ level is about 1·3 Mev higher (Leland and Agnew 1951, Titterton and Brinkley 1951). This analysis has been confirmed by later work, and so the indications of a doublet structure in the low-energy resonance found by some authors must be ascribed to a statistical fluctuation in their measurements.

The resonance scattering occurs in the presence of the usual potential scattering, and there is interference between them. Bloch (1940) has shown that the differential cross section due to the S-wave potential scattering and the resonance P-wave scattering is

$$\frac{d\sigma}{d\Omega} = \frac{1}{k^2}\left|\sin\delta_0 \exp(i\delta_0) + \left(\frac{\Gamma_{3/2}}{E_{3/2}-E-\frac{1}{2}i\Gamma_{3/2}} + \frac{1}{2}\frac{\Gamma_{1/2}}{E_{1/2}-E-\frac{1}{2}i\Gamma_{1/2}}\right)\cos\theta\right|^2$$
$$+ \frac{1}{4k^2}\sin^2\theta\left|\frac{\Gamma_{3/2}}{E_{3/2}-E-\frac{1}{2}i\Gamma_{3/2}} - \frac{\Gamma_{1/2}}{E_{1/2}-E-\frac{1}{2}i\Gamma_{1/2}}\right|^2 \quad . \quad . \quad . \quad (4)$$

where $E_{1/2}$ and $E_{3/2}$ are the resonance energies of the $P_{1/2}$ and $P_{3/2}$ levels respectively, $\Gamma_{1/2}$ and $\Gamma_{3/2}$ their respective widths, and δ_0 the S-wave phase shift. In the case of proton–alpha scattering there is a Coulomb term as well, which interferes with both the potential and the resonance terms.

The resonance parameters are related to the phase shift in the resonance region by the equation

$$\tan\delta = \frac{\frac{1}{2}\Gamma}{E_r - E} \quad . \quad . \quad . \quad . \quad . \quad . \quad . \quad (5)$$

so that the resonance energy E_r, when the cross section is at a maximum, occurs when $\delta=\frac{1}{2}\pi$. These relations enable E_r and Γ to be deduced from the energy variation of the phase shifts when the resonance is large and isolated, and the potential scattering is small.

Adair (1952) has used the more developed theory of Wigner and Eisenbud (1947) to study the resonances in detail. The total nuclear phase shift $\delta_l^{\pm}$ can be written as the sum of the resonance or compound nucleus phase shift $\beta_l^{\pm}$ and the potential hard sphere phase shift ϕ_l

$$\delta_l^{\pm}=\beta_l^{\pm}+\phi_l \qquad (6)$$

where the subscripts are the values of the orbital angular momentum, the superscripts the two spin states and

$$\tan\beta_l^{\pm}=\sum_{\lambda}\frac{\frac{1}{2}\Gamma_\lambda}{E_\lambda+\Delta_\lambda-E}; \qquad \tan\phi_l=\left(\frac{F_l}{G_l}\right)_{r=a} \qquad (7)$$

where Γ_λ, the width of the λth level of the compound nucleus, is given by

$$\Gamma_\lambda=\frac{2k\gamma_\lambda^2}{(F_l^2+G_l^2)_{r=a}} \qquad (8)$$

and Δ_λ, the level shift, by

$$\Delta_\lambda=-\frac{\gamma_\lambda^2}{a}\left[\frac{d\ln(F_l^2+G_l^2)^{1/2}}{d\ln(kr)}+l\right]_{r=a} \qquad (9)$$

where F_l and G_l are the regular and irregular Coulomb wave functions for orbital angular momentum l, and γ_λ is the reduced width of the λth level, and E_λ is the energy at which

$$\left(\frac{d\ln r\chi}{d\ln r}\right)_{r=a}=-l \qquad (10)$$

in which χ is the normalized internal wave function.

The resonance energy is conveniently defined as $E_r=E_\lambda+\Delta$. Adair found that the best fit to the proton–alpha scattering data is obtained with the nuclear radius $a=2{\cdot}9\times10^{-13}$ cm, $\gamma^2(P_{3/2})=\gamma^2(P_{1/2})=17{\cdot}6$ Mev cm, $E_\lambda(P_{3/2})=3{\cdot}65$ Mev, and the doublet splitting $E_\lambda(P_{1/2})-E_\lambda(P_{3/2})=5$ Mev. The data do not determine the parameters of the $P_{1/2}$ level very accurately.

This work was continued by Dodder and Gammel (1952), who studied the variation of the phase shifts with energy. The above relation between the total, resonance and potential phase shifts may, with the help of the relation (Blatt and Weisskopf 1952)

$$G_lF_l'-F_lG_l'=k \qquad (11)$$

be written in the form

$$aY=-\frac{ka/FG}{1+(F/G)\cot\delta}+\frac{kaF'}{F} \qquad (12)$$

where the prime denotes differentiation with respect to kr. The logarithmic derivative Y of the wave function was evaluated from this relation using

the proton–alpha phase shifts derived by Critchfield and Dodder (1949) from the data of Freier *et al.* (1949) and the values of F_l and G_l tabulated by Bloch *et al.* (1951).

They found that aY is a linear function of energy, which is to be expected from the one-level approximation

$$aY \sim \frac{a}{\gamma_\lambda^2}(E_\lambda - E). \qquad \ldots\ldots (13)$$

Table 8. Nuclear Resonance in Neutron–Alpha Scattering

Author	Energy (Lab)	Angles (CM)	$J=\frac{3}{2}$ $l=1$		Notes
			E_r	Γ	
Staub* 1939	0·5–6	171–180	~1	0·2	Found resonance for backward scattering attributed it to a P-level in ^{5}He
Gaerttner* 1939	~1	—	—	—	Possible splitting indicated.
Staub* 1940 a, b	0·4–3	171–180	~1	0·4	Found indication of doublet structure, splitting. Sign of splitting undetermined
Bonner* 1940	0·5–1·3	0–180	~1·1	1·2	
Barschall* 1940	2·5–3·1	—	—	—	Interpreted by Wheeler* 1940 as showing large P-wave splitting.
Hudspeth* 1940	0·6–2·5	160–180	~1	–	No evidence of double peak.
Hall* 1947	0·6–1·6	150–180	~1	—	Found total σ by assuming only S and P-waves. Showed slight indication of splitting of 1 MeV resonance.
Bashkin* 1950, 1951	0·4–6·4	0–180	1·15	—	Resonance peak shows no splitting.
Adair 1952	0–2·73	50–180			Agrees with widely-split inverted P doublet.
Hughes* 1956	—	—	1·15 ± 0·05	1·4 ± 0·2	Review Article.

From these curves they found the resonance parameters to be $E_\lambda = -4{\cdot}1$ MeV, $\gamma_\lambda^2 = 25 \times 10^{-13}$ MeV cm for the $P_{3/2}$ level, and $E_\lambda = 3{\cdot}4$ MeV, $\gamma_\lambda^2 = 106 \times 10^{-13}$ MeV cm for the $P_{1/2}$ level. The $P_{1/2}$ level is thus found to be considerably broader than the $P_{3/2}$ level, unlike the results of Adair. More recent work at higher energies (cf. § 9) have not shown the $P_{1/2}$ phase shift to pass through 90°, so there is no virtual level at all, although

it is possible to define some formal resonance energy. The energy variation of aY for the $S_{1/2}$ wave was found to be negligible, showing that there is no S resonance.

Assuming that, when allowance has been made for the shift of the levels due to the Coulomb forces, these parameters characterize the P resonance in neutron–alpha scattering also, and that the S-wave function has the same logarithmic derivative at the nuclear surface in both cases, Dodder and Gammel also calculated the energy variation of the total cross section for neutron–alpha scattering, and found good agreement with the experimental results of Bashkin, Mooring and Petree (1951).

Table 9. Nuclear Resonances in Proton–Alpha Scattering

Author	Energy (Lab)	Angles (CM)	$J=\frac{3}{2}$ $l=1$		Notes
			E_r	Γ	
Heydenburg* 1941	1–3	37–149	~2	~1	Resonance detected. No indication of doublet structure.
Freier* 1949	0·95–3·58	12·5–16·8	~2·2	—	

Since the interpretation of a scattering process in terms of a nuclear resonance is applicable only in the vicinity of the resonance, and all the information given by the resonance parameters is also contained in the phase shifts, it is more convenient to work in terms of phase shifts alone. The above resonance analysis is still used, however, to estimate the values of the phase shifts at higher energies from those found at lower energies. The values obtained are useful as first approximations in the iteration procedure for the determination of the phase shifts from the experimental data.

The investigations of the neutron–alpha and proton–alpha scattering that make use of the concept of nuclear resonance, and the resonance parameters found are summarized in tables 8 and 9.

§ 9. Phase Shift Analysis

Faxen and Holtsmark (1927) showed that the differential scattering cross section can be decomposed into a sum over the possible values of the orbital angular momentum l

$$\sigma(\theta)=|f(\theta)|^2$$

where
$$f(\theta)=\frac{1}{2ik}\sum_l (2l+1)[\exp(2i\delta_l)-1]\,P_l(\cos\theta) \quad . \quad . \quad . \quad (14)$$

where k is the nucleon wave number and P_l is a Legendre polynomial.

Wheeler and Barschall (1940) found that the observed (Barschall and Kanner 1940) differential scattering cross section for neutron–alpha collisions cannot be fitted by the first two terms of this formula, that is by the S and P waves, which are the only ones expected to contribute significantly at the energies concerned.

This suggested that the scattering depends on the orientation of the spin of the incident nucleon with respect to the orbital angular momentum. These must be combined together, so there are in general two values $l\pm\frac{1}{2}$ of the total angular momentum J for each value of the orbital angular momentum corresponding to the two possible orientations of the spin of the scattered nucleon. It is convenient to designate the possible scattering states $S_{1/2}$, $P_{1/2}$, $P_{3/2}$, $D_{3/2}$, $D_{5/2}$ etc., and the corresponding phase shifts δ_0, δ_1^-, δ_1^+, δ_2^-, δ_2^+, etc.

The formula for the differential cross section in this case was found by Mott (1932) and Bloch (1940) to be

$$\sigma(\theta)=|A|^2+|B|^2$$

where
$$A=\frac{1}{2ik}\sum_l\{(l+1)[\exp(2i\delta_l^+)-1]+l[\exp(2i\delta_l^-)-1]\}P_l(\cos\theta),$$

$$B=\frac{1}{2ik}\sum_l[\exp(2i\delta_l^+)-\exp(2i\delta_l^-)]P_l^1(\cos\theta) \quad . \quad . \quad . \quad . \quad (15)$$

where P_l^1 is an associated Legendre polynomial.

The total cross section is given by

$$\sigma_T=\frac{4\pi}{k^2}\sum_l\{(l+1)\sin^2\delta_l^+ + l\sin^2\delta_l^-\}. \quad . \quad . \quad . \quad . \quad (16)$$

Wheeler and Barschall found that it is possible to fit the observed neutron–alpha data with these formulae using only $S_{1/2}$, $P_{1/2}$ and $P_{3/2}$ waves. The large value of $(\delta_1^+-\delta_1^-)$ indicated the presence of a strong spin–orbit force between the alpha-particle and the scattered neutron.

A small number of phase shifts suffices to specify the differential cross section and, furthermore, most theories of nuclear collisions give a series of wave equations that may be solved for the phase shifts. It is therefore important to analyse the experimental differential cross sections in terms of phase shifts, so that comparisons with theories may be made.

The analysis is simpler in the neutron–alpha case, so this will be described first. At lower energies (less than about 5 Mev), the D waves may be neglected, and even at higher energies it is usual to neglect them as a first approximation, and seek a solution in terms of $S_{1/2}$, $P_{1/2}$ and $P_{3/2}$ waves alone. In the absence of D waves, the differential cross section as a function of $\cos\theta$ is paraboloid, and a least squares fit to the data easily gives the three phase shifts. Alternatively, the total cross section and the differential cross sections at 90° and 180° when inserted into (15) and (16) give three equations that can be solved for the phase shifts.

Graphical and mechanical methods of analysing the data have been described by Ashkin and Vosko (1953), Laubenstein and Laubenstein (1951), Seagrave (1953) and Clementel and Villi (1955). The latter pointed out that the problem of analysing nucleon–alpha particle collisions is mathematically identical with that of pion–nucleon collisions, so that the methods developed during the study of the latter problem may be applied also to the former. An electrical analogue computer to perform the phase analysis has been constructed by Baldinger (1952).

The higher phase shifts may be found by an iterative method. First approximate values of the S and P phases are found by neglecting higher phases, and then the D phases are included. For each trial set of phase shifts the corresponding differential cross section is calculated and compared by the method of least squares with that determined experimentally. The trial phase shifts are systematically varied until the best fit is found. These phase-shift analyses are greatly facilitated by an electronic computer programmed to calculate the differential cross section from the phase shifts according to eqn. (15).

Equations (15) and (16) for the total and differential cross sections are still valid for proton–alpha scattering, but the phase shifts $\delta_l^{\pm}$ now refer to the combined effect of Coulomb and nuclear scattering. These phase shifts tend to zero very slowly as l increases. It is therefore necessary to get rid of the Coulomb contribution so that only the rapidly converging nuclear phase shifts are left. This may be done by writing the total phase shift as the sum of Coulomb and nuclear parts:

$$\zeta_l^{\pm}=\eta_l+\delta_l^{\pm} \quad . \quad . \quad . \quad . \quad . \quad . \quad . \quad . \quad (17)$$

in which we have kept the symbol $\delta_l^{\pm}$ for the nuclear phase shift and written $\zeta_l^{\pm}$ for the total and η_l for the Coulomb phase shifts respectively. These nuclear phase shifts are not equal to the corresponding phase shifts derived from neutron-alpha scattering. But they vary in a similar way with energy, and would be equal if the Born approximation were valid in the enery region concerned. If the $\delta^{\pm}$ of (15) are replaced by the $\zeta^{\pm}$ of (17), (15) becomes

$$\left.\begin{aligned} A'(\theta)&=\frac{1}{2ik}\sum_l (2l+1)[\exp(2i\eta_l)-1]P_l(\cos\theta) \\ &\quad+\frac{1}{2ik}\sum_l \{(l+1)[\exp(2i\delta_l^{+})-1]+l[(\exp 2i\delta_l^{-})-1]\} \\ &\quad\times(\exp 2i\eta_l)P_l(\cos\theta), \\ B'(\theta)&=\frac{1}{2ik}\sum_l \{\exp(2i\delta_l^{\,\prime})-\exp(2i\delta_l\ )\}\exp(2i\eta_l)P_l^{1}(\cos\theta). \end{aligned}\right\} \quad . \quad (18)$$

The first term in $A'(\theta)$ is the scattering amplitude for pure Coulomb scattering, while the other terms in $A'(\theta)$ and $B'(\theta)$ are sums of products of Coulomb and nuclear parts. If the D and higher phase shifts are neglected, the experimentally determined differential cross sections at three selected angles may be expressed in terms of the three unknown

phase shifts. These equations may be solved graphically, and the sets of solutions used to compute the whole differential cross section. Comparison between these and the observed cross section usually permits most of the solutions to be discarded as non-physical. The acceptable sets of phase shifts may be systematically varied to improve the agreement with experiment. When approximate values of the S and P phase shifts have been found the D phase shifts may be introduced and the whole procedure repeated using five experimentally-determined differential cross sections to give five equations for the unknown phase shifts.

It is a little difficult to estimate the accuracy of these phase-shift analyses. Dodder and Gammel (1952) point out that if all phase shifts except one are kept fixed, the remaining one cannot be altered by more than about a tenth of a degree without destroying the agreement with experiment, but that several phase shifts may be simultaneously varied by several degrees without seriously impairing the fit. They estimate that the $S_{1/2}$ phase shifts they obtain are subject to an uncertainty of about 5°, and the P phase-shifts to one of about 2°.

These analyses are complex and time-consuming procedures, so a simpler and more elegant method of finding the phase shifts has been developed by Lustig and Blatt (1955). They avoid the necessity of

Table 10. Phase-Shift Analyses for Neutron–Alpha Collisions

Author	Data	Method	Phases
Huber* 1952	Huber* 1952	Baldinger 1952 Analogue Computer	S, P, D
Seagrave 1953	Seagrave 1953	Graphical	S, P, D
Clementel* 1955	Adair 1952	Graphical	S, P

matching at selected angles and then fitting over the rest of the angular range by working directly with expressions akin to the total cross section. In this way all the experimental data are used at the same time on an equal footing.

They begin by expressing the differential cross section as the sum of a pure Coulomb term, a pure nuclear term and a Coulomb–nuclear interference term. This may be done using the formalism of Blatt and Biedenharn (1952). The pure Coulomb contribution can then be subtracted from both the experimental results and the theoretical formula. The remaining experimental cross section still diverges at small angles due to the Coulomb–nuclear interference term, and in any case experimental difficulties are such that accurate measurements cannot be made in this region. The whole cross section is therefore weighted by a function that tends rapidly to zero in the Coulomb region, and to unity for larger angles. The resulting weighted cross section is everywhere known and finite.

It is convenient to seek first a solution in terms of S and P waves only. The theoretical and experimental cross sections are weighted in turn by

the first three Legendre polynomials and integrated over the angular range. This gives three equations which can be solved for the three phase shifts by an iterative process. The D waves may now be included and five moment equations obtained and solved in a similar way using the previous results for the S and P phase shifts for the first order of

Fig. 9

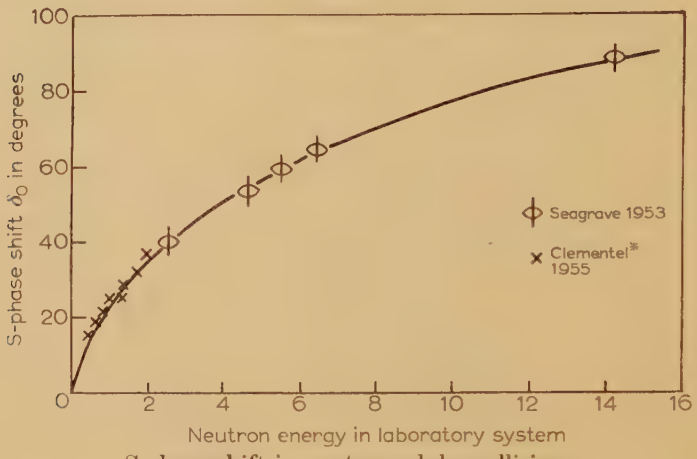

S phase-shift in neutron–alpha collisions.

Fig. 10

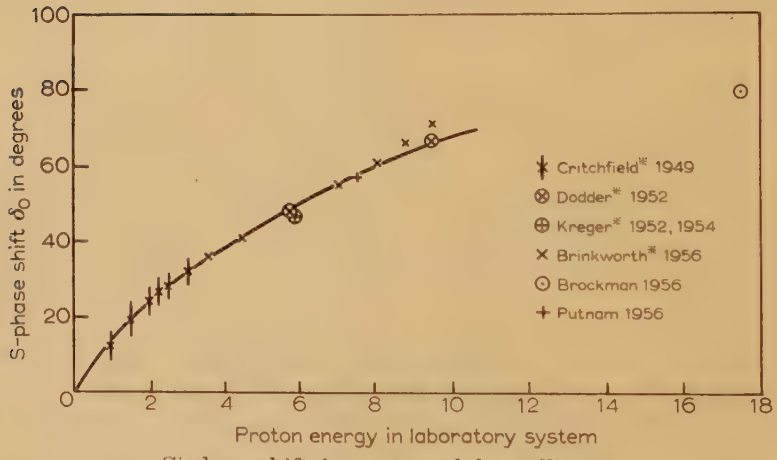

S phase-shift in proton–alpha collisions.

iteration. Lustig and Blatt have performed the integrations of the weighted theoretical formula, and tabulated the coefficients of the resulting expressions.

So far the method of Lustig and Blatt has been applied only to the data of Kreger *et al.* (1954). It would be desirable to apply it also to the data of other experimenters, although not all of these are of sufficient accuracy to justify the inclusion of the D phase shifts.

It is found, in general, that the experimental data do not uniquely determine the phase-shifts ; there are several sets in equally good accord

Fig. 11

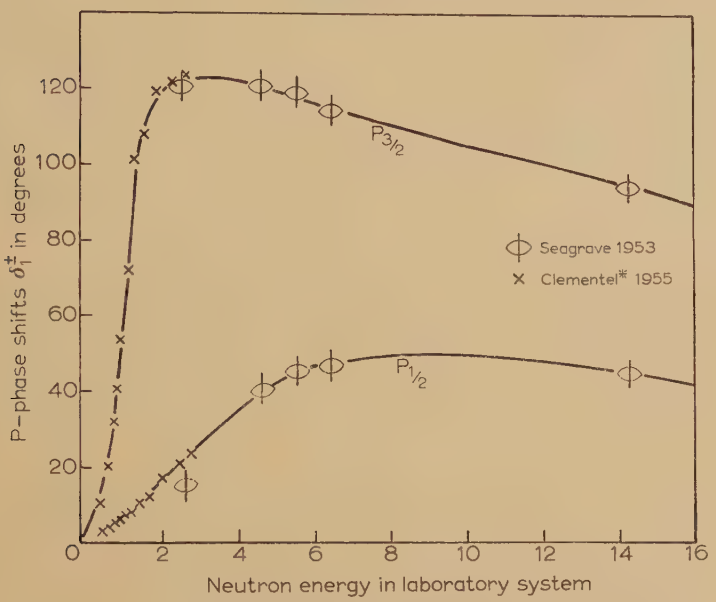

P phase-shift in neutron–alpha collisions.

Fig. 12

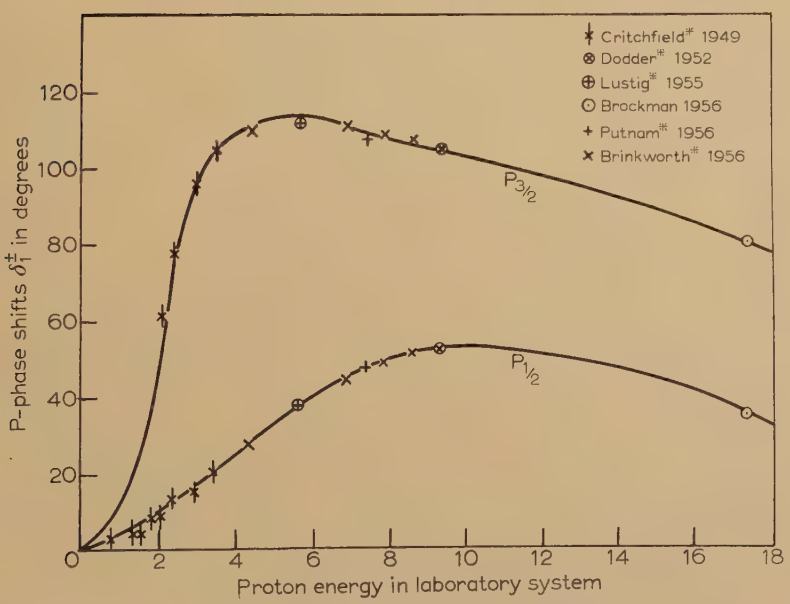

P phase-shift in proton–alpha collisions.

Fig. 13

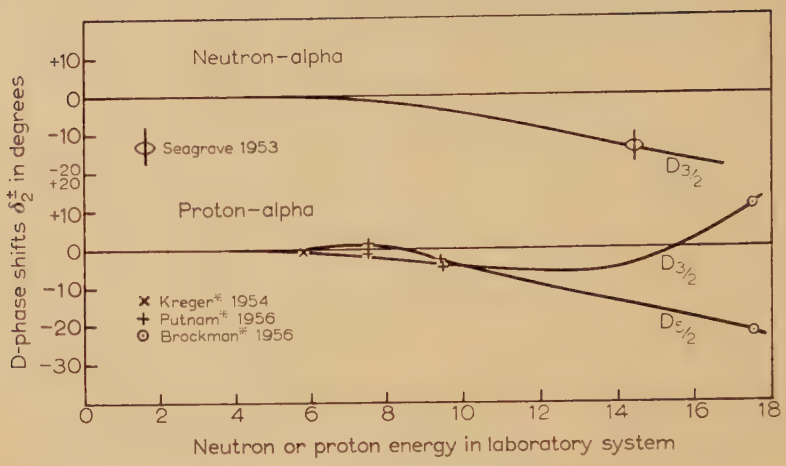

D phase-shifts in neutron–alpha and proton–alpha collisions.

Table 11. Phase-Shift Analyses for Proton–Alpha Collisions

Author	Data	Method	Phases
Critchfield* 1949	Freier* 1949	Iteration	S, P
Kreger* 1952	Kreger* 1952	Iteration	S, P
Dodder* 1952	Putnam/Kreger* 1952	Iteration using IBM computer	S, P, D
Lustig* 1955	Kreger* 1954	Lustig* 1955	S, P, D
Brinkworth*1956	All	Interpolation	S, P
Brockman 1956	Brockman 1956	Iteration+IBM	S, P, D, F
Putnam* 1956 a, b	Putnam*1956a, b	Iteration+IBM	S, P, D

Table 12. The D Phase-Shifts

Author	Energy	$D_{3/2}$	$D_{5/2}$	N—α or P—α	Notes
Putnam 1952	9·48	−8·84	−5·03	P—α	Analysed by Dodder* 1952
Seagrave 1953	14·3	−14±5	—	N—α	
Kreger* 1954	5·78	−1·30	−0·49	P—α	Analysed by Lustig* 1955
Putnam*1956a, b	7·5	−1·87	+0·44	P—α	
Putnam*1956a, b	9·48	−5·73	−3·21	P—α	Revised analysis.
Brockman 1956	17·5	+10·9	−22·2	P—α	

with it. In particular there is no way of determining from the differential cross section whether the P-state doublet is normal or inverted. This ambiguity is exactly analogous to the Fermi–Yang ambiguity for pion–nucleon scattering. It has been resolved in the nucleon–alpha-particle case by a study of the scattering of polarized protons by alpha-particles, and the doublet was found to be inverted (see § 5).

The main characteristics of the phase-shift analyses that have been made are given in tables 10 and 11, and the phase shifts themselves plotted in figs. 9 to 13. The phase shifts corresponding to the normal P-phase doublet are not included. The rather meagre data on the D-phases are given in table 12.

§ 10. Phenomenological Theories

In § 9 it was shown that the differential cross sections for nucleon–alpha collisions as a function of energy could be conveniently described by a series of nuclear phase shifts. In addition the characteristics of the collisions in the region of 1 Mev can be well accounted for by the resonance theory of nuclear interactions. This is simply another way of describing the same data.

When this is done, there still remains the most fundamental problem of accounting for the variation of the phase shifts with energy in terms of the properties of the interacting particles.

The earliest attempt to do this was by Chadwick and Bieler on purely classical lines. They accounted for the observed departures from Rutherford's law by assuming that the alpha-particle becomes flattened as it approaches the proton into the form of an oblate spheroid of semi-axes 8×10^{-13} cm and 4×10^{-13} cm. More elaborate calculations along these lines were made by Darwin (1921) but none of them gave good agreement with the observed differential cross sections, and in any case it became clear that a more thorough-going quantum-mechanical approach was needed.

Taylor (1932 a b,) made a quantum-mechanical calculation taking the Coulomb field but not the proton spin into account, and adjusted a square well nuclear potential to give the best fit to the experimental results.

Primakoff and Goldsmith (1939) tried to correlate some of the early measurements of proton–alpha and neutron–alpha scattering by assuming the nuclear forces to be charge independent. The proton–alpha cross section was obtained by adding the Coulomb force to the phase shifts obtained from the neutron–alpha data using eqn. (18). No detailed results were given.

Another approach makes use of the $0{\cdot}8\pm0{\cdot}3$ Mev by which the binding energy of lithium 5 exceeds that of helium 5. Assuming that the level schemes of these nuclei are otherwise similar, it might be expected that the resonance in proton–alpha scattering would occur at an energy of about 0·8 Mev higher than the 1·05 Mev of neutron–alpha scattering, i.e. at

1·85 MeV. The phase shifts for proton–alpha scattering may therefore be expected to be similar to those for neutron–alpha scattering, but with the $P_{3/2}$ phase shift passing through $\frac{1}{2}\pi$ at 1·85 MeV.

The simplest nuclear model that can be used is the hard sphere, and this may be expected to be quite tolerable outside the resonance regions in view of the exceptional stability of the alpha-particle. If the wave functions are accordingly made to vanish on the nuclear surface, the phase shifts are given by

$$\tan \delta_l = (-1)^{l+1} \frac{j_l(ka)}{j_{-l}(ka)} \quad . \quad . \quad . \quad . \quad . \quad (19)$$

where the j's are spherical Bessel functions.

For $l=0$, this becomes

$$\delta_0 = \pi - ka \text{ radians}$$
$$= 180 - 11{\cdot}3aE_{\text{cm}}^{1/2} \text{ degrees.}$$

The experimental S-phase shifts for neutron–alpha and proton–alpha scattering are plotted in figs. 14 and 15 as a function of $E_{\text{cm}}^{1/2}$. The neutron–alpha results fit the above relation very well for $a \sim 2{\cdot}4 \times 10^{-13}$ cm and the proton–alpha results are in quite good agreement with it if $a \sim 2{\cdot}0 \times 10^{-13}$ cm. The higher hard sphere or potential scattering phase shifts are small compared with the resonance phase shifts over most of the energy region. They are also plotted in figs. 14 and 15.

Dancoff (1940) used second-order perturbation theory with a square well potential and exponential wave function to estimate the effect of the simplest types of spin–orbit force. He found that, on two different models, the Thomas spin–orbit force splits the P-levels to form an inverted doublet, but that the splitting is only of the order of a few kilovolts, which is several orders of magnitude too small. This indicates that the observed splitting cannot be due solely to the relativistic spin–orbit precession.

He also studied the effect of tensor forces, using the closure approximation to evaluate the contributions due to the many intermediate states. This showed that the tensor force splits the P-levels into a normal doublet with a very small separation, except in the case when the interaction potential is singular near the origin, when it can be quite large.

These results need, however, to be treated with some reserve owing to the approximations used to obtain them. It has since been shown experimentally that there is not even a virtual $P_{1/2}$ level as the corresponding phase shift does not pass through 90°; the bound state approximation used by Dancoff is therefore inadequate.

This work was developed by Feingold and Wigner (1952) and Feingold (1956), who calculated the splitting of the P-levels by a variational method that includes the effect of configuration interaction. The variational function had a tensor component, and was treated as a perturbation on a central force oscillator wave function. He calculated

the doublet splitting for Gaussian and Yukawa potentials, and found that the tensor force gives an inverted doublet with a separation that depends quite strongly on the nuclear radius chosen. For a reasonable choice of radius the splitting is of the order of 1 MeV, which is rather

Fig. 14

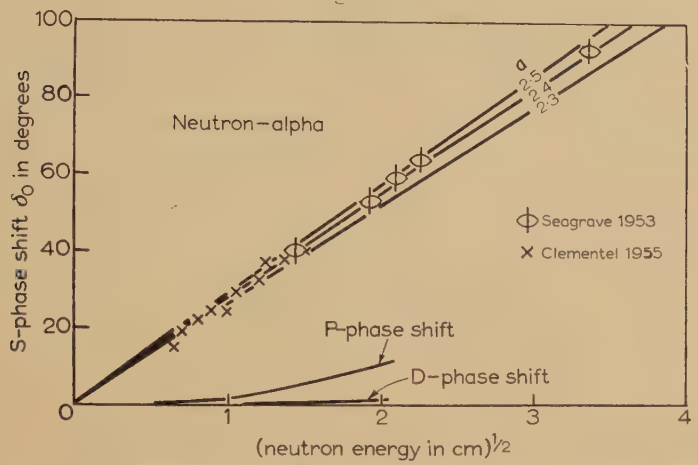

Comparison of S phase-shifts for neutron–alpha collisions with hard sphere formula.

Fig. 15

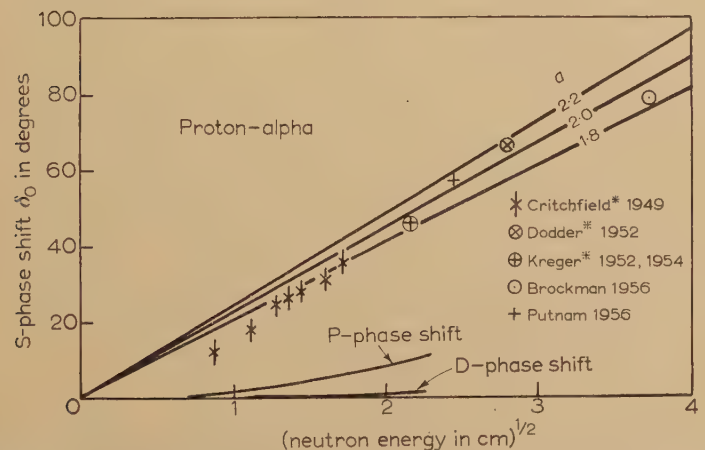

Comparison of S phase-shifts for proton–alpha collisions with hard sphere formula.

smaller than the observed value of about 2·6 MeV, but of the correct order of magnitude. He was unable to account for the discrepancy between this result and Dancoff's by the different potentials and nuclear radii chosen. Nevertheless, for the reasons already given, the results of such a perturbation calculation need to be treated with reserve.

Several calculations have been made by treating the collision as a two-particle one and postulating a central and a spin–orbit force between the neutron and the alpha-particle. The inclusion of such spin–orbit forces in the phenomenological potential was first suggested by Blanchard *et al.* (1951) and it has been shown by Blanchard and Avery (1951) and Adair (1952) that the nucleon–alpha interaction can be reasonably well represented by the model of a single particle moving in the average potential of the closed shell core of the alpha-particle. Further support for the use of spin–orbit forces comes from the work of Mayer (1949, 1950) and of Haxel *et al.* (1949) on the spins and magnetic moments of heavy nuclei, and from that of Koester *et al.* (1951) on the lower excited states of light nuclei (Inglis 1953, Mayer and Jensen 1955).

Hochberg (1953) used a square well potential of the form

$$V=(1+\beta \mathbf{l}\,.\,\boldsymbol{\sigma})V(r) \qquad . \quad . \quad . \quad . \quad . \quad . \quad (20)$$

where

$$V(r)=V_0 \text{ for } r<a$$

$$=0 \quad \text{for } r>a,$$

and found that the S and P phase-shifts obtained agree quite well with those determined experimentally when the depth of the well $V_0=-70{\cdot}9$ Mev, its radius $a=2{\cdot}5\times10^{-13}$ cm, and $\beta=0{\cdot}150$. The differential equation in this case is exactly soluble by the method of Camac and Bethe (1948).

Bürgel (1952) made a similar calculation and found that the best agreement with experiment when $V_0=-33{\cdot}0$ Mev, $a=2{\cdot}55\times10^{-13}$ cm, and $\beta=0{\cdot}103$.

Hochberg also found that the experimental variation of phase shifts with energy is rather steeper at higher energies for $l=0$ and less steep for $l=1$ than the calculated variation, and attributed this to the neglect of velocity dependent forces. These are effectively repulsive and proportional to the incident neutron energy, and this tends to reduce the positive phase shifts at higher energies.

Sack *et al.* (1954) calculated the S and P phase-shifts for proton–alpha scattering using a nucleon–nucleus interaction of the form

$$V=\left[1-\beta \mathbf{l}\,.\,\boldsymbol{\sigma}\,\frac{1}{r}\,\frac{d}{dr}\right]V(r) \qquad . \quad . \quad . \quad . \quad . \quad (21)$$

having a spin–orbit term of the Thomas type. Calculations were made for square, Gauss and exponential wells. These shapes give a regular progression from concentrated potentials with external spin–orbit interaction to long-tail wells with concentrated spin–orbit interaction. They found that the exponential well gave a P-phase splitting increasing too rapidly with energy; the square well a splitting increasing too slowly with energy; and the Gaussian well a satisfactory overall fit. This is

shown in fig. 16. The analytic forms of these potential wells, together with the parameters giving the best agreement with experiment are as follows :

Square well : $V_0 = -19{\cdot}65$ Mev, $a = 3{\cdot}21 \times 10^{-13}$ cm, $\beta = 12{\cdot}2\ (\hbar/Mc)^2$

Gaussian well : $V(r) = V_0 \exp[-(r/a)^2]$

with $V_0 = -47{\cdot}32$ Mev, $a = 2{\cdot}30 \times 10^{-13}$ cm, $\beta = 7{\cdot}4\ (\hbar/Mc)^2$

Exponential well : $V(r) = V_0 \exp[-(r/a)]$

with $V_0 = -155{\cdot}5$ Mev, $a = 0{\cdot}862 \times 10^{-13}$ cm, $\beta = 5\ (\hbar/Mc)^2$. . . . . (22)

Fig. 16

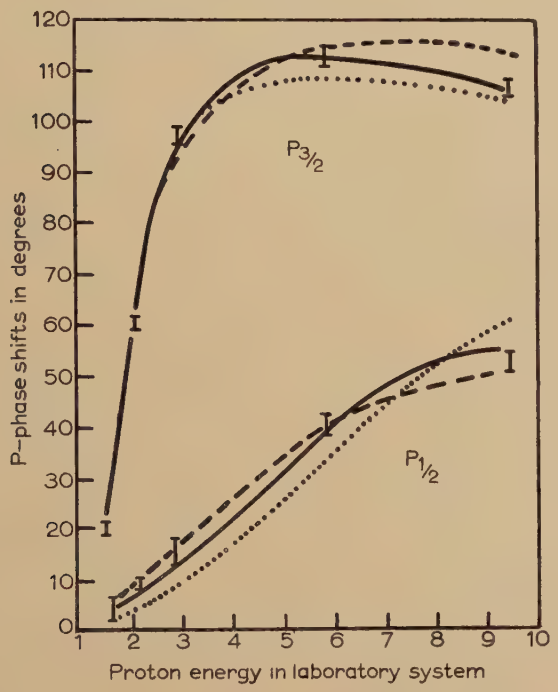

P phase-shifts for proton–alpha scattering calculated by Sack *et al.* The I represent the experimental phase-shifts, and the curves the best fits for the three well shapes : . . . . . square well ; ——— Gaussian well ; – – – – – exponential well.

The spin–orbit parameter required by the theory of the Thomas term is $\beta = \frac{1}{4}(\hbar/Mc)^2$, which is much smaller than any of the values needed to fit the experimental data. This confirms the first conclusion of Dancoff, and indicates that the P-phase splitting is not simply a relativistic correction, but a major effect.

A similar nucleon–nucleus interaction has been used by Levintov, Miller and Shamshev (1957) to interpret the results of Chamberlain *et al.* (1956) on polarization in proton–alpha scattering at 315 Mev. They used the Born approximation to evaluate the polarized cross section, and showed how the form of the polarization curve can give information on the radial variation of the ordinary and spin–orbit parts of the nucleon–nucleus interaction.

The ultimate aim of the theoretical study of nucleon–alpha collisions is to show that all its characteristics can be accounted for by the same nuclear interactions that will account for all other types of collision. This is difficult for two main reasons. In the first place even the nucleon–nucleon interaction is not at all well understood. Some of the proposed analytic forms fit some of the data and others the rest of it. One to fit all the data can be constructed only by incorporating so many adjustable parameters that it becomes questionable whether it bears much relation to reality. The second difficulty is that nucleon–alpha scattering is a five-body problem, and all the interactions between the ten pairs of nucleons must be taken into account. Strictly speaking this problem is insoluble, and so efforts are directed towards finding approximate methods of treatment that render the problem tractable mathematically and yet not too inaccurate physically.

The first attempt along these lines was by Nogami (1942). He assumed that the force between each pair of nucleons is given by

$$v_{ij}=(mM+hH+bB+w)V(r_{ij}) \quad . \quad . \quad . \quad . \quad . \quad (23)$$

where M, H and B are the Majorana, Heisenberg and Bartlett exchange operators, m, h, b and w are numerical parameters such that

$$m+h+w+b=1 \quad \text{and} \quad m+w-(h+b)=x$$

where $x(\sim 0{\cdot}6)$ is the ratio of the ^{1}S to the ^{3}S interaction in the neutron–proton system.

The Schrödinger wave equation for the five-particle system was reduced to a manageable mathematical form by expressing the total wave function Ψ as the antisymmetrized sum of products of the alpha-particle wave function and the scattered nucleon by the method of resonating group structure of Wheeler (1937)

$$\begin{aligned}\Psi=&\alpha(1)\,\chi(\widetilde{23},\,\widetilde{45})\,F(1)\,\phi(-1)+\alpha(2)\,\chi(31,\,\widetilde{45})\,F(2)\,\phi(-2)\\&+\alpha(3)\,\chi(\widetilde{12},\,\widetilde{45})\,F(3)\,\phi(-3) \quad . \quad . \quad . \quad . \quad . \quad . \quad (24)\end{aligned}$$

where $\phi(-1)$ and $F(1)$ are the spatial wave functions of the alpha-particle 2345 and the neutron 1 and χ $(\widetilde{23},\,45)$ and $\alpha(1)$ their respective spin wave functions. Particles 1, 2, and 3 are neutrons, and 4 and 5 protons. This expansion of Ψ is only approximate, since it neglects the deformation of the alpha-particle.

The Gaussian form was chosen for the spatial part of the interaction potential :

$$V(r_{ij}) = V_0 \exp(-\beta r_{ij}^2) \quad . \quad . \quad . \quad . \quad . \quad . \quad (25)$$

and for the wave functions of the alpha-particle clusters

$$\phi(-1) = N \exp\{\alpha \sum_{i>j=2}^{5} r_{ij}^2\} \quad \text{etc.} \quad . \quad . \quad . \quad . \quad (26)$$

The parameters V, α and β were chosen to give the best agreement with the low-energy scattering data and the binding energies of the deuteron and the alpha-particles.

Nogami solved the resulting integro-differential equation for the S-wave by the method of Flügge (1938), after neglecting several of the smaller integrals, and found qualitative agreement with experiment.

This work was repeated by Hochberg, Massey and Underhill (1954), who solved the integro-differential equation exactly taking all the integrals into account. The values they used for the parameters of the wave function and potential are : $\alpha = 0{\cdot}0789 \times 10^{26}$ cm^{-2} ; $\beta = 0{\cdot}2657 \times 10^{26}$cm^{-2}; $V_0 = -45$ Mev.

The variation of S-phase shift with energy for neutron–alpha scattering was calculated for the symmetrical exchange and for the Serber exchange force ; the former gives the better agreement with experiment. The calculations were repeated for proton–alpha scattering, with a similar result. In this case a Coulomb term $(e^2/r_{45})\delta_{45}$ was added to the interaction potential.

Bransden and McKee (1954) have made similar calculations, but they calculated the phase-shifts by the Hulthen–Kohn variational method with a trial function of the form used by Swan (1953) in his calculations on neutron–triton collisions. The results agree with those given above in favouring Majorana–Heisenberg and symmetrical exchange forces rather than the unsaturated ordinary and Serber interactions, although there are considerable numerical differences between the two sets of results, due probably to the different approximations used in obtaining them.

Hochberg *et al.* (1955) extended their calculations to the P-phase shifts by adding to the nucleon interaction a spin–orbit term of the form

$$(SV_0/\hbar^2)(\mathbf{s}_i + \mathbf{s}_j) \cdot \mathbf{r}_{ij} \times (\mathbf{p}_i - \mathbf{p}_j) \exp(-\beta r_{ij}^2). \quad . \quad . \quad . \quad (27)$$

This term does not affect the S-phase but can be made to produce any desired splitting of the P-phases just by altering the magnitude of the parameter S. It was found by exact numerical solution of the wave equation that a value $S = 0{\cdot}1$ gives satisfactory agreement with experiment. This is in good agreement with the strength of the spin–orbit force used in Mayer's shell theory of the nucleus (Hughes and Le Couteur 1950) and by Blin-Stoyle (1955) to account for the level splitting in lead 208.

They found also that the symmetrical exchange force that agrees best with the experimental S-phases gives a mean P-phase that is too small, while the Serber force gives the correct value. A mixture of the two types

of force was therefore chosen that gave the best fit to both the S-phase and the mean P-phase. It is the near-Serber force, composed of nine-tenths Serber force and one-tenth symmetrical exchange force, and has the following constants :

$$m=0{\cdot}2583+0{\cdot}3250x\ ; \quad h=0{\cdot}2583-0{\cdot}3250x\ ;$$
$$w=0{\cdot}2417+0{\cdot}1750x\ ; \quad b=0{\cdot}2417-0{\cdot}1750x. \qquad (28)$$

An essentially similar calculation was made by Van der Spuy (1956), but instead of solving the wave equation exactly he derived approximate relations between the phase parameters and the interaction parameters, and used them to solve the problem for square and Gaussian potential wells.

Although it is possible to account satisfactorily for the S and P wave scattering by assuming the nuclear interaction to be composed of central and spin–orbit parts, there is still the effect of the tensor force to be investigated. Neither the central force nor the spin–orbit force can account for the observed quadrupole moment of the deuteron ; the tensor force can, and accordingly the presence of a tensor component in the nuclear interaction must be recognized. Since the tensor force can also split the P levels in nucleon–alpha scattering it is important to find out whether the whole of this splitting can be ascribed to the tensor force and, if not, the relative contributions to it of the tensor and spin–orbit forces respectively.

The early calculations of Dancoff (1940) indicated that the tensor forces produced a splitting of the wrong sign and negligible magnitude. Similar but more elaborate work of Feingold (1956) showed that the tensor splitting could be of the correct sign and have the order-of-magnitude observed experimentally.

In view of the uncertainty of these conclusions a more detailed attempt to evaluate the tensor force splitting was made by Sugie, *et al.* (1957). They assumed that the nuclear interaction was given by the near-Serber central component used by Hochberg *et al.* with the addition of a tensor component

$$V_{ij}{}^{T}=(mM+w)\,S_{ij}\,V(r_{ij}) \qquad (29)$$

where S_{ij} is the tensor operator

$$S_{ij}=\{3\,(\boldsymbol{\sigma}_i\,.\,\mathbf{r}_{ij})(\boldsymbol{\sigma}_i\,.\,\mathbf{r}_{ij})-r_{ij}{}^{2}\,(\boldsymbol{\sigma}_i\,.\,\boldsymbol{\sigma}_j)\}/r_{ij}{}^{2} \qquad (30)$$

in which σ_i and σ_j are Pauli spin operators. There are only two exchange components because the tensor force contributes only to the triplet state of the nucleon pair.

The tensor force mixes a small amount of D state with the predominantly S ground state of the alpha-particle. Only the most important D-state was taken into account, namely the symmetric one of the form

$$\{3(\boldsymbol{\sigma}_2\,.\,\mathbf{r}_{23})(\boldsymbol{\sigma}_4\,.\,\mathbf{r}_{45})+3(\boldsymbol{\sigma}_2\,.\,\mathbf{r}_{45})(\boldsymbol{\sigma}_4\,.\,\mathbf{r}_{23})-2\,(\mathbf{r}_{23}\,.\,\mathbf{r}_{45})(\boldsymbol{\sigma}_2\,.\,\boldsymbol{\sigma}_4)\}\chi. \qquad (31)$$

The alpha-particle radial wave function and the radial part of the interaction potential were chosen to be of Gaussian form to facilitate

the mathematical work. The parameters were adjusted to give the best fit to the low-energy scattering data, the binding energies of the deuteron and alpha-particle, and the quadrupole moment of the deuteron. The values chosen were : $\alpha=0{\cdot}0975\times10^{-26}$ cm^{-2} ; $\beta=0{\cdot}443\times10^{-26}$ cm^{-2} ; $\beta_T=0{\cdot}290\times10^{-26}$ cm^{-2} ; $V_0=-44{\cdot}3$ Mev ; $V_0{}^T=30{\cdot}7$ Mev.

The Schrödinger wave equation was simplified by using the resonating group expansion of the total wave function, and solved numerically with an electronic computer. It was found that the P-phase splitting due to the tensor force is of the correct sign and of magnitude about 30% of that observed experimentally. This figure is subject to considerable uncertainty because of the neglect of the other five D states of the alpha-particle, and the approximations inherent in the use of Gaussian wave functions and potentials and in the method of solution of the wave equation, but it does indicate that the tensor forces make a substantial contribution to the splitting of the P-phases.

Few calculations have been made at higher energies, and these have applied approximate methods to find the cross sections directly, instead of making a phase-shift analysis. Thus Heidmann (1950) has used the Born approximation with a nuclear interaction of the Serber type and Gaussian wave functions and potentials to calculate the differential cross sections for elastic neutron–alpha scattering and the corresponding $n(\alpha, t)d$ and stripping reactions for incident alpha-particles of 90 Mev. Considering the approximations used, his results are in excellent agreement with the experimental work of Tannenwald (1952, 1953).

This work has been extended by Squires (private communication), who calculated the differential cross section for neutron–alpha scattering using the Born approximation with symmetrical exchange or Serber interactions and Gaussian or Yukawa potentials and Gaussian wave functions. On comparing his results with those of Tannenwald he found that the Gaussian and Yukawa potentials were equally good, but that, with the assumption of an undeformed alpha-particle, only the Serber interaction was in accord with experiment.

Squires went on to estimate the effect of the deformation of the alpha-particle by the incident neutron, using both the impulse approximation (Chew and Goldberger 1952) and the static potential approximation. Although there are many uncertainties in the calculation, the deformation is found to be considerable ; it is greater if the radial dependence of the potential is Gaussian than if it is of the Yukawa form, and increases with decreasing energy and with the amount of tensor force in the nuclear interaction. This indicates that it is likely to be important at lower energies, where it has often been neglected.

Acknowledgments

I am greatly indebted to Dr. A. Herzenberg, M. J. Brinkworth and E. J. Squires for valuable discussions and suggestions, and to Professor H. S. W. Massey, F.R.S., in whose Department this work was begun.

References

Adair, R. K., *Phys. Rev.*, 1951, **82,** 750 ; 1952, **86,** 155.

Ajzenberg, F., and Lauritson, T., *Rev. mod. Phys.*, 1952, **24,** 321 ; 1955. **27,** 77.

Allred, J. C., 1950, *Phys. Rev.*, **77,** 753.

Alston, M. H., Crewe, A. V., Evans, W. H., Green, L. L., and Willmott, J. C., 1954, *Proc. phys. Soc. Lond. A*, **67,** 657.

Argo, H. V., Gittings, H. T., Hemmendinger, A., Jarvis, G. A., and Taschek, R. F., 1950. *Phys. Rev.*, **78,** 691.

Ashkin, J., and Vosko, S. H., 1953, *Phys. Rev.*, **91,** 1248.

Atkins, A. L., 1952 *Thesis*, Illinois (quoted Kreger, Jentschke and Kruger, 1954).

Baldinger, E., Huber, P., and Staub, H., 1938, *Helv. phys. acta*, **11,** 245.

Baldinger, E., 1952, *Helv. phys. acta*, **25,** 446.

Barschall., H. H., and Kanner, M. H., 1940, *Phys. Rev.*, **58,** 590.

Bashkin, S., Mooring, F. P., and Petree, B., 1951, *Phys. Rev.*, **82,** 378.

Bashkin, S., Petree, B., Mooring, F. P., and Peterson, R. E., 1950, *Phys. Rev.*, **77,** 748.

Benveniste, J., and Cork, B., 1951, *Phys. Rev.*, **83,** 894 ; 1953, *Ibid.*, **89,** 422.

Bethe, H. A., and Bacher, R. F., 1936, *Rev. mod. Phys.*, **8,** 147.

Blanchard, C. H., and Avery, R., 1950, *Phys. Rev.*, **81,** 35.

Blanchard, C. H., Avery, R., and Sachs, R. G., 1951, *Phys. Rev.*, **78,** 292.

Blatt, J. F., and Weisskopf., V. F., 1952; *Theoretical Nuclear Physics* (New York : J. Wiley and Sons) p. 330.

Blatt, J. M., and Biedenharn, L. C., 1952, *Rev. mod. Phys.*, **24,** 258.

Blin-Stoyle, R. J., 1955, *Phil. Mag.*, **46,** 973.

Bloch, F., 1940, *Phys. Rev.*, **58,** 829.

Bloch, I., Hull, M. H., Broyles, A. A., Bouricius, W. G., Freeman, B. E., and Breit, G., 1951, *Rev. mod. Phys.*, **23,** 147.

Bonner, T. W., and Hudspeth, E., 1940, *Phys. Rev.*, **57,** 1187.

Braden, C. H., 1951, *Phys. Rev.*, **84,** 762.

Bradner, H., and Isbell, W., 1957, *Phys. Rev.*, **108,** 463.

Bransden, B. H., and McKee, J. S. C., 1954, *Phil. Mag.*, **45,** 869.

Brinkworth, M. J., and Rose, B., 1956, *Nuovo Cim.*, **3,** 195.

Brockman, K. W., 1956, *Phys. Rev.*, **102,** 391.

Brussel, M. K., and Williams, J. H., 1957, *Phys. Rev.*, **106,** 286.

Burcham, W. E., 1957, *Handb. Physik.*, **40,** 65.

Bürgel, B. (quoted in 1952, *Helv. phys. acta*, **25,** 439).

Butler, S. T., 1951, *Proc. roy. Soc. Lond.* A, **208,** 559.

Camac, M., and Bethe, H. A., 1948, *Phys. Rev.*, **73,** 191.

Carroll, H., 1941, *Phys. Rev.*, **60,** 702.

Carroll, H., and Dunning, J. R., 1938, *Phys. Rev.*, **54,** 541.

Chadwick, J., and Bieler, E. S., 1921, *Phil. Mag.*, **42,** 923.

Chamberlain, O., Segrè, E., Tripp, R., Wiegand, C., and Ypsilantis, T., 1954, *Phys. Rev.*, **96,** 807 ; 1956, *Ibid.*, **102,** 1659.

Chew, G. F., and Goldberger, M. L., 1950, *Phys. Rev.*, **77,** 470 ; 1952, *Ibid.*, **87,** 778.

Clementel, E., and Villi, C., 1955, *Nuovo Cim.*, **2,** 1121.

Cook, L. J., McMillan, E. M., Peterson, J. M., and Sewell, D. C., 1949, *Phys. Rev.*, **75,** 7.

Coon, J. H., 1953 (quoted Seagrave).

Coon, J. H., Graves, E. R., and Barschall, H. H., 1952, *Phys. Rev.*, **88,** 562.

Coon, J. H., and Henkel, R. J., 1952 (quoted Ajzenberg and Lauritson 1952).

Cork, B., 1951, *Phys. Rev.*, **83,** 893 ; 1953, *Ibid.*, **89,** 78.

Cork, B., and Hartsough, W., 1954, *Phys. Rev.*, **96,** 859, 1267.

Crane, H. R., Delsasso, L. A., Fowler, W. A., and Lauritsen, C. C., 1935, *Phys. Rev.*, **48,** 125.
Critchfield, C. L., and Dodder, D. C., 1949, *Phys. Rev.*, **76,** 602.
Dancoff, S. M., 1939, *Phys. Rev.*, **56,** 384 ; 1940, *Ibid.*, **58,** 326.
Darwin, C. G., 1921, *Phil. Mag.*, **41,** 486.
Day, R. B., and Henkel, R. L., 1953, *Phys. Rev.*, **92,** 358.
Dodder, D. C., 1949, *Phys. Rev.*, **76,** 683.
Dodder, D. C., and Gammel, J. L., 1952, *Phys. Rev.*, **88,** 520. (See footnote 30 in Seagrave 1953.)
Eisberg, R. M., 1956 a, *Phys. Rev.*, **102,** 1104 ; 1956 b, *Bull. Amer. phys. Soc.*, **1,** 19.
Faxen, H., and Holtsmark, J., 1927, *Z. Phys.*, **45,** 307.
Feenberg, E., 1936, *Phys. Rev.*, **49,** 328.
Feingold, A. M., 1956, *Phys. Rev.*, **101,** 258.
Feingold, A. M., and Wigner, E. P., 1952 (quoted Adair 1952).
Fermi, E., 1954, *Nuovo Cim.*, **11,** 407.
Flügge, S., 1938, *Z. Phys.*, **108,** 545.
Ford, F. C., 1953, *U.C.R.L.* 2148.
Frank, E., 1934, *Z. Phys.*, **90,** 764.
Freemantle, R. G., Grotdal, T., Gibson, W. M., McKeague, R., Prowse, D. J., and Rotblat, J., 1954, *Phil. Mag.*, **45,** 1090.
Freier, G., Lampi, E., Sleator, W., and Williams, J. H., 1949, *Phys. Rev.*, **75,** 1345.
Gaerttner, E. R., Pardue, L. A., and Streib, J. F., 1939, *Phys. Rev.*, **56,** 856.
Goldstein, H., 1950, *Phys. Rev.*, **79,** 740.
Hall, T. A., and Koontz, P. G., 1947, *Phys. Rev.*, **72,** 196.
Harris, S. P., 1950, *Phys. Rev.*, **80,** 20.
Hatton, J., and Preston, G., 1949, *Nature, Lond.*, **164,** 143.
Haxel, O., Jensen, J. H. D., and Suess, H. E., 1949, *Phys. Rev.*, **75,** 1766.
Heidmann, J., 1950, *Phil. Mag.*, **41,** 444.
Heitler, H., May, A. N., and Powell, C. F., 1947, *Proc. roy. Soc.* A, **190,** 180.
Henkel, R. L., and Perry, J. E., 1955 (quoted Ajzenberg and Lauritson, 1955)
Heusinkveld, M., and Freier, G., 1952, *Phys. Rev.*, **85,** 80.
Heydenburg, N. P., and Ramsey, N. F., 1941, *Phys. Rev.*, **60,** 42.
Heydenburg, N. P., and Roberts, R. B., 1939, *Phys. Rev.*, **56,** 1092.
Hibdon, C. T., and Muelhause, C. O., 1951, *Argonne National Laboratory Report* 4680.
Hillman, P., Stahl, R. H., and Ramsey, N. F., 1954, *Phys. Rev.*, **96,** 115.
Hochberg, S., 1953, *Thesis*, London (unpublished).
Hochberg, S., Massey, H. S. W., Robertson, H., and Underhill, L. H., 1955, *Proc. phys. Soc. Lond.* A, **68,** 746.
Hochberg, S., Massey, H. S. W., and Underhill, L. H., 1954, *Proc. phys. Soc. Lond.* A, **67,** 957.
Huber, P., and Baldinger, E., 1952, *Helv. phys. acta*, **25,** 435.
Hudspeth, E., and Dunlop, H., 1940, *Phys. Rev.*, **57,** 971.
Hughes, D. J., and Carter, R. S., 1956, *Neutron Cross Sections* (Brookhaven National Laboratory), p. 8.
Hughes, D. J., and Harvey, J. A., 1955, *Neutron Cross Sections* (New York : McGraw-Hill).
Hughes, J., and Le Couteur, K. J., 1950, *Proc. phys. Soc. Lond.* A, **63,** 1219.
Inglis, D. R., 1953, *Rev. mod. Phys.*, **25,** 390.
Johnston, R., 1957 (see Bradner and Isbell 1957).
Juveland, A. C., and Jentschke, W. K., 1956, *Z. Phys.*, **144,** 521.
Koester, L. J., Jackson, H. L., and Adair, R. K., 1951, *Phys. Rev.*, **83,** 1250.
Kreger, W. E., Jentschke, W. K., and Kruger, R. G., 1954, *Phys. Rev.*, **93,** 837.

Kreger, W. E., Kerman, R. O., and Jentschke, W. K., 1952, *Phys. Rev.*, **86**, 593.
Landau, L., and Smorodinsky, J., 1944, *J. Phys., Moscow*, **8**, 154.
Lasinio, G. Jona, and Monetti, G. C., 1957, *Nuovo Cim.*, **6**, 987.
Laubenstein, R. A., and Laubenstein, M. J. W., 1951, *Phys. Rev.*, **84**, 18.
Lauritsen, C. C., and Crane, H. R., 1934, *Phys. Rev.*, **46**, 537.
Leland, W. T., and Agnew, H. M., 1951, *Phys. Rev.*, **82**, 559.
Lepore, J. V., 1950, *Phys. Rev.*, **79**, 137.
Levintov, I. I., 1955, *Dokl. Acad. Sci. U.S.S.R.*, **103**, 803.
Levintov, I. I., Miller, A. V., and Shamshev, U. N., 1957, *Nuclear Phys.*, **3**, 221.
Levintov, I. I., Miller, A. V., Shamshev, V. N., and Tarumov, E. Z., 1956, *Physica*, **22**, 1181.
Lustig, H., and Blatt, J. M., 1953, *Phys. Rev.*, **91**, 453 ; 1955, *Ibid.*, **100**, 777.
Marsden, E., 1914, *Phil. Mag.*, **27**, 824.
Marshall, L., and Marhsall, J., 1955, *Phys. Rev.*, **98**, 1398.
Mayer, M. G., 1949, *Phys. Rev.*, **75**, 1969 ; 1950, *Ibid.*, **78**, 16.
Mayer, M. G., and Jensen, J. H. D., 1955, *Elementary Theory of Nuclear Shell Structure* (New York : Wiley and Sons).
Miller, P. D., Phillips, G. C., Henry, R. R., and Erdwin, J., 1957, *Bull. Amer. phys. Soc.*, **2**, 104.
Mohr, C. B. O., and Pringle, G. E., 1937, *Proc. roy. Soc.* A, **160**, 190.
Mott, N. F., 1932, *Proc. roy. Soc.* A, **135**, 429.
Mott, N. F., and Massey, H. S. W., 1949, *The Theory of Atomic Collisions*, 2nd ed. (Oxford : Clarendon Press), p. 48.
Moulthrop, P. H., 1955, *Phys. Rev.*, **99**, 1509.
Nogami, M., 1942, *Proc. phys.-math. Soc. Japan*, **24**, 26 ; 1946, *J. phys. Soc. Japan*, **1**, 11.
Pollard, E., and Margenau, H., 1935 a, *Phys. Rev.*, **47**, 833 ; 1935 b, *Ibid.*, **48**, 402.
Pose, H., and Diebner, K., 1934, *Z. Phys.*, **90**, 773.
Primakoff, H., and Goldsmith, H. H., 1939, *Phys. Rev.*, **55**, 1117.
Putnam, T. M., 1952, *Phys. Rev.*, **87**, 932.
Putnam, T. M., Brolley, J. E., and Rosen, L., 1956 a, *Bull. Amer. phys. Soc.*, **1**, 9 ; 1956 b, *Phys. Rev.*, **104**, 1303.
Robertson, H. H., 1956, *Proc. Camb. phil. Soc.*, **52**, 538.
Rosen, L., and Brolley, J. E., 1957, *Phys. Rev.*, **107**, 1454.
Ruhla, C., 1954, *J. Phys. Radium*, **15**, 451.
Rutherford, E., 1911, *Phil. Mag.*, **21**, 669 ; 1919, *Ibid.*, **37**, 537.
Sack, S., Biedenharn, L. C., and Breit, G., 1954, *Phys. Rev.*, **93**, 321.
Schwinger, J., 1940, *Phys. Rev.*, **58**, 1004 ; 1946, *Ibid.*, **69**, 681.
Scott, M. J. 1957, *Bull. Amer. phys. Soc.*, **2**, 349.
Scott, M. J., and Segel, R. E., 1955, *Phys. Rev.*, **100**, 1244.
Seagrave, J. D., 1953, *Phys. Rev.*, **92**, 1222.
Shaw, D. F., 1955, *Proc. phys. Soc. Lond.* A, **68**, 43.
Simon, A., and Welton, T. A., 1953, *Phys. Rev.*, **90**, 1036 ; 1954, *Ibid.*, **93**, 1435.
Smith, J. R., 1954, *Phys. Rev.*, **95**, 730.
Squires, E. J., 1957 (private communication).
Staub, H., and Stephens, W. E., 1939, *Phys. Rev.*, **55**, 131.
Staub, H., and Tatel, H., 1940 a, *Phys. Rev.*, **57**, 936 ; 1940 b, *Ibid.*, **58**, 820.
Striebel, H. R., and Huber, P., 1957, *Helv. phys. acta.*, **30**, 67.
Sugie, A., Hodgson, P. E., and Robertson, H. H., 1957, *Proc. phys. Soc. Lond.* A, **70**, 1.
Swan, P., 1953, *Proc. phys. Soc. Lond.* A, **66**, 238, 740.

Swartz, C., 1952, *Phys. Rev.*, **85,** 73.
Tamor, S., 1954, *Phys. Rev.*, **94,** 1087 ; 1955, *Ibid.*, **97,** 1077.
Tamura, T., 1954, *Progr. theor. Phys., Japan*, **11,** 335.
Tannenwald, P. E., 1952, *Phys. Rev.*, **87,** 205 ; 1953, *Ibid.*, **89,** 508.
Taschek, R. F., Argo, H. V. Hemmendinger, A., and Jarvis, G. A., 1949, *Phys. Rev.*, **76,** 325.
Taylor, H. M., 1932 a, *Proc. roy. Soc.* A, **136,** 605 ; 1932 b, *Nature, Lond.*, **129,** 56.
Teem, J. M., Selove, W., and Kruse, U. E., 1955, *Phys. Rev.*, **98,** 259.
Titterton, W. E., and Brinkley, T. A., 1951, *Proc. phys. Soc. Lond.* A, **64,** 212.
Tracy, J., and Powell, W. M., 1950, *Phys. Rev.*, **77,** 594.
Tsein San-Tsiang, 1940 a, *Thesis*, A 2797, Paris ; 1940 b, *J. phys. Radium*, **1,** 1.
Tyren, H., Tibell, G., and Maris, Th. A., 1957, *Nuclear Phys.*, **4,** 277.
Vanecian, R. A., and Fedchenco, E. D., 1956, *Physica*, **22,** 1124.
Van der Spuy, E., 1956, *Nuclear Phys.*, **1,** 381.
Volland, W., 1937, *Z. Phys.*, **105,** 104.
Werner, F., 1954, *Master's Thesis*, Pennsylvania (quoted Feingold 1956).
Wheeler, J. A., 1937, *Phys. Rev.*, **52,** 1107.
Wheeler, J. A., and Barschall, H. H., 1940, *Phys. Rev.*, **58,** 682.
White, R. E., and Farley, F. J. M., 1957, *Nuclear Phys.*, **3,** 476.
Wickersham, A. F., 1954, *U.C.R.L.* 2662 ; 1957, *Phys. Rev.*, **107,** 1050.
Wigner, E. P., and Eisenbud, L., 1947, *Phys. Rev.*, **72,** 29.
Williams, J. H., and Rasmussen, S. W., 1955, *Phys. Rev.*, **98,** 56.
Williams, J. H., Shepherd, W. G., and Haxby, R. O., 1937, *Phys. Rev.*, **52,** 390.

Spin-disorder Effects in the Electrical Resistivities of Metals and Alloys

By B. R. Coles
Department of Physics, Imperial College, London, S.W.7

Contents

§ 1. Introduction.

§ 2. Resistivity Anomalies and Magnetic Ordering in Rare Earth Metals.
2.1. Gadolinium.
2.2. Dysprosium and Erbium.
2.3. Quantitative comparisons.

§ 3. Atomic and Magnetic Ordering in Transition Metal Alloys.
3.1. Au_3Mn, AuMn, and Au_2Mn.
3.2. Ni_3Mn and Ni_3Cr.

§ 4. The Transition Metals.
4.1. Manganese.
4.2. Palladium and nickel.
4.3. Iron.
4.4. Other metals.
4.4.1. Second and third transition group metals.
4.4.2. Titanium.
4.4.3. Chromium.

§ 5. Dilute Alloys
5.1. Solid solutions in ferro- and antiferromagnetic metals.
5.2. Dilute alloys of transition metals in noble metals.

§ 1. Introduction

It has long been recognized that exchange interaction effects between conduction electrons and unpaired electrons localized on particular atoms might have important consequences for many properties of metals and alloys. It has recently been pointed out (Kasuya 1956 a, Yosida 1958, Friedel and de Gennes 1958, Elliott and Roycroft, to be published) that, if an interaction of this type is sufficiently large, the disordered exchange field in a lattice the atoms of which possess localized but randomly orientated spins would scatter conduction electrons moving through it, and give rise to an appreciable term in the electrical resistance. This term may conveniently be described as the spin-disorder resistivity, and upon ordering of the atomic spins (in either a ferromagnetic or antiferromagnetic manner) it should decrease markedly. Conspicuous anomalies in electrical resistivity at temperatures of magnetic ordering

should therefore be shown by materials possessing localized spins. On the other hand, it has been shown by Mott (1936) that a very satisfactory account of the resistivity anomaly at the Curie point of nickel can be given in terms of a collective band model of the electrons which provide the spontaneous magnetization. This model is based on the assumption that the current is carried mainly by electrons in one band (the s-band), but that the mean free path is determined by transitions to another band (the d-band) which contains the magnetic carriers. The two models have been discussed by Mott and Stevens (1957) ; spin disorder scattering should occur to a greater or less extent in all ferro- or antiferromagnetic materials ; s–d transitions only in certain metals in which the magnetic electrons can be described as partly occupying a band. This is the case in nickel and cobalt but not in iron or the rare earths.

It can easily be seen, moreover, that the two models predict resistivity behaviours differing in their detailed characters. In a material possessing localized spins, the excess (spin-disorder) resistivity should be temperature-independent above the Curie or Néel temperature. Matthiessen's Rule might therefore be extended to allow the resistivity to be expressed as the sum of three terms—the lattice (or ideal) resistivity, the impurity resistivity, and the spin-disorder resistivity. (Such an extension will only be valid for a spatially ordered array of localized spins. In an alloy which is a disordered solid solution possessing localized moments a spin-disorder term will exist well below the magnetic ordering temperature ; the spins will be aligned, but they will be distributed at random over some fraction of the lattice points. Such materials are considered in § 5.) On the collective band model a separation of resistivity terms is not possible, for the states to which the conduction electrons make transitions in resistivity-producing processes differ above and below the Curie temperature. It should thus be possible, in principle, to gain valuable information from resistivity measurements about the types of wave-function appropriately to be used to describe the magnetically active electrons in particular materials. Examples of the suggested use of resistance data in this way have been given by Mott and Stevens (1957) and are discussed in § 4.3.

Even on the localized spin model the states to and from which the conduction electrons make transitions may depend on the degree of magnetic order. With such a model the exchange interaction between the conduction and localized electrons produces, in aligning the spins of the latter, a polarization of the former (Pratt 1957), with the consequent use of states in the conduction band above the Fermi surface of the unpolarized configuration. The extent of this polarization, and therefore its effects on conduction electron transition probabilities, are not yet known. Furthermore the exchange field of, say, a monatomic body-centred cubic lattice will have a periodicity for antiferromagnetic ordering different from that for ferromagnetic ordering, and the spectrum of allowed conduction band states will be correspondingly affected (see

Slater 1951 a). Fortunately the good results obtained by a naïve application of the concept of spin-disorder scattering to resistivity data suggest that these complications can often be ignored.

The objects of this review are to bring together some of the more significant experimental results that receive a natural explanation in terms of spin-disorder scattering ; to present briefly some of the situations where the collective model is highly successful ; and to discuss the light shed by electrical measurements on the electronic structures of the transition metals and their alloys.

§ 2. Resistivity Anomalies and Magnetic Ordering in Rare Earth Metals

The most straightforward examples of magnetic behaviour associated with localized electrons in metals are provided by the rare earth metals, where the 4f electron shell is incomplete. The susceptibilities of these elements at high temperatures are well described by expressions of the Curie–Weiss type, and at lower temperatures magnetic properties and specific heat measurements show magnetic ordering effects, of both ferro- and antiferromagnetic character, to be taking place. The experimental data have been reviewed by Spedding *et al.* (1957). From the slopes of the inverse susceptibility versus temperature plots effective moments may be derived, and for all the elements with at least half-filled 4f shells those for the metals are in good agreement with those calculated for the free trivalent ions.

2.1. *Gadolinium*

The behaviour of gadolinium is particularly simple. This metal is paramagnetic above 290°K and ferromagnetic below that temperature. The low temperature saturation intensity of magnetization (Elliott *et al.* 1953) and the temperature dependence of the high temperature susceptibility (Trombe 1937) indicate that $S=J=7/2$, and this value is in excellent agreement with that derived by Hofmann *et al.* (1956) from the magnetic entropy indicated by the specific heat data of Elliott *et al.* (1954). The temperature dependence of the electrical resistivity (Legvold *et al.* 1953) is shown in fig. 1, and it can be seen that this shows a behaviour conforming closely to that expected from a simple model of spin-disorder scattering. Above the Curie temperature the resistivity can be separated into a temperature-independent term of about 120 microhm cm and a term linear in the temperature, the coefficient of T being about 0·08 microhm cm per degree. The saturation magnetic moment follows the $T^{3/2}$ law closely ; and, in contrast to the resistivity behaviour associated with ordering (by the formation of a superlattice) of the *electrical* potential in an alloy, it is not possible to examine the variation with temperature of the resistivity of gadolinium for a given high degree of order in the exchange field. One cannot therefore compare the high-temperature and

low-temperature temperature dependences in the hope of bringing to light any change in the configuration of the conduction electron band. The resistivity is, in fact, almost linear between about 35°K and the

Fig. 1

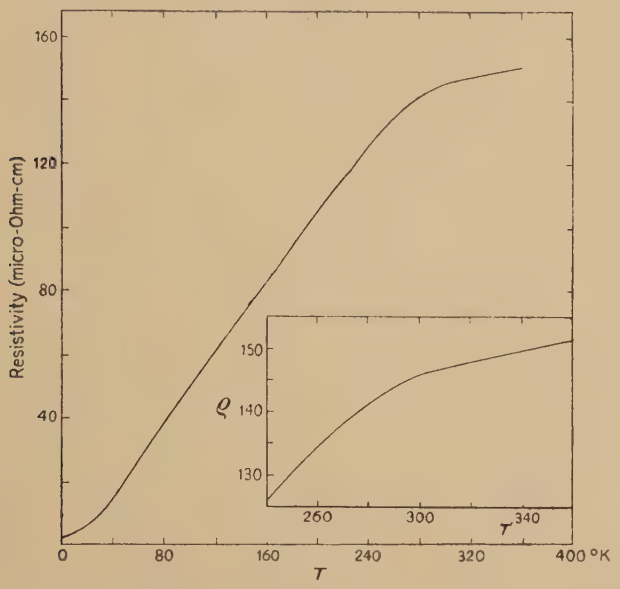

The electrical resistivity of gadolinium (microhm cm).

Curie temperature. Gadolinium has been used as an example in the theoretical treatments of spin-disorder scattering given by Kasuya (1956 a) and Friedel and de Gennes (1958).

2.2. *Dysprosium and Erbium*

Dysprosium, holmium, and erbium have paramagnetic susceptibilities of the Curie–Weiss type at high temperatures, and on cooling show the behaviour typical of antiferromagnetic materials ; the Néel temperatures are approximately 175°, 132°, and 84°K, respectively (Spedding *et al.* 1957). At still lower temperatures, however, ferromagnetic behaviour is shown by all three (below about 85°, 19·4°, and 19·9°K respectively), and for each metal two well-marked maxima are found in the specific heat curves (Griffel *et al.* 1956, Gerstein *et al.* 1957, Skochdopole *et al.* 1955).

Electrical resistivity data are available (Legvold *et al.* 1953) for dysprosium (fig. 2) and erbium (fig. 4). For both metals a marked change in slope of the resistivity–temperature curve takes place slightly below the Néel temperature, but little further change takes place during the transition to ferromagnetism. This is in agreement with the predictions of a simple model of spin-disorder scattering, in which the *character* of the magnetic ordering is unimportant. It is interesting to compare

the resistivity curve for dysprosium (fig. 2) with fig. 3, which shows the magnetic entropy curve (Griffel *et al.* 1956). For dysprosium and erbium

Fig. 2

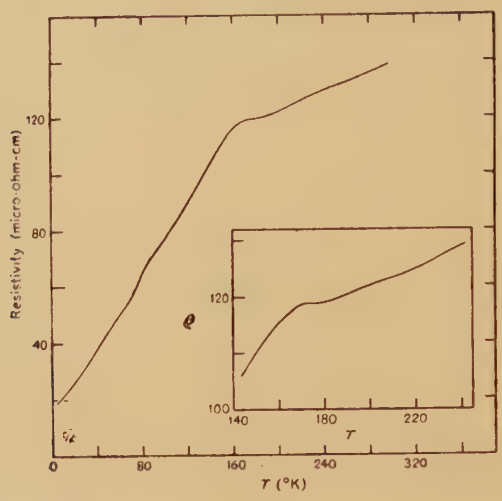

The electrical resistivity of dysprosium (microhm cm).

Fig. 3

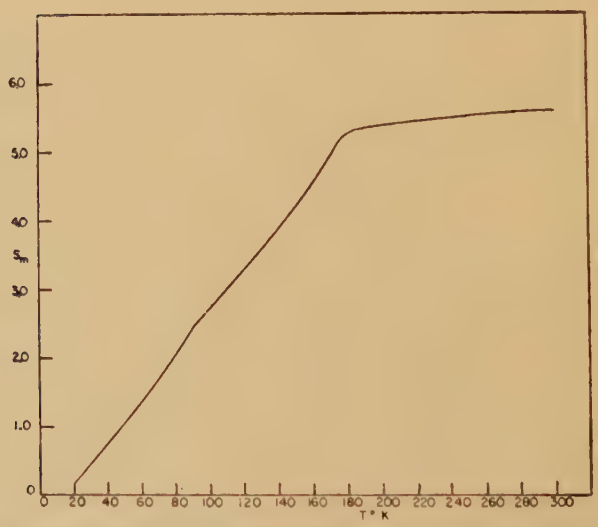

The magnetic entropy of dysprosium (cal. per g atom per degree).

it is less easy than for gadolinium to separate the temperature-independent and temperature-dependent terms in the resistivity, but approximate values for the former term are 75 microhm cm for dysprosium ($S=5/2$, $J=15/2$) and 42 microhm cm for erbium ($S=3/2$, $J=15/2$).

It is significant that immediately below the Néel temperature the resistivities of both dysprosium and erbium fall less rapidly. It will be seen later (§ 4.1) that α-manganese shows an even clearer example of such behaviour, and theoretical treatments (Friedel and de Gennes *loc cit.*, Elliott and Roycroft, to be published) suggest that it may prove possible to account for such effects in terms of short range ordering.

Fig. 4

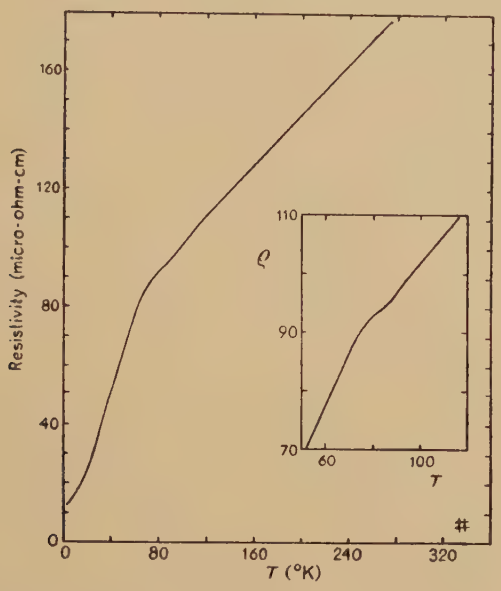

The electrical resistivity of erbium (microhm cm).

The excess scattering of the conduction electrons is analogous to the critical scattering of neutrons by iron in the vicinity of the Curie temperature (Wilkinson and Shull 1956). It is not easy to see, however, why gadolinium and some other materials show no sign of such an effect.

2.3. *Quantitative Comparisons*

If the electronic structures of the different rare earth metals differed only in the configuration of the 4f shell, it might be possible to gain some indications of the dependence on that configuration of the effective perturbation of the exchange field from the magnitude of the spin-disorder terms in the resistivities of the different metals. The validity of the assumption of similar conduction electron configurations can be explored in a crude fashion by the comparison of the lattice scattering above the temperatures of magnetic ordering. For similar Debye temperatures and similar conduction electron configurations one would expect similar values of $d\rho/dT$. The observed resistivity-temperature curves have been collected together by Spedding and Daane (1956).

At temperatures close to 300°K the slope of these curves is not very far from 0·16 microhm cm per degree for lanthanum, praseodymium, neodymium, and dysprosium, but it decreases rapidly with increasing temperature for the first three elements, falling to less than half the above figure at 1000°K. The value for erbium is considerably larger (about 0·5 microhm cm per degree at 240°K); while that for gadolinium, as pointed out above, is only about 0·08 microhm cm per degree at 320°K. These variations suggest that it would be very misleading to assume that the conduction electron configurations of all the rare earth metals are closely similar, and that the transitions producing resistivity are between similar states. The general form of the curves for lanthanum, praseodymium, and neodymium is sufficiently constant to make the assumption plausible for them, but it is quite evident that the resistivity behaviour of the later elements referred to differs in more than the presence of a magnetic ordering anomaly. It may be that increasing admixture of 5d character in the wave functions describing the conduction electrons modifies the conduction band significantly. Evidence for the existence of such effects may become available when specific heat measurements have been extended to temperatures low enough to make possible the unambiguous extraction of the term due to the electrons.

If the localized spin configurations and the conduction electron configurations differ for gadolinium, dysprosium, and erbium no reliable information about the dependence of the spin-disorder resistivity term on either of these configurations can be derived from the experimental data. It may be significant, however, that this term is much larger (about 120 microhm cm) for gadolinium with $S=J=7/2$ than for dysprosium (75 microhm cm, $S=5/2$, $J=15/2$) or for erbium (42 microhm cm, $S=3/2$, $J=15/2$).

§ 3. Atomic And Magnetic Ordering in Transition Metal Alloys

It has been pointed out in § 1 that in most solid solution alloys spin-disorder effects will be complicated by the atomic disorder produced by the random distribution of the solute atoms over a certain fraction of the lattice sites. Ordered binary alloys in which atoms of one or both of the constituent metals carry spin moments should prove easier to discuss.

In a simple binary alloy capable of atomic ordering where neither type of atom has a moment (Cu_3Au, for example) one may write the total resistivity ρ as

$$\rho=\rho_A+\rho_T, \qquad (3.1)$$

where ρ_A is the term arising from atomic disorder and ρ_T that from the lattice vibrations. In a crude but useful approximation this may be rewritten as

$$\rho=(P_A+P_T)F, \qquad (3.2)$$

where P_A and P_T represent the perturbations produced by the atomic and thermal disorder of the lattice respectively, and F is a factor depending upon the conduction electron configuration and involving the number of current carriers, their effective masses, and the density of states to which they can make transitions. Slater (1951 b) has pointed out that the Brillouin zone for the ordered state will differ from that for the disordered one. In particular, if the zone for the disordered alloy is half full the Fermi surface in the ordered zone structure will, for many types of ordering, lie near planes of energy discontinuity. This should lead, in general, to a diminution of the freedom of the electrons (an increase in the factor F of (3.2)) ; and the existence of such an effect is demonstrated by the measurements of the Hall coefficient by Komar and Sidorov (1941), who find the sign of the coefficient for Cu_3Au to change from negative to positive on ordering. In the resistivity of this alloy the increase in F on ordering is masked by the marked fall in P_A, which is appreciably greater than P_T for the disordered alloy at the temperature of ordering.

In a binary alloy containing localized spin moments eqn. (3.2) will become

$$\rho=(P_A+P_S+P_T)F, \quad . \quad . \quad . \quad . \quad . \quad . \quad (3.3)$$

where P_S represents the perturbation due to disordered spins. This simple separation of the perturbations cannot in fact be valid when P_A is large (see Yosida 1957), for the localized spins are then disordered in both distribution and orientation, but in the alloys to be considered here this is not important. From expression (3.3) it is obvious that, if the critical temperature for atomic ordering is higher than that for magnetic ordering, the term P_SF will constitute at certain temperatures a large portion of the total resistivity, which will therefore be sensitive to changes in F. Some indication of the magnitude of such changes can be derived from an examination of the term P_TF, but allowance has then to be made for any changes in the elastic constants on atomic ordering. (Preliminary results of such an examination for Cu_3Au suggest a change in F on ordering by a factor of almost 2.) A further subdivision of the Brillouin zone of the conduction electrons, with further possible changes in F, can take place on antiferromagnetic spin ordering (Slater 1951 a). As pointed out in the discussion of gadolinium in § 2.1 it is not yet possible to separate the P_TF term from the P_SF term below the magnetic ordering temperature. Developments in the theoretical examination on a spin-wave model of P_S (Friedel and de Gennes 1958, Elliott and Roycroft, to be published) may make such a separation possible.

3.1. Au_3Mn, AuMn, *and* Au_2Mn

In general it is not easy to decide when it is appropriate to describe the d-electrons of transition metal atoms in metallic phases by localized

wave functions, and when a collective description should be used. In certain alloys, however, magnetic and electrical data suggest that the localized wave function view point is correct. A particularly straightforward example of the occurrence of atomic and magnetic ordering effects is provided by the alloy Au_3Mn. This alloy has a disordered face-centred cubic structure at high temperatures, with a transition to an ordered structure at 900°K. This structure is probably orthorhombic (Giansoldati and Linde 1955). At low temperatures the ordered alloy is antiferromagnetic (Meyer 1957), with a Néel temperature (θ_N) of 145°K. The magnetic properties suggest a $3d^6$ configuration† for the manganese atom, so that the average number of conduction electrons per atom is

Fig. 5

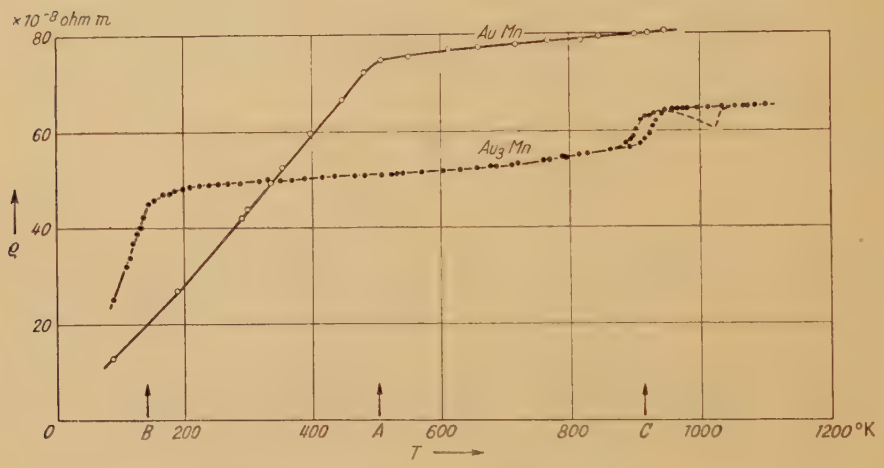

The electrical resistivity of Au_3Mn and AuMn.

1·0 as in pure gold. The electrical resistivity has been measured over a considerable temperature range by Giansoldati and Linde (1955), and their results are shown in fig. 5. It is immediately apparent that the principal source of the large high temperature resistivity is the spin-disorder scattering term, for the change on atomic ordering is only about 7 microhm cm. It is unlikely that a larger change in $P_\lambda F$ (see expression (3.3)) is offset by an increase of $P_\sigma F$, for the constancy of the temperature variation above and below 900°K indicates that little change

† Such configurations are still not known with certainty. In copper–manganese alloys (Myers 1956) the effective moment derived from inverse susceptibility-temperature curves (which is $\sqrt{4S(S+1)}$ if orbital effects are quenched) indicates $S = 2$ corresponding to a $3d^6$ configuration; but Owen *et al.* (1957) conclude from electron spin resonance measurements that the manganese atoms are in $3d^5(^6S)$ states, although their own susceptibility measurements give an effective moment close to that found by Myers.

in $P_T F$ occurs. The coefficient of T in the term linear in temperature at high temperatures is rather small, being only about $8{\cdot}3 \times 10^{-3}$ microhm cm per degree which is very close to the value for pure gold. This is strong support for the suggestion that the number of conduction electrons and the states between which they make transitions closely resemble those of gold, for any increase in Debye temperature on alloying would tend slightly to reduce the ordinary lattice term in the resistivity, while any possibility of scattering into empty states in a d-band would increase it greatly. Extrapolation to 0°K indicates a spin-disorder term of about 50 microhm cm. This is rather smaller than the corresponding terms in gadolinium, dysprosium, and pure manganese (§ 4.1), but if the conduction electrons on which the spin-disorder perturbation P_S operates are similar to those of pure gold (so that F is small) the value of P_S may be quite as large as in those elements, in which F is likely to be considerably larger.

Fig. 6

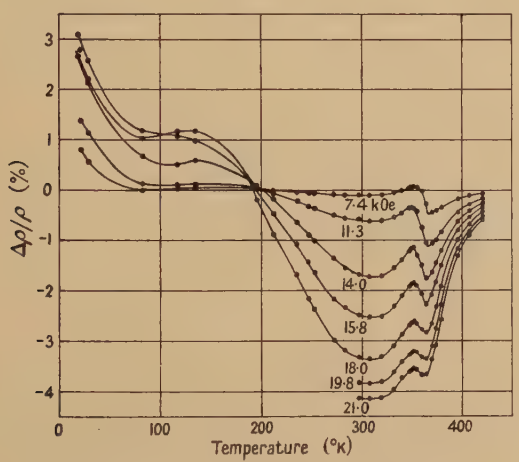

The magneto-resistance of Au_2Mn.

Closely similar effects are shown by the AuMn alloy, the data for which are included in fig. 5. In this alloy the change in crystal symmetry when atomic ordering, here of the CuAu type, takes place, is to a tetragonal lattice. The spin-disorder term in the resistivity is about 70 microhm cm, and the coefficient of T above the Néel temperature is about 11×10^{-3} microhm cm per degree.

Smith and Street (1957) have recently published the results of an investigation of the resistivity and magneto-resistance of Au_2Mn. This alloy has a more complicated crystal structure than either of those discussed above, and shows the remarkable property of ' metamagnetism ' (Meyer and Taglang 1956), whereby a phase change from antiferromagnetic to ferromagnetic ordering can be produced by a critical field of

about 15 kilogauss. The resistivity in zero field falls sharply below the Néel temperature (90°c), but behaves less simply than Au_3Mn at higher temperatures, so that no simple separation into spin-disorder and lattice scattering terms is possible. Smith and Street interpret their results in terms of a band of Bloch-type states for the magnetically active electrons, and discuss in such terms the marked decrease in resistance that accompanies the field-induced transition to a ferromagnetic condition. The susceptibility, however, conforms well to a Curie–Weiss relation with an effective moment slightly larger than the spin-only moment for a $3d^6$ configuration of the manganese atoms, and the saturation magnetization in the ferromagnetic state yields a moment about 12% less than that for complete alignment of manganese atoms in that configuration (Meyer and Taglang 1956). There thus seems to be justification for the use of a localized moment model, and the resistivity decrease (fig. 6) can be given a satisfactory qualitative interpretation in terms of a conduction electron/localized spin interaction of the type we have been considering. When the magnetic order changes from the antiferromagnetic to the ferromagnetic type there will be a change in the periodicity of the exchange field seen by the conduction electrons, a change in the Brillouin zone structure and size (Slater 1951 a), and a change, consequently, in the freedom of the conduction electrons. If these effects lead to an appreciable decrease in the quantity F in the expression (3.3) a fall in resistivity will follow, even when no change takes place in the *degree* of magnetic ordering.

Disordered substitutional solid solutions of manganese in gold show magnetic ordering effects and spin-disorder scattering, and these will be considered in § 5.2.

3.2. Ni_3Mn *and* Ni_3Cr

For many alloys of nickel a collective band treatment of the magnetically active electrons gives good results ; but the alloy Ni_3Mn may perhaps be more appropriately described in terms of localized spin moments on the manganese atoms, with much smaller localized or collective moments associated with the nickel atoms. Neutron diffraction studies (Shull and Wilkinson 1955) of the ordered alloy, which has a Cu_3Au structure, indicate moments of about 3 and 0·3 Bohr magnetons for the manganese and nickel atoms respectively. Since the alloy is ferromagnetic it resembles Au_3Mn in showing both atomic and magnetic ordering. The critical temperature (T_c) for the former is about 580°c, and that (θ_c) for the latter is about 460°c. Careful electrical resistivity measurements have been made by Kaya and Nakayama (1940), and these (fig. 7) show the usual fall of the spin-disorder term on cooling below θ_c. The magnitude of this term is of the order of 75 microhm cm ; but these paration of T_c and θ_c is too small to allow accurate extrapolation, and the highest degree of atomic ordering is probably not obtained until some way below θ_c. The most remarkable feature of these results is that the alloy shows a slight *increase* of resistance

on atomic ordering, although this ordering is certainly of the long range type. This peculiar behaviour can be understood in terms of a spin-disorder model for the principal term in the resistivity at high temperatures.

If we adopt the somewhat naïve model implied by the relation (3.3), and further postulate that the quantity F increases on atomic ordering (as it does in Cu_3Au), then the observed behaviour follows. When P_S is large the increase in the P_SF term below T_c will easily counterbalance the decrease taking place in P_AF when P_A, the atomic disorder perturbation,

Fig. 7

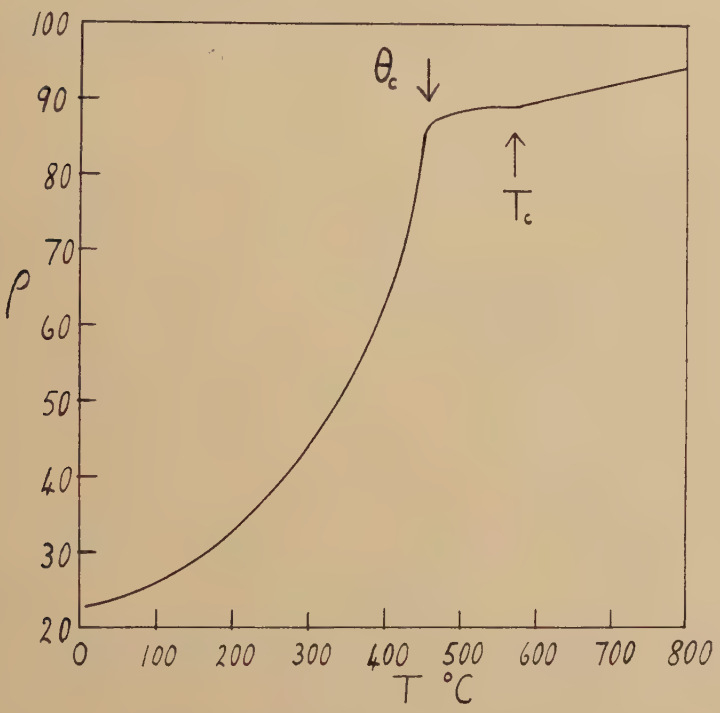

The electrical resistivity of Ni_3Mn (microhm cm).

falls to a small value. The increase in F on atomic ordering required for this explanation to hold will only be about 15%, if P_S is (as in Au_3Mn) about seven times larger than P_A. This increase is quite small compared with that of 100% suggested above for Cu_3Au. The proximity of the temperatures T_c and θ_c makes a comparison of the P_TF term above and below T_c impossible.

Above T_c the slope of the resistivity-temperature curve is about 2×10^{-2} microhm cm per degree. This is only about half that for paramagnetic nickel or palladium, and suggests that scattering of conduction electrons into any empty d-*band* states plays a very much smaller part in Ni_3Mn than it does in pure nickel.

One is tempted, by the success of the spin-disorder treatment in dealing with Ni_3Mn, to apply it to a discussion of the anomalous increase in the resistivity of Ni_3Cr (fig. 8) observed on low temperature annealing (Taylor and Hinton 1952). Since a specific heat anomaly is associated with this behaviour and no change in the symmetry of the lattice is observed by x-ray diffraction techniques an atomic ordering effect is to be suspected. However, neutron diffraction measurements (Roberts and Swalin 1957, G. Bacon, private communication) produce no evidence for any long-range atomic order. Since some change, and one which can be reversed by cold-working (Koster and Rocholl 1957), does take place the only interpretation remaining would appear to involve short-range order. The electrical resistivity remains very large down to 4·2°K, showing no

Fig. 8

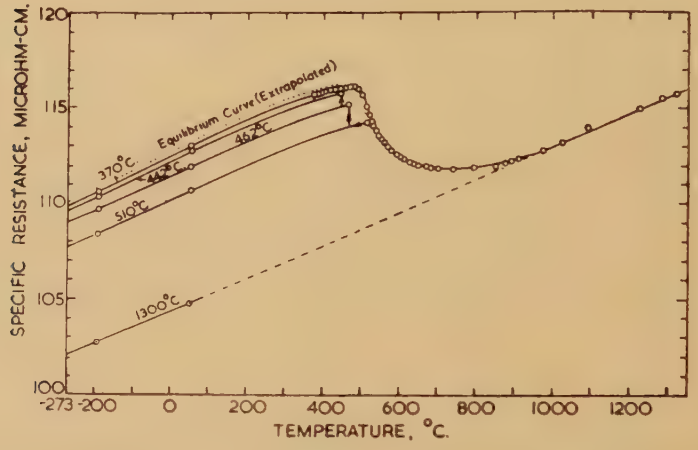

The electrical resistivity of Ni_3Cr (microhm cm).

marked fall of the magnetic ordering type (Coles, unpublished), and susceptibility data of Arrott (1954) on an alloy slightly richer in nickel show appreciable magnetic ordering effects only at still lower temperatures. Thus there is, as yet, no real evidence to indicate the presence of a large spin-disorder term in the resistivity of Ni_3Cr. On the other hand, it should be noted that the slope of the resistivity–temperature curve is only about $8{\cdot}7 \times 10^{-3}$ microhm cm per degree, which is of the same order as that for the noble metals. This means (unless the Debye θ is exceptionally large) that the quantity F is small, so that the very high observed value of ρ requires a very large value of either P_S or P_A. High values of P_A are found in solid solutions of germanium or arsenic in copper but the explanations normally given (cf. Mott and Jones 1936, Friedel 1956) of these effects are in terms of a description that seems unlikely to hold for the extensive solid solution of one transition metal in another.

§ 4. The Transition Metals

A completely satisfactory description of the electronic structures of the transition metals and their alloys, which will account for their physical properties and alloying behaviour, has yet to be given. Many of the features required of such a description and some of the experimental data have recently been considered by Mott and Stevens (1957), and an earlier review in this journal (Hume-Rothery and Coles 1954) gives a general account of the crystal structures, physical properties, and alloying behaviour. All these metals show magnetic behaviour associated in some way with the presence of electrons in partly occupied d-levels, and one of the main points to be resolved for any particular material concerns the type of wave-function to be used in describing these electrons. Making

	Ti[h]	V[b]	Cr[b]	Mn	Fe[b]	Co[f, h]	Ni[f]
Electrons with type A wave functions (in 3d band)	—	—	~0·2	—	—	8·5	9·5
Electrons with type B wave functions (in hybridized band)	4	5	~5·8	~6†	6	—	—
Electrons with type C wave functions (in non-conducting states)	—	—	—	~1†	2	—	—
Electrons in 4s band	—	—	—	—	—	0·5	0·5

† These figures are averages over the four different types of atom in the complex α-manganese structure.

b=Body-centred cubic. f=Face-centred cubic. h=c.p. hexagonal.

a slightly arbitrary classification one may consider : A. Functions which are of the simple Bloch type but which are predominantly d in character. B. Functions which are of the simple Bloch type but which are too strongly hybridized (from mixtures of d, s, and p states) to be connected with any particularly atomic levels. C. Functions which are not of the simple Bloch type† but are localized on particular atoms. Type A functions make up a narrow energy band containing part of the Fermi surface, type B functions make up a broad energy band containing part of the Fermi surface, and type C functions do not contribute to the Fermi surface and may be described as non-conducting. Mott and Stevens argue that a collective band of type A functions (overlapped by a conduction band of almost free-electron character) exists in nickel and palladium, the end members of the first and second transition groups ;

† We shall not be concerned here with the possibility of arriving at these functions (Mott 1956, Mott and Stevens *loc. cit.*) via Wannier functions built up from Bloch functions.

but that in iron and perhaps manganese some electrons have non-conducting, type C wave functions, the outer electrons in these metals having type B wave functions. In chromium there may be some overlap into inner 3d functions of the type existing in iron, but the number of electrons in such states is not likely to be integral ; if not, they must contribute to the current and so should be classed as type A. The same may be true of manganese. In such a scheme the approximate configurations (in electrons per atom) of the metals of the first transition group would be those shown in the Table.

Palladium in the second transition group is closely similar to nickel, but there are indications that only type B wave functions are used by the earlier elements of the second and third transition groups.

In the following sections the behaviour of the resistivity of some of these elements will be considered in the light of such a scheme.

4.1. *Manganese*

Metallic manganese can exist with four different crystal structures, but neither of the simple ones, δ body-centred cubic or γ face-centred cubic, is stable at room temperature. The stable low temperature form is a complex cubic structure, and is antiferromagnetic (Shull and Wilkinson 1953) with a Néel temperature close to 100°K. A detailed consideration of the magnetic structure, as revealed by neutron diffraction, has been presented by Kaspar and Roberts (1956) who give different possible schemes for assigning spin moments to four crystallographically distinct types of atom. The mean moment per atom is about 1·1 Bohr magnetons per atom† but Kaspar and Roberts conclude that one type of atom carries no moment. The specific heat has an anomaly associated with the antiferromagnetic ordering, and Tauer and Weiss (1957) have shown that the magnitude of this is in agreement with what would be expected from the moments assigned.

The electrical resistivity of α-manganese has been measured down to 2°K by White and Woods (1957 a), and their results are shown in fig. 9. The resistivity falls sharply below about 60°K, folllowing a T^2 dependence below about 30°K. It seems highly probable that the sharp fall is associated with the ordering of the spin system, and extrapolation of the high temperature data gives a spin disorder term ($P_S F$) of about 112 microhm cm. If the high temperature resistivity is assumed to be linear in temperature, the coefficient of T is approximately 7×10^{-2} microhm cm per degree, which is not quite twice that shown by palladium. These relative values of the lattice scattering terms for manganese and palladium seem not unreasonable when the densities of states into which conduction electrons may be scattered at their respective

† The original figure given by Shull and Wilkinson is corrected by Shull and Wollan (1956).

Fermi surfaces are proportional to 33×10^{-4} and 22×10^{-4}. These figures are the values, in calories per mole per (degree)^2, of the coefficients of the linear terms in the low temperature specific heats (Guthrie *et al.* 1955, Hoare and Yates 1957). If, however, the conduction electrons in manganese have type B wave functions it is not possible to estimate their effective number ; palladium is discussed in detail below.

A significant feature of the results shown in fig. 9 is that the resistivity *rises* when magnetic ordering first takes place, reaching a maximum about 20° below the Néel temperature, which therefore lies at a minimum in the

Fig. 9

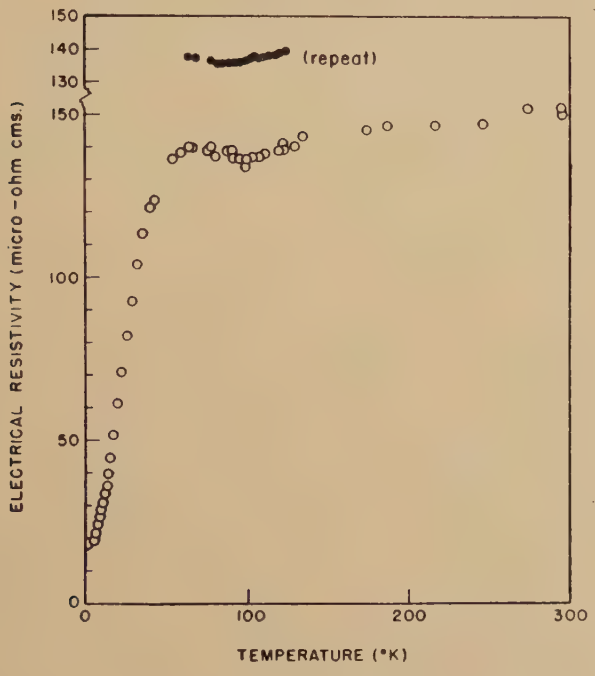

The electrical resistivity of α-manganese (microhm cm).

resistivity–temperature curve. Related behaviour for dysprosium was mentioned in § 2.2 and tentatively ascribed to short-range order effects analogous to those causing the critical scattering of neutrons. The theoretical treatment of Elliott and Roycroft predicts a maximum, but one that occurs *at* the critical temperature for magnetic ordering, not below it. It is conceivable, therefore, that other factors are involved, and that even the first stages of magnetic ordering have significant effects on the conduction electron configuration. If magnetic ordering decreased the freedom of the conduction electrons (through a mechanism of the type mentioned in § 1) more rapidly at first than it decreased the spin-order perturbation, such an increase could occur.

4.2. *Palladium and Nickel*

The ' classical ' d-band model of a transition metal (Mott 1935, Stoner 1947) describes the electronic structure in terms of two overlapping bands ; one, in which the density of states is high, of type A states, and one closely-similar to a free-electron conduction band. The most striking successes of this model were in the interpretation of the physical

Fig. 10

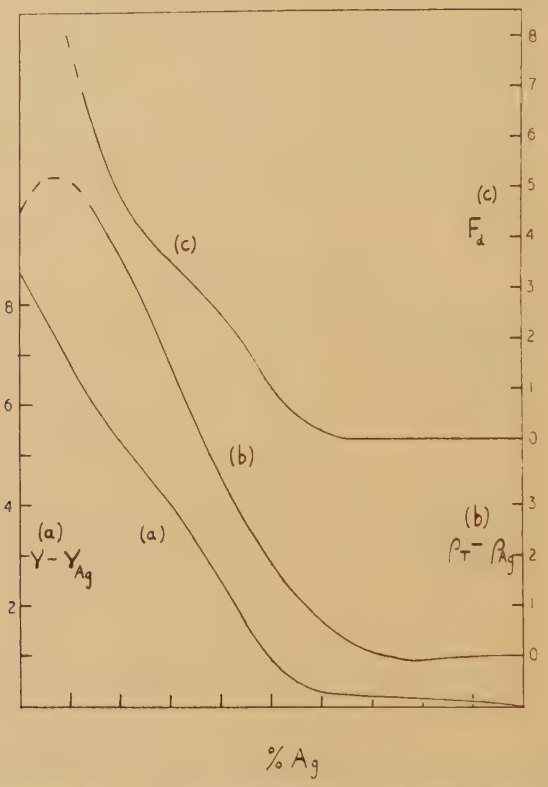

Experimental measures of $N_d(E)_F$, the density of states at the Fermi surface in the d-band of palladium–silver alloys as a function of silver content. (*a*) $\gamma - \gamma_{Ag}$ from the specific heat data at low temperatures (millijoules per mole per (degree)^2). (*b*) $\rho_T - \rho_{Ag}$ from the lattice scattering resistivity at room temperature (microhm cm). (*c*) F_d from the residual resistivity (arbitrary units).

properties of palladium, nickel, and some of their alloys: and in view of the emergence of the concept of spin-disorder scattering it may be useful to review some of the experimental results which are satisfactorily discussed in terms of the old model.

In palladium and nickel the Fermi surface is assumed to lie at an energy slightly lower than that of the top of the d-band, so that there are 0·5 or 0·6 empty d-band states and an equal number of occupied s-band states.

It is further assumed that in ferromagnetic nickel the magnetization of the d-band is complete at low temperatures, so that all d-band states of one direction (five per atom) are filled. Mott (1935) ascribed the high resistivity of these metals to the high probability of processes in which the s-electrons, which are the principal current carriers, are scattered into empty d-band states and relax back into the s-band. In later papers (Mott 1936 a, b) he showed that it is a reasonable assumption to take the time of relaxation as inversely proportional to the density of states $(N_d(E)_F)$ in the d-band at the Fermi surface, and that this assumption leads to a satisfactory discussion (cf. Mott and Jones 1936, Jones 1956) of the resistivity and thermo-electric power of palladium and its alloys with silver. This model also provides a satisfactory interpretation of the anomaly in the resistivity of nickel at the Curie point (θ_c), for it may be described as arising from the ability of s-band electrons of both spins to make spin-conserving transitions into empty d-band states above θ_c. It should be noted that here the anomaly is connected with changes in the states between which transitions take place, and not with any change in the nature of the perturbation (the thermal disorder of the lattice) bringing about the transitions. In the simple notation of expression (3.3) this description takes $P_\uparrow$ to be zero at all temperatures and F to be larger for $T>\theta_c$ than for $T<\theta_c$.

Recent experimental results, especially for alloys of palladium with silver and of nickel with copper, make possible a detailed examination of the validity of this d-band model. Additions of the noble metal should, if the d-band is collective, decrease the number of empty states in it and the value of $N_d(E)_F$. The variation with silver content of $N_d(E)_F$ in the palladium–silver alloys is given directly by the measured variation of γ, the coefficient of T in the term in the low temperature specific heat which is linear in the temperature, and this variation (Hoare and Yates 1957) is shown in fig. 10. Also shown in this figure are two separate measures of $N_d(E)_F$ that may be derived from resistivity data (J. C. Taylor, to be published). One of these $(\rho_T-\rho_{Ag})$ is the excess over that of silver of the lattice scattering contribution† $(P_T F)$ to the electrical resistivity at room temperature ; and the other (F_d) is an estimate of the quantity F in the $s \rightarrow d$ scattering portion of the residual resistivity $(P_\downarrow F)$, F_d being obtained by making reasonable assumptions about the concentration dependence of $P_\downarrow$. On the band model the lattice scattering contribution should differ from that in pure silver in a manner governed mainly by the value of $N_d(E)_F$, and the experimental results show behaviour qualitatively of this type, except for the alloys very rich in palladium where (as shown by Hall effect and thermoelectric power data) d-band holes make a contribution to the conduction. The concentration dependence of F_d

† In deriving this quantity the measured difference between the room temperature resistance and the residual resistance has to be corrected for the appreciable temperature variation (through the factor F) of $P_\downarrow F$; this variation as shown later, can provide other information about the electronic structure.

derived from the residual resistivity is in even better agreement with what might be expected from a proportionality between F_d and $N_d(E)_F$.

The band model also deals successfully with the departure of the resistivity of palladium from linearity in temperature at high temperatures. The high temperature resistivity can be expressed, ignoring the effects of expansion on the Debye temperature, as

$$\rho = BT(1 - AT^2) \quad . \quad . \quad . \quad . \quad . \quad . \quad (5.1)$$

where A and B are constants, and Mott (*loc. cit.*) has shown that the coefficient A depends largely on $d \log_e N_d(E)/dE$. The value of A for pure palladium can be derived from the high temperature data of Conybeare (1937); and from the lower temperature data of Taylor for the palladium–silver alloys, where

$$\rho = (\rho_R + BT)(1 - AT^2), \quad . \quad . \quad . \quad . \quad . \quad (5.2)$$

Fig. 11

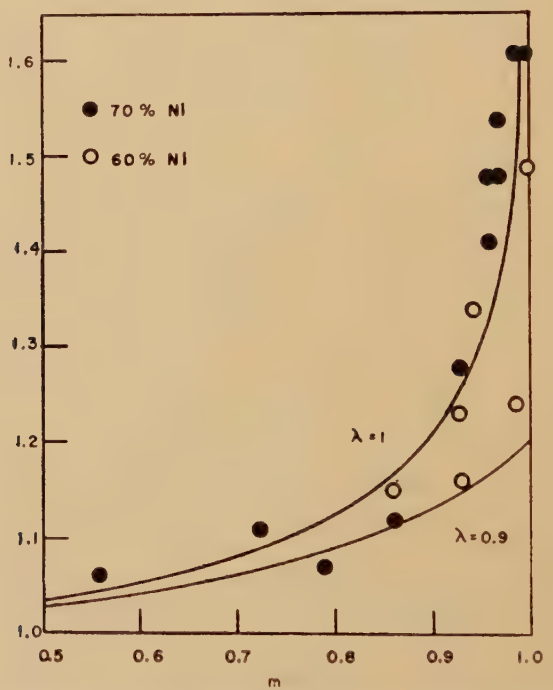

Reduced Hall coefficient (r) of nickel–copper alloys versus reduced magnetization (m). $\lambda = 1$, theoretical curve for complete magnetization at 0°K. $\lambda = 0{\cdot}9$, theoretical curve for 90% magnetization at 0°K.

the large value of ρ_R makes it possible to derive values of A corresponding to more highly occupied configurations of the d-band. These values agree in general magnitude with those suggested by the $N_d(E)$ versus energy curve derived from the specific heat measurements, and with those derived, using the same band model, from the absolute thermo-electric powers of the alloys (Taylor and Coles 1956).

A collective band model has been used to discuss the magnetic properties of the nickel-rich nickel–copper alloys (Wohlfarth 1949), and also their electrical resistivities (Mott 1936 a). Recently measurements of the Hall coefficients of these alloys above and below their Curie points (Allison and Pugh 1956) have provided additional support for the model. In an alloy in which at low temperatures all empty d-band states have parallel spins, the s-band electrons with spins parallel and antiparallel to these states will have different mobilities, for those with antiparallel spins will not be able to make spin-conserving transitions into empty d-states. Above the Curie temperature, however, all s-electrons will have similar mobilities, since the occupation of the two halves of the d-band will be the same. Using a two-band model (the two types of carrier differing only in mobility, not in sign or number) Allison and Pugh derive the dependence on reduced magnetization, m or $M_{\mathrm{sat}}(T)/M_{\mathrm{sat}}(0)$, of a reduced Hall coefficient (r) defined as the ratio of the ordinary Hall coefficient at the temperature T to that at temperatures well above the Curie point. Figure 11 shows that the experimental results are in good agreement with the theoretical curve if it is assumed that the magnetization of the d-band is complete at 0°K, but in marked disagreement with the assumption of only 90% alignment of the d-band holes at low temperatures.

Fig. 12

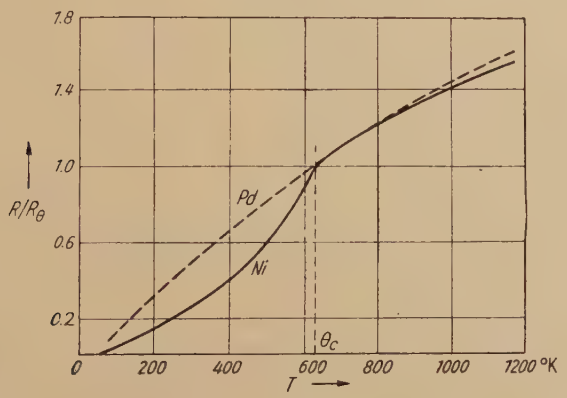

Reduced resistivity (R/R_θ) as a function of temperature for nickel and palladium; θ for both curves is the Curie temperature of nickel.

It might be argued that, although s → d scattering effects play a part in the resistivities of nickel and palladium, a spin-disorder term in the resistivity of nickel does exist above the Curie temperature. The experimental data for the pure metals (Gerritsen 1956) shown in fig. 12 make this seem improbable. The resistivity of palladium falls, as the temperature is lowered, in a straightforward manner; and, although magnetic ordering does not occur, there is no sign of a spin-disorder term in the resistivity. Figure 12 shows that the high temperature resistivity

of nickel behaves in a very similar manner, with a curvature satisfactorily explained on the band model.

In view of the close similarities between the electronic structures of the pure metals, the alloys of nickel with palladium should show effects governed largely by the variation in the spontaneous magnetization of the d-band holes. Electrical resistivities in this system have been measured by Schindler *et al.* (1956, 1957), and the departure of their residual resistivity data from a simple parabolic dependence on concentration has been interpreted (Overhauser and Schindler 1957) in terms of the variation in relative magnetization and a particular band form. At high temperatures, where the alloys are paramagnetic for all concentrations, the maximum resistivity is found at the equiatomic composition as expected.

4.3. *Iron*

The properties of iron differ in a number of significant respects from those of nickel, and a straightforward collective band model of the type used successfully for the latter is not adequate for the former. Attempts to discuss the magnetic properties of iron and its alloys on such a model (Stoner 1946, Hume-Rothery and Coles 1954) have found it necessary to postulate that the d-band of iron is incompletely magnetized at 0°K, d-band holes of both spins being present, and also that the density of states at the Fermi surface in the two half-bands is approximately the same. With these assumptions it is possible to give an account of the magnetic behaviour of the iron–cobalt alloys (Coles and Bitler 1956); but they do not seem to provide as satisfactory a basis for the discussion of the electrical properties.

In a recent paper Mott and Stevens (1957) have discussed theoretical models and experimental data for iron. They conclude that the electronic structure is that shown in the table, two 3d electrons with coupled spins being located on each atom in the body-centred cubic structure. They follow the suggestion of Griffith (1956) in assigning 3d wave-functions of the e_g type to these localized electrons; and that of Zener (1951) in ascribing some of the extra 0·2 Bohr magnetons per atom in the saturation moment to a magnetization of the conduction electrons, through the medium of which the atomic moments are aligned. The interactions involved in this alignment mechanism have been treated theoretically by Kasuya (1956 b) and Pratt (1957). A sharp distinction, as shown in the table, between the electronic structures of iron on the one hand, and cobalt and nickel on the other, is suggested by the x-ray scattering data of Weiss (to be published), which are quoted by Mott and Stevens. Here we shall consider the extent to which the electrical properties of iron are in conformity with a localized moment model.

Iron at room temperature is a moderately good conductor ($\rho = 10$ microhm cm) with a positive Hall coefficient (Foner and Pugh 1953). The resistivity temperature curve (fig. 13) shows a marked anomaly at the Curie temperature (1033°K), but the proximity of the transformation

to the face-centred cubic structure (γ) makes the temperature range over which the magnetically disordered body-centred cubic structure is stable too small for any detailed comparison with nickel to be possible. The various sources of experimental data (Powell 1939, 1953, Pallister 1949) show clearly that the slope of the curve varies rapidly between the Curie temperature (θ) and the α/γ change point ; at the bottom of this range it is similar (on a reduced resistivity plot) to that of nickel, but falls to a much lower value at the top of the range. In view of the pronounced ' tail ' observed in the magnetic specific heat above θ one is probably justified in regarding the lower value of the slope as more reliable. At higher temperatures (above 1680°K) the body-centred cubic structure again becomes stable, and comparison of the resistance in this region with

Fig. 13

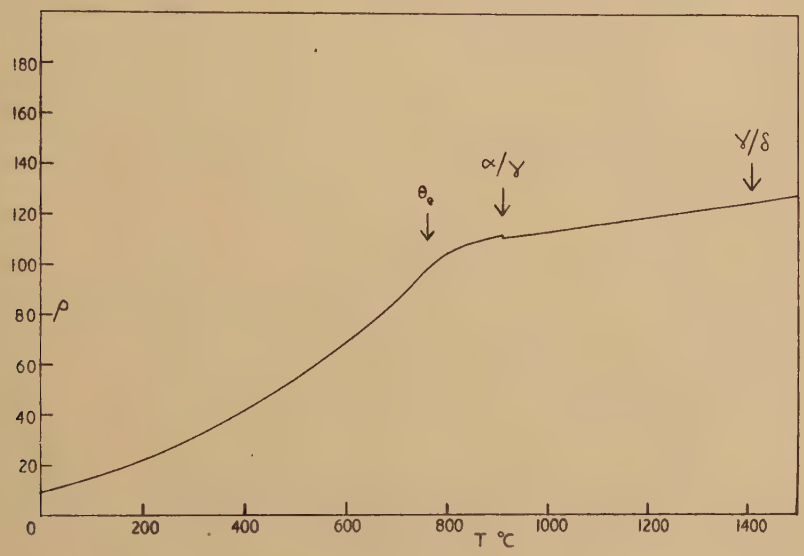

The electrical resistivity of iron (microhm cm).

its value just above θ suggests that the resistivity of paramagnetic body-centred cubic iron (like that of gadolinium) does contain an appreciable temperature-independent term. A reasonable value for this would seem to be about 70 microhm cm, and the slope of the resistivity–temperature curve is about 0·03 microhm cm per degree. At temperatures below θ, however, the reduced resistivity curve (ρ/ρ_θ *vs* T/θ) of iron resembles that of nickel, not that of gadolinium (see fig. 7 of Mott and Stevens *loc. cit*) : this presumably reflects the fact that the magnetization of gadolinium follows the $T^{3/2}$ law whereas that of iron (like that of nickel) does not.

It is difficult to see how a Curie point anomaly of the magnitude of that observed in iron could be explained in terms of the type of band model applied to nickel. For such a model to explain the magnetic properties

of iron one must postulate, as pointed out above, d-band holes of both spin directions and similar densities of states, $N_d(E)$, at the Fermi surface in both half-bands. With such a configuration and a time of relaxation inversely proportional to $N_d(E)$, conduction electrons of both spins would have similar transition probabilities for s → d scattering above and below the Curie point, unless the density of states curve had a high peak midway between the positions of the Fermi level in the two half bands.

The resistivity–temperature curve for γ-iron has a very similar appearance to that suggested for α-iron, were it stable, over the same temperature range, the changes in resistivity at the two transition points being very small. This would seem to indicate the presence of a spin-disorder term similar to that postulated for the α-form ; but Mott and Stevens, on the basis of neutron diffraction data for face-centred cubic iron–manganese alloys which indicate smaller moments for the iron atoms, consider γ-iron to have an electronic structure more like that of nickel than that of α-iron.

Further experimental comparisons of the properties of α-iron and nickel are desirable, and one such experiment, referred to by Mott and Stevens, has recently been performed (Coles, to be published). Reverting to the notation of § 3, we may write the resistivity of a pure metal as

$$\rho=(P_S+P_T)F.$$

The suggested difference between iron and nickel may be stated in terms of this expression as follows : in iron at high temperatures exchange interaction between conduction electrons and randomly orientated localized moments gives a large spin-disorder perturbation, P_S, which falls to zero during the alignment of the moments without any change in the quantity F, which depends on conduction electrons and the states to which they make transitions ; in nickel no P_S term exists at any temperature, and the Curie point anomaly arises from the difference in F produced by the change in relative occupation of the two halves of the d-band into which conduction electrons are scattered. If, now, another perturbation (P_A) is introduced by the addition of a small amount of an alloying addition, the new term in the resistivity P_AF should have a larger value above the Curie temperature than at 0°K for nickel, but the same value at both temperatures for iron. The predicted resistivity behaviour is shown in fig. 14 (from the paper of Mott and Stevens). For the actual experiment ruthenium was chosen as an addition to iron, and palladium as an addition to nickel, because the corresponding positions in the Periodic Table of solvent and solute make it likely that the disturbance to the electronic structure will be small. (The magnetic properties (Stoner 1946) show little change on alloying of this sort.) The observed difference, $\Delta\rho$, between the resistivity of the alloy and that of the pure metal is as shown in fig. 14 for liquid helium temperatures and temperatures just above the Curie point, in confirmation of the above descriptions of

iron and nickel. At temperatures of the order $\frac{1}{2}\theta$, however, $\Delta\rho$ is appreciably larger than its value at very low temperatures in both systems.

Fig. 14

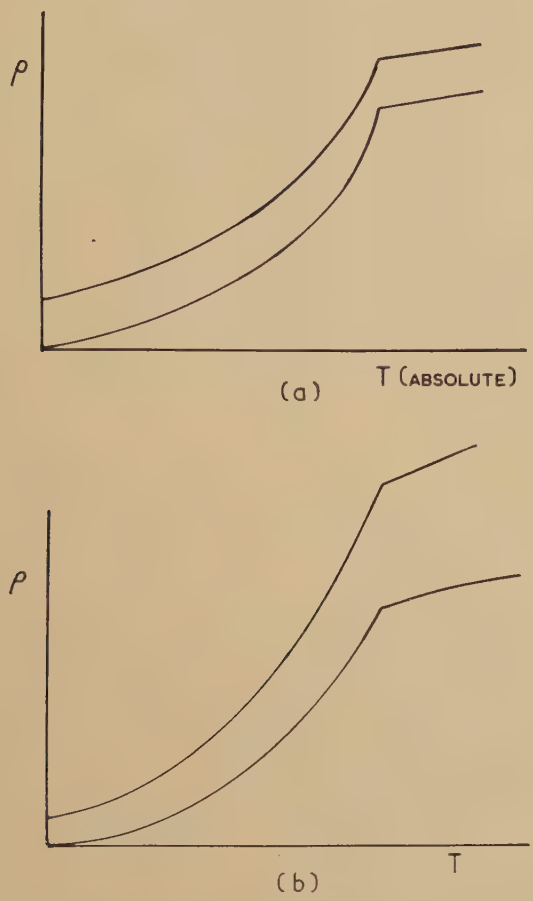

Predicted behaviour of the electrical resistivity of iron and nickel alloys. (*a*) Iron and iron–ruthenium. (*b*) Nickel and nickel–palladium.

4.4 *Other Metals*

4.4.1. *Second and third transition group metals*

No magnetic ordering effects have been observed in the earlier members of the first transition group or in any members of the second and third transition groups. The resistivity–temperature curves (Potter 1937, 1941, White and Woods 1957 b, c) have been examined at both high and low temperatures, and these give no indication of the presence of a temperature-independent term that can be associated with the presence of spin-disorder scattering. It has been emphasized in § 4.2 that the electronic structure of palladium, at the end of the second transition

group, must be very like that of nickel ; and platinum, at the end of the third would seem (Wohlfarth 1948) to bear a general, although less close, resemblance to these. The other members of the second and third groups, however, have properties more similar, in their general character, to those of the early members of the first group (cf. Hume-Rothery and Coles 1954). It therefore seems probable that the electronic structures of all but the final members of the second and third groups involve only wave-functions of type B (see table), and that the point at which type A functions become favourable in the second group lies closer to the end of the group than in the first, and perhaps closer again in the third. It is not yet clear why electrons with type C functions, which would give resistivity effects, are not found in the second and third groups. It may be remarked, although it could be only a chance correlation, that nickel, cobalt, palladium, and platinum (for which d-bands overlapped by s-type conduction bands are postulated) have negative Hall coefficients ; while iron, ruthenium, rhodium, rhenium, osmium, and iridium have positive coefficients (Justi and Kohler 1951).

4.4.2. *Titanium*

Interesting resistivity behaviour is shown by titanium. The close-packed hexagonal α-form of titanium, stable at room temperature, has a very high resistivity with a normal temperature dependence at low temperatures. About 100° below the transformation at 1175°K to the body-centred cubic β-form the slope of the resistivity–temperature curve begins to decrease very markedly, and for the β phase (the resistivity of which is somewhat lower than that of the α phase at the transformation temperature) the curve is almost horizontal over a considerable temperature range (McQuillan 1950). Similar behaviour is shown by zirconium (Adenstedt 1952) and hafnium (Fast 1952). The β-structure in pure titanium cannot be retained at low temperatures by quenching, but this can be done in the titanium–niobium alloys. The electrical resistivities of these alloys have been examined by Ames and McQuillan (1954) in the hope of discovering the form of the resistivity–temperature curve for β-titanium at lower temperatures. Their results are shown in fig. 15, and it seems from them that the room temperature resistivity of β-titanium would be about the same ($\sim$145 microhm cm) as that at higher temperatures. It is possible, therefore, that this contains a large and almost temperature-independent term arising from spin-disorder effects ; and that in the body-centred cubic form of titanium, as in that of iron, localized type C electrons exist.

4.4.3. *Chromium*

A small localized moment is ascribed to chromium in the table on the basis of neutron diffraction data (Shull and Wollan 1956), but the electrical resistivity shows no anomalous behaviour at the temperature ($\sim$470°K) of the supposed antiferromagnetic ordering. The electrical

resistivity at low temperatures shows a normal behaviour, but there seems to exist some anomaly at temperatures close to 320°K (Sully *et al.* 1952). Other physical properties, and mechanical ones, show anomalies at this temperature, and these effects have not yet been explained.

Fig. 15

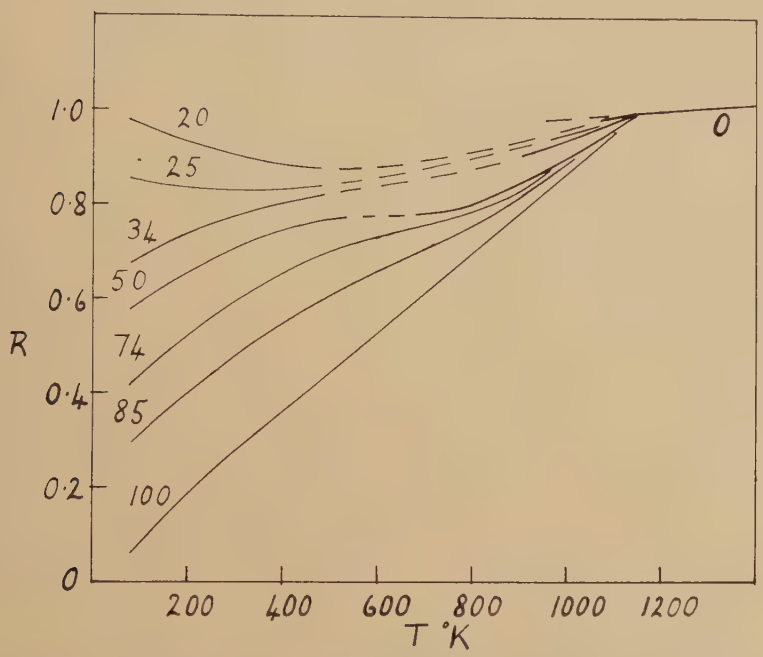

The electrical resistivity of body-centred cubic (β) titanium–niobium alloys relative to that at 1173°K. The curves are numbered with the percentage of niobium. In the temperature range where the curves are broken the α-phase precipitates.

The room temperature resistivity of these alloys falls regularly with the niobium content, and the value for pure β-titanium given by extrapolation is about 150 microhm cm.

§ 5. Dilute Alloys

5.1. *Solid Solutions in Ferro- and Antiferromagnetic Metals*

The electrical resistivities of dilute solid solutions in ferro- and antiferromagnetic metals have not received the attention that has been given those of solid solutions in copper, silver, and gold ; but such data are of great potential interest in the study of spin-disorder effects. The use of resistivity measurements to examine the electronic structures of iron and nickel has been demonstrated in § 4.3.

When a small amount of an alloying element is added, at absolute zero, to a ferro- or antiferromagnetic pure metal possessing completely aligned localized moments, two sources of perturbation capable of

contributing to the resistivity will be introduced. One (P_A) will be the normal atomic disorder perturbation of the electric field, similar to that produced by, say, zinc in copper ; and the other (P_S) will arise from the disordered exchange field of the solvent moments. The latter term will exist even if the solute carries a moment equal to that of the solvent, for the exchange interaction with the conduction electrons will differ in the atomic cell containing a solute atom. There may also, of course, be a change in the number of conduction electrons and the nature of the states between which they make transitions, but this will in general be small for small additions of a solute.

Since spin-disorder resistivity terms are large it will be necessary to achieve a high degree of purity in metals containing aligned localized moments if low values of the residual resistivity are to be reached. It can be seen from figs. 1, 2, and 4 that large residual resistivities are observed for the rare earth metals, even when their purity is kept high. A more striking effect of strain and gaseous impurity is shown by manganese, where White and Woods (1957 a) found an unannealed specimen to have a resistance of 330 microhm cm at 4·2°K, compared with a value of less than 20 microhm cm for a vacuum annealed specimen at the same temperature. This effect may be connected with the suppression of spin ordering at low temperatures, for the value for the unannealed specimen rose only to 378 microhm cm at room temperature where the resistivity of the annealed specimen was 150 microhm cm.

It is of interest to compare the magnitudes of the effects of alloying on the resistivities of iron and nickel in the light of the discussion of § 4.3. The addition of 1 atm% of ruthenium gives a residual resistivity contribution of about 3 microhm cm to iron, whereas the rate of increase of the residual resistivity of nickel with palladium content is about 0·17 microhm cm per atm% (Schindler *et al.* 1956). In both alloy systems the solvent and solute occupy analogous positions in the Periodic Table, so that the change expected of the conduction electron configuration should be small. The marked difference in residual resistivity observed is additional support for the electronic structures postulated.

That spatial disorder of aligned spins can give as large a resistivity term as the orientational disorder of regularly arranged moments is shown by the resistivity behaviour of the alloy Fe_3Al (Bennett 1952). This alloy is ferromagnetic at room temperature in both ordered and disordered states ; but the resistivity of the disordered alloy is very much larger than that of the ordered alloy, and is closely similar to that given by extrapolation of results for the ordered alloy from above its Curie temperature. Similar behaviour is shown by the alloy Fe_3Si (Glaser and Ivanick 1956).

5.2. *Dilute Alloys of Transition Metals in Noble Metals*

Some extremely interesting effects can be produced by the solution of small amounts of transition metals in copper, silver, and gold. The

concept of spin-disorder scattering contributes greatly to our understanding of these, and it has become apparent, for example, that the large increase in resistivity produced is due more to such scattering than to atomic disorder scattering. Solid solutions of manganese in copper have, in particular, been studied extensively, and the results of many different types of measurement have been discussed by Gorter *et al.* (1956) and by Owen *et al.* (1957).

These alloys are paramagnetic at high temperatures with susceptibilities accurately described by expressions of the Curie–Weiss type (Myers 1956, Owen *et al.*, *loc. cit.*). In theoretical treatments a $3d^5$ configuration has normally been assumed for the manganese atom, although the effective moments given by the susceptibility data are closer to that for the $3d^6$ configurations. At very low temperatures alloys with as little as 0·1% of manganese become antiferromagnetic, the Néel temperature increasing with manganese content, and alloys with

Fig. 16

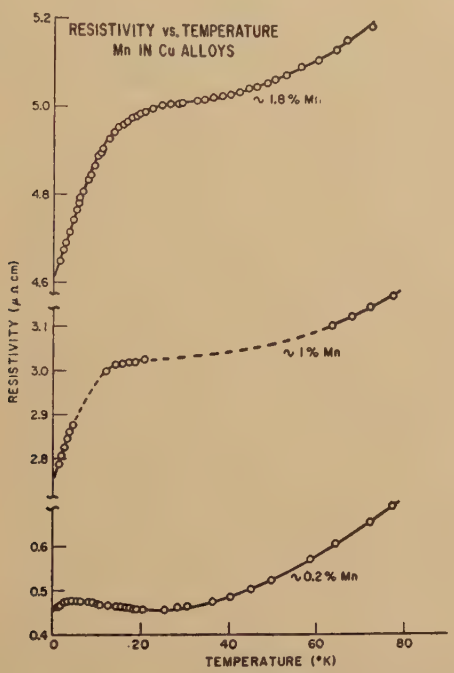

Low temperature electrical resistivity of dilute copper–manganese alloys.

large manganese contents (>13%) show antiferromagnetic ordering effects when examined by neutron diffraction techniques (Meneghetti and Sidhu 1957). In manganese-rich alloys (Bacon *et al.* 1957) long-range antiferromagnetic ordering is found, accompanied by a distortion of the lattice from cubic to tetragonal.

The electrical resistivities of all alloys with more than about 1% manganese show a straightforward decrease in resistivity on being cooled through the temperature of magnetic order (Otter 1956, Bacon *et al.*, *loc. cit.*); but they do not, of course, tend to very low values at very low temperatures because the atomic disorder, and hence also the *spatial* disorder of the localized moments, is still present. The magnitude of the effect is indicated by the results of Schmitt and Jacobs (1956) shown in fig. 16. For alloys with smaller concentrations of manganese the results are at first sight more complex. (Figure 17 shows data of Gerritsen and

Fig. 17

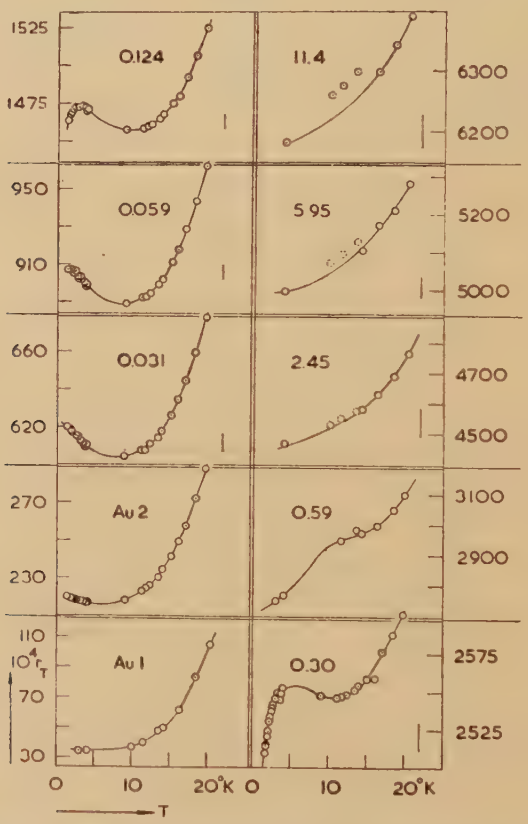

Electrical resistivity, relative to that at 0°c, for dilute gold–manganese alloys; the numbers on the curves are the percentages of manganese.

Linde (1952) for gold–manganese alloys.) This complexity arises from the fact that with these concentrations the temperature of magnetic ordering is close to that at which a resistivity minimum is observed. The occurrence of such minima in the resistivity of many dilute alloys is still not adequately explained: but there is, as yet, no evidence that it is associated in any fundamental way with spin-disorder scattering.

(This and other features of the low temperature electrical properties of metals and alloys are discussed by MacDonald 1956.) As the magnetic ordering temperature falls, on reducing the manganese content, through the temperature range of the minimum, the resistivity–temperature curve shows first a point of inflection, and later a maximum below the minimum. As might be expected, negative magneto-resistive effects are found in such materials (Gerritsen 1953, Gerritsen and Linde 1951); Schmitt and Jacobs (1956, 1957) have shown that these can be correlated simply with the relative magnetization, proving that the decrease is associated (like the fall at low temperatures) with the ordering of the moments.

The theory of these effects in the resistivity (excluding the minimum) has been developed by Yosida (1957), following the phenomenological treatment of Schmitt (1956). He finds it necessary to postulate an exchange integral for the s–d interaction larger than the free ion value by a factor of about 1·7 in order to get quantitative agreement with the experimental observations.

Similar effects are shown by alloys of chromium and iron in solution in gold, and of manganese in silver. It is of interest to note that, in spite of the great similarities of electronic structure between gold and copper, the solutions of manganese in the former (including disordered Au_3Mn) show magnetic ordering of ferromagnetic character (Meyer 1956, 1957) in contrast to the antiferromagnetism of the copper–manganese alloys.

Acknowledgments

This review is based upon a talk given by the author to a conference in Cambridge in June 1957, and his thanks are due to many of those who attended for helpful discussions; in particular to Professor N. F. Mott, Dr. R. J. Weiss, Dr. R. J. Elliott, Dr. W. M. Lomer, Dr. W. Marshall, and Dr. J. Friedel. Dr. A. I. Schindler (of the Naval Research Laboratory, Washington), Dr. R. J. Elliott, and Mr. J. C. Taylor kindly gave permission for reference to be made to their unpublished work.

The sources of the following figures are also gratefully acknowledged:

Figures 1, 2 and 4 from Spedding, F. H., Legvold, S., Daane, A. H., and Jennings, L. D., 1957, *Prog. Low Temp. Physics*, Chapter 12 (Amsterdam: North Holland Publishing Co.) (figs. 15, 20, 27).

Figure 3 from Griffel, M., Skochdopole, R. E., and Spedding, F. H., 1956, *J. chem. Phys.*, **25,** 75 (fig 2).

Figures 5 and 12 from Gerritsen, A. N., 1956, *Handbuch der Physik*, **19,** 187 (figs. 55 and 25 a).

Figure 6 from Smith, J. H., and Street, R., 1957, *Proc. phys. Soc. Lond.* B, **70,** 1067 (fig. 2).

Figure 8 from Taylor, A., and Hinton, K. G., 1952, *J. Inst. Met.*, **81,** 169 (fig. 2).

Figure 9 from White, G. K., and Woods, S. B., 1957, *Canad. J. Phys.*, **35,** 346 (fig. 1).

Figure 11 from Allison, F. E., and Pugh, E. M., 1956, *Phys. Rev.*, **102,** 1281 (fig. 8).

Figure 16 from Schmitt, R. W., and Jacobs, I. S., 1956, *Canad. J. Phys.*, **34,** 1285 (fig. 1).

Figure 17 from Gerritsen, A. N., and Linde, J. O., 1952, *Physica*, **18,** 877 (fig. 2).

References

Adenstedt, H. K., 1952, *Trans. Amer. Soc. Metals*, **44**, 949.
Allison, F. E., and Pugh, E. M., 1956, *Phys. Rev.*, **102**, 1281.
Ames, S. L., and McQuillan, A. D., 1954, *Acta Met.*, **2**, 831.
Arrott, A., 1954, *Thesis*, Carnegie Inst. of Technology.
Bacon, G. E., Dunmur, I. W., Smith, J. H., and Street, R., 1957, *Proc. roy. Soc.*, **241**, 223.
Bennett, W. D., 1952, *J. Iron St. Inst.*, **171**, 372.
Coles, B. R., and Bitler, W. R., 1956, *Phil. Mag.*, **1**, 477.
Conybeare, J. G. G., 1937, *Proc. phys. Soc. Lond.*, **49**, 29.
Elliott, J. F., and Legvold, S., and Spedding, F. H., 1953, *Phys. Rev.*, **91**, 28 ; 1954, *Ibid.*, **94**, 1143.
Fast, J. D., 1952, *J. appl. Phys.*, **23**, 350.
Foner, S., and Pugh, E. M., 1953, *Phys. Rev.*, **91**, 20.
Friedel, J., 1956, *Canad. J. Phys.*, **34**, 1190.
Friedel, J., and de Gennes, P. G., 1958, *J. Phys. Chem. Solids* (in press).
Gerstein, B. C., Griffel, M., Jennings, L. D., Miller, R. E., Skochdopole, R. E., and Spedding, F. H., 1957, *J. chem. Phys.*, **27**, 394.
Gerritsen, A. N., 1953, *Physica*, **19**, 61 ; 1956, *Handbuch der Physik*, **19**, 187.
Gerritsen, A. N., and Linde, J. O., 1951, *Physica*, **17**, 584 ; 1952, *Ibid.*, **18**, 877.
Giansoldati, A., and Linde, J. O., 1955, *J. Phys. Radium*, **16**, 341.
Glaser, F. W., and Ivanick, W., 1956, *J. Metals*, **206**, 1290.
Gorter, C. J., van den Berg, G. J., and de Nobel, J., 1956, *Canad. J. Phys.*, **34**, 1281.
Griffel, M., Skochdopole, R. E., Spedding, F. H., 1956, *J. chem. Phys.*, **25**, 75.
Griffith, J. S., 1956, *J. Inorg. Nuclear Chem.*, **3**, 15.
Guthrie, G. L., Friedberg, S. A., and Goldman, J. E., 1955, *Bull. Amer. phys. Soc.*, **30**(i), 42.
Hoare, F. E., and Yates, B., 1957, *Proc. roy. Soc.* A, **240**, 42.
Hofmann, J. H., Paskin, A., Tauer, K. J., and Weiss, R. J., 1956, *J. Phys. Chem. Solids*, **1**, 45.
Hume-Rothery, W., and Coles, B. R., 1954, *Advance Phys.*, **3**, 149.
Jones, H., 1956, *Handbuch der Physik*, **19**, 297.
Justi, E., and Kohler, M., 1951, *Abh. Braunschweig wiss. Gesell*, **3**, 44.
Kasper, J. S., and Roberts, B. W., 1956, *Phys. Rev.*, **101**, 537.
Kasuya, T., 1956 a, *Progr. theor. Phys., Japan*, **16**, 58 ; 1956 b, *Ibid.*, **16**, 45.
Kaya, S., and Nakayama, N., 1940, *Proc. phys.-math. Soc., Japan*, **22**, 126.
Komar, A., and Sidorov, S., 1941, *J. Phys., Moscow*, **4**, 552.
Koster, W., and Rocholl, P., 1957, *Z. Metallk.*, **48**, 485.
Legvold, S., Spedding, F. H., Barson, F., and Elliott, J. F., 1953, *Rev. mod. Phys.*, **25**, 129.
MacDonald, D. K. C., 1956, *Handbuch der Physik*, **14**, 137.
McQuillan, A. D., 1950, *J. Inst. Met.*, **78**, 249.
Meneghetti, D., and Sidhu, S. S., 1957, *Phys. Rev.*, **105**, 130.
Meyer, A. J.-P., 1956, *C. R. Acad. Sci., Paris*, **242**, 2315 ; 1957, *Ibid.*, **244**, 2028.
Meyer, A. J.-P., and Taglang, P., 1956, *J. Phys. Radium*, **17**, 457.
Mott, N. F., 1935, *Proc. phys. Soc., Lond.*, **47**, 571 ; 1936 a, *Proc. roy. Soc.* A, **153**, 699 ; 1936 b, *Ibid.*, **156**, 368 ; 1956, *Canad. J. Phys.*, **34**, 1356.
Mott, N. F., and Jones, H., 1936, *The Theory of the Properties of Metals and Alloys* (Oxford : Clarendon Press).
Mott, N. F., and Stevens, K. W. H., 1957, *Phil. Mag.*, **2**, 1364.
Myers, H. P., 1956, *Canad. J. Phys.*, **34**, 527.

Otter, F. A., 1956, *J. appl. Phys.*, **27,** 196.
Overhauser, A. W., and Schindler, A. I., 1957, *J. appl. Phys.*, **28,** 544.
Owen, J., Browne, M. E., Arp, V., and Kip, A. F., 1957, *J. Phys. Chem. Solids*, **2,** 85.
Pallister, P. R., 1949, *J. Iron. St. Inst.*, **161,** 87.
Potter, H. H., 1937, *Proc. phys. Soc., Lond.*, **49,** 671 ; 1941, *Ibid.*, **53,** 695.
Powell, R. W., 1939, *Proc. phys. Soc. Lond.*, **51,** 416 ; 1953, *Phil Mag.*, **44,** 772.
Pratt, G. W., 1957, *Phys. Rev.*, **81,** 440.
Roberts, B. W., and Swalin, R. A., 1957, *J. Metals*, **9,** 845.
Schindler, A. I., Smith, R. J., and Salkovitz, E. I., 1956, *J Phys. Chem. Solids*, **1,** 39 ; 1957, *Phys. Rev.*, **108,** 921.
Schmitt, R. W., 1956, *Phys. Rev.*, **103,** 83.
Schmitt, R. W. ,and Jacobs, I. S., 1956, *Canad. J. Phys.*, **34,** 1285 ; 1957, *J. Phys. Chem. Solids*, **3,** 224.
Shull, C. G., and Wilkinson, M. K., 1953, *Rev. mod. Phys.*, **25,** 100 ; 1955, *Phys. Rev.*, **97,** 304.
Shull, C. G., and Wollan, E. O., 1956, *Solid State Physics*, Vol. 2 (New York : Academic Press), p. 138.
Skochdopole, R. E., Griffel, M., and Spedding, F. H., 1955, *J. chem. Phys.*, **23,** 2258.
Slater, J. C., 1951 a, *Phys. Rev.*, **82,** 538 ; 1951 b, *Ibid.*, **84,** 179.
Smith, J. H., and Street, R., 1957, *Proc. phys. Soc., Lond.* B, **70,** 1089.
Spedding, F. H., and Daane, A. H., 1956, *Progr. Nucl. Energy* (5), **1,** 413.
Spedding, F. H., Legvold, S., Daane, A. H., and Jennings, L. D., 1957, *Progress in Low Temperature Physics* (ed. Gorter) (Amsterdam : North Holland Publishing Co.), p. 368.
Stoner, E. C., 1947, *Rep. Progr. Phys.*, **11,** 43.
Sully, A. H., Brandes, E. A., and Mitchell, K. W., 1952, *J. Inst. Met.*, **81,** 585.
Tauer, K. J., and Weiss, R. J., 1957, *J. Phys. Chem. Solids*, **2,** 237.
Taylor, J. C., and Coles, B. R., 1956, *Phys. Rev.*, **102,** 27.
Taylor, A., and Hinton, K. G., 1952, *J. Inst. Met.*, **81,** 169.
Trombe, F., 1937, *Ann. Phys., Paris*, **7,** 383.
White, G. K., and Woods, S. B., 1957 a, *Canad. J. Phys.*, **35,** 346 ; 1957 b, *Ibid.*, **35,** 248 ; 1957 c, *Ibid.*, **35,** 656.
Wilkinson, M. K., and Shull, C. G., 1956, *Phys. Rev.*, **103,** 516.
Wohlfarth, E. P., 1948, *Proc. Leeds phil. lit. Soc.*, **5,** 89 ; 1949, *Proc. roy. Soc.* A, **195,** 434.
Yosida, K., 1957, *Phys. Rev.*, **107,** 396.
Zener, C., 1951, *Phys. Rev.*, **81,** 440.

Metal Fatigue

By N. Thompson
H. H. Wills Physical Laboratory, University of Bristol

and N. J. Wadsworth
Royal Aircraft Establishment, Farnborough, Hants.

CONTENTS

PART I

§ 1. Experimental Methods.
1.1. Type of stress.
1.2. Uniformity of stress.
1.3. Control of stress.
1.4. Mean Stress.
1.5. Anisotropy effects.
1.6. Metallurgical effects.
1.7. Surface finish.
1.8. Environment.
1.9. Temperature.
1.10. Speed of Testing.
1.11. Stress level.

PART II

§ 1. General.

§ 2. Metallographic Observations.
2.1. Slip under alternating stresses.
2.2. Observations of incipient cracks.
2.3. Extrusion.

§ 3. Changes in Mechanical Properties.
3.1. Introduction.
3.2. First stage—initial hardening.
3.3. Second stage
3.3.1. Pure metals.
3.3.2. Alloys.
3.4. Bauschinger effect.

§ 4. The Fatigue Limit and Related Phenomena.
4.1. Introduction.
4.2. Experimental results.
4.3. Discussion.
4.4. Further related experiments.

§ 5. Notch Effect and Crack Propagation.
5.1. Introduction.
5.2. General results.
5.3. Non-propagating cracks.
5.4. Theory of crack propagation.

§ 6. Experiments using X-rays.
§ 7. Surface Effects.
7.1. Introduction.
7.2. Mechanical effects.
7.3. Chemical effects.

§ 8. Annealing Experiments.

§ 9. The Effect of Fatigue on Diffusion.

PART III

Discussion.

Preface

It is now more than a hundred years since attention was first drawn to the failure in service of the axles of railway wagons, by a process which has since come to be described as 'fatigue'. In that period, and more particularly in recent years, a very large amount of experimental work has been done, mainly with the object of assessing different materials, and of providing data for designers. By comparison, research workers concerned primarily with the more academic aspects of the behaviour of metals under applied stresses have paid very little attention to the problem of fatigue. This is rather unfortunate; no theory of 'work hardening', for example, can be considered to be satisfactory if it does not permit of an extension which accounts for the behaviour of the metal when the applied stress is removed and reversed—a process which is the first step towards a fatigue experiment.

The purpose of the present paper is to review the current position in respect of some of the basic problems; if it succeeds in arousing a more general interest in such problems, some part of the writers' object will have been achieved. Potential readers are envisaged as being physicists interested in the strength of metals rather than engineers or metallurgists interested in physical speculations. This idea has influenced the content not a little: it has been thought proper, for example, to explain what is meant by a 'rotating cantilever machine' but to assume that the difference between an edge and a screw dislocation is already known. Part I, in fact, sets out very briefly what might be called the background of experimental techniques. Part II summarizes some of the very large number of experimental results, while Part III discusses, briefly, some of the current ideas on the interpretation of these results.

PART I

§ 1. Experimental Methods

Before considering the results of experimental work on fatigue, which is our main concern, it is proposed to describe very briefly some of the experimental methods. This procedure is considered necessary since, in this field of study more than in most, the conclusions drawn are likely to be influenced by the technique adopted. In addition, it will serve to familiarize the non-specialist reader with some of the vocabulary.

A typical fatigue experiment consists of subjecting a specimen to repeated cycles of stress until, after many repetitions, the specimen breaks. The specimen may be a structure—ranging from a single rivetted joint to a complete aircraft; work of this kind will not concern us here. Alternatively it may be a single piece of metal of prescribed form— a test piece; in this case it is the properties of the material itself which are under investigation; this is our present concern. The successive cycles of stress may all be (nominally) identical, or they may vary in some regular or irregular manner,

according to a pre-determined programme: the latter procedure (programme testing) is receiving increasing attention in connection with the performance rating of aircraft, but only the former type of experiment will be discussed here. The number of cycles of stress that elapse before failure may range from 10^2 to 10^9: the region of greatest technical interest, and in which most work has been done, is about 10^5 to 10^8. The size of the specimen may range from less than a millimetre to 10–20 cm in diameter. Other observations that can be made in addition to the number of stress cycles to failure will be mentioned later. We proceed now to list the ways in which one fatigue test can differ from another

1.1. *Type of Stress*

The applied stress may be uniaxial, biaxial or triaxial. The first is exemplified by (i) a bar tested in alternating axial tension and compression (push–pull); a number of commerical fatigue machines operate in this way. (ii) A cylindrical rod tested in ' rotating bending '; this is the cheapest and commonest technical method of fatigue testing. The cylinder is rotated and is loaded transversely in a fixed direction. The surface layers experience a sinusoidally varying tension–compression cycle. (iii) A bar or flat strip tested in ' reverse bending '; this is also a fairly common technical method of testing. The strip is clamped at one (or more) point and constrained to flex to and fro. Again the surface layers experience an alternating tensile–compressive stress.

A biaxial stress is met in its simplest form in the alternating torsion test. The specimen, usually cylindrical and either solid or hollow, is clamped at one end, while the other end executes torsional oscillations.

If a force, rather than a pure couple, is applied to the free end of such a specimen, then combined bending and torsion can be produced and, by suitably choosing the point of application of the force, all conditions intermediate between pure bending and almost pure torsion can be achieved. A biaxial stress can also be produced in a thin walled cylinder by applying a fluctuating internal pressure; if an axial load is applied externally in synchronism it is possible to vary the ratio of the two components.

Experiments on triaxial stresses are very rare (except in so far as local states of triaxial stress are always produced incidentally when a notched specimen is used, see § 5). One technique is to subject a thick-walled cylinder to a fluctuating hydrostatic pressure (see Morrison *et al.* 1956).

By far the largest amount of experimental work has been done using machines that produce uniaxial stresses. The effort involved in covering more complex stress systems as a matter of routine is in general prohibitive, and such investigations as have been made have usually been carried out with reference to the mechanism of fatigue rather than for the evaluation of materials. It may be that work of this kind will ultimately prove of great value in solving the problems of fatigue but, partly because it lies outside the present authors' sphere of competence, and partly to avoid too much complication, it will not be considered in any detail.

1.2. *Uniformity of Stress*

In many experiments the stress is macroscopically uniform along the length of the specimen (e.g. axial push–pull, reverse torsion and some types of rotating bending and reverse bending machines), or else varies only comparatively slowly along the length. Such test-pieces are usually called ' plain ' or ' un-notched '. In other cases some singularity is deliberately introduced which gives rise to a local concentration of stress in its neighbourhood. The singularity may take the form of a circumferential groove, a transverse hole or an abrupt change of section (fillet). For simplicity, all such test-pieces are referred to as ' notched '. The reasons for using notched specimens and the results obtained are considered in more detail in § 5. It should be noted, however, that even with a nominally plain test-piece it is impossible to avoid some stress concentration at the ends, where it is held in the grips of the testing machine. With suitable design, such effects can be reduced to such a level that they do not affect the validity of observations made in the central portion ('gauge length ') of the test-piece.

Confining our attention for the moment to ' plain ' test-pieces, we note that on a macroscopic scale the stress may either be uniform throughout the volume under test, or it may not. (On the scale of the grain-size of the material under test the stresses will always be non-uniform.) Uniform stress is very difficult to achieve. In a push–pull test one can get near to it if the (parallel) centre portion of the specimen is long enough so that end effects are small: but in an effort to achieve this result the specimen may be made so slender that it tends to buckle under compression—which again implies non-uniform stressing. In addition it is very difficult on some types of machine to ensure that the loading is truly axial both on the tensile and compressive half-cycles. Attempts have been made to obtain uniform stressing in pure shear for observations on very slow alternating stresses, but not, as far as is known, for fatigue testing of the more usual kind. It is, in practice, more difficult than push–pull, and equally complicated by end effects. Alternating torsion of a hollow cylinder, whose wall thickness is small compared to its radius approximates to a uniform shear.

All other forms of testing produce non-uniform stresses. In particular, the two most usual techniques—rotating bending and reverse bending—produce stresses which range from zero on the axis to a maximum on the surface. The same is true of torsion tests, if the specimen is a solid bar, as is usual. It would be surprising if the difference between these conditions and those of uniform stressing had no effect on fatigue phenomena, and, indeed there is no doubt that such differences exist. For example, the fraction of the total life for which an obvious crack is present in the specimen is greater in the case of non-uniform stress—as might be expected. The relationship between the two types of test is however not simple and, at the moment, not completely understood, although empirical relations of restricted validity have been suggested.

Besides the radial variation just mentioned, the stress may be either uniform or non-uniform along the length of the specimen. (We are not,

of course, at the moment considering notched specimens.) These considerations apply particularly to rotating bending and reverse bending tests. The simplest arrangement, with a specimen clamped at one end and loaded at the other clearly gives rise to a longitudinal stress gradient, if the specimen is of constant cross section; such an arrangement is very common and is described as ' single point loading '. By appropriately tapering the specimen towards the free end, a considerable region of constant stress can be produced, but such specimens are more costly than simpler shapes.

In a rotating bending test, by applying two equal loads in opposite directions to the free end of a uniform bar clamped at the other end, a region of constant stress can be produced (two-point loading). Some linkage mechanism usually ensures equality of the two loads. A similar result is achieved by four-point loading, in which the bar is supported at the two ends and subjected to two equal and symmetrically disposed loads in the same direction. By using a hollow cylinder with thin walls tapering in thickness towards the free end, and single point loading, an approximation to uniform stressing can be achieved, but again the specimens are rather costly. In those reverse bend tests where the specimen is either a fixed–free or a free–free reed, driven at its resonant frequency, the stress distribution is that appropriate to the particular mode excited.

The importance of these longitudinal variations of stress is particularly in connection with statistical problems. All fatigue tests have something of the character of testing a chain and recording the strength of the weakest link. The results are more subject to variation than are those of many mechanical tests –although one suspects that a knowledge of this fact is sometimes made an excuse for slovenly experimentation or bad planning. On this basis any specimen of finite size might be regarded as a ' sample ' of the population comprising all the material of that particular batch. The smaller the volume (or area ?) of material which is subjected to the maximum stress, the smaller is the ' sample ' which is being tested; one might therefore expect a greater variation in the results of individual experiments but a higher mean value. A number of workers have considered such statistical aspects of fatigue testing in some detail, and some have tried to explain as purely statistical results some phenomena which others believe to represent real physical effects. These statistical questions are not discussed further here: those interested may be referred to the work of Afanasiev (1940, 1941), Weibull (1949, 1952, 1954, 1955), Freudenthal (1946), Epremian and Mehl (1952), McClintock (1955), etc.

1.3. *Control of Stress*

Most fatigue experiments are run under conditions which ensure that the peak values of the applied *stress* are approximately constant throughout the test—a condition described, for brevity, as a test at constant stress. (More exactly, the applied *load* is kept constant: the accuracy to which this implies constant stress depends on the extent to which the cyclic stress–

strain curve for the different parts of the specimen changes during the run.) These conditions apply to almost all rotating bending tests and most push–pull types.

Alternatively the amplitude of *strain* may be kept constant; this is not uncommon in reverse bend tests, where one end of the specimen is clamped, and the other end constrained to move through a fixed excursion. Sometimes the results of such observations are, in fact, presented in terms of strain amplitude. More often, however, they are converted into stresses merely by multiplying by an elastic modulus: such a procedure is less misleading if, as is sometimes done, the result is referred to as a ' nominal stress '. In some work the strain amplitude is deliberately adjusted several times during the course of a test, in an attempt to maintain the stress amplitude approximately constant despite the changes taking place in the properties of the specimen.

Rarely, with some electronic devices, the power input to the specimen is held constant during a test; both stress and strain will then change to an extent which depends on the variation of damping capacity of the material.

Some special techniques of fatigue testing have been proposed from time to time in which the stress (or strain) is deliberately changed (usually increased) either continuously or discontinuously during a test. Such techniques are usually designed to expedite the processes of routine testing and will not concern us here.

Finally a word must be said about the way in which the load is applied at the beginning of an experiment. There are, broadly, two possibilities. In most rotating bending tests and many push–pull machines the stress is built up from zero to its maximum value with the frequency of the oscillations at its normal value. Alternatively, as in many reverse bend machines operating at constant strain, the full amplitude is achieved in the first half cycle, while the speed is gradually built up from rest to its normal running value. There is little doubt that these differences will produce different crystal textures during the early stages of a fatigue test although only a little direct experimental work seems to have been done. Whether the differences will seriously affect the later stage of a test is more doubtful; no careful comparison appears to have been made (but see p. 148).

1.4. *Mean Stress*

In all that has been said so far, it has been tacitly assumed that the mean stress is zero, i.e. the maximum tensile and compressive stresses are equal. This is the commonest type of fatigue test. However it is of considerable technological interest to know how a material behaves when the cycle of stress is not symmetrical, and many such observations have been made. The superposed mean stress is usually tensile, although some examples have been reported of fatigue failures in push–pull when the stress was entirely compressive during the whole cycle (see Wallgren 1953.) The ratio of mean stress to stress amplitude commonly lies within

the range from zero to unity, although some observations have been made with a small alternating stress superposed on a comparatively large steady stress; such experiments are more nearly akin to creep than to fatigue (see Kennedy 1956), Allen and Forrest 1956).

The presence of a superposed mean stress usually has the effect of reducing the fatigue life for a given stress amplitude. The stress amplitude is, very roughly, still the dominant factor, but the effects of the mean stress are by no means negligible. If the results of x-ray investigations are considered, however, the presence of even a small mean stress can exert a considerable influence. With some types of equipment it is very easy to apply such a small mean stress unwittingly, and it may be that this circumstance explains the discordant results obtained by the earlier workers who used x-ray methods. We return to this point again in § 6, but, apart from this, lack of space and a desire to avoid excessive complication will prevent any further reference in this article to the effect of a superposed mean stress.

1.5. *Anisotropy Effects*

The material from which a fatigue specimen is made is quite likely to be anisotropic. If it has been rolled or extruded, the individual grains are likely to be much elongated, and inclusions or cavities will be drawn out into long 'stringers'. If it has been re-crystallized after such treatment, or even if it is cast metal, there may be a preferred orientation of the individual grains. Specimens cut from rolled sheet, for example, may give different results according as the length of the specimen lies along or across the rolling direction. The differences may be large enough to be of considerable technological importance but their main interest in so far as we are concerned here is that they serve to confuse still further an already complex subject, and make more difficult a comparison of the results of different investigations.

1.6. *Metallurgical Effects*

Under this heading we may include the whole previous thermal and mechanical history of the material from which the specimens are made. Many of the earlier papers and, regrettably, some modern ones also, give completely inadequate accounts of the nature of the material on which the observations are being made. The chemical composition is obviously important—although no one could blame the author of a paper for not specifying the amount of a trace element which was only shown to be important by later work (e.g. nitrogen in steel). The nature and amount of working, cold or hot, the temperature and duration of annealing processes, rates of heating and cooling and even the time elapsed between these operations and the carrying out of the test may all be important in some cases.

In so far as such treatments give rise to internal stresses either deliberately (e.g. case-hardening) or accidentally (quenching stresses) their

importance is obvious; but again, such effects are not our present concern. Any treatment which increases the 'hardness' of the material (using the term loosely) will also be important, since it will increase the level of stresses needed to produce slip in the metallic crystals: as we will see later, the fundamental processes of fatigue are largely associated with slip in the grains.

It is also reasonably well established that the grain size of the material is a relevant factor although one must be cautious lest any result attributed to a difference in grain size be due to some other consequence of the thermal and mechanical history that was necessary to produce the different grain sizes. It appears possible that both the absolute size of the grains, and their size relative to the scale of the test piece (particularly with notched specimens) may be concerned.

Another and rather less obvious point is that if the material is in any way metallurgically unstable, then during a fatigue test, changes may take place much more rapidly than in the resting material. One or two examples have been reported (see § 9), but much more could profitably be done; it is possible that phenomena of this kind may be not only important in connection with the properties of complex technical alloys, but may also throw light on the mechanism of fatigue itself.

1.7. *Surface Finish*

Since a fatigue fracture usually starts at the free surface of the test piece, the nature of this surface is an important factor in fatigue investigations. We refer not so much to special surface treatments, such as nitriding, shot peening, surface rolling, electro-plating, etc.—although these are technically important and have been considerably investigated—but more to the incidental surface treatment that may be given during the manufacture of a test piece. Relevant factors are the surface roughness—the direction as well as the severity of residual scratches being important—and also the depth and severity of the surface cold work that results from machining. Until the basic mechanism of fatigue is better understood it would seem that the wisest plan would be to avoid these complications as far as possible. One way, perhaps the best way, to achieve this is to machine the surface with progressively finer cuts, to polish the machined surface with progressively finer abrasive, and to finish the polished surface with an electro-polishing technique wherever possible. This procedure is tedious, and not always practicable; for example, it is difficult to ensure the same kind of surface finish on a plain specimen, and at the bottom of a very sharp notch. But where it is not followed, the possibility of the results being affected by surface finish must be borne in mind.

1.8. *Environment*

If a fatigue test is carried out in an environment that is obviously and deliberately corrosive, the phenomena are usually referred to as 'corrosion fatigue'; such effects are outside the scope of this article. But there are,

in addition, a number of reliable results showing, for example, that the absence of air, or immersion in paraffin can have a considerable effect on the fatigue of at least some metals. Since almost all normal tests are carried out in ordinary laboratory air, we can at least say that this factor does not complicate the comparison of one set of results with another. The question of why the atmosphere should affect fatigue is taken up again in § 7.

1.9. *Temperature*

The temperature is an obvious variable likely to affect fatigue. Many investigations have been made above room temperature, but very few indeed at low temperatures. This is likely to be a fruitful field of study in the future. Apart from general effects which may be common to all substances, we may expect special effects, particularly with alloys, which may be quite striking, and peculiar to the material under investigation. The common system of iron + carbon, for example, shows an anomalous behaviour at only moderately elevated temperature (§ 4.4).

Apart from temperature changes deliberately produced, the energy dissipated in the specimen during a fatigue test may itself raise the temperature. With a large specimen of a material which has a high damping capacity, a test carried out at high stress may produce a temperature rise of several hundred degrees. The amount of this temperature rise, and the distribution of temperature in the specimen, will depend not only on the properties of the material itself, but also on the conditions of test, such as the shape and size of the specimen, the stress distribution, and the speed of testing (number of stress cycles per second). Unless the actual specimen temperature is measured (or at least estimated!) quite erroneous deductions may be made from a comparison of different experiments.

1. 10. *Speed of Testing*

By this term is usually understood the number of cycles of stress per minute. Normal engineering practice is to run machines at about 1500 to 6000 c.p.m. (cycles per minute) although with the development of faster running machinery there has been an increasing interest in higher testing speeds.

1.11. *Stress Level*

As already indicated, the amplitude of the cycle of stress to which the specimen is subjected is the most important single variable in determining its life.

PART II

§ 1. General

The results of a series of fatigue tests are usually exhibited as a graph of stress, plotted on either linear or a logarithmic scale, against the number of cycles to fracture, plotted logarithmically (usually called an S–N curve). Apart from the convenience of the experimenter, and of the designer who

uses the data, there appears to be no reason why stress should necessarily be taken as ordinate. A possible alternative which, in the light of later discussion might perhaps be of greater significance, would be the cyclic strain. The practical problems of making experiments on this basis would be considerable, and only one or two published papers deal with the possibility: it might perhaps repay more attention.

Fig. 1

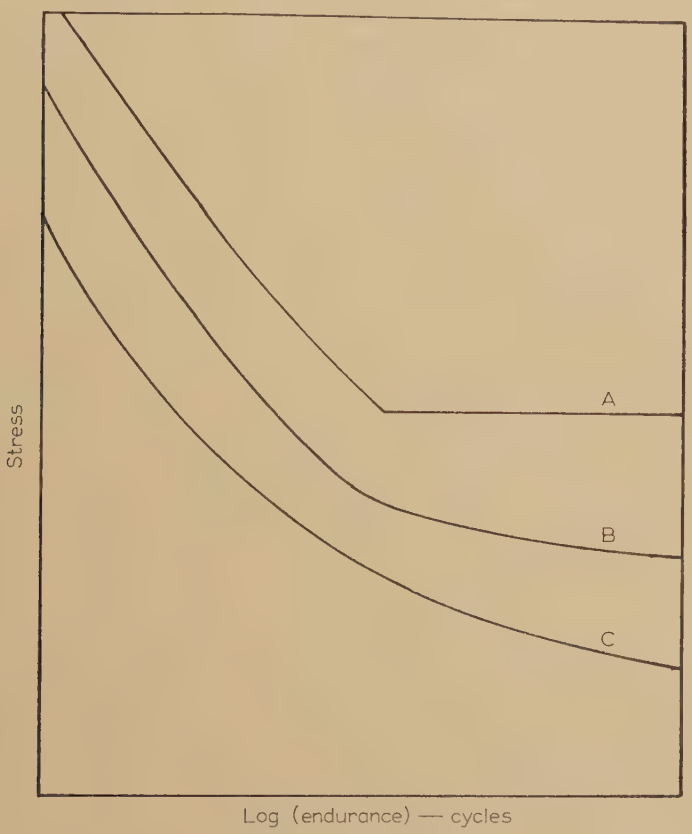

Typical fatigue curves.

Characteristic forms for S–N curves are shown in fig. 1. Some materials show a more or less well defined elbow in the curve beyond which it is, within the limits of experimental error, horizontal (*A*). This stress, below which fatigue failure does not occur in any accessible time, is called the *fatigue limit*. For materials which do not show such a limit, a similar quantity called the *endurance limit*, is defined as the stress needed to produce failure in some specified (large) number of cycles (often 10^8). The same term is also used, more loosely, to denote a stress below which the specimen will last for a large number of cycles, without specifying

exactly how many. In many cases the S–N curve, although not horizontal, has only a very small slope beyond the endurance limit (B).

One must ask whether the total *number* of cycles of stress is the proper measure of endurance. To a first approximation this appears to be so. Over a fairly wide range, the frequency of the variations has only a small effect. The lower limit of practicable testing speeds is set by the excessive time needed to complete a useful number of stress cycles: speeds down to 10 cycles per minute have been used. More interest has attached to the other extreme, and there are a few isolated experiments up to $\sim 10^6$ c.p.m. The practical difficulty here lies in evaluating the stress that is being applied. The available evidence suggests that, if the speed is varied over a sufficiently wide range, there is a tendency for fatigue strength to increase as frequency increases. This was reported in an early paper by Jenkin and Lehman (1929) and has since been confirmed by Wade and Grootenhuis (1956) up to 200 000 c.p.m., and by Lomas *et al.* (1956) up to 150 000 c.p.m. There are however considerable differences between the detailed results of the different observers which are possibly to be traced to the difficulty of stress calibration already mentioned.

In addition to any general effect that may exist, there will also be specific effects peculiar to certain materials tested at temperatures sufficiently high that metallurgical changes (either spontaneous or induced by the fatigue test itself) are in progress during the test. Under these conditions the absolute duration of the test in minutes will be of importance, as well as its duration measured in numbers of stress cycles. The so-called anomalous speed effect in mild steels in the temperature range 150°–350°c is to be included in this category (see § 4.4).

In one or two cases it has proved impossible to obtain an S–N curve of any kind. Either the specimen broke immediately on reaching the desired level of stress (or before it was reached) or else it did not break at all. Such behaviour has been reported for single crystals of zinc tested at the temperature of liquid oxygen (Fegredo 1957) and some similar results have been obtained in a preliminary investigation of γ brass by Sines (private communication). It is particularly interesting to note that Fegredo's crystals were 'hardened' by the fatigue stressing, in that the static tensile properties of the crystal were very much altered. Other brittle materials do not seem to have been investigated, but it is perhaps relevant to note that in McCammon and Rosenberg's (1957) observations on fatigue at low temperatures, both zinc and iron show abnormal S–N curves, fatigue occurring only in a very restricted range of stress (see also Gough and Cox (1930a on the fatigue of antimony).

The production of a S–N curve represents about the least that can usefully be done in an experiment on fatigue, and in many routine tests it is all that is necessary. More than this will be needed before the mechanism of fatigue is understood. An examination of the fracture is an obvious next step. A characteristic feature of a fatigue fracture is that it takes place without any obvious plastic deformation. The fracture

surface runs, in simple cases, approximately normal to the principal tensile stress: for example in a push–pull test it is approximately a plane normal to the tensile axis, while in a torsion test the fracture surface tends to be helicoidal. With more complex stress systems, no simple rule can be given. In an individual grain the crack often lies along a slip plane, or a series of slip planes, and this would suggest that the shear stress might be the important consideration. McClintock (1952b) has made one suggestion for reconciling these apparently discordant observations.

An examination of the fracture surface itself is sometimes made; this usually reveals clearly the point or, more rarely, points of origin of the fracture, and can be valuable in what may be called technical post-mortems. A more detailed examination of the fracture surfaces reveals some evidence of local plastic deformation but such a procedure is less likely to give useful information in fatigue than in other fields of study, since the surfaces may well have been affected by rubbing or banging together after fracture.

There is a general impression that fatigue fracture takes place suddenly, after a large number of cycles of stress, and without any previous warning. This is, at best, no more than a half truth. Most testing machines incorporate an automatic cut-out which stops the test when fracture is imminent. Such devices usually depend on the reduced stiffness of a partly fractured member, or on the out-of-balance of the resulting motions: more rarely, the increased power needed to maintain the motion in the presence of a crack is used to operate the device. It is not in general possible to make devices of this kind sufficiently sensitive to detect the earlier stages of the formation of the fatal crack. In the later stages the crack does, indeed, grow very quickly (see § 5) but its growth will be greatly influenced by the macroscopic re-distribution of stress due to its own presence. Studies on the more interesting earlier stages tend to be rare owing to the difficulty of detecting an incipient fatigue crack when small. (The obvious trick of deliberately introducing a stress concentration, so that one knows where to look for the crack does not really help very much, since it simultaneously introduces unknown complications into the stress field.) There are a number of devices available to assist the early detection of fatigue cracks: these include the use of fluorescent liquids (to be drawn into the crack during stressing and subsequently detected when the surface liquid is removed) and magnetic methods (to reveal the discontinuities in magnetic flux which are found at a crack in a ferromagnetic specimen). The alternative appears to be the patient searching of the whole specimen surface, suitably prepared, with a microscope. In addition to measurements of the rate of crack growth, metallographic observations relating to path to grain and twin boundaries, slip lines, etc. are of interest; such studies are summarized in § 2.

The application of x-ray techniques to fatigue has given some interesting results which are summarized in § 6; most of the work has been done by

observing the reflections from 'a typical point on the specimen'. The difficulty of anticipating the path of the crack and making more detailed observations on the changes which precede cracking are even worse with x-rays than with optical methods, and, as far as is known, this has never been done.

In general, observations on the effect of fatigue on most physical parameters is likely to produce information only indirectly connected with the central problem of fatigue *fracture*. This is because most quantities represent an average taken over an appreciable volume of material, whereas the development and progress of a fatigue crack is concerned primarily with events at a singular point in the specimen. There are in fact very few reports on the effect of fatigue on electrical, magnetic and thermal properties: such effects, if they exist, will be very small.

The so-called structure sensitive properties such as mechanical strength represent a more hopeful line of investigation. The aspect which has received most attention is the measurement of internal friction (damping, hysteresis loop, cyclic plastic strain:—although perhaps not identical, such terms all relate to the same physical phenomenon). This has the advantage that measurements can be made without interrupting the progress of the fatigue test, although sometimes this is not done. A second possibility is to measure changes in 'hardness' caused by fatigue stresses. This may in some contexts mean the resistance of the specimen to a static stress of the same kind as that used in fatigue, e.g. a push–pull test is stopped and a 'static' tensile test is carried out on the partly fatigued specimen. Alternatively, it may mean the resistance to a quite different set of stresses, e.g. those imposed by an indentation hardness tester. Work of this kind is discussed in § 3.

The effect of fatigue on the metallurgical condition of the test piece has been remarked in only a few instances (see, for instance, § 9). The changes observed need to be looked for with care, and it may well be that further work on these lines would be worthwhile. In a similar category is the measurement of stored energy of deformation in a fatigue specimen: very little indeed has been done on this most promising line.

§ 2. Metallographic Observations

2.1. *Slip under Alternating Stresses*

Ewing and Humphrey (1903) were perhaps the first to make a detailed study of the surface appearance of specimens during fatigue tests to investigate the formation of cracks. They tested annealed Swedish iron in rotating bending and photographed the surface at intervals during the test. The surface of the specimen was polished and then etched to remove the work hardened surface layer before starting. The stresses used were below the yield point of the original material. Very few slip lines were produced by the first few thousand cycles but as the test progressed more slip lines formed. The new lines appeared close alongside the existing

ones, producing bands of slip. These bands grew wider and more intense as the test continued, but between them there were large areas in which no slip was visible. The appearance was quite different from that of a specimen strained unidirectionally in which the slip lines were much more evenly spaced. The roughened surface of the fatigue slip bands was often 'decidely above the level of the other parts of the crystal'. At lower stresses there were fewer bands and they tended to be shorter and less intense than at higher stresses. Fatigue cracks formed in the broadened slip bands but it was difficult to decide at what stage they formed as both slip bands and fine cracks looked dark. To distinguish between the two, the specimen was polished mechanically and etched occasionally during the test. This removed the surface roughness associated with the slip bands but widened the cracks, making them more visible. In this way it was found that many slip bands had cracks in them at the end of the test, the proportion being higher in specimens which had longer lives. The cracks spread across the grains, sometimes jumping from one slip band to another, and then spread across neighbouring grains.

Since 1903 many investigators have studied the fatigue slip bands formed in many other pure metals. They find that the description given by Ewing and Humphrey (1903) applied equally well to almost all pure metals.

Gough and co-workers investigated the slip mechanism in more detail. They fatigued single crystal specimens of aluminium (Gough, Wright and Hanson 1926, Gough, Hanson and Wright 1927, Gough 1928 a), silver (Gough and Cox 1931), copper (Gough 1933), zinc (Gough and Cox 1929, 1930 b), iron (Gough and Hanson 1923, Gough 1928 b), antimony (Gough and Cox 1930 a) and bismuth (Gough 1933) in torsion. The results are summarized by Gough (1933). Torsion has the advantage that the stress acting on the various planes differs in different parts of the crystal and thus, if the various parts do not interact appreciably with each other, a single test corresponds to uniform stress tests on a large number of crystals of different orientation but all with identical impurities, structure etc. For an investigation of slip systems this is a big advantage. It was found that the assumption that the interaction between different parts of the crystal could be neglected was valid. The slip planes and directions which operated in fatigue were the same as those operative in unidirectional tests, and the active slip system in each part of the crystal was the system which had the largest shear stress on it at that part. Different systems operated at different places round the crystal and the transition from one to another was very sharp.

Aluminium was the face-centred cubic metal most thoroughly investigated. It slipped on the close-packed $\{111\}$ planes in the close-packed $\langle 110 \rangle$ directions. If the crystals were fatigued at a stress a little below their endurance limit slip bands appeared on the surface on the predicted planes. As the stressing continued the bands became more numerous. The rate of slipping could be seen by polishing the surface at intervals and

watching the slip bands reappear. When the stress was below the endurance limit a stage was reached when no further visible slip occurred and the stressing apparently had no effect. The places which continued slipping longest were those with the greatest resolved shear stress on the active slip system. If the stress were above the endurance limit the rate of production of slip bands still decreased during the test, but usually did not drop to zero before cracks had appeared and the specimen had broken. The cracks occurred in the region which had slipped most extensively, and started in the visible slip bands.

In reversed torsion tests the maximum shear stress and the maximum range of shear stress occur on the same slip planes. To determine which of these was responsible for the slip under alternating stress, two single crystals were tested in reversed torsion with a superimposed steady tensile or compressive end load (Gough 1933). The maximum shear stress now acted on a different plane from that with the maximum range of shear stress. It was found that in the very early stages of the test the absolute value of the maximum shear stress determined the slip system but that very soon the slip changed to the plane with the maximum range of stress and most slip occurred there. Fatigue cracks eventually formed in the latter plane. Thus in a fatigue test it is the *range* of stress which is principally responsible for slip and failure. Experiments on other face-centred cubic metals, silver and copper, gave essentially similar results.

When α-iron was tested the slip bands had a rather different appearance, in that, as in unidirectional tests, the slip plane was ill-defined. Apart from this difference slip occurred much as in the face-centred cubic materials. Fatigue cracks formed in the positions of maximum resolved shear stress.

Zinc was tested by Gough and Cox (1929, 1930 b) as an example of a hexagonal metal. Slip occurred on the close packed basal (0001) plane in the close packed $\langle 10\bar{1}0 \rangle$ direction. In addition twins were formed and these slipped on their basal plane. The fatigue crack took one of three paths. It either went along the basal plane of the crystal, along the basal plane of the twin or along the twin-matrix interface. Bullen (1953) fatigued polycrystalline zinc at various stresses and found that twin formation was most marked during tests at high stress. At lower stresses it was less common but considerable movement of existing grain boundaries occurred. The boundaries moved in jerks and left a black line behind in each place at which they paused. Movements of up to 150 μ occurred. Sometimes cracks formed in these boundaries. Similar movements of twin boundaries were seen in cadmium crystals by Thompson and Wadsworth (1957) and again cracks formed in the boundaries. This mode of deformation does not appear to occur in face-centred cubic metals although grain boundary migration has been observed (see p. 91).

Two metals with a rhombohedral lattice, antimony and bismuth, were tested: neither showed any slip bands, but numerous twins were produced. Cracks occurred along the cleavage planes and also along the twinning

planes. It was found that after cracks had formed they spread very slowly in spite of the apparently sharp ends and the brittle nature of the metals.

In unidirectional tests, slip bands seen under low and moderate magnification appear generally as quite straight sharp lines which are, in the main, fairly evenly distributed over each grain. (We must except iron and other body-centred cubic metals where the slip plane is often ill-defined.) The slip bands produced in fatigue are more wavy and irregular, and although their general direction is that of the trace of a crystallographic plane, they are clearly not exactly straight. Moreover, as the test proceeds, new slip lines tend to form beside the old ones, and the bands of slip become very broad with the intervening regions apparently free from slip. Figures 2 (*a*) and 2 (*b*) (Pl. 1) illustrate this difference.

Under the electron microscope the slip bands formed in unidirectional tests are seen to consist of parallel straight lines of various heights (Kuhlmann-Wilsdorf *et al.* 1952, Kuhlmann-Wilsdorf and Wilsdorf 1953, Seeger *et al.* 1957) whereas the slip bands formed in fatigue tests have a much less regular appearance and usually the individual slip lines, when these are visible, appear to be curved (Craig 1952, Forsyth 1953 a, Wever *et al.* 1955, Love 1952). The cause of this difference is not clear.

2.2. *Observations of Incipient Cracks*

There have been many subsequent researches which have attempted to investigate the slip processes in more detail and to discover how and when the cracks form. In most tests large cracks are only present in the specimen for the last few per cent of the life but small cracks may be present considerably earlier. They have been detected either by variations on the repolishing and etching technique used by Ewing and Humphrey or by taking replicas of the surface and examining these.

Thompson *et al.* (1956) studied the fatigue of annealed copper and outlined the growth of cracks from an early stage of the test. The specimens were stressed in push–pull and cracks were detected by electropolishing the surface. The usual slip bands appeared early in the test and became more numerous as the test proceeded. A light electropolish (removing a layer 2μ thick from the surface) sufficed to remove the roughness associated with the slip bands. This normally made the bands invisible but a few became accentuated and were called 'persistent slip bands'. The cracks eventually grew from these persistent bands and it seems probable that they themselves were in fact cracks. The first appeared after about 5% of the specimen life (of a few million cycles). Figures 3–6, Pl. 2, show the early stages of the development of a crack, while fig. 7, Pl. 2, shows a crack which eventually caused the failure of the specimen. This picture was taken after 42% of the specimen life. Thus almost the whole of the test was spent in propagating cracks, one of which had spread out of the grain in which it started before half of the test had elapsed. The cracks frequently started in a slip band which lay very close

to a twin boundary (or perhaps in the twin boundary itself). This observation has been confirmed by more numerous observations made later on copper by Bown (unpublished). The reason for this is not known: but clearly the twin boundary is not an essential, since some cracks do start in the middle of grains, and a similar sequence of events has been observed in tests on single crystals.

If the specimens were electropolished repeatedly, the persistent bands were eventually removed. No new ones were ever uncovered during this process, showing that they only formed on the surface of the specimens in spite of the macroscopically uniform stress throughout its volume. Most of the marks were not more than 10 microns deep and after 25% of the life of polycrystals none were deeper than 30 microns. If these were polished off and the specimen re-tested, the slip bands reformed and became persistent again. In many cases the pattern of the new slip lines reproduced in some detail that which had been removed, showing that slip was still active on the same planes. These new marks could be removed by a similar electropolish and the process could be repeated many times. After 2·25 times the normal life of one specimen (well outside the experimental scatter) the specimen was unbroken and looked as good as new. This showed that the fatigue damage only occurred at the surface, an idea further supported by the considerable effect of the surrounding atmosphere on fatigue life. (This effect is discussed in more detail in § 7.)

There is however some unresolved confusion about the occurrence and interpretation of persistent slip bands. Kemsley (1957a) applied a similar electropolishing technique to copper specimens and was only able to find persistent slip bands in specimens fatigued at low stresses (giving lives of about 10^7 cycles) and then only if they were electropolished in the early stages of the test. It is possible that small differences in polishing technique or in the impurities present caused this difference.

The metallography of iron during fatigue is of particular interest in view of the definite fatigue limit usually found for such material. One might reasonably expect some marked difference in appearance according as the stress is below or above the limit. This was investigated by Gough and Hanson (1923) who fatigued Armco iron (0·012%C) in rotating bending. They fatigued a number of specimens at constant stress and photographed the surface, but made no attempt to detect cracks in the early stages, or to watch them grow. Specimens fatigued above or just below the fatigue limit showed essentially the same slip band structure, the most common form at low stresses being a mass of fine slip covering most of some grains with other grains clear. Specimens run at lower stresses showed less slip. The observation that there is no difference between the appearance of specimens fatigued above or below the fatigue limit is confirmed by Hempel and co-workers (Wever *et al.* 1955, Hempel 1956a, b). Specimens of polycrystalline 99% iron with 0·09%C and 0·009%N were fatigued in reversed bending and showed a fatigue limit of 18 kg mm^{-2}. A number

of specimens were run at stresses below the fatigue limit and their surfaces examined. Slip bands formed in the usual manner on a specimen run at 17·5 kg mm $^{-2}$. They became more numerous as the test proceeded (fig. 8, Pl. 3) and the electron microscope showed a very rough surface with some narrow ditches in the slip bands, fig. 9, Pl. 4. This specimen was however unbroken after $4{\cdot}6 \times 10^7$ cycles and so was apparently stressed below its fatigue limit. If lower stresses were used slip bands appeared more slowly. At 16 kg mm^{-2} they took about 3×10^4 cycles to appear while at 13·8 kg mm $^{-2}$ none were visible after $14{\cdot}8 \times 10^6$ cycles. This slower rate of production may correspond to the considerably slower rate of energy dissipation at the lower stresses (see § 3.3), but it is clear that slip still occurs. It is apparent from these experiments that specimens stressed just below the fatigue limit cannot be distinguished from those fatigued above it by their surface appearance. The mechanism producing the fatigue limit does not work by preventing slip bands from forming or ditches from forming in them.

Clearly more work is needed to find at what stage the discontinuity representing the fatigue limit occurs. Experiments on single crystals might be useful but those which have been done to date (Gough 1928 b, McClintock 1952 a, Lipsitt and Horne 1956 b, Hempel *et al.* 1957) have not included the determination of the fatigue limit.

Hunter and Fricke (1954) have studied the fatigue of aluminium and aluminium alloys and watched cracks form in the slip bands. They found that in pure (99·9%) aluminium tested in reversed bending the first slip appeared after about 0·5% of the fatigue life, and that the rate of production of slip lines decreased after about 10% of the life. They did not electropolish their specimens and were unable to detect cracks appreciably before failure. If magnesium were added to the aluminium (Hunter and Fricke 1955) the metal was hardened and its endurance increased. Even 1% of magnesium increased the endurance limit (for 10^8 cycles) to a stress greater than that needed to give a life of 5000 cycles on pure aluminium. At these higher stresses slip first appeared even earlier in the test than in pure aluminium specimens of comparable life and some cracks were visible after 1% of the total life. The rest of the time was spent propagating the cracks. Further magnesium additions strengthened the metal further. Slip was visible very early in the test, sometimes after only one cycle, but remained scarce and few cracks formed. These spread slowly and over 90% of the test was still spent in their propagation.

Some experiments on pure (99·99%) aluminium were made by Smith and Harries (Smith 1957). They fatigued annealed specimens in reversed bend at 1500 c.p.m. and found virtually the same sequence of events as were found with copper and iron, incipient cracks forming after 5% of the life. The chief difference was that some grain boundaries became persistent in the same manner as slip bands and often developed into macroscopic cracks. Grain boundary cracks were more common at 300°C than at

room temperature and were fewer at −73°c and completely absent at −180°c. As would be expected a reduction of test speed (to 70 c.p.m.) had the same effect as an increase in temperature. The lives of these specimens were considerably shorter than those of Thompson *et al.'s* copper specimens and it is possible that the greater preponderance of grain boundary cracks may be due to this as well as to the different material and frequency. Kemsley (1957 c) has shown that copper specimens tested at room temperature have a higher proportion of grain boundary cracks at shorter lives. Figure 10, Pl. 5, shows stages in the growth of cracks in an aluminium specimen with a life of $2{\cdot}3\times10^5$ cycles. The first two pictures show the surface after 11% of the life before and after electropolishing. Parts of the slip bands are persistent and so is part of the grain boundary. On further fatiguing no slip occurred near the black part of the grain boundary showing that it was indeed a crack at that stage. By 33% of the life it had spread as shown in the last picture.

The above experiments on copper, iron and aluminium indicate the slow rate of growth of cracks in a pure metal, but give no indication of how they are formed. Accordingly Smith (1957) made a series of experiments at lower stresses and it was found that if the stress were such as to give a life of 10^7 cycles then the short incipient cracks (persistent slip bands) appeared dotted. If the stress were reduced still more this feature became more pronounced. Oxide electron microscope replicas were taken of the surface before and after electropolishing and these dots were seen to be pointed pits in the surface a few microns deep. Figures 11 and 12, Pl. 6, show electron micrographs of the pits illustrating their shape. It appears probable that these lie in the slip plane.

These results have been confirmed by Bown (unpublished) who found qualitatively similar effects on copper at very low stresses. Prolonged testing at a stress at which such discontinuous markings were produced (up to several hundred million cycles) failed to produce any fatigue failure, so that it is not yet established whether in this case such marks have any bearing on the production of a crack. Similar markings with every appearance of holes have however been seen by Jacquet ahead of a fatigue crack in brass (Jacquet 1956). Forsyth and Stubbington (1955) have also seen roughly similar pits in the slip bands of pure aluminium. Figure 13, Pl. 6, shows the holes revealed by electropolishing. Clearly the holes must have been considerably deeper than they are wide or they would have been completely removed during the electropolishing. Similar marks were seen in an alloy of 7·5% Zn, 2·5% Mg in aluminium (Forsyth 1957 a). In this case the spots were visible in the slip bands before electropolishing. They appeared as small black dots regularly spaced with a mean spacing of about $0{\cdot}36\,\mu$ but were very much deeper than they were wide; they were still clearly visible after an electropolish which removed $4\,\mu$ from the surface. When sections were cut roughly perpendicular to the surface the holes normally appeared as dots but occasionally sections were seen showing that they were tubes approximately straight

and parallel. Figure 14, Pl. 6, shows a section with typical rows of dots at A and a section through the tubes at B. The formation of these tubes was not dependent on the heat treatment given to the material and occurred whether the alloy was solution treated, age hardened or over-aged.

It is possible that these pits represent an early stage of crack formation and later on in the test they join up to produce macroscopic surface cracks, as indeed the pits shown in fig. 12, Pl. 6, are already doing.

In addition to these observations of pits, Forsyth has investigated the fatigue of pure aluminium and of many aluminium alloys at a variety of temperatures, and also of copper, nickel and their alloys. He has used polishes and etches which are more sensitive than those used to remove slip bands in the previous work. The early work (Forsyth 1951) was done on a solid solution of $\frac{1}{2}\%$ Ag in Al—a stable alloy in which the silver causes little hardening. (Subsequent work on pure aluminium shows essentially similar behaviour.) He found that it was possible to etch up many of the regions which had been slipping. It appeared that the material in the slip bands had been heavily deformed, as the electron micrographs show it to be, and had been polygonized into subgrains of slightly different orientations. Figure 15, Pl. 7, shows polygonized region lying along slip bands while fig. 16, Pl. 7, shows a more heavily deformed region in which traces of the slip bands are no longer visible. The polygonization was most marked in specimens fatigued at high stresses and in extreme cases differences of orientation of up to 30° could be shown by x-rays and etch-pits. The polygonization leading to differential etching was less marked if the specimen were fatigued at low temperature or if an alloy with a high recrystallization temperature (Al–1% Mn) were used. The polygonization was specially marked near the tip of propagating cracks and Forsyth points out (Forsyth 1956) that cracks must always propagate through this polygonized material.

Connected with this polygonization was the moving of grain boundaries away from the end of slip band (Forsyth 1953 a). Figure 17, Pl. 7, shows such a place. In some cases the position of the old boundary was still clearly visible showing that the boundary has moved through the metal rather than that the metal itself had moved. The distorted metal in the next grain near the end of the slip band must have recrystallized with the orientation of the first grain. Similar polygonization boundaries and grain boundary movement have been seen on fatigued copper and Armco iron (Forsyth 1951).

The intense deformation occurring in slip bands has also been etched up on copper by Kemsley (1956, 1957 a, b) who finds that temperatures of 350°–800°c are needed to remove it. Similarly Jacquet (1956) fatigued brass (67% Cu) and etched up the slip bands. He found that if the brass were annealed at 550°c for one hour and re-etched the straight traces of the etched slip bands were replaced by a diffuse polygonized structure. Figures 18 and 19, Pl. 8, show this. It seems that in these last

two cases the metal has possibly not polygonized during the test but that the etch was selecting the regions with large internal stresses.

If the aluminium were cold rolled before fatiguing the slip bands were short and tended to outline the subgrains produced by the cold work (Forsyth and Stubbington 1954). The electron microscope shows that the slip lines are even more curved than in annealed metals. In the most intense slip bands the cold work stresses were relieved and the material recrystallized to form larger subgrains of apparently softer material in which most of the subsequent fatigue deformation occurred and in which the fatigue cracks formed. Figure 20, Pl. 9, shows such a region. (This recrystallization is similar to that found by Kenyon (1950) in some samples of heavily cold drawn copper wire, and which was responsible for a considerable reduction in fatigue strength.) If the aluminium specimens were tested at −195°c the recrystallization was suppressed and almost no polygonization occurred.

2.3. *Extrusion*

The most intriguing outcome of this work is undoubtedly the discovery of 'extrusion'. Ewing and Humphrey (1903) found that the surface of broad slip bands frequently rose above the surface of the surrounding material but the rise was gradual and progressive across the band. Forsyth found that in some cases a section of the material is extruded from a slip band to a considerable height. The extruded portion is clearly defined and has definite edges.

This phenomenon was first seen on an unstable, partially age-hardened solid solution of 4% copper in aluminium (Forsyth 1953b, 1955). When this alloy was fatigued fine slip bands formed and towards the end of the test thin ribbons of metal were extruded from them. Figure 21, Pl. 9, shows the slip lines and extrusions. Typically the extrusions were 10 μ high and very thin. They had a metallic lustre and an attempt to measure their thickness interferometrically showed they were less than 0·1 μ thick. If a specimen containing them were repolished and etched the slip bands could be seen as shallow grooves, and there were cracks visible which had been widened by the etch. Figure 22, Pl. 9, shows this.

Extrusions only formed if slight ordering or clustering of solute atoms were allowed to take place before the test either by using a low solution heat treatment temperature or by allowing some ageing. If the alloy were aged to peak hardness or over-aged much less extrusion occurred. This indicates that an ageing phenomenon was involved, an impression confirmed by the fact that extrusion was almost suppressed at −25°c and completely so at −196°c, the alloy then deforming in a manner similar to pure aluminium. Similarly, considerably supersaturated aluminium–zinc alloys gave extrusion while unsaturated or only slightly supersaturated ones did not. The effect was found on other supersaturated alloys tested. It was established that the same effect took place at low

speeds of testing (60 c.p.m.) and that extrusion took place in a few cycles after a period of fatiguing†. Cracks formed and spread rapidly as soon as extrusion had occurred.

Tests at higher temperatures (Forsyth and Stubbington 1957) indicated in more detail the processes involved. The extrusions became thicker and more irregular as the temperature was raised. Figure 23, Pl. 9, shows a thick extrusion from aluminium–4% copper fatigued at 250°c. When the specimen was repolished and etched not only were cracks seen in the slip bands but the slip bands themselves etched differently from the rest of the grain. The whole appearance is consistent with the idea that over-ageing is much more rapid in the slip band than outside and that the extrusion and cracking takes place in the softer over-aged material. (It is unfortunate that the extruded material was too thin to be analysed chemically to see if it still contains 4% of copper.) The over-aged zone narrows as the temperature is lowered and the extrusion becomes thinner and eventually disappears if the temperature is lowered sufficiently. Extrusion continues to lower temperatures on faster ageing alloys.

Hanstock (1954) has made observations on the over-ageing of commerical age hardened aluminium alloys although without finding extrusions. He showed that bands of precipitate occurred at and below the surface of the metal. Measurements made on the internal friction of these specimens indicated that precipitation occurred after an incubation period. Cracks eventually formed in these precipitation bands. This is very similar to Forsyth's observations except that the direction of the bands of precipitation seen by Hanstock seems to be determined solely by the direction of the shear stress and not by the orientation of the individual grains. Figure 24, Pl. 10, shows some precipitation bands and associated cracks.

Since these observations were made, extrusions have been found to occur on many other materials including pure metals and stable alloys. Aluminium showed the effect at room temperature if it had been cold rolled before testing (Forsyth and Stubbington 1955). Small amounts of cold rolling (5–10% reduction) produced thin extrusion as shown in fig. 25, Pl. 10, while greater amounts (50%) led to partial recrystallization and block extrusion. Even greater cold reduction hardened the metal so much that the slip bands were broken up into short lengths outlining the substructure and extrusion was not seen.

In aluminium some cold work was necessary for extrusion to occur and theories based on local softening of initially hard material could still be applied. However subsequently extrusion has been observed on various stable copper–nickel alloys (Stubbington and Forsyth 1957) and on annealed pure copper (Thompson *et al.* 1956). The extrusion found on these metals is rather smaller than that produced on unstable aluminium alloys, being typically 1–2 μ high but it is similar in other

† This is not true of extrusion in all materials.

respects. Work on an annealed single crystal of copper of known orientation showed that the extrusion occurred along the slip plane in the most highly stressed slip direction and did not occur where this direction was parallel to the surface (Wadsworth, unpublished).

An unexpected effect occurred when a 68% nickel–32% copper alloy (Monel metal) was fatigued at 300°c (Stubbington and Forsyth 1957). Much extrusion took place from the slip bands and when the specimen was etched after repolishing the slip bands were attacked less than the surrounding alloy, as they were in the unstable aluminium–4% copper. However in this case the solid solution is stable. One is tempted to think that the composition is changed locally as the precipitates show it to be in the aluminium–4% copper alloy; but an alternative explanation is that the different etching behaviour is caused by an increase in the amount of disorder in the slip planes, possibly followed by local polygonization, as in pure aluminium.

Extrusion has been seen on unstable alloys, pure annealed metals, on work-hardened pure metals, on stable solid solutions and on silver bromide (see below). The width of the extruded portion varies from less than $0{\cdot}1\,\mu$ to blocks at least $3\,\mu$ wide and the height from barely detectable rises to $10\,\mu$. There seems to be a continuous gradation from rough slip bands with a series of hills and valleys in them to the longest and thinest extrusion.

The motions associated with slip band roughening do not necessarily take place right through the crystal; it is possible for some parts of the surface to rise and others to fall without leaving gaps. This is illustrated in fig. 26, Pl. 11, which is a photograph taken by Forsyth (1951) showing a grain of aluminium–$\frac{1}{2}$% Ag in a fatigued specimen. This grain slipped first on one slip system and then on a second. The displacements on the second system, in this case roughly parallel to the surface, are shown by the movement of the lines left by the first. It will be seen that relative displacements on the second system of about $5\,\mu$ occur and that these can disappear in distances of only a few tens of microns in the direction of the displacement. (Compare ringed regions.) If this had occurred perpendicularly to the surface a very rough slip band would have been formed with no cracks beneath.

If motion upwards can occur to form extrusions with no gaps being left behind the reverse should be possible and Forsyth (1957 b) has shown this to happen on crystals of silver bromide. This material deforms in a similar manner to metals, producing broad slip bands in fatigue, and is transparent. Extrusions occurred and interference fringes showed that they were tapered. When the underside of the surface was examined it was found that 'negative extrusions' had also occurred producing deep crevasses. Figure 27, Pl. 11, shows these. Some parts of the active band have risen above the original surface and others have sunk.

Cottrell and Hull (1957) have fatigued copper in push–pull and taken replicas of the surface. By suitable shadowing techniques it was possible

to emphasize either raised or lowered portions and both extrusions and intrusions were seen. Both were similar in appearance. Figure 28, Pl. 12, shows some of the intrusions. The intrusions clearly could grow in cracks and fig. 29, Pl. 12 (Wever *et al.* 1955) shows a crack in fatigued iron with small extrusions at the edge. Wood and Segall (1957 b) give a photograph showing a similar crack in copper.

Figure 30, Pl. 13, shows an electron micrograph of a shadowed replica of part of a fatigue slip band on copper. It illustrates the very wavy nature of the local slip in spite of the generally straight, crystallographic, nature of the edges of the band. It also shows that intrusions and extrusions can occur close together in the same band. The black regions A, represent intrusions or extrusions. The (carbon) replica was shadowed in opposite directions on the two sides, so that extrusions cast shadows (light on print) to the left and intrusions cast shadows to the right. Such shadows can be seen at B and C respectively. These intrusions are similar in some ways to the pits found in slip bands by Smith and Harries (figs. 11 and 12, Pl. 6) and by Forsyth (fig. 13, Pl. 6) and already described. The pits are however much narrower than the intrusions or extrusions. It is not clear if the mechanism of formation is the same in both cases but it is clear that either are possible nuclei for cracks.

§ 3. Changes in Mechanical Properties

3.1. *Introduction*

In their classic work in the 1920's Gough and his co-workers described the basic changes in mechanical properties which occur during fatigue tests on fairly pure metals (see Gough 1922, Gough and Hanson 1923, Gough, Hanson and Wright 1927, Gough 1938 and Haigh 1928). They tested various metals in push–pull and observed the changes in the energy dissipated in the specimen during the test. This may be measured in two ways, either by plotting the mechanical hysteresis loop or by measuring the rate of heat production in the specimen. Haigh (1928) used the latter method as it enabled measurements to be made continuously during the test. Thermocouples were placed at the centre and ends of the specimen thus measuring the temperature gradient along its length. This was approximately proportional to the rate of production of heat. Haigh found that when a soft specimen was stressed at a stress greater than its yield point the rate of energy dissipation was initially large but decreased rapidly and became approximately constant. During this stage both the 'elastic limit' and the Brinnell hardness of the specimen increased. If the stress were below the endurance limit, no further changes occurred until the stress was increased further. When this happened there was a further brief period of rapid energy release and then the rate settled down to a new steady value. This could be repeated many times. However when the stress was increased to a value beyond the endurance limit a gradual increase in rate of heat production occurred

after the initial drop. The rate continued to rise steadily until the end of the test, when it increased very rapidly just before the specimen fractured. Figure 31 shows the results of measurements made by Haigh on copper and illustrates these points.

Following Haigh it is convenient to divide the test into three parts. The first is the initial 'heat pulse' which normally lasts a few thousand cycles. The second is the majority of the test in which there is usually a slow increase in heat production; this is followed by the third stage, in which the dissipation rises rapidly immediately before fracture. The first and second stages will be described in more detail (§§ 3.2 and 3.3). The third stage is associated with the final stages of the propagation of the fatigue crack and will not be considered further. Section 3.4 discusses the related phenomena of the Bauschinger effect.

Fig. 31

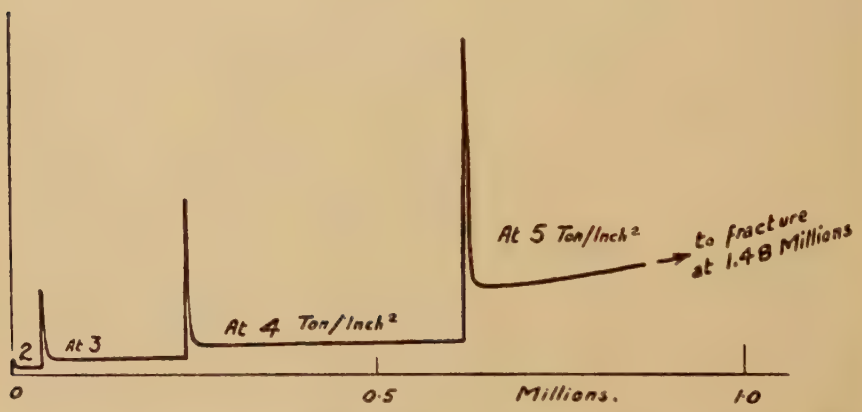

Rate of heat production during push-pull test on copper. (Haigh 1928.)

3.2. *First Stage–Initial Hardening*

Apart from noting that the 'first stage' only occurred when the specimen was stressed above its yield point, that there was no difference in the behaviour above or below the endurance limit and that it usually occupied some thousand cycles but could last longer, Gough and Haigh did not study it in detail. It was obviously not an essential stage in the fatigue process. However the manner in which the hardening of soft specimens occurs under cyclic stress is of interest in its own right as an example of work hardening, and is also of importance in determining the state of annealed metals during the remainder of the test. The latter point is illustrated by two experiments at low temperatures, the first of which demonstrates the difference between unidirectional and cyclic hardening while the second shows that different cycling treatments can lead to different states.

Broom, Molineux and Whittaker (1956) tested annealed specimens of commercially pure aluminium in push–pull at −183°C. They found that if the cyclic stress were increased slowly over some thousands of cycles it was possible to harden the specimen to such an extent that its endurance limit (for 10^5 cycles) was greater than its original ultimate tensile strength at that temperature. At room temperature the hardening was less effective.

McCammon and Rosenberg (1957) have made a series of experiments on annealed copper polycrystals at hydrogen and helium temperatures. They found that if the cyclic stress were increased to its full value in about 2000 cycles the fatigue life (of the order of 10^6 cycles) was about 8 times as long as if the full stress were applied suddenly. Fortunately for normal fatigue tests this effect was absent at room temperature.

(These two effects should be distinguished from the 'coaxing' of steels (see § 4) in that coaxing occurs at stresses below the yield point of the metal and without appreciable plastic flow whereas this cyclic hardening only occurs above the yield point and involves considerable plastic flow. In addition the coaxing of steels is appreciable at room temperature whereas the effects of cyclic hardening quoted above only occurred at much lower temperatures.)

A number of experimenters have studied the initial hardening, using a variety of methods of measurement.

3.2.1.

If the fatigue test is of the simple push–pull type, one possibility is to stop the test after a known number of cycles, and determine a static stress–strain curve for the fatigued specimen, to compare with a similar curve relating to a similar specimen, unfatigued. This was done by Bullen *et al.* (1953) on copper using a stress of ±11 200 lb per in^2. Hardening was rapid in the first 100 cycles, the 0·05% proof stress increasing from 3200 to 10 400 lb per in^2. The hardness continued to increase more slowly during the rest of the test, the proof stress reaching 14 000 lb per in^2 after 10^6 cycles (see fig. 32). Similar, though less detailed, measurements have been made by Polakowski and Palchoudhuri (1954) on a number of pure metals and alloys. The static tests were done in compression to avoid possible complications from the opening of incipient fatigue cracks. In every case the soft metals hardened considerably during fatigue.

More recently, Broom and Ham (1957) have extended the work of Bullen *et al.* by making observations on copper both at room temperature and at 90°K. The initial hardening was still observed at the low temperature, but the more prolonged and more gradual subsequent changes seemed to have been suppressed.

3.2.2.

Davies *et al.* (1956) have followed the changes in indentation hardness during a rotating bending test on annealed copper. The Vickers diamond hardness rose from 38 to values round about 70, higher fatigue stresses

producing only a very slight increase in the latter figure. As before, most of the hardening occurred in the first 1000 cycles.

3.2.3.

Some of the techniques for investigating damping capacity are suitable for use at the strain-amplitudes that are normally encountered in a fatigue test, and can be used to indicate changes in the area of the hysteresis loop, giving yet another measure of the increase of 'hardness'. The experiments of Haigh, mentioned above, were of this character. Wadsworth (1957 b) using an electromagnetic type of fatigue machine running at 1000 c.p.s. has made some approximate measurements of this kind. He expresses his results in terms of the quantity $1/Q$, which is proportional to the ratio of the energy dissipated per cycle to the total vibrational energy.

Fig. 32

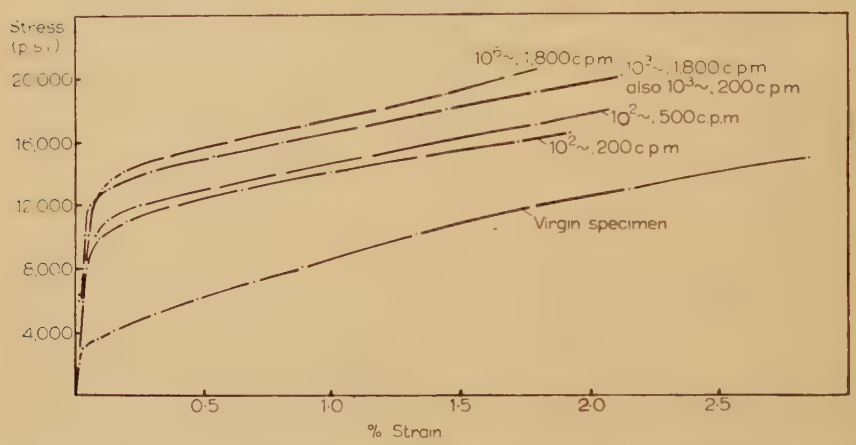

Tensile stress–strain curves on specimens subjected to the cyclic stressing indicated. (Bullen, Head and Wood 1953.)

Owing to the large initial energy dissipation at the stresses used, it took about 1000 cycles for the machine to reach operating stress. The amplitude of the stress cycles was then held constant and the specimen hardened rapidly. Figure 33 shows the results of measurements made at successively higher stresses on a copper single crystal. In each case cycles were measured from the time operating stress was reached. At all stresses the crystal hardened in a similar manner, and any changes after the first few thousand cycles were too small to be detected. (The lower initial values of $1/Q$ in the tests at higher stresses reflect the increased time needed to reach these stresses rather than a fundamental change.) Similar hardening curves were obtained for polycrystalline specimens of copper, aluminium, silver and nickel. In all these cases hardening was virtually complete in about 6000 cycles.

Cadmium single crystals also hardened under similar conditions, but much more slowly. The process was still incomplete after 10^6 cycles. Figure 34 shows a typical set of results. This much slower rate is possibly connected with the fact that cadmium has only one slip plane, whereas the other metals have four.

Fig. 33

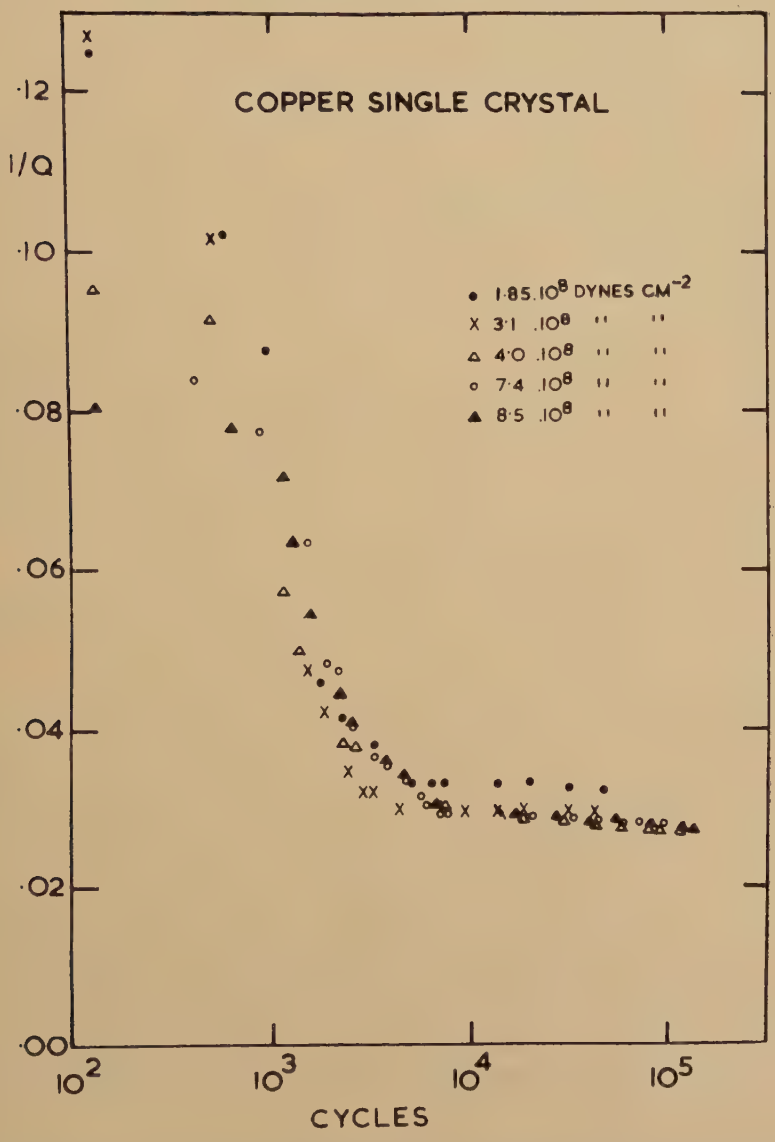

Energy dissipation during fatigue testing of a copper single crystal at successively higher stresses as indicated. (Wadsworth 1957 b.)

3.2.4.

More detailed studies of the initial work-hardening have been made by a number of workers using very much slower cycles of stress than are usual in ordinary fatigue testing (say, of the order of one cycle per minute). The measurements can be made in two different, but equivalent, ways: (i) by measuring the increase in peak stress during cycles of constant strain (or, better still, constant *plastic* strain); (ii) by measuring the decrease in loop width (cyclic plastic strain) during cycles of constant stress.

Fig. 34

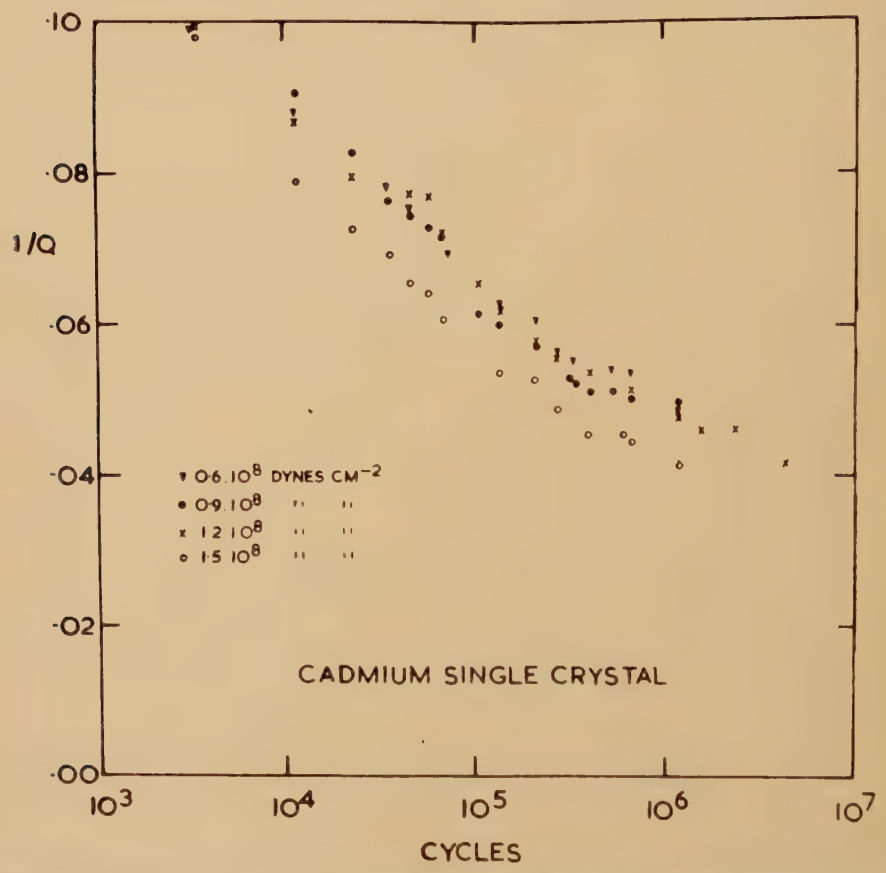

Energy dissipation during fatigue testing of a cadmium single crystal at successively higher stresses, as indicated. (Wadsworth 1957 b.)

The former method was adopted by Wood and Davies (1953) using polycrystalline copper specimens. The peak stress increased steadily as the specimen hardened. Figure 35 taken from Wood (1956) shows, effectively, this stress plotted against the cumulative plastic strain (i.e. $\sum|\epsilon|$) and compared with the unidirectional stress–strain curve. (The quantities actually shown are torque and twist, the observations

being made in torsion.) It will be seen that the hardening for a given total strain is less when the strain-amplitude is small than when it is larger, and that both are less than the hardening produced by unidirectional stressing. Similar results have been obtained for aluminium single crystals (Rider, unpublished).

Fig. 35

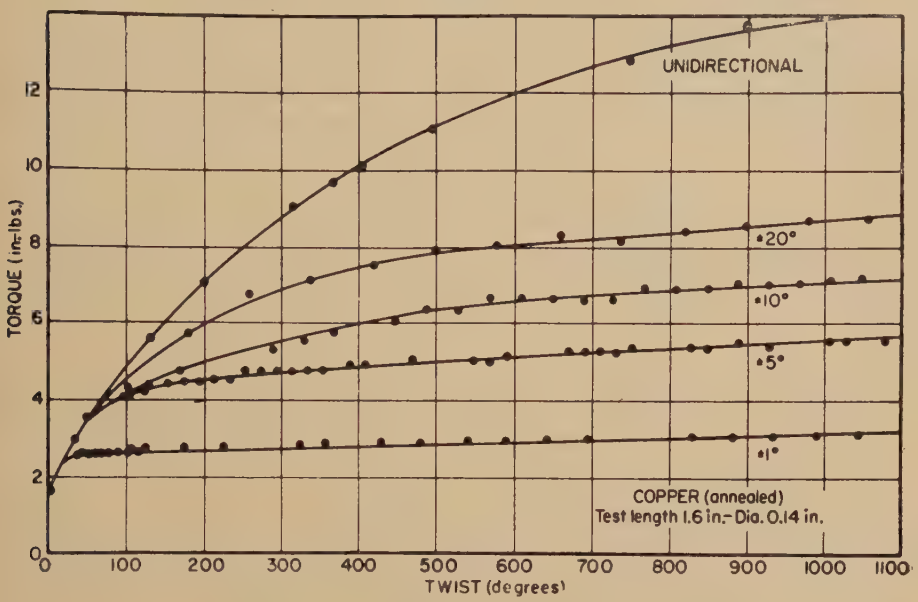

Torque *vs.* twist curves, for different amplitudes of alternating torsion, as indicated. (Wood 1956.)

As explained later in connection with the Bauschinger effect (§ 3.4) particular interest attaches to observations of this kind made on single crystals. Such observations were made by Held (1940) using crystals of tin tested in 'pure shear'. The strain amplitude is not stated, but appears to have been large, since considerable distortion of the surface was observed after about 100 cycles and complete fracture followed in a few hundred cycles. The peak stress increased rapidly at first, and then more slowly; the increase was greater at a low temperature (−78°C) than at a high temperature (+100°C). The rate of hardening produced by alternating strain was much less than that due to cycles of strain between zero and a fixed maximum, always in the same sense. The difference was much less at 100°C than at room temperature.

Paterson (1955) worked with copper crystals, at room temperature, and tested them in push–pull. The plastic strain amplitude was kept constant at a value which corresponded to a resolved shear strain of 0·83%. Curves of cyclic strain hardening are given for about 25 crystals, of a well distributed variety of orientations. The general pattern of these

curves, in its dependence on crystal orientation, is very similar to that obtained by Paterson himself and also by many other workers for pure face-centred cubic metals deformed unidirectionally. In particular, the same phenomenon of 'easy-glide' appears in both sets of data. The scale of the two sets of curves is qualitatively similar also, with the one striking exception that the region of easy-glide is prolonged to much greater total strains when these are alternating in sign.

Scholl (1957) experimented with aluminium crystals tested in shear at room temperature. The strains used were fairly large (1·5–8·2%) and the cycles were not symmetrical about zero, but always had zero strain as the lower limit. The peak stress (both positive and negative) increased for about the first 10 cycles and then decreased again. This does not agree with Paterson's results on copper, but it should be noted that the two investigations differ in several ways: Scholl's strains were much larger, and probably less homogeneous; the cycles of strain were not symmetrical; and the aluminium, at room temperature, was effectively much hotter than the copper.

3.2.5.

The second procedure mentioned in § 3.2.4, has been used by Thompson *et al.* (1955) and by Charsley (1957) using single crystals of aluminium. The order of magnitude of the loop widths (tensile plastic strains) involved in these measurements was from 10^{-3} to 10^{-5} and were thus considerably smaller than that used by Paterson. The empirical relation $W = An^{-q}$, (W = loop width; n = number of cycles of stress) in many cases fitted the observations fairly well for $10 < n < 1000$. The index q is a measure of the rate of hardening; this rate was considerably smaller for crystals oriented for single slip than for those in which double or multiple slip was to be expected. Thus both these results and those of Paterson indicate that the orientation dependence of the rate of hardening is qualitatively the same for alternating stresses as for direct stresses.

The rate of initial hardening found in these tests is considerably slower than that found by Wadsworth on his copper single crystal. It is possible that prolongation of the slow tests beyond 1000 cycles might have revealed a closer similarity but it seems more probable that the difference is due to the difference in the speeds of the two tests (a ratio of about $10^5 : 1$). Appreciable amounts of creep occurred during the slow tests, so presumably appreciable recovery was possible; there was much less time for this in the high speed tests.

It should be noted that the initial hardening stage may be absent if the material is not fully annealed before the fatigue test is begun. This was recorded by Haigh (1928) in his early work and was found also by Wadsworth (1957 b) in his experiments on copper. If the original material had been previously cold worked, the initial stage may be one of a pronounced softening. Polakowski (1952) has drawn particular attention to this point, making measurements on aluminium and copper, initially

cold rolled, and using as a criterion of softening a decrease in the 'yield point' in a tensile test, or an increase in ductility. The work was extended by Polakowski and Palchoudhuri (1954) using conditions of fatigue testing more nearly akin to usual practice, and recording both changes in indentation hardness and in the tensile stress–strain curve. Wood subjected copper specimens to slow cycles of torsion of constant strain amplitude. If the material were previously cold worked the peak stress gradually decreased, whereas for annealed material it increased. Similar observations on a stainless steel have been made by Coffin and Read (1956). Broom and Ham (1957) made the interesting observation that the softening of a hardened copper specimen was very much less if the fatigue testing were done at 90°K.

In the case of mild steel and similar materials, a further complication arises owing to the strain-ageing effects discussed more fully in § 4. Variations of energy dissipation, for example, are markedly affected by a resting period even at room temperature (Lazan and Wu 1951). The classical experiments of Bairstow (1910) and later of Gough and Hanson (1923) both record measurements at low stresses in which the energy dissipation was initially almost zero, but gradually increased to a steady value. It seems likely that this behaviour is related to the strain-ageing.

The general conclusions to be drawn from all this work is that the processes of cyclic work hardening are not, to a first approximation, very different from those of unidirectional work-hardening. In face-centred cubic crystals the distribution of slip lines on the surface is similar, and the orientation and stress dependence of hardening rates are also much alike. The characteristic differences between face-centred cubic and hexagonal crystals have been shown qualitatively to exist. Starting from a fully annealed crystal, the hardness increases rapidly at first, and later at a decreasing rate. If the strain-amplitude is sufficiently large, this hardening may eventually give place to a softening, representing the second of Haigh's three stages.

3.3. *The Second Stage*

The second stage comprises the major part of the fatigue test. The published results are summarized in two groups comprising pure metals and alloys respectively.

3.3.1. *Pure metals*

The gradual rise in hysteresis loss which normally occurs during the second stage of the test on pure metals is very stress sensitive. Thus, for simplicity of interpretation of the results obtained, it is desirable to carry out tests with the stress uniform through the significant volume of material.

Thompson and Wadsworth (1957) made some measurements on polycrystalline copper tested in push–pull. $1/Q$ (see § 3.2.3) was measured during the test under operating conditions. The specimens were annealed for one hour at 400°C before the test and this was insufficient to soften the

metal completely, so no first stage hardening was seen. The energy dissipation at the start of the test was low and if the stress were below the endurance limit, no change occurred. If the stress were above the limit, then the energy dissipation increased steadily during the test until the specimen finally broke. This is identical with the second stage behaviour

Fig. 36

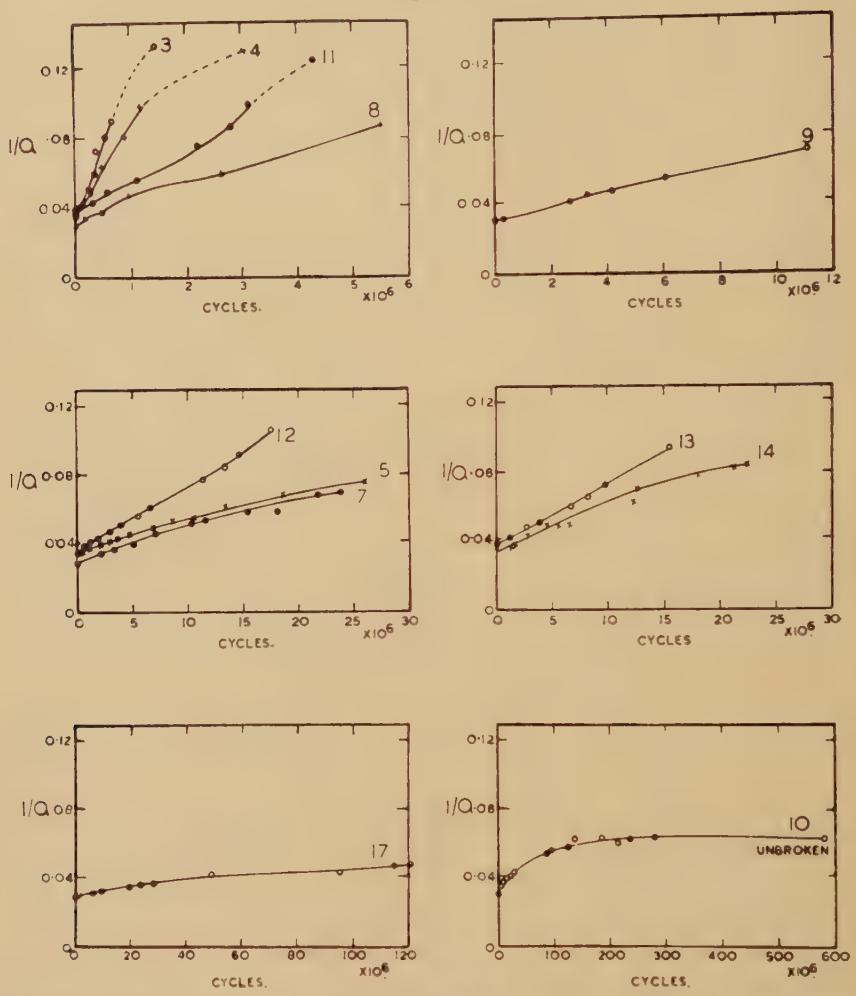

Variation of energy dissipation during fatigue of copper : twleve specimens at different stresses. (Note different time-scales). The number against a curve refers to the corresponding point on Fig. 37. (Thompson and Wadsworth 1957).

observed by Haigh. The results are shown in fig. 36. The rate of rise of $1/Q$ is obviously correlated with the fatigue life of the specimen and varies with stress in the same rapid way. Figure 37 shows the correlation between the initial rate of rise of $1/Q$ and fatigue life. This correlation is

better than that between final $1/Q$ and life and is in fact about as good as that between stress and life; i.e. the life could be predicted about as accurately from the initial rate of rise of $1/Q$ as it could from the applied stress. The two lines of fig. 37 refer to two groups of specimens, one batch being annealed at 400°C and the other at 500–600°C for one hour before testing. (The latter group showed the first stage hardening and for this group the rate of rise of $1/Q$ was determined after the completion of this first stage.) It is of interest to note that the difference between the two lines is considerably less than the difference between the two corresponding S–N curves. The S–N curves are displaced by a factor of 100 : 1 in life whereas the rate-of-rise curves differ by a factor of only 1 : 2.

Fig. 37

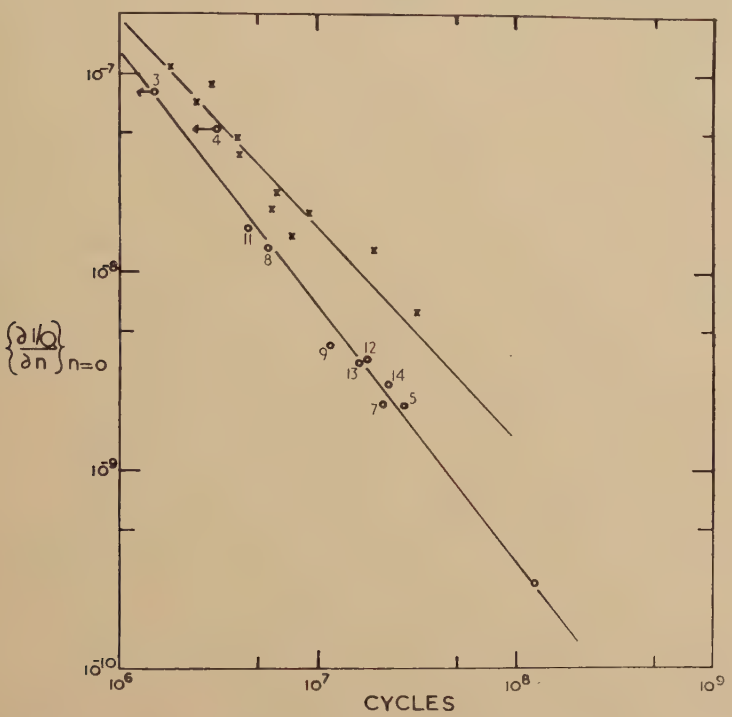

Initial rate of rise of energy loss, correlated with fatigue life. ○ annealed 400°C before test : × annealed 500°C.

It was shown that the energy dissipation was a bulk phenomenon and was not affected by removing the surface material or by surrounding the specimen by nitrogen, both of which treatments increased the fatigue life. On the other hand a partially fatigued specimen could be returned almost to its original state, as measured by energy dissipation, by an anneal at 600°C for 1 hour without affecting its life in any way. These results indicate that the energy dissipation is not directly related to crack formation—which is considered to be primarily a surface phenomenon—but

occurs throughout the volume of the specimen. It is probable that it is associated with the broad fatigue slip bands which appear on the specimen during fatigue; the results of measurements on other metals help to confirm this. For example, aluminium and silver polycrystals and copper single crystals (Wadsworth 1957 b) gave a very similar rise in $1/Q$ when stressed above the endurance limit and all showed many fatigue slip bands. The rate of increase of $1/Q$ was stress dependent in a similar way. Nickel and duralumin polycrystals (Bown and Thompson, unpublished) did not produce a detectable rise in $1/Q$ (the machine was not sensitive to very small increases), and showed few or no slip bands, when the test was carried out at fairly low stresses. At high stresses, nickel showed a rather slow, but steady rise of $1/Q$ throughout stage two, and a correspondingly greater number of slip lines on the surface. Cadmium single crystals (Thompson and Wadsworth 1957) showed no increase in $1/Q$ and no slip bands until they suddenly twinned. On further stressing, the edges of the twin bands became black, $1/Q$ increased rapidly and the specimen broke shortly afterwards along the black bands.

Duce (1950) tested a number of materials, both pure metals and alloys, in alternating torsion at 1500 c.p.m. at approximately constant strain. At intervals during the test the machine was stopped and a mechanical hysteresis loop was plotted at a speed of 1 c.p.m. From this the dynamic modulus (stress range/strain range $=\tan\beta$) and the total energy dissipated (ΔE) were determined. If the hysteresis loop were of the shape found by Thompson *et al.* (1955), then as the area ΔE increased, the dynamic modulus ($\tan\beta$) must decrease, and *vice versa*. In Thompson and Wadsworth's experiments (unpublished) this did indeed happen, to approximately the extent predicted, in all stages of the experiments. This correlation occurred again in the first stage of all Duce's tests: ΔE decreased and $\tan\beta$ increased for nickel, copper, magnesium and aluminium while for iron ΔE increased and $\tan\beta$ decreased as was observed by Bairstow (1910).

In the second stage, however, for most metals, including copper, both ΔE and $\tan\beta$ decreased slightly (a few per cent). The explanation of this is not clear. The drop in ΔE may indicate that the slow continuation of Stage I hardening in the bulk of the specimen stressed below the endurance limit masked the Stage II softening of the surface layers. The drop in $\tan\beta$ might similarly be attributed to the Stage II softening of the surface layers, if the conditions were such that their contribution dominated the total stiffness of the specimen. The only alternative appears to be the assumption of a slow change in the elastic modulus appropriate to the unloading curve sufficient to mask the continuing Stage I increase due to the narrowing of the hysteresis loop; such an effect has not been reported elsewhere. None of the above suggestions really carry conviction, however, and the dilemma remains unresolved. Magnesium alone of the metals tested showed the expected fall of ΔE and rise of $\tan\beta$ in Stage II.

While the amount of plastic flow in each cycle (strains of the order of 10^{-4}) generally increases during the second stage of fatigue tests when the

stress is both uniform and of constant amplitude (Stage II softening) the stress needed to produce *large* strains continues to increase slowly. A number of the investigations already quoted in connection with Stage I hardening were continued to show this effect. Polakowski and Palchoudhuri (1954), Broom and Ham (1957) and Bullen *et al.* (1953) (see fig. 32 of this work) show it by the gradual raising of the static stress–strain curve with increasing number of stress cycles. Davies *et al.* (1956) show it by diamond pyramid hardness measurements: in this case there is a suggestion that the hardness eventually falls slightly. It is also claimed that the peak value of hardness reached is almost independent of the nominal fatigue stress, over the range 11 200 to 18 000 lb per in^2. The significance of this somewhat complex observation is, at the moment, not clear.

Broom and Ham (1957) give some interesting results on the temperature dependence of the hardening produced by fatigue in copper. Measuring this quantity by the ratio of static flow stresses at 293°K and 90°K they show that it is greater for specimens hardened by 10^5 cycles of fatigue, than for others subjected to the same stress once only. The temperature dependence of fatigue hardening is comparable with that of material damaged by neutron irradiation, from which they concluded that vacant lattice sites probably play an important role in fatigue hardening.

If a specimen has been heavily work hardened before a fatigue test, the softening already mentioned continues slowly throughout the fatigue life, and again a greater effect is produced by longer cycling or higher stress (cf. Polakowski and Palchoudhuri (1954) also Broom and Ham 1957). Unfortunately only stresses above the endurance limit were used, so that it is not possible to tell how closely the softening is connected with fatigue; it does, however, appear to be very stress sensitive.

Kenyon (1950) microscopically examined hard drawn copper wire fatigued at room temperature and found that some specimens had partially recrystallized, producing abnormally large grains. These grains were much softer than the others, having a (Knoop) hardness of 70 as against 135 for the unrecrystallized grains. Fatigue cracks formed in the large, soft grains and specimens containing them had shorter lives than those without. More specimens showed this recrystallization when the test temperature was raised to 70°C.

3.3.2. *Alloys*

In general it appears that stable alloys behave in essentially the same way as pure metals under fatigue stresses. Haigh (1928) made energy dissipation measurements and found that ductile brasses showed rapid initial hardening and then stress dependent softening in the same way as copper. Polakowski and Palchoudhuri (1954) showed that the effect of fatigue on the compression stress–strain curve of a number of stable alloys (tin, bronze, copper–nickel and aluminium–1·2% magnesium) was similar to that on pure metals as already described. If the alloy had been annealed it hardened progressively and if it were initially work

hardened, it softened. Coffin and Read (1956) worked with cold worked stainless steel fatigued in push–pull at constant strain. They found that the maximum stress reached decreased considerably during the test. Little change occurred with annealed stainless steel.

The effect on unstable alloys and those showing a yield point is rather different. The behaviour of carbon steels will be discussed separately (§4); we deal here only with non-ferrous alloys. Hanstock (Hanstock and Murray 1946, Hanstock 1947, 1948, 1954, 1956) has made a series of investigations into the variation of damping during the fatigue testing of aluminium alloys. The specimens were fatigued in torsion in a resonance machine which allowed the energy loss in the specimen to be measured very accurately. In general it was found that the energy loss was very low at low stresses but increased rapidly when a 'critical strain' was passed. This critical strain is comparable with the limit of proportionality in a static test and its value depends somewhat on the sensitivity of the test criterion used. It is however a useful concept. This strain was very low ($\sim 10^{-4}$) for annealed metals, higher (10^{-3}) for solution treated or over-aged alloys and higher still (3×10^{-3}) for fully hardened alloys.

When a fully hardened precipitation hardening alloy such as L 65 (4·4% Cu, 0·6% Mg, 0·7% Si, 0·6% Mn) was fatigued at a strain in the region of its critical strain its energy loss remained fairly constant for a time and then started to increase at an increasing rate. The higher the strain the shorter was the induction period and the more rapid the rise. Figure 38 shows some examples. While the damping increased, the critical strain decreased to perhaps half its original value. During the increase in damping, fatigue cracks appeared. A series of experiments showed that the damping was caused by local structural changes in the alloy rather than by crack formation. Firstly, the value of damping at which the cracks were first seen varied irregularly from specimen to specimen. Secondly, it was shown that a specimen which had been fatigued to produce a large increase in damping could be returned to its original state (as measured by energy dissipation) by heat-treating it to dissolve any precipitate and then re-ageing. This treatment also appeared to remove the fatigue damage if there were no cracks present; if the specimens were re-fatigued they softened in the same way as fresh specimens and did not have an unusually short fatigue life. If cracks had already formed, the damping was still reduced by the second heat treatment showing that it was not due to the cracks, although in this case the specimen soon broke on re-fatiguing. In DTD 683 (5·3% Zn, 2·7% Mg, 0·4% Cu, 0·5% Mn) similar changes in damping occurred, and the bands of precipitate could be seen to form in planes of maximum shear stress. The cracks formed in these bands. Figure 24, Pl. 10, shows precipitation bands and cracks. The chief difference between the behaviour of the two materials was that while in L 65 the specimen broke soon after cracks had formed in DTD 683 the cracks took longer to spread and the damping, after rising to a high value ($5 \cdot 10 \times 10^{-3}$), decreased slowly for the rest of the test. The explanation of this difference is not clear.

If the alloy L 65 were tested in the solution-treated condition, its critical strain was initially fairly low, but when fatigued above this level it hardened at first and the critical strain increased. In this way the critical strain could be increased by a factor of 2, almost as much as by thermal ageing at 185°C. The macroscopic hardness also increased.

Fig. 38

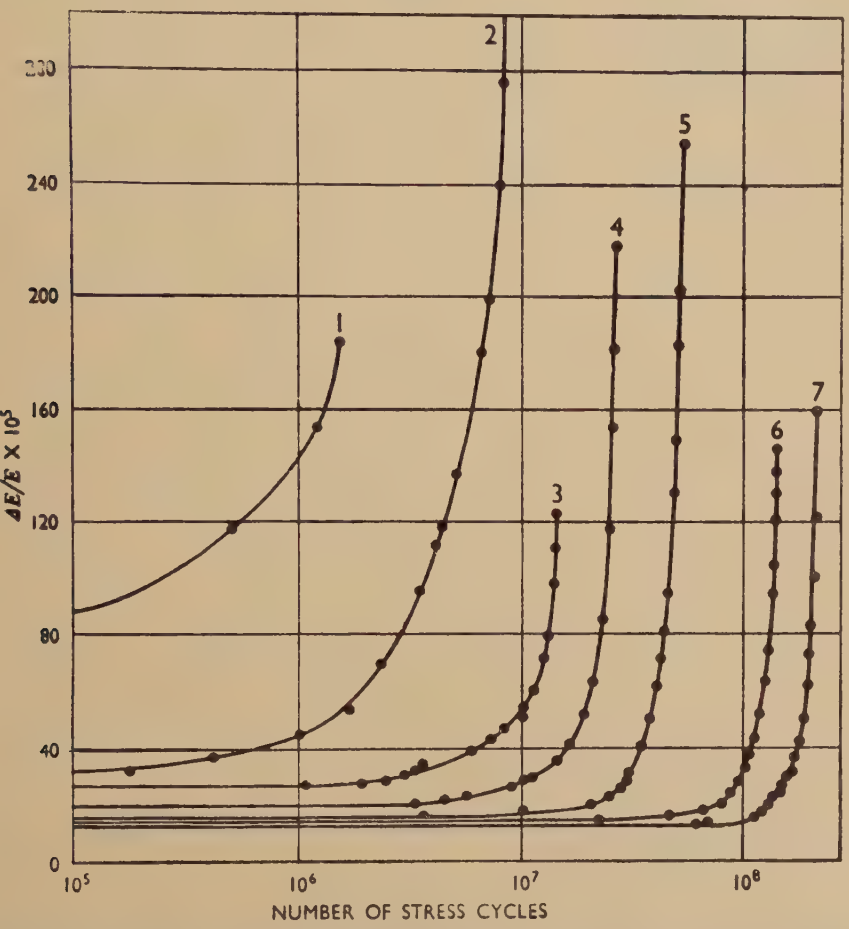

Changes in energy dissipation of aluminium alloy L 65 during cyclic stressing at various strain levels, i.e.

1. 48×10^{-4}
2. 45×10^{-4}
3. $42{\cdot}5 \times 10^{-4}$
4. 40×10^{-4}
5. $37{\cdot}5 \times 10^{-4}$
6. 35×10^{-4}
7. $32{\cdot}5 \times 10^{-4}$

(Hanstock 1956)

Broom, Molineux and Whittaker (1956) showed that the indentation hardness increased from 70 to 100 in a similar test. There was however one significant difference between cyclic strain hardening and thermal

hardening. Thermal hardening occurred generally throughout the specimen, and the damping increased gradually as the stress was raised. Cyclic strain hardening however only occurred in the regions which slipped under the applied strain and so when the strain was increased the new regions came into play, the damping was still large. Figure 39 shows this difference. If the fatiguing were continued, the energy loss started to increase again and the specimen finally broke. This increase is presumably similar to that associated with the local over-ageing of hardened specimens (see fig. 38).

Fig. 39

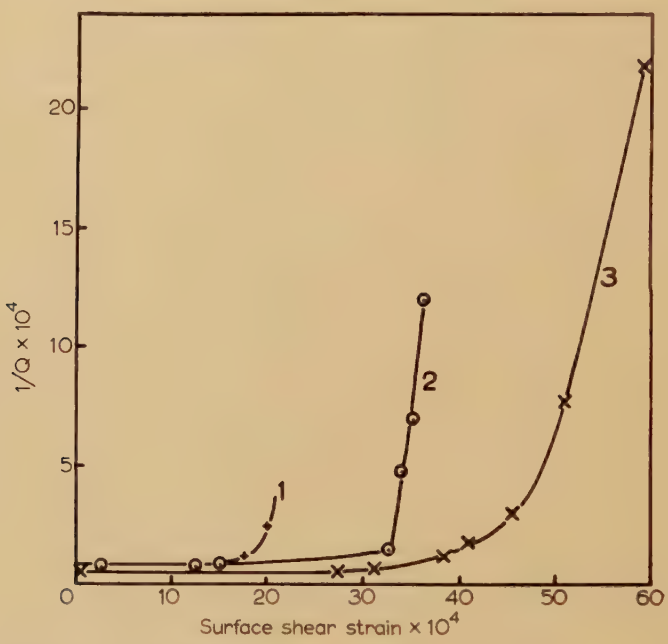

Energy dissipation in aluminium alloy L 65.

(i) As quenched after solution treatment.

(ii) After 4×10^6 cycles of alternating stress of gradually increasing magnitude.

(iii) Thermally aged to optimum static strength. (After Hanstock 1956.)

To summarize, the changes produced by fatiguing were in all cases a movement towards equilibrium such as could be produced by heating. The solution heat treated specimens became harder and the fully aged specimens became softer and precipitates could be seen. The changes were local rather than general.

Lazan (Lazan and Demer 1951, Lazan 1954) has measured the damping capacity of a large number of commercial materials during fatigue tests at various stresses. He finds that there is a stress, the 'cyclic stress sensitivity limit', below which the damping remains constant, however many cycles of stress are applied. In this region the energy dissipated

per cycle is usually proportional to something between the second and third power of the stress. (If the hysteresis loop remained the same shape the area would be proportional to the square of the stress.) Above the cyclic stress sensitivity limit the damping varies as the test proceeds and usually the mean value increases more rapidly with stress than it

Fig. 40

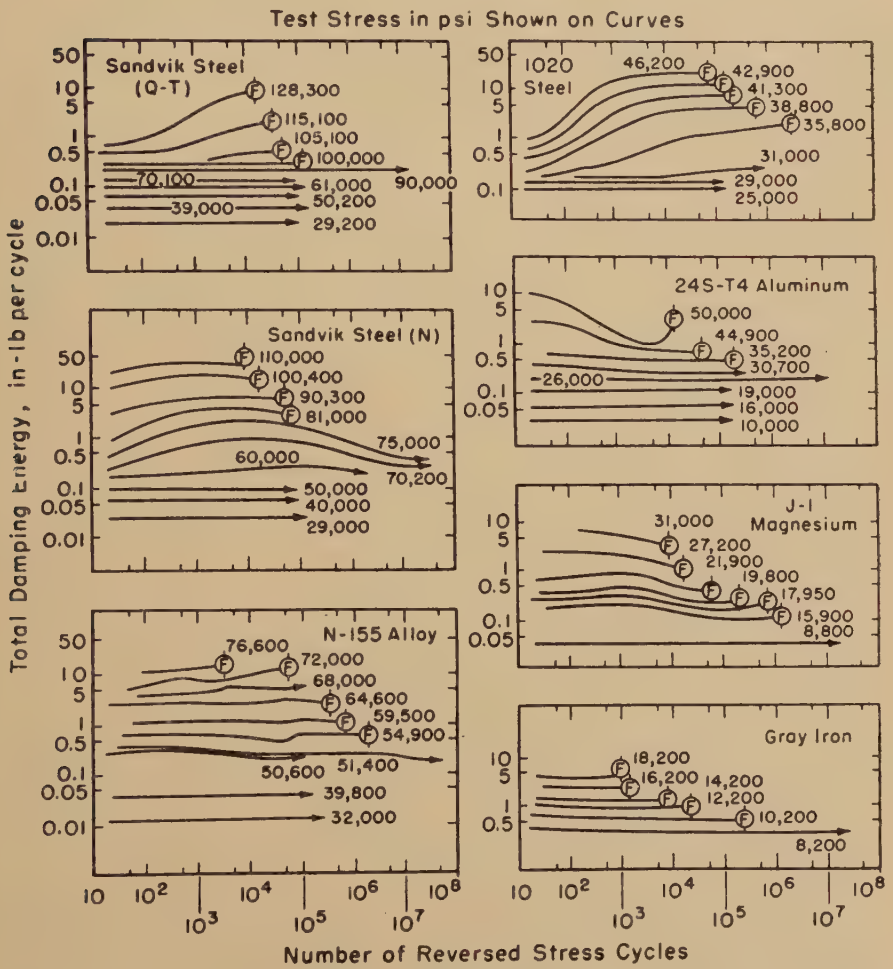

Changes of energy dissipation during fatigue of various materials. (Lazan 1954.)

did below the limit. The variation of damping with number of cycles above the limit may take any form. Some materials showed a steady increase, some an increase followed by a levelling off or a decrease, and some a decrease or a decrease followed by a rise. The cyclic stress sensitivity limit was of the same order as the endurance limit (for 2×10^7 cycles) but was not directly connected with it. The ratio of the two

varied in extreme cases between 0·33 and 1·10. Figure 40 shows how the damping varied for a number of materials. The 24S–T4 aluminium was naturally aged but behaved, at high stresses at least, in a manner characteristic for Hanstock's incompletely aged alloys. Apparently further local hardening was possible under the higher fatigue stresses. No attempt was made to study the metallographic changes which occurred during the test and no detailed explanations of the observations can be given.

The lack of coincidence of the cyclic stress sensitivity limit and the endurance limit is of interest and shows that in many alloys structural changes associated with changes in damping can occur without leading to the eventual failure of the specimen while in other metals the specimen can fail without the incipient failure being detectable by damping changes.

3.4. *Bauschinger Effect*

We have hitherto been concerned entirely with the *area* of the hysteresis loop, as a measure of the damping, and not with its *shape*. To a good first approximation, the unloading quadrants of such a loop are straight lines (elastic); the loading quadrants are smooth curves, and, save in exceptional circumstances, the loop is symmetrical. The transition from elastic unloading to plastic deformation during reverse loading takes place smoothly at, or shortly after, zero stress; sometimes the beginnings of the process can be just detected before zero stress is reached. If, having reached zero stress, the specimen is re-loaded *in the original sense*, the result is, again to a first approximation, an elastic straight line, at least until the previous maximum stress is approached. Thus the behaviour of the specimen is asymmetrical, being 'softer' for reversed stressing than for a second stressing in the same sense. (see fig. 41).

This asymmetrical behaviour is known as the Bauschinger Effect. The original experiments of Bauschinger (1886) and the few other early papers on the same subject, were concerned mainly with iron and steel, and thus the results were complicated by the phenomena of strain-ageing; later work has however shown that the effect is quite general. In the case of polycrystalline specimens an explanation has been suggested based on the anisotropy (elastic and plastic) of the individual grains. The principle can be seen by considering two neighbouring grains which undergo the same (tensile) strain, but which have different stress–strain curves. On unloading, both are taken to behave elastically; when the applied load is zero one will be in tension and other in compression. On re-loading in the same sense to the same stress, both will again behave elastically. But on loading in the opposite sense, the residual stress in the softer grain is in the direction to make it yield even earlier than before. Thus not only is the behaviour asymmetrical, but the combination is softer for the reverse stressing than it was in the virgin state.

Ideas of this kind were elaborated in a series of papers by Masing (1923, 1926, also Masing and Mauksch 1925a, 1925b, 1926) and, in more detail, although in a somewhat different context by Afanasiev (1940, 1941).

Rahlfs and Masing (1950) have used a model of this kind in an attempt to calculate the shape of the hysteresis loop from the shape of the initial loading curve. A comparison with experimental results obtained from torsion tests on wires of various materials showed considerable disagreement in some instances. Although such calculations are so difficult that it is perhaps unreasonable to expect them to be successful, it is clear that an effect of this kind must be present, and such a view has gained general acceptance. It is another matter, however, to assume that this is the

Fig. 41

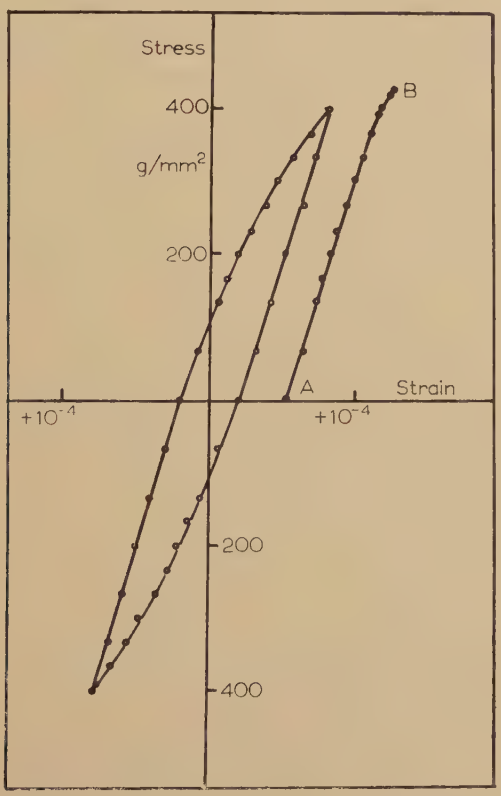

Hysteresis loop of aluminium single crystal, and reloading curve AB—to illustrate Bauschinger effect.

complete explanation. In such arguments it is assumed that the individual grains, if isolated, would show no Bauschinger effect, but Woolley (1953) analysing some of his own results on the torsion of thin-walled cylinders maintains that they are inconsistent with this view.

A more direct approach is to carry out experiments on single crystals. It has been pointed out by a number of authors (e.g. Swift 1944) that such experiments must be carried out under conditions of uniform strain.

If the observations are made in bending or in torsion, for example, then the macroscopic non-uniformity of stress will produce a spurious Bauschinger effect in the same way as the microscopic non-uniformities considered above. Of the few papers that have appeared on this topic about half describe experiments in tension–compression and the remainder in 'pure' shear. Both are difficult techniques but the former is more likely to approximate to the desired conditions than the latter. Some workers observe only one cycle of stress on each specimen (e.g. Edwards and Washburn 1954, Weinberg 1953, Buckley and Entwistle 1956) and most concern themselves with strains of 1% or more, which are large compared to those normally encountered in fatigue. Nevertheless such studies are relevant to the problem of fatigue, as they may throw light on the behaviour of dislocations under an alternating stress.

Fig. 42

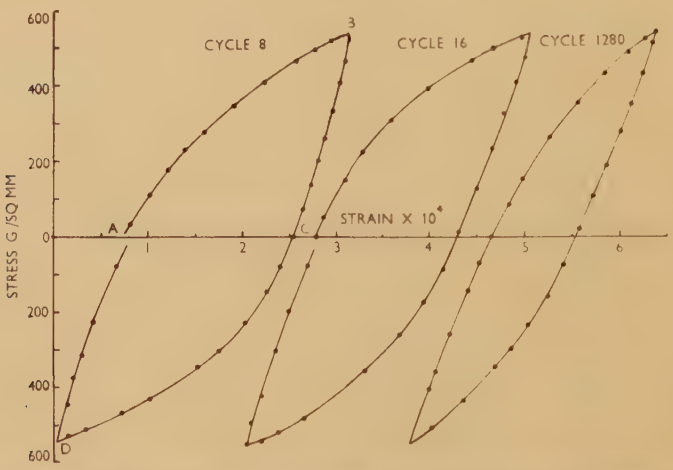

Typical hysteresis loops for a single crystal of aluminium. (From Thompson, Coogan and Rider 1955.)

The metals so far investigated as single crystals are brass, tin, cadmium, zinc, copper and—most extensively—aluminium, in addition to the early work on iron. All experimenters are in agreement that a single crystal does indeed show a Bauschinger effect; qualitatively the phenomenon is well marked with a single crystal as with a polycrystal. Figure 42 shows some typical hysteresis loops obtained in push-pull on aluminium by Rider (1953).

Buckley and Entwistle (1956), following Woolley (1953), adopt an arbitrary, but convenient, single parameter as a measure of the Bauschinger effect; this is (approximately) the plastic strain at a specified fraction (e.g. 3/4) of the preceding maximum stress and is called by them the 'Bauschinger strain'. Their results on aluminium show that the Bauschinger strain increases continuously with the amount of preceding

strain hardening—a result in qualitative agreement with the early work of Sachs and Shoji (1927) on brass. There is strong evidence for a sharp drop in this rate of increase when the pre-stress exceeds the upper limit of the easy-glide range. This they interpret as evidence that the Bauschinger strain is caused by slip on the same slip system as was operative during the pre-strain.

There are three characteristic features of the shape of a hysteresis loop which call for explanation in terms of any theory; and no dislocation theory of work hardening can be considered to be satisfactory unless it permits of an extension which would give such an explanation.

1. The Bauschinger effect itself, i.e. the asymmetrical form of the stress–strain relation.

2. The fact that the transition from the almost straight, elastic, unloading portion of the cycle to the curved, partly plastic, loading portion, although gradual, always takes place at about zero stress, irrespective of what the maximum stress may have been.

3. The fact that the initial portions of the unloading curves are—if no complications arise due to creep—purely elastic, within the limits of error of such observations as have been made.

No attempt has yet been made to work out a dislocation theory in any detail, although the problem has been discussed by Thompson, Coogan and Rider (1955), Seeger (1954) and Buckley and Entwistle (1956). When the strain-amplitude is small (which is the situation most nearly relevant to fatigue) the suggestion made is that the plastic deformation is due to a to-and-fro motion of individual dislocations through the crystal. The alternative possibility, of the generation by Frank–Read sources of groups of dislocations of opposite sign on alternate half cycles has not been shown to be impossible. The existence of something in the nature of a 'friction' force acting on the dislocations is necessary to account for the third of the above points. The production of 'jogs' and of vacant lattice sites (or interstitial atoms) by crossing dislocations could give such an effect. More generally, the motion of a dislocation through an internal stress field which varied in a random manner would act similarly.

If, in addition, the order of magnitude of the friction force were always about one half of the peak stress that had just been applied to the crystal, then the second of the above points would be qualitatively accounted for; no definite suggestion has yet been made as to why this would be so. From this point, the existence of the Bauschinger effect follows without difficulty; in fact, the problem is not so much to account for the ease of plastic deformation in the third quadrant of a hysteresis loop, as to account for its absence in the second quadrant.

One possible line of attack on the problem is the observation of slip lines at different stages in the cycle. This is open to the objection that what is observed on the surface may not be representative of what is happening in the interior. It is particularly unfortunate therefore that

the very few observations that have been made have been confined to aluminium. Louat and Hatherley (1954) state that after a forward strain of the order of 0·1%, which produced a few visible slip lines, no changes in the surface appearance were detected until the reverse stress was about twice the maximum forward stress. At this point new slip lines were produced and one of the old slip lines suddenly changed its appearance in such a way as to suggest either the reversal of slip on the original plane, or slip in the reverse direction on a plane very close to the original. Buckley and Entwistle (1956) removed the forward slip markings by electropolishing, and showed that no slip marks appeared under reversed stress until the pre-stress had been exceeded. Charsley (1957),

Fig. 43

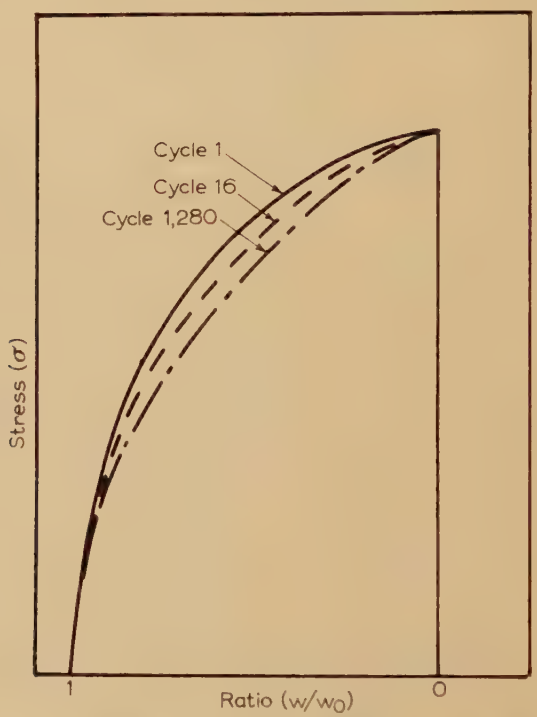

Change in shape of hysteresis loop during continued cyclic stressing. w=loop width at stress σ; w_0= loop width at zero stress. (Charsley, unpublished.)

in a more extensive study, also showed no change in the old slip marks and the production of no new ones until the reverse stress considerably exceeded the forward stress. In all three experiments there was considerable Bauschinger strain, which must therefore have been due entirely to fine slip, or to slip which did not reach the free surface. Further observations on these lines on materials other than aluminium, might be very fruitful,

Experiments on the effect of an increased temperature on the Bauschinger effect are very few (Sachs and Shoji 1927, Masing and Mauksch 1925a, 1925b, Polakowski 1951) and inconclusive: there appears to be very little support for the contention that it is possible to anneal out the Bauschinger effect at a lower temperature than that necessary to produce softening of a cold worked crystal.

If the series of alternating stresses is continued beyond the first cycle, the hysteresis loop changes both in size and shape. The changes in loop which accompany the reduction in width previously discussed have been little investigated, apart from unpublished work by Coogan, Rider and Charsley. These observations show that, with aluminium single crystals at least, the unloading sections of the curve continue to be almost straight and elastic, and the plastic deformation continues to be first noticeable at about zero stress (see fig. 42). The amount of plastic deformation in the loading sections becomes progressively less, but the whole remains a smooth curve. By plotting the ratio of the loop width at any stress to the loop width at zero stress (fig. 43) it can be shown that, as the loop shrinks, the reduction in width is more marked near the peak stress than near the zero stress: the change is, however, not very pronounced and to a first approximation, the narrowing of the loop can be described as a progressive reduction of all non-elastic strains in the same ratio.

§ 4. The Fatigue Limit and Related Phenomena

4.1. *Introduction*

It has already been mentioned that iron and many ferrous alloys show a charactersitic 'fatigue limit' (see fig. 1, curve *A*). A little above this stress level, the fatigue life is finite, and of the order of 10^6 cycles; below it, the life is so very much longer that it is usually regarded as infinite. A recent extensive series of experiments by Clayton-Cave *et al.* (1955) illustrate the characteristic behaviour. The experiments were made on about 400 specimens prepared under controlled conditions from a single cast of commercial steel (EN 24). These specimens were very carefully machined and mechanically polished to a metallographic standard, and the whole test carried out with the greatest care. Figure 44 shows the results; each point represents the failure of a single specimen at the stress shown; lives longer than 4×10^7 cycles were recorded as 'unbroken'.

It will be seen that it is not possible with this material to choose a stress that will give a mean life of, say, 10^7 cycles, in any real sense. Nevertheless the transition from 'finite' to 'infinite' life does not take place sharply. If the fatigue limit be defined as the stress at which 50% of the specimens have a life exceeding N cycles, than it lies between 46·0 and 45·5 tons/in^2 according as N is taken to be 2×10^6 or 40×10^6. Figure 45 shows similar results for another material. The essential physical point remains clear—that, within a small range of stress there is a large qualitative change in behaviour; this is what we mean by a fatigue 'limit'.

Fig. 44

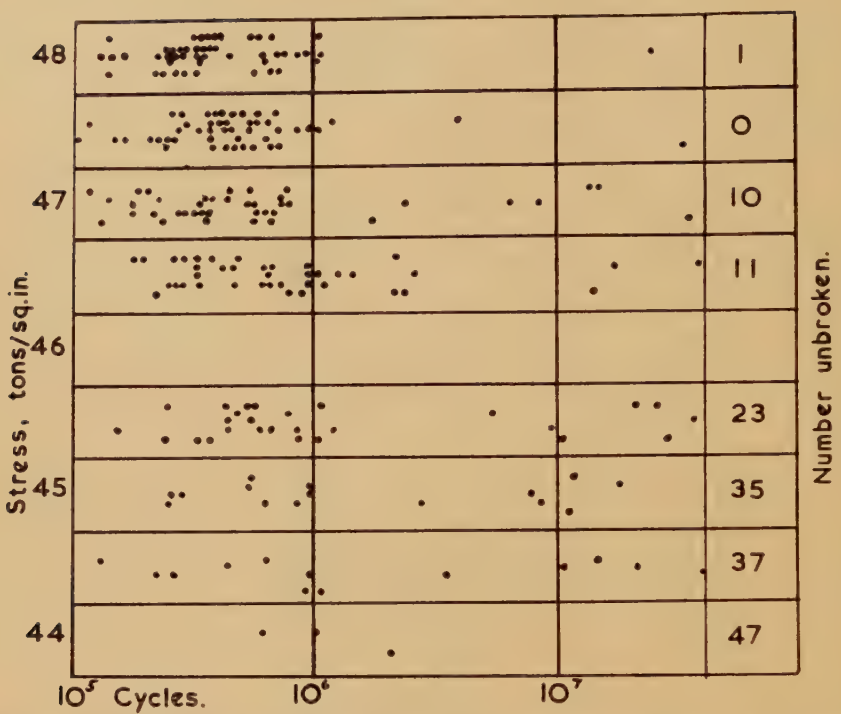

Endurance of 400 specimens of steel EN 24. (After Clayton-Cave *et al.* 1955.)

Fig. 45

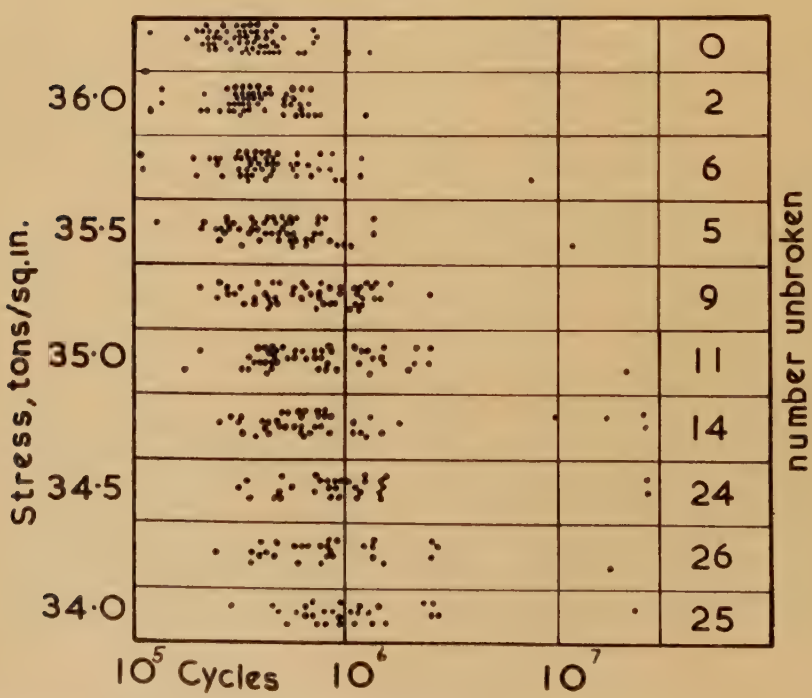

Endurance of 550 specimens of steel EN 100. (After Clayton-Cave *et al.* 1955.)

In general, non-ferrous materials do not show any comparable discontinuity in the S–N curve, at least up to the point at which normal technical fatigue testing stops (of the order of 10^8 cycles). One exception to this generalization is provided by a group of aluminium alloys, containing between 2% and 7% of magnesium, and about $\frac{1}{2}$% of manganese. Existing data on these materials † are compatible with the existence of a fatigue limit although no extensive investigation has been made comparable with that mentioned above on a steel. In view of later discussion in this section it is interesting to note that these same Al–Mg–Mn alloys show a sharp yield-point similar to that of an annealed mild steel and also exhibit markings comparable to Lüder's bands (see Phillips *et al.* 1952).

Even with ferrous materials it is by no means certain that all alloys show the characteristic discontinuity in the S–N curve. Almost all ferritic alloys and those in which ferritic regions predominate probably do. It is more doubtful whether it can be asserted that austenitic (i.e. face-centred cubic) alloys do not; at the moment this appears possible, but there are (somewhat surprisingly) not enough sufficiently careful and sufficiently numerous sets of observations to enable a firm conclusion to be drawn.

4.2. *Experimental Results*

Before attempting any hypothesis to account for the occurrence of a fatigue limit in some materials we propose to summarize a number of experimental papers which seem to be relevant. It is not absolutely certain that the phenomena recorded are always peculiar to those materials which show a fatigue limit; but they have all been observed on such materials and in many cases there appears to be some connection.

(*a*) *Under-stressing and coaxing*

One of the more striking effects is that which has come to be known as 'understressing' or 'coaxing'. Essentially, a fatigue specimen is tested for many cycles at a stress below the fatigue limit: if it is then subsequently tested at a stress above the fatigue limit, it is found that its life has been significantly increased (under-stressing). If the stress is increased in small steps, the specimen remaining unbroken, the duration of the test at each stress level can be much greater than the normal life of a fresh specimen at that stress. In this way the material can be made to withstand stresses considerably above the fatigue limit for very long periods (coaxing). Many striking examples are given in the literature: see, for example, Gough (1926).

A systematic investigation of the effect has been made by Sinclair (1952). Five different materials were used: (i) a 70–30 brass; (ii) an aluminium alloy 75 S–T 6; (iii) two ferritic steels, SAE 2340 hot rolled, quenched and tempered, and SAE 1045 hot rolled; and (iv) ingot iron (0·012% C) fully annealed after machining.

† See Research Bulletin of Aluminium Laboratories Ltd., No. 1 (1952).

An extensive series of observations were made, using four different values of stress increment and two different values for the length of test at each stress. All three ferrous materials showed the expected coaxing effect but it was conspicuously absent with both the brass and the aluminium alloy. (Another paper by Dolan and Brown (1952) also reports complete failure to show any coaxing in 75 S–T 6 aluminium.) Two other points from Sinclair's work should be noted: (i) The final fracture stress after coaxing was the greater when the size of the stress increment was less, and when the duration of each phase was longer; thus the effect is more marked when the stress is built up more slowly. (ii) A second group of specimens of the same ingot iron, in which the final machining and polishing was done after annealing, showed little or no coaxing. Such a treatment would leave the important surface layers violently cold-worked and possibly partly strain-aged.

Some earlier results of Memmler and Laute (1930) and also of Kommers (1943) also emphasize the point that the understressing treatment must be prolonged before it has any considerable effect. The latter used an ingot iron (fatigue limit =26 200 p.s.i.) which was understressed at 26 000 p.s.i. for various times: after each treatment the new fatigue limit was determined. Five million cycles of understressing raised the fatigue limit by about 6%, while after forty million cycles of understressing the increase was about 20%. No further increase could be achieved.

(*b*) *Effect of decarburization*

One or two very interesting papers have recently been published dealing with the effect of decarburization on the fatigue characteristic of mild steels. The most careful work is probably that of Lipsitt and Horne (1956a) who used a material originally containing 0·09% C. The specimens were very carefully prepared, including a final electropolish, and the tests carried out in push–pull. The decarburizing treatment was 100 hr in wet hydrogen at 940°c and was estimated to reduce the carbon content to 0·003–0·005% and the nitrogen to 0·00018%.

The general effect (fig. 46) was to depress the S–N curve in the mortal region, i.e. to reduce the life for a given stress. But in addition the 'knee' of the curve—i.e. the point at which it turns to become horizontal—was shifted to longer lives. There is even some doubt as to whether the knee exists at all or whether the phenomenon of the fatigue limit has not disappeared altogether. In view of the long lives involved ($\sim 10^8$ cycles) it will be very tedious to obtain conclusive evidence on this point, but it is clearly something that should be done.

Another similar investigation was made by Rally and Sinclair (1955) using a steel containing nominally 0·15–0·20% C. In this case the tests were done in rotating bending. The decarburization (wet hydrogen at 705°c for 14 days) was not sufficient to remove all traces of the yield-point from the static tensile curve. The effect on the fatigue curve is shown in

fig. 47. It will be seen that the knee of the curve has again been moved to a lower stress and a longer life, but in this instance there is little doubt that it still exists.

A third related experiment was made by Levy and Sinclair (1955). Here no attempt was made to investigate the fatigue limit, but the life at

Fig. 46

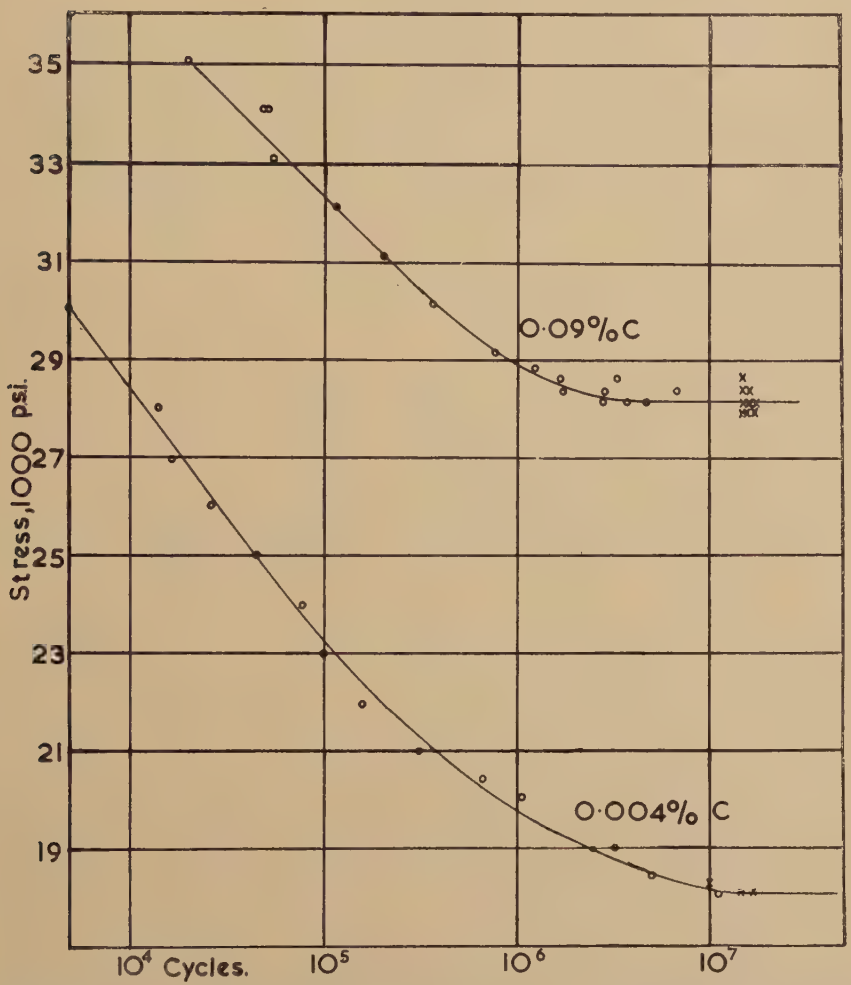

S–N curves for iron specimens, before and after decarburizing treatment. Tests in push–pull. (After Lipsitt and Horne 1956 a.)

a constant stress and various temperatures was measured. The initial material showed a pronounced maximum in the fatigue life at about 230°c (this point is discussed again on p. 130, see fig. 50). When the steel decarburized (4 days at 705°c in wet hydrogen) the maximum

disappeared; and a similar maximum re-appeared when the decarburized material was subsequently nitrided (24 hours at 705°c in ammonia).

These three investigations serve to show that the presence of carbon (nitrogen) in solution in α iron has a very marked effect on fatigue behaviour. An attempt at interpretation will be given later; in the meantime, it is clear that more experimental work under carefully controlled conditions would be very valuable.

(*c*) *Damping capacity*

Observations on the energy dissipated per cycle when the peak stress is of the same order as the fatigue limit are also of interest. The experimental difficulties are considerable, and the number of papers giving trustworthy results appears to be very small. One of the more recent and more thorough investigations is that of Lazan and Wu (1951) using a

Fig. 47

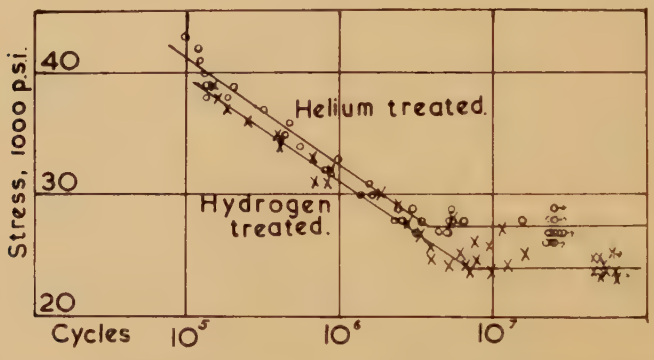

S–N curves for iron specimens before and after decarburizing treatment. Tests in rotating-bending. (After Rally and Sinclair 1955.)

commercial steel (SAE 1020). This was tested in rotating bending, single point loading, but by using tapered specimens in the form of thin-walled tubes the stress was made approximately constant (to within about 10%) over the whole volume of material tested. The damping was measured by observing the lateral displacement of the free (loaded) end of the specimen when rotating. Figure 48 shows some of the results replotted on linear scales from the published (smoothed) curves, which were on logarithmic scales. Three points may be noticed: firstly, the damping is not zero—that is some cyclic plastic deformation is taking place—below the fatigue limit which is quoted as 35 000–36 000 p.s.i. Measurements at low damping are likely to be the least reliable, using this particular technique, but the results are unambiguous: in addition, the same fact has been remarked upon by other workers also, for example, Gough and Hanson (1923). Secondly, the damping increases with continued stressing, at first rapidly and then more slowly. At stresses

below the fatigue limit, this increase is much more gradual than at higher stresses. Thirdly, it will be seen that the general level of the damping, after the initial increase is over, is low when the stress is below the fatigue limit, and increases rapidly when this stress is exceeded. (It should be remembered that the stress was not exactly homogeneous throughout the volume, even macroscopically, and that, owing to the elastic anisotropy of the individual grains, the micro-stresses will show an even greater spread.)

Fig. 48

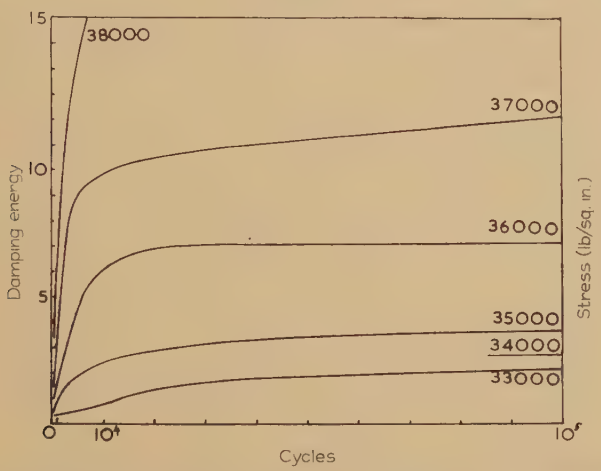

Variation of damping during fatigue test of mild steel, at stresses indicated. (Adapted from Lazan and Wu 1951.)

In this connection it is interesting to recall some of the earlier work done by Gough, Moore and Kommers, and others, around 1920. The starting point was the desire to evolve some method of determining the fatigue limit without prolonged endurance testing of many specimens. Following up the earlier work of Stromeyer (1914), Gough (1926) measured the rate of evolution of heat in a fatigue specimen as a function of stress, as the stress was increased in steps from zero. When the temperature rise (α area of hysteresis loop) was plotted against stress, a straight line resulted when the stress was small, but a more or less well marked discontinuity appeared at a critical stress, indicating that the hysteresis loop had begun to increase more rapidly. This critical stress, it was suggested, was the fatigue limit.

A second line of approach, explored simultaneously, was to measure the alternating strain as the stress was gradually increased from zero. Both Gough (1926), and independently, Lea (1923) did this in a rotating bending machine by using a delicate optical lever to measure the change in slope of the free end of a single cantilever specimen. Again, when this strain was plotted against increasing stress, a discontinuity in the curve was said to coincide with the fatigue limit. (It will be appreciated that

this arrangement measures an effective or secant elastic modulus, as was done later by Lazen and Wu, and therefore really detects the same quantity as the thermal method, namely, a sudden widening of the hysteresis loop.)

In fact, the two critical stresses agreed very well, and both were in good agreement with the fatigue limit determined by more conventional methods, for many of the materials tested. Figure 49 summarizes the results obtained by both Gough and by Moore and Kommers, for about

Fig. 49

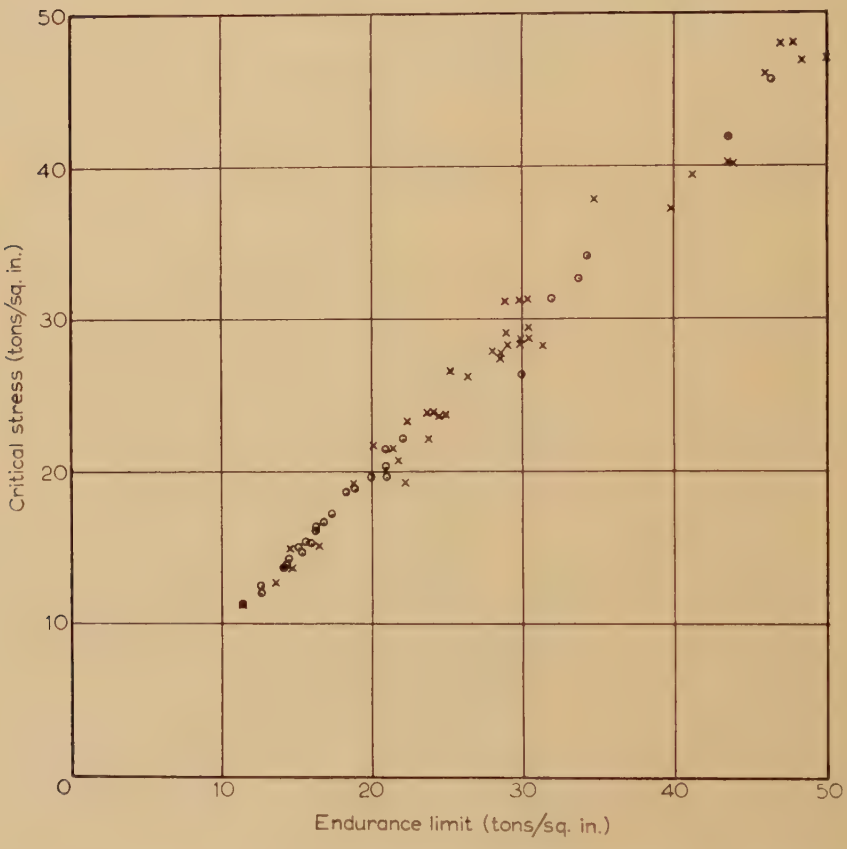

Relation between endurance limit and critical stress determined by temperature rise method. ○ N.P.L. results; × Illinois Expt. Station results: both quoted by Gough (1926).

70 ferrous alloys and shows the extent of this agreement. With non-ferrous materials the discontinuities in the curves were much less well marked —the published examples show a gradual departure from a straight line rather than any pronounced kink. Only a few results are given, and the agreement with normal endurance values is less satisfactory. The

technique is now not mentioned in the literature as a method of determining fatigue 'limits' probably because of this limitation to one type of material.

(*d*) *Metallographic observations*

Reference must also be made to the work of Hempel and his associates during the past years. From among many other interesting observations, two in particular concern us here. The material used was an iron with about 0·02% C annealed 1 hour at 930°C and air cooled, and the fatigue tests were done in push–pull. For some of the work the specimens were given a static tensile pre-strain before the fatigue test. If this strain exceeded about 6% then it was found, on completion of the subsequent fatigue test, that small particles of precipitate were visible, mainly in the slip bands produced during the tensile straining. (Sander and Hempel 1952, Hempel and Houdremont 1953). Electrochemical separation of the precipitate particles, followed by an x-ray determination of their crystal structure, showed that the precipitate was cementite (Fe_3C). Further observations showed that such precipitation did not occur if the stress during the fatigue test were below the fatigue limit for the material under the conditions of the test. When conditions were favourable for producing the precipitate, the amount of it increased as the fatigue test continued; if the stress were not homogeneous, the amount of precipitate was greater in those regions where the stress was greater and, other things being equal, was greater on the surface of the specimen than in the interior. If the fatigue stress were well above the fatigue limit, no precipitate was visible at the conclusion of the test; but if the life of the specimen were prolonged by a coaxing treatment, precipitate particles were seen.

Subsidiary experiments showed that the following procedures did *not* produce similar precipitation:

1. Fatigue testing without previous tensile strain.
2. Fatigue testing followed by tensile strain.
3. Tensile strain followed by a low temperature anneal.
4. Tensile strain, followed by prolonged fatigue testing at a stress below the fatigue limit, either with or without a subsequent mild annealing treatment.
5. Tensile strain, followed by a short fatigue test at high stress, and a subsequent mild anneal.
6. Tensile strain, followed by a fatigue test at any stress level carried out a low temperature (−180°C).

In the present context, perhaps the most significant observation was that it was not possible, under any circumstances, to observe the formation of precipitates if the fatigue stress were below the fatigue limit. At slightly higher stresses, however, the precipitation was very marked, and at still higher stresses, the specimen broke before the precipitates were formed.

(*e*) *X-ray observations*

The second aspect of the work of Hempel's school to which reference must be made is the x-ray observations: these are described more fully in § 6. The more important results are that little or no change in the sharpness of x-ray reflections from annealed material is produced by fatigue stresses below the fatigue limit, but that above this stress an increase in the amount of blurring is often observable after as few as 10^3 cycles. (All the evidence of this last point is not entirely consistent.) The blurred reflections on initially cold-worked specimens become sharper as a result of stressing above their fatigue limit. Both of these changes are inhibited by a coaxing treatment.

4.3. *Discussion*

Turning now to more speculative matters, it seems possible that much of the behaviour just summarized can be related to the effects of carbon (and nitrogen) present in interstitial solution in the body-centred (ferritic) lattice. The effects on the static mechanical properties of iron have received a good deal of attention in recent years. Explanations, based on the interaction of such solute atoms with dislocations, and stemming from the original suggestion of Cottrell, are now agreed by most workers in broad outline, although some points of details remain unresolved. The phenomena concerned, i.e. the existence of upper and lower yield points, strain-rate effects, strain-ageing and blue brittleness, Lüder's bands, etc., are too well known to need recapitulation here.

By comparison, very little has been written about the effects on 'dynamic' properties such as damping and the various aspects of fatigue behaviour. It is now suggested that the *fatigue limit* occupies a similar place in the field of alternating stresses to that filled by the *yield point* in unidirectional stressing. At stresses above the fatigue limit, the locking of dislocations by carbon atoms is readily broken down; below the fatigue limit, most dislocations are still effectively locked.

If this is correct, then, in the simplest cases, the fatigue limit and the yield point should be approximately equal. The agreement is, in fact, not good, but such a comparison is not as easy as might appear at first sight. Neither quantity is easy to measure at all accurately; the former depends on the mode of stressing, on the method of surface preparation, and possibly on grain size, speed etc.; the latter is sensitive to axiality of loading and also shows speed effects. The number of experiments on simple, low-carbon steels in which all the relevant variables were controlled and recorded is not very large, and the results show a considerable variation. Values for the fatigue limit range from 24 000 to 28 000 p.s.i., while yield point results range from 28 000 to 35 000 p.s.i. or more. A careful comparison using modern techniques, would be very valuable. It would also follow that the result should be independent of the carbon content over a considerable range. This has been demonstrated for the lower yield point by Petch (1953) but existing data are inadequate to draw any conclusion about the fatigue limit.

If the carbon content is reduced to a very low value, it is well known that the characteristic yield point phenomena almost disappear. It is clear from the results of the three papers quoted above that an equally striking change takes place in the fatigue limit. These results provide the most direct evidence available to date in support of the contention that the two are related.

We consider next the experiments on carbide precipitation. The general lines on which these observations are to be explained are probably clear enough, and were suggested by the original authors (see also Houdremont in discussion of paper by Hempel *et al.* 1952). The carbon will be initially present as supersaturated solution. The fatigue testing confers upon it sufficient mobility, even at room temperature, to diffuse and form precipitates. (For the effect of fatigue on rate of diffusion of carbon, see Schenck and Schmidtmann 1954, see also § 9 of this article.) The role of the previous plastic deformation is possibly to produce the local regions of distorted lattice in the slip bands (? =groups of dislocations) which constitute a favourable situation for the nucleation of the precipitate particles. It is known (see, for example, Harper 1951) that carbon atoms migrate readily to dislocations; such an aggregation on a close group of dislocations would be a likely place for a precipitate particle to nucleate. This cannot, however, be a complete explanation: if it were, a mild annealing treatment following cold work would produce similar results by speeding up the migration of carbon in the usual way. In fact this was observed not to take place.

x-ray results tell the same story. Below the fatigue limit, little or no effect is observed; above this level of stress, some at least of the grains are considerably distorted, which indicates immediately that movement of dislocations has been taking place. It is not proposed to discuss here the converse effect, i.e. the re-sharpening of x-ray reflections made diffuse by cold-work, when the fatigue stress is sufficiently high. The fatigue *limit* does not enter into these effects as a critical stress. But the inhibition of these change by fatiguing at stresses below the fatigue limit is more relevant. These effects are clearly to be related to coaxing and the three will be considered together.

The fact that such effects can be produced at all by fatiguing below the fatigue limit indicates that some permanent (i.e. non-elastic) changes are caused in the crystals, and suggests that we must refine our hypothesis to this extent, that we envisage *some* dislocation movement below the limit, together with a very large increase on passing this limit. It is obvious from the metallographic observations already discussed that this must take place to some extent, at least in the surface layers. The idea is supported also by the observations on damping. It has already been mentioned that, although small, this is not zero below the fatigue limit. The classical papers of Bairstow (1910) and the later work of Gough and Hanson (1923) and of Lazan and Wu (1951) demonstrate that this small damping may increase very slowly during continued stressing below the fatigue limit.

In this connection, a recent suggestion by Gibbs (1957) is interesting. He points out that if a dislocation is pinned at intervals by impurity atoms, and if an applied stress causes a small loop of the dislocation to break away from its pinning points, then there will be a tendency for the length of this loop to increase as the remaining impurity atoms diffuse *along* the dislocation away from the free loop. Moreover—an important point in the present connection—the effect is independent of the sign of the stress, and thus will be cumulative under the action of an alternating stress. The displaced impurity (carbon) atoms will accumulate around the nodes of the dislocation network, and will act like a finely divided precipitate. It is possible that an explanation of coaxing and the associated phenomena may be found on these lines, although the problem has not yet been examined in detail. It would, for example, be interesting to observe the effect of low temperatures on the occurrence of coaxing in a simple material.

An interesting result, readily understandable on the basis of these ideas, was obtained by Tapsell (quoted by Gough 1926, p. 249). He used a technique similar to those described in § 4 (*c*) above for measuring the energy dissipation, but applied it to push–pull tests. A specimen of medium carbon steel showed a pronounced kink on the graph of temperature versus stress, when tested as described. When the stress was reduced to zero, and the test repeated however, there was no detectable discontinuity in the curve: moreover the energy dissipated per cycle at stresses below the previous fatigue limit was now very much larger than it had been on the first test. The parallel with the well-known effects of 'overstraining' in a simple tensile test is very close.

In this connection two other isolated and interesting observations may be mentioned; in both, confirmation under carefully controlled conditions using modern techniques would be valuable. The first is by Moore and Ver (1930) using a plain carbon steel (0·20% C) fatigued in reverse bending. Four point loading was used, so that a long central section was subjected to a constant bending moment. In this section there were two regions in which the diameter was reduced. Fatigue fracture occurred in one of these regions. A plain cylindrical tensile specimen was then machined from the broken piece so that about half of its gauge length came from the second reduced diameter region of the fatigue specimen, while the other half came from the portion of larger diameter. Thus both halves of the new gauge length had previously been subjected to the same number of cycles of fatigue stress, in the one half at a level almost high enough to produce failure, and in the other half at a much lower level. The interesting point is that although Lüder's bands were propagated in the normal manner through the low-stress portion, they were not propagated at all through the other half. Since, according to current ideas, the Lüder's band phenomenon is closely related to the breaking away of dislocations from their anchoring atmospheres of carbon, this suggests that this process had already occurred in the high stress region, but not in the low stress region—in agreement with the ideas put forward above.

The second experiment was done by Memmler and Laute (1930) on a steel with 0·05%C using a push–pull machine. They report that by subjecting a specimen to a prolonged fatigue test (40×10^6 cycles) at a stress *just below* the fatigue limit, and then carrying out a normal tensile test on the unbroken specimen, it was possible to reduce, or even eliminate, the characteristic upper yield point without causing any other significant alteration in the stress–strain curve. Again this suggests that a considerable number of dislocations had been freed from the locking action of the carbon by this understressing.

4.4. *Further Related Experiments*

Although not strictly concerned with the fatigue *limit*, this would appear to be the appropriate place to mention one or two experimental papers which are probably all concerned with the effects of interstitial carbon on damping and fatigue properties.

(*a*) *Strain-ageing effects*

Guest and Lea (1916) when making observations on what they called torsional hysteresis of a mild steel (0·15%C) using very slow rates of cycling remarked that if the specimen were allowed to rest at room temperature under zero stress, the width of the hysteresis loop was reduced. Furthermore, this decrease was accelerated if the temperature were raised to 100°C. A similar effect was reported by Case (1938). The observed damping was increased by as much as ten times if the specimen were violently overstrained in torsion; this damping again decreased on standing at room temperature, and again decreased more rapidly at rather higher temperatures. Lazan and Wu (1951) give some results on a specimen which had been fatigued for a large number of cycles below the fatigue limit. On resting at room temperature the damping decreased (after a curious but unambiguous initial increase!) falling to about 50% of its value in the order of 10^4 min. Although insufficient quantitative data are available to establish the point with certainty, it is fairly clear that in all this work we have the equivalent of 'strain-ageing', i.e. the re-locking of previously mobile dislocations by the diffusion of carbon atoms to them.

If the above is correct, then it might be expected that such a rest pause, or mild annealing treatment would have the effect of prolonging the fatigue life. Results which appear to support this conclusion are to be found in a paper by Daeves *et al.* (1940). Two different steels were used, containing 0·06% and 0·42%C respectively, specimens being tested in rotating bending at a stress which gave an endurance of about 10^5 cycles in each case. Some of the tests were interrupted, for varying times (1 minute to 3 days) at varying intervals (every 5000 cycles, or 10 000 or 20 000 or 40 000) and during the interruption the specimens were annealed at varying temperatures (20–210°C, but usually 140°C). Taking the mean endurance of batches of 4–6 specimens, it was found that the effect

of the interposed annealing treatment was always to increase the life, the effect being greater when (*a*) the pause was longer, (*b*) the pauses were more frequent, (*c*) the temperature was higher. Bollenrath and Cornelius (1940) investigated the effect of rest pauses (6–24 hours long) interposed at intervals ($\simeq 10\%$ of the expected life) during fatigue tests of eight different alloys, i.e. one aluminium, two magnesium, one copper, one brass and three steels. The only material showing any significant effect was a plain steel with a carbon content of only 0·02% carbon. In this case the life at stresses just above the fatigue limit was increased about a hundred-fold. Lissner (1955) investigated similarly four different steels under carefully controlled conditions, interposing rest pauses, either at room temperature, or at 100°c and lasting for 24 hours, at intervals during a test. Two of the three annealed plain carbon steels showed an increase in life due to this treatment, but a hardened, Ni–Cr steel did not. On the other hand, Siebel and Stähli (1942) and Möller and Hempel (1954), using different procedures involving interposed annealing, both concluded that there was no such increase. It should be noted however that in both these experiments the annealing temperature was much higher (550°c and 930°c respectively), so that they are not strictly comparable with the others.

(*b*) *Effect of high temperatures*

The effect of temperature on the fatigue characteristics of mild steels is also of considerable interest although there does not appear to have been an exhaustive and systematic investigation. Very few observations have been made below room temperature, and most of these refer to alloy steels. The general tendency is for the fatigue limit to rise slightly as the temperature falls, the increase amounting to between 5 and 20% at temperatures of the order of −40 to −80°c (see, for example, Henry and Coyne 1942).

This downward trend with rising temperature continues for a little way above room temperature (Rally and Sinclair 1955), and then, with a further increase in temperature, as has been known for some time, the fatigue characteristics are 'improved'— i.e. the fatigue limit is higher, and the life in the mortal range is greater at a specified stress. The first point is illustrated by some results of Moore and Alleman (1931) on a 0·17% C steel. The fatigue limit increased from 30 000 p.s.i. at room temperature to 39 000 p.s.i. at 290°c. The second point is shown by the measurements of Levy and Sinclair (1955) on a 0·18% C steel. Several specimens were tested at a constant (nominal) stress of 35 000 p.s.i. and fig. 50 shows a marked rise in fatigue life, to a maximum in the neighbourhood of 230°c.

At still higher temperatures the trend is reversed. The life for a given stress falls rapidly (fig. 50) and the fatigue limit, as such, disappears. Moore and Alleman, for example, show a steadily falling S–N curve as far

as 4×10^7 cycles for tests carried out at 430°c. At still higher temperatures, the endurance is very much less, and there is still no trace of a fatigue limit.

Confirmation of these results is to be found in the work of Forrest (see Forrest and Tapsell 1954), Allen and Forrest 1956, Forrest 1957). The latter papers shows clearly a maximum in the fatigue limit at about 350°c in qualitative agreement with Levy and Sinclair. The quantitative agreement between two sets of results is not however very good, even

Fig. 50

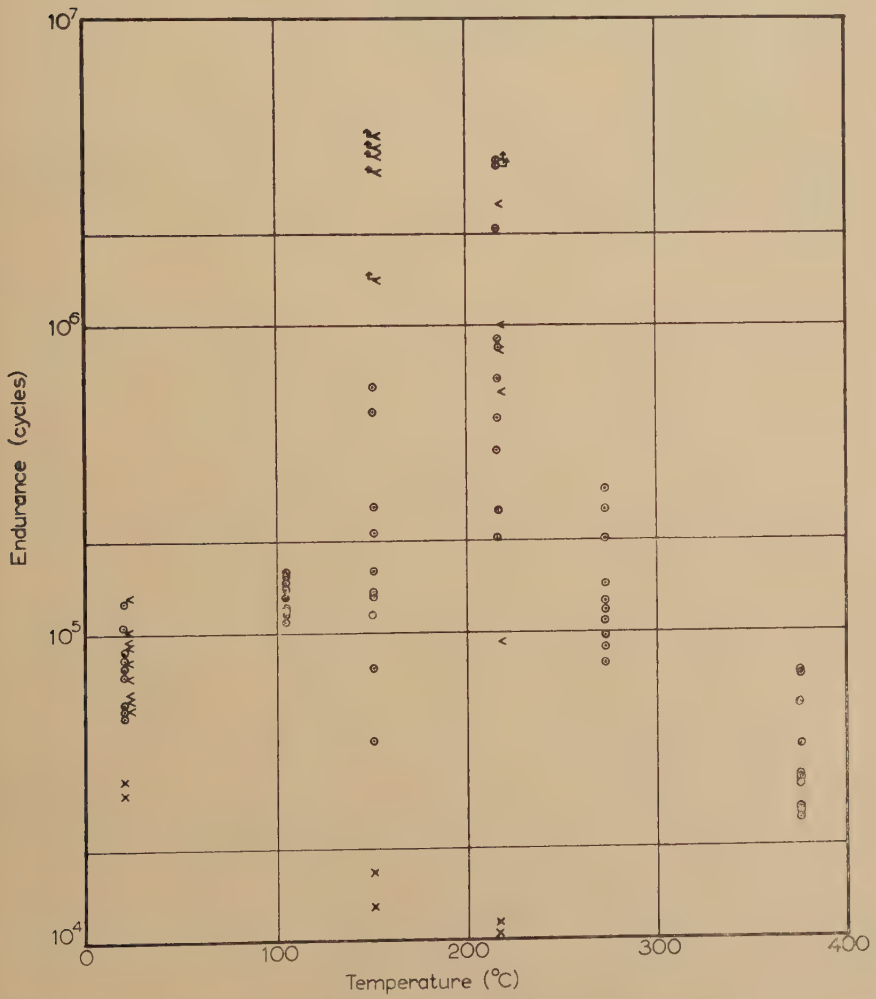

Endurance of mild steel specimens tested in rotating bending at 35 000 lbs/sq. in. and temperatures as shown. ○ material as received ; × carbon and nitrogen reduced (wet hydrogen treated) ; < nitrogen restored (ammonia treated). (After Levy and Sinclair 1955.)

though the material and conditions of test were similar: it is possible that the explanation of the divergence is to be found in differences of heat treatment, or surface preparation or even composition (? nitrogen).

The explanation of the maximum advanced by Levy and Sinclair, and supported by Forrest, is that it is a strain-ageing effect. At the temperatures concerned the interstitial carbon (nitrogen) atoms have sufficient mobility to diffuse through distances of the order of 10^{-6} cm during one half cycle of stress. This will enable them to form an 'atmosphere' around the dislocations and so inhibit the occurrence of slip in the next half cycle. At temperatures below the maximum the diffusion rate is too small to permit any appreciable amount of locking to take place in this manner. At temperatures above the maximum the interstitial atoms are not sufficiently condensed.

This hypothesis is qualitatively satisfactory and receives strong support from the fact that when Levy and Sinclair annealed their material in wet hydrogen, so as to remove the dissolved carbon and nitrogen, the maximum in the curve disappeared (fig. 50). Furthermore, on heating in ammonia, to replace some of the nitrogen, the maximum returned.

(*c*) *Speed effect*

At these higher temperatures another phenomenon appears, namely, the so-called speed effect. At ordinary temperatures the fatigue failure of a test piece is determined almost entirely by the *number* of cycles of stress to which it has been subjected, and the frequency of the vibration has very little effect. At higher temperatures, however, the speed does become important. The effect is usually in the sense that the endurance in the mortal range is greater when the speed of testing is higher. This has suggested to numerous workers that the total *time* of testing rather than the total *number* of cycles should be considered as the significant variable. In general, neither method of representing the results gives a relation between stress and life which is independent of speed (see, for example, fig. 51 (*a*) for data on an aluminium alloy, RR 58). The fact that such speed effects become more noticeable at higher temperatures has led a number of authors to suggest, in general terms, some connection with creep processes. Another way of presenting the argument might be as follows: Since slip plays an important part in fatigue failure, and since slip is a time-dependent process at elevated temperatures, we might expect that fatigue would also depend on the time for which each half-cycle of stress is applied. As an approximate measure of the amount of slip per half cycle we may take the cycle plastic strain, i.e. the width of the hysteresis loop. Thus if the cyclic strain is used to characterize a fatigue test, rather than the applied stress, we might expect the speed effect to disappear.

The paper by Forrest and Tapsell (1952 b) includes results on the dynamic stress–strain curves which enable the change to be made. Figure 51 (*b*)

shows the results on RR 58 re-plotted in this way ; the points lie sufficiently close to a single curve to suggest that it would be interesting to obtain further data of the same kind.

Fig. 51

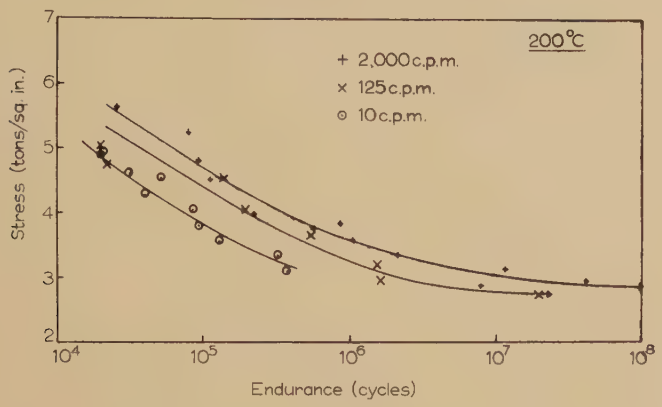

(*a*)

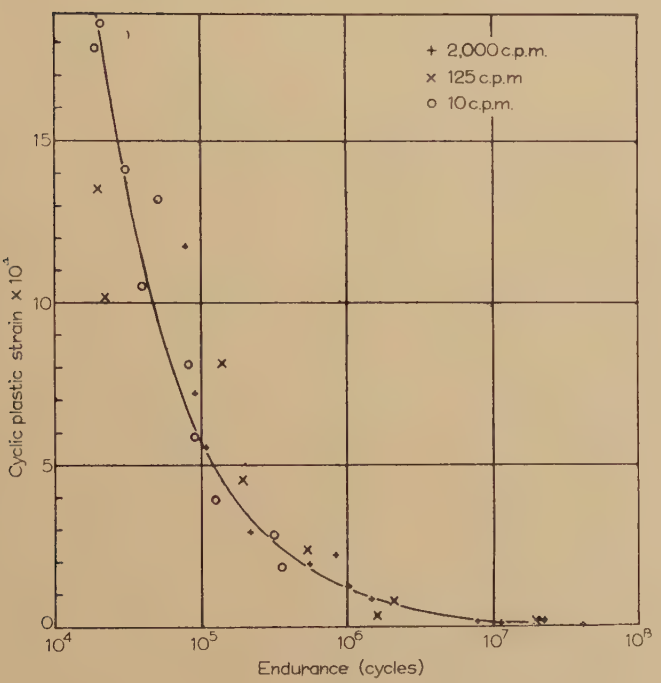

(*b*)

(*a*) S–N curves for alloy RR 58, tested in push–pull at 200°c : + at 2000 cycles/min ; × at 125 cycles/min ; ○ at 10 cycles/min. (Forrest and Tapsell 1952 b.)

(*b*) Same data as (*a*) re-calculated in terms of cyclic plastic strain, instead of stress.

A speed effect of the above kind would be expected to be a general phenomenon, not confined to one class of material. But with mild steels in the temperature range 150–350°C, one finds an anomalous speed effect, in which a lower speed leads to greater fatigue strength. This is closely bound up with the maximum in the fatigue strength already discussed. Since, at lower speeds, the time available for diffusion of the carbon is greater, adequate locking of the dislocations can take place at a lower temperature: i.e. the position of the maximum should be displaced to lower temperatures at lower speeds. The consequent crossing of the curves leads directly to the anomalous speed effect, as is shown clearly by the results of Forrest (1957).

§ 5. Notch Effect and Crack Propagation

5.1. *Introduction*

It has been known since the time that fatigue first attracted attention, that singularities of geometrical form which give rise to local variations of stress are often the seat of the initial failure, and that they sometimes produce disastrous consequences which at first sight seem altogether out of proportion to the magnitude of the cause. The feature which gives rise to the local stress concentration may take many forms—a notch, groove or sharp re-entrant angle, a hole deliberately made or a defect such as a cavity or slag inclusion in the material; in the present context all such singularities are referred to as 'notches'. To investigate the effect of such stress-raisers under controlled laboratory conditions, they are usually made to take the form of circumferential grooves around cylindrical specimens or, alternatively, transverse holes through rods, bars or strips.

By a suitable choice of the shape of the 'notch' it is sometimes possible to obtain a situation in which the stress distribution can be calculated—at least approximately—by the methods of classical elasticity. A few exact solutions for special cases have been published, and a collection of such results, some only approximate, has been given by Neuber (1937) (see also Cox 1953). It should perhaps be remarked now—as will be emphasized later—that such solutions, even when exact, refer to an elastic, homogeneous, isotropic and continuous solid; it is doubtful whether any of these adjectives could be applied to a real specimen on the scale on which it seems most appropriate to consider the phenomena of the initiation and propagation of a fatigue crack. Where the conditions do not lend themselves to mathematical analysis, an alternative approach is to determine the stress-distribution in a scale model by the methods of photoelasticity. Such methods have hitherto been applicable mainly to two-dimensional problems, and even here are difficult to apply where very high stresses are concentrated in very small volumes. The ratio of the calculated peak stress in a notched specimen to the maximum nominal stress is known as the 'stress concentration factor'—sometimes with the additional adjective 'theoretical': it will be denoted here by the

symbol K_t. The 'nominal stress' in this context means the stress calculated by elementary formulae which take no cognisance of stress concentration effects; in the case of a push–pull specimen, for example, it would usually be the total load divided by the minimum cross sectional area.

In view of its very great importance in engineering, an enormous amount of experimental work has been done on the fatigue behaviour of notched specimens. In many cases the investigators have contented themselves with a determination of the fatigue limit (or some similar quantity) for a notched specimen, and have then compared it with corresponding quantity for a plain specimen under similar conditions. In such an investigation the 'stress' referred to is always the nominal stress as defined above. Some workers have gone a little further and made a comparison of the S–N curves for plain and notched specimens. Nevertheless it is the almost universal practice to measure the effect of a notch on fatigue behaviour by a single number, usually taken as the ratio of two stresses, and usually again as the ratio of the fatigue limits, for plain and notched specimens. This quantity is known as the 'strength reduction factor' (or sometimes 'effective stress concentration factor' etc.) and will be denoted here by the symbol K_f. (When the cycles of stress are not symmetrical about zero, the proper definition of K_f is a matter of some difficulty, but that will not concern us here.)

If it were true that the maximum stress is the only factor relevant to the question of whether or not a fatigue crack is initiated, and if the initiation of a crack always led eventually to complete failure, then it might be reasonable to expect that the two quantities K_t and K_f, the latter calculated with reference to the fatigue *limit* would be equal to one another. In almost all cases this equality is not found, and the discrepancy is frequently measured by a quantity called the 'notch sensitivity' q, defined as

$$q=(K_f-1)/(K_t-1).$$

With only very rare exceptions, q is found to be less than unity. A very large amount of experimental work has been done to determine K_f or q or both for a wide variety of materials, using specimens of all sorts of shapes and sizes, and much ingenuity has been exercised in trying to rationalize the results obtained.

A review article dealing with work of this kind was contributed by Paterson to the symposium on fatigue in Melbourne in 1946, and later another critical appraisal was given by Yen and Dolan (1952).

5.2. *General Results*

There are a number of factors relevant to this problem which should be mentioned before embarking on a detailed discussion. Firstly, it is now known that details of surface finish can have a very important influence on fatigue behaviour. Even when this is appreciated—and its importance was not realized when much of the earlier work was done—it is still very difficult to ensure the same conditions at the bottom of a sharp notch as on the surface of a plain specimen. Since it is almost

inevitable that the volume (or area) of material subjected to the maximum stress is much smaller in a notched specimen than in a plain one, this alone might be expected to lead to differences in the results. There is little doubt that this factor must operate to some extent. (In cast iron, for example, there is little difference between the strength of a notched and a plain specimen: this has been attributed to the fact that the graphite flakes in the material act like a very large number of small, but acute notches, and the addition of one more artificial notch makes little difference.) But it is most improbable that the whole explanation is to be found on these lines, and, indeed, Cox (1956) has given good arguments against such a viewpoint.

Fig. 52

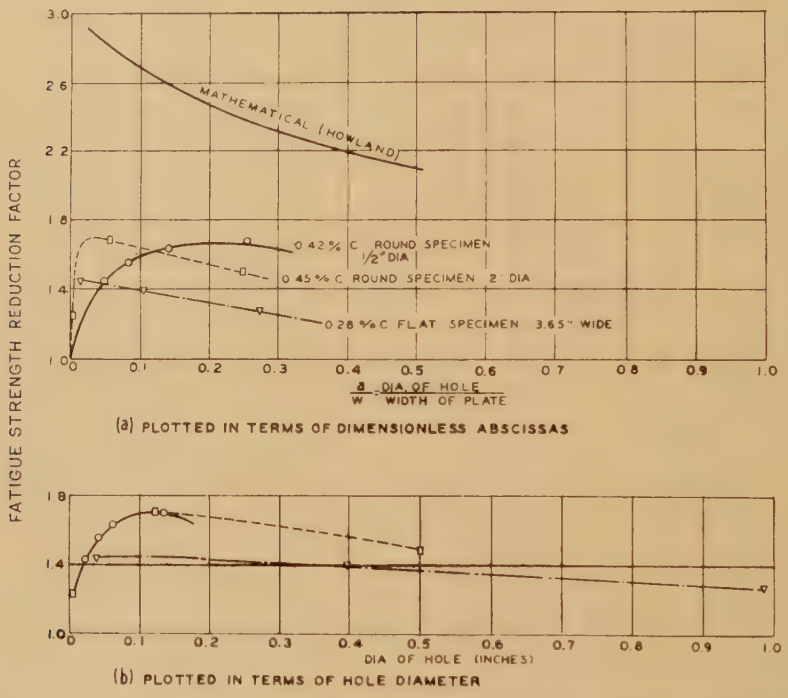

Fatigue strength reduction factor of steel specimens as a function of the size of a transverse hole. (Peterson 1933.)

From the confusion of results relating to 'notch sensitivity' two points at least stand out clearly: (1) The notch sensitivity, either as defined above, or with any other less precise connotation, varies from one material to another. But, however defined, it is not to be regarded as a constant characteristic of a material. (2) With any one material, the 'notch sensitivity' depends on the absolute size of the test piece. (One complicating factor may be mentioned now, and not further considered: The energy dissipated during fatigue may be sufficient to cause an appreciable rise in temperature of the specimen, particularly at higher testing speeds.

The temperature attained by specimens of a given material will thus depend on their size, even if they are geometrically similar; and if the properties of the material are sensitive to temperature, this will give

Fig. 53

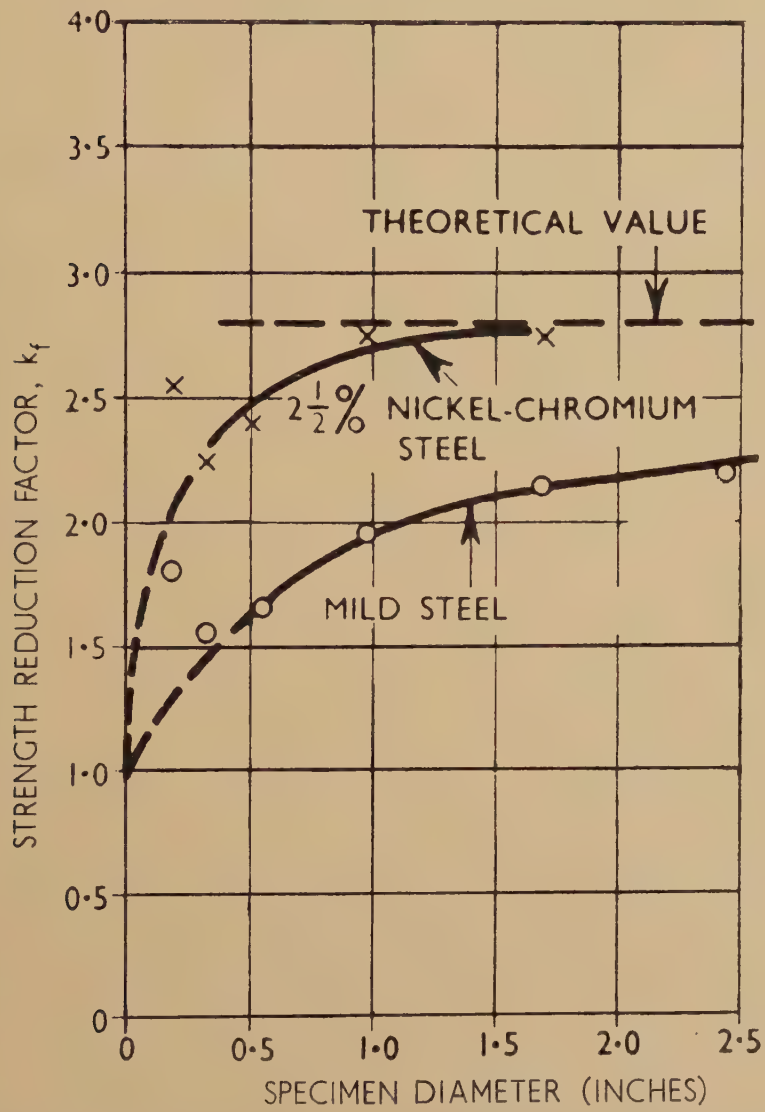

Size effect with transversely bored specimens tested in push–pull. Hole diameter = 1/6 specimen diameter. (Phillips and Heywood 1951.)

rise to a spurious 'size effect'. Similarly, when comparing the behaviour of specimens of different shapes, the possibility of complications of this kind should not be overlooked.)

The general trend of all the investigations is that q tends to its theoretical value of unity when the scale of the experiment becomes sufficiently large. Two examples of papers bearing on this point will suffice. Peterson (1933) reports experiments on round bars tested by bending and on flat specimens, each with transverse holes of various diameters. The results are summarized in fig. 52. Similarly Phillips and Heywood (1951) tested round bars of two different steels in push–pull, the notch again taking the form of a transverse hole (fig. 53). The graphs show the same general form in all cases.

By contrast, no such comparable 'size effect' is found when a plain specimen is tested in push–pull (see, for example, Peterson 1930, Phillips and Heywood 1951). If a plain specimen is tested in bending (or torsion) on the other hand so that a stress gradient exists at the surface, a 'size effect' re-appears. This was shown, for example, by Morkovin and Moore (1944), and Vitovec (1953) gives a collection of data on technical materials illustrating the same point. Forrest and Tapsell (1952a) have pointed out that the plastic flow which occurs in the regions of maximum stress will cause a redistribution of stress and a reduction in the maximum value. The amount of plastic strain at each stress may be measured in a test under uniform stress. In this way they were able to account for the fact that their specimens (plain steel cylinders tested in rotating bending) showed a bigger size effect at 450°C than at room temperature.

In a recent paper, Forrest (1956) has applied the same ideas to a consideration of notch effect. The theoretical (elastic) solution for the stresses around the notch is taken to give the real strains, even when some parts of the material are plastically deformed. The dynamic stress–strain curve, determined independently using a plain specimen, then gives the approximate real stresses. The specimens used took the form of transversely bored, square-section bars of various materials, tested in push–pull. They were all the same shape and size, having a theoretical (elastic) stress concentration factor K_t of 2·3. Figure 54 shows the calculated (plastic) stress concentration K_t' compared with the experimental strength reduction factor K_f. Although the agreement is far from perfect, it is sufficiently good to suggest that the cyclic plastic deformation at the root of a notch is an important factor, and goes a considerable way towards reconciling the difference between K_f and K_t at least when the notch is not very acute.

One refinement of the theory has been suggested, in slightly different ways, by a number of writers. This is the idea that, where the stress is not uniform – as at the root of a notch – the fatigue behaviour should be determined not by the maximum value of stress but by a value averaged in some way over a finite volume including the point of maximum stress. In this simple form the suggestion is incontrovertible if the general theory is to be applicable to the sharpest of notches—for example, the tip of a fatigue crack itself. On such a scale the concept of 'the stress at a point' ceases to have any strict physical meaning.

One of the earlier proponents of this idea was Neuber (1937) who based his argument on just this point, that classical elasticity rested on an assumption of infinite divisibility of matter, whereas real solids were non-homogeneous, when regarded on a sufficiently small scale. He proposed to substitute for the maximum stress, another value, averaged

Fig. 54

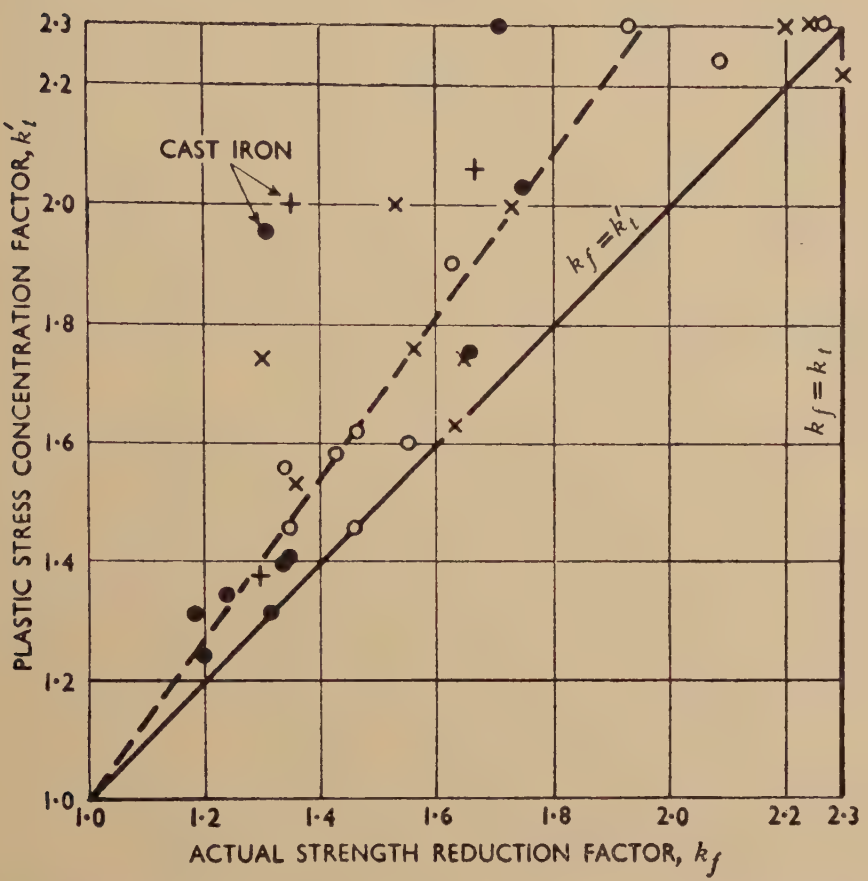

Comparison of calculated stress concentration factor with allowance for plastic deformation (K_t'), and experimental strength reduction factor (K_f). Various materials : Basis of comparison : × 10^7 cycles ; ○ 10^6 cycles ; • 10^5 cycles ; + 10^6 and 10^7 cycles. (Forrest 1956.)

over the surface of an 'elementary particle', and showed that the effect was to replace, in the algebraic formulae, the radius of curvature at the root of the (very sharp) notch by the radius of the 'elementary particle'. Shortcomings of this simple treatment were to be taken up by choosing the size of the elementary particle to give the best fit with experiment. Further, the transition from blunt to very sharp notches was made by

choosing, quite arbitrarily, an algebraic expression which assumed the correct form in the two limiting cases. In the present notation this is

$$\frac{K_e-1}{K_t-1}=\frac{1}{1+\sqrt{(\rho/r)}}$$

where ρ is the radius of the elementary particle and r is the radius at the root of the crack. An expression of this kind has been found to fit experimental data in some cases, but the necessary values of ρ range from 0·5 cm to 0·0002 cm and seem to bear no obvious relation to any physical quantity.

An alternative approach, which leads to essentially similar results, is the suggestion that not only the maximum stress, but also the stress gradient, is relevant to the problem. In other words, it is not sufficient that the peak stress (calculated from elasticity theory) shall reach a certain value: the stress must exceed a critical value everywhere within a critical volume. Since the stress gradient at the root of a notch varies inversely with the radius of curvature, this approach will lead to formulae in which the ratio K_e/K_t becomes smaller as r decreases. Such expressions, largely empirical, have been given by Afanasiev (1948) and by Heywood (1947).

5.3. *Non-Propagating Cracks*

A recent series of researches at M.E.R.L. under the general direction of Phillips, have shed a great deal of new light on this problem. A paper by Frost (1956) gives the results of an extensive series of experiments on three materials—a plain carbon steel, a nickel chrome steel and an aluminium alloy. Cylindrical specimens were tested either in push–pull, or in rotating bending. The notch was a circumferential groove the form of which was carefully controlled. Figure 55 shows the results of one series obtained in push–pull on the aluminium alloy; the diameter of bar and depth of notch were held constant, and the radius of curvature at the root varied. For each value of root radius, sufficient specimens were tested to give a reasonably reliable value for the fatigue 'limit'. (The point on fig. 55 plotted at zero radius is the fatigue limit for a plain specimen that had been previously cracked in rotating-bending: the conditions are thus not exactly similar to those obtaining for the other points.)

The striking feature of the results is that the strength of a notched specimen passes through a minimum as the acuity of the notch is increased. Similar results, albeit less well supported, had previously been obtained by other workers, notably by Mann (1953) and Hyler *et al.* (1954). In the case of the other materials tested by Frost, and for the aluminium alloy tested in rotating bending, both depth of notch and root radius were varied. However, all the results can be contained on a single diagram if the abscissa is taken as the theoretical stress-concentration factor K_t (calculated, e.g. from Neuber's formulae), and the ordinate is made equal to the experimental strength reduction factor K_f. Figure 56 shows such a diagram for the aluminium alloy used; it includes also some points

from other published work. The data for the two other materials are of the same form, but less complete. They all show that for mild notches, K_t and K_f tend to equality, and that as the severity of the notch (measured by K_t) increases, K_f does not increase but tends to a limit, possibly after first passing through a maximum value. Similar results, although again less complete, have been obtained by Frost and Dugdale (1957) on mild steel plates tested in push–pull, when the edges of the plates are symmetrically notched with varying degrees of severity (see also Frost and Phillips 1957).

Fig. 55

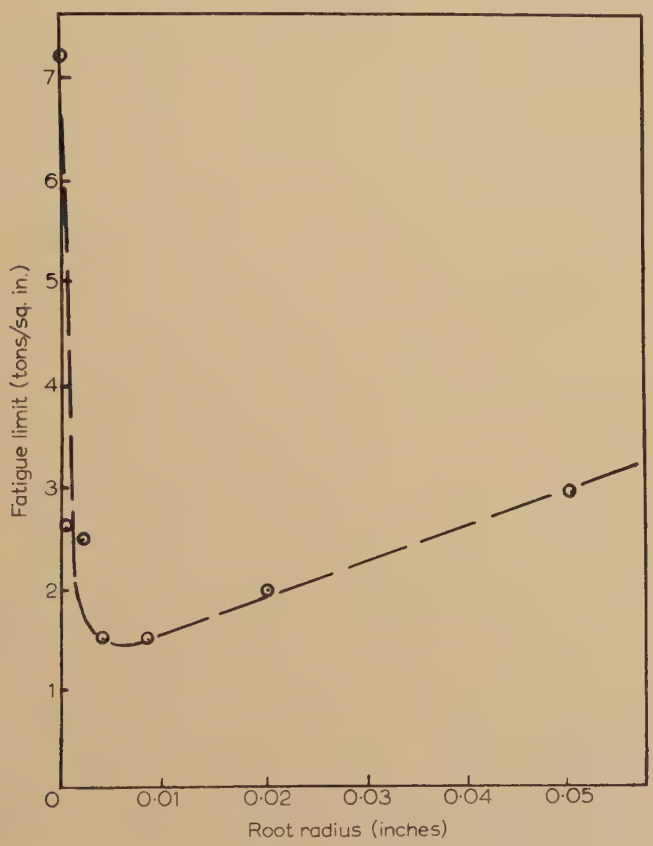

Fatigue limit of an aluminium alloy tested in push–pull. Specimen diameter=1·7 in.; notch depth=0·2 in. Radius at root of notch varied as shown. (From Frost 1956.)

The general trend of all these results is in line with previous observations, but what is quite new is the fact that, in the most severe notches, fatigue cracks were observed to start at the root of the notch, progress so far, and then stop. This observation has been the focus of attention of the whole series of papers. There are occasional earlier references in the

literature to such non-propagating cracks, e.g. Toolin (1953) but no previous systematic investigation. The first of the series of papers (Fenner *et al.* 1951) briefly describes experiments on mild steel bars with a circumferential V groove, tested in push-pull. For example, a specimen sectioned after 5×10^4 cycles at a low (nominal) stress showed the presence of cracks, while another, similar, specimen withstood $2{\cdot}5 \times 10^7$ cycles at the same stress and on sectioning showed a similar crack. Frost (1955) gives similar and more extensive data on an age hardening aluminium alloy. The general conclusions were that a crack would penetrate fairly rapidly ($\simeq 10^5$ cycles) to its final depth and thereafter go no further (up to $2{\cdot}8 \times 10^7$ cycles). The maximum depth of penetration increased as the applied stress increased. Frost and Dugdale (1957) experimented with mild steel plates notched at the edges, to enable the progress of the

Fig. 56

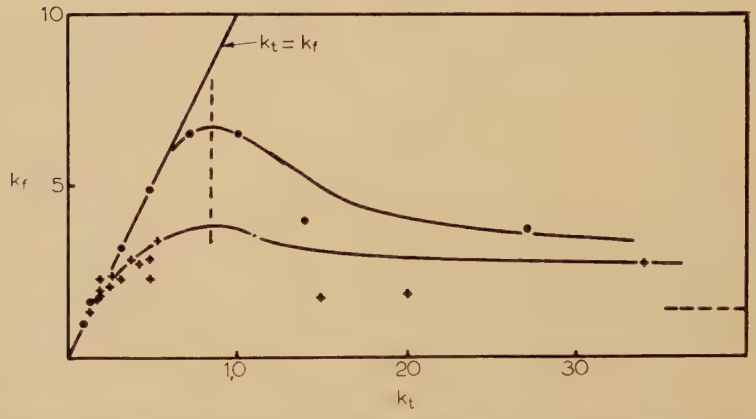

Relation between fatigue strength reduction factor (K_f) and elastic stress concentration factor (K_t) for aluminium alloy. • observations in push–pull ; + observations in rotating bending. (From Frost 1956.)

crack to be followed throughout the test. The measurements show that the cracks really do reach a constant length (and do not merely grow very slowly) under these conditions; thus this may perhaps be assumed to be true also in cylindrical bars. Unlike the earlier results neither the final crack length nor the time to reach that length shows any regularity; this is perhaps partly due to the greater difficulty of controlling the test conditions, and partly to a lack of sufficiently numerous data to smooth out inevitable irregularities.

The relevance of these non-propagating cracks to the question of notch sensitivity, is that on these materials at least, they always appear, and only appear, when the notch is so sharp that the simple relation between K_t and K_f, which holds for blunter notches, is beginning to break down. For example, in fig. 56 non-propagating cracks were found in all specimens represented by points to the right of the line through the maximum of the

curve. The presence of a non-propagating crack is thus associated with the breakdown of the simple relation between K_f and K_t. But a different picture emerges if we enquire, not what is the least stress that will cause the specimen to break completely in, say, 10^7 cycles, but, what is the least stress that will cause a crack to appear in 10^7 cycles. The paper by Frost and Dugdale provided evidence on this point. Four different notches were used, and the following table shows, in addition to K_t, calculated according to Peterson (1953) two values of K_f, the former based on the fatigue limit (i.e. stress to fracture) and the latter based on the stress to form a crack.

More, and more extensive, data are clearly needed, but the table does suggest that the theoretical (elastic) stress at the root of the notch may be the dominant factor that determines whether or not a crack will form: having formed, some other factors determine—in the case of sharp notches—whether it gives rise to total failure.

Root radius (in.)	K_t	K_f	
		Fracture	Crack
0·004	12·5	4·1	8·7
0·010	8·2	3·8	6·8
0·020	6·1	4·1	5·0
0·050	4·0	3·3	3·3

5.4. *Theory of Crack Propagation*

A rather different approach to the problem of crack propagation has been made by Head (1953, 1956) whose work follows on from a much earlier paper by Orowan (1939). Orowan considered the behaviour of a small plastic inclusion, embedded in a purely elastic matrix when the whole was subjected to symmetrical cycles of constant stress. It was assumed that the behaviour of the plastic inclusion could be described by a stress–strain curve, and that it showed no Bauschinger effect—i.e. (*a*) plastic deformation on one half-cycle did not begin until the stress had risen to the maximum value reached on the previous half-cycle, and (*b*) once plastic deformation had begun, the relation between stress and strain in any one half-cycle was the same as would have been obtained if the stress had continued to increase indefinitely in the previous half-cycle. The inclusion thus progressively hardens under the action of the alternating stress, and, as it does so, the distribution of load between the inclusion and its immediate (elastic) surroundings alters. The alteration is in the sense that the amplitude of the cycles of strain in the inclusion gets progressively less, while at the same time the amplitude of stress gets bigger. The stress amplitude tends to a finite limit, depending on the geometry and on the relative elastic moduli of inclusion and matrix,

and the second basic assumption of the Orowan theory was that if this limit were above a certain value characteristic of the material, the plastic inclusion would crack after a finite number of cycles of stress; if, on the other hand, the limiting stress were less than the characteristic 'fracture stress' no failure would result. On the basis of these ideas, Orowan proceeded to discuss the form of the relation between stress and fatigue life, and to attempt to account for the existence of the fatigue limit.

Head took up the development by pointing out that the small volume of material at the tip of an advancing fatigue crack was in just such a situation as Orowan had envisaged. When it had passed through all the stages just described, and finally cracked, the fatigue crack had grown a little longer and the whole process was repeated on the next element of volume. In order to develop this idea quantitatively Head replaced the real fatigue specimen by an idealized model, designed to reproduce all the essential features. The crack was considered to be growing across a sheet of material, stressed in alternating tension–compression. The strip through which it would propagate was represented by an infinite series of rigid plastic 'elements', to be stressed in push–pull following the sequence already described. Each of these was joined to an elastic element at each end, to represent the elastic constraint of the surroundings. The points of junction were connected, each to its neighbour on either side through an elastic shear element, to represent the characteristic that, as the crack grew longer, an increased stress would be transmitted to the unbroken material ahead of it.

The mathematical problem is complex, and a full statement cannot be given here. Head obtains approximate solutions for two limiting cases and shows in his second paper that the errors introduced by the mathematical approximations (as distinct from the physical assumptions) are not serious.

The most interesting result is the equation which gives the rate at which the length of the fatigue crack (l) increases, in terms of the number of cycles of stress (n). This is

$$\frac{1}{\sqrt{l}} = \frac{F}{E\sqrt{a}} f(\sigma, \sigma_0, \sigma_1).(N-n).$$

Here E is the elastic (Young's) modulus; F is the coefficient of work hardening, i.e. the slope of the stress–plastic strain curve (assumed linear); a is a constant with the dimensions of a length, and is the half-width of the strip of material involved in the crack propagation mechanism, and N is a constant– formally the number of cycles of stress to produce a crack of infinite length. The function f involves the applied stress σ, the yield stress σ_0, and the fracture stress σ_1, and its form depends on the relative value of the three quantities.

The amount of experimental evidence available for comparing with this formula is very limited. The crack observed must be small compared to the dimensions of the specimen, to avoid the complication of a macroscopic

redistribution of stress, and should really be large compared to the grain size, if the assumption of homogeneity is to be justified. Head quotes the results of three earlier investigations, all on steel, in which the growth of a crack around the circumference of a cylindrical test piece was observed. All three give a reasonably linear relation between l and n. Wadsworth (1957 a) has since added another observation on copper, but again on a cylindrical specimen. McClintock and Ryan (1954) have investigated the stress-dependence of the rate of growth, assuming the validity of the general form of the above equation. The theory predicts that the quantity

$$\frac{d(1/\sqrt{l})}{dn}\frac{(\sigma_0-\sigma)^2}{\sigma^3}=K$$

should be constant; McClintock and Ryan find that 'almost all' their values of K lie within a range of $\pm 50\%$ of the mean value, provided that the value of the constant σ_0 is taken some 50% larger than its static value. The absolute value of the quantity K as found from experiment is, however, less than the value calculated from theory by a factor lying between 10 and 100. Head found a similar discrepancy in the less extensive comparison which he was able to make and attributed it (amongst other things) to the fact that total amount of plastic deformation (summed without reference to sign) which can be obtained before fracture under an alternating stress is very much greater than the corresponding quantity under unidirectional loading.

It will be noted that the stress at the tip of the crack—however long or sharp that may be—is finite and equal to σ_1. The physical explanation of why long cracks grow faster than short ones may be said to lie in the fact that the plastic zone ahead of the tip is bigger for long cracks (it is of the order of magnitude $(a)^{1/2}$) and therefore an increasingly longer section is brought to the point at which it fractures on every successive cycle.

If, now the crack is advancing into a region in which the 'applied' stress is getting progressively less—as, for example, growing away from the root of a deliberate notch—the rate of growth will not increase as rapidly as predicted by the above expression. It is difficult to see how this could stop crack growth completely and, in any case, it cannot be the whole story since numerous examples have been recorded of a crack growing to a distance large compared to the radius of the notch from which it started, and then coming to a standstill.

Another important point is the effect of progressive cyclic work hardening on the mechanical properties of the material ahead of the crack. Before the crack reaches it, this material is subjected to many cycles of increasing stress. If the crack starts by growing slowly, the stress will increase very slowly. And if the material is such that it can be strengthened by a 'coaxing' procedure, these conditions are ideal for showing the effect. If this factor is in fact important, non-propagating cracks should be most easily produced in ferritic steels; and if, as appears probable, coaxing is

related to strain-ageing it should be more difficult (but perhaps not impossible) to obtain similar results with face-centred cubic metals.

The success of Head's model is rather striking, but it is doubtful if much useful purpose would be served by attempts to refine it on points of detail. It is valuable in drawing attention to the dangers of applying elasticity theory to problems in which plastic deformation plays an essential part. Its main weakness lies, perhaps, in the assumption that there does exist a critical stress σ_1, above which the material fractures. More generally, it is surprising that a model based essentially on the concepts of macroscopic physics should be so successful in accounting for events, the important parts of which take place in very small volumes. It is well known that the usual bulk properties of solids are not manifest if measurements are made on sufficiently small volumes (cf. the properties of metal whiskers, etc.); and the gradual extension of a crack as envisaged by Head does indeed concern only a small volume near its tip. The same idea can be expressed in another way by pointing out that a slowly growing fatigue crack may well be increasing in length at an average rate of one atom per cycle or even less: to treat such a process by the concepts of macroscopic physics is a bold stroke and it is perhaps surprising that it is so successful. There are, however, practically no published papers which even attempt a more detailed study, either experimentally or theoretically.

One factor which will clearly be of importance is the effect of the grain boundaries. It is well known that grain size exerts an important influence on fatigue properties of metals, but it is always difficult to separate the effect of grain size per se, from the effect of concomitant differences produced by the procedures adopted to give rise to the different sizes. The general opinion is that a small grain size is to be associated with higher fatigue strength. Perhaps the least doubtful results are those obtained on the simplest materials: Walker and Craig (1949) and later Sinclair and Craig (1952) experimented with annealed α brass in bending. Both investigations show that the stress to produce a given fatigue life increases as the grain size decreases. The relation between the two is probably not simple; the latter authors suggest $\sigma = a\,d$ (d grain size) but in the discussion it is pointed out that $\sigma = a\,d^{1/2}$ fits the results as well. The former set of results approximate to $\sigma = a - b\,d$. Qualitatively similar results have been obtained by Duce (1950) on nickel tested in reverse torsion (constant strain machine) (fig. 58). The curves are not continued to sufficiently low stresses to show the effect on the endurance limit, but the effect on life in the mortal range is qualitatively the same as for brass.

The above deal with plain specimens: there are two papers concerned with the effect of grain size on notched specimens. Karry and Dolan (1953) experimented with α brass and Peterson (1938) collects together results on steels. Both lots of data show the same general trend—that the notch sensitivity increases as the grain size becomes smaller. As far

as is known, no attempt has been made to investigate separately the effect of grain size on crack initiation and crack propagation. Since it appears that, in each grain, the plane of the crack is strongly influenced by crystallographic considerations, and since neighbouring grains are, in general, randomly orientated with respect to one another, the passage of a crack from one grain to the next is likely to be a matter of some difficulty. It might be expected therefore that a crack would propagate more quickly in a large grained specimen. An observation by Lipsitt *et al.* (1955) supports this view. Fatigue specimens were cut out of rolled bars of an aluminium alloy with the length of the specimen at right angles to the

Fig. 57

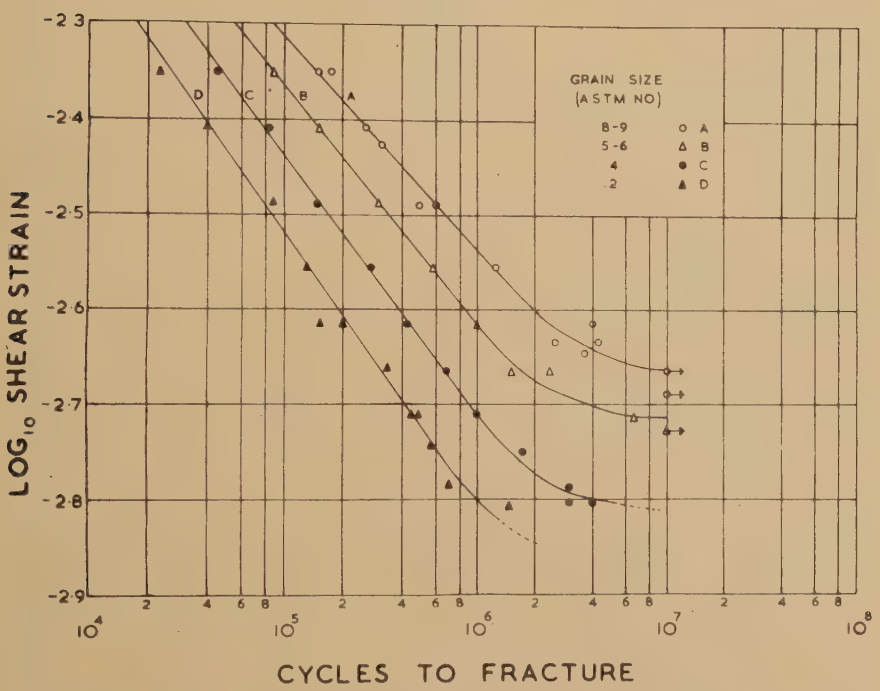

Effect of grain size on the fatigue of nickel tested in alternating torsion. (Duce 1950.)

direction of rolling, and tested (as grooved cylinders) in rotating bending. The crack appeared to start at many places around the root of the notch, and spread inwards. The method of fabrication had produced grains elongated in the direction of rolling, and the final 'core' of the fatigue specimen, which was easily distinguishable from the region across which the fatigue crack had propagated relatively slowly, was usually elliptical in shape, with its minor axis parallel to the long axis of the grains. A more direct investigation of this problem would be of considerable interest particularly in view of the relations between grain size and the fracture

strength of brittle materials on the one hand, and the lower yield point of iron on the other (see, for example, Stroh 1955 b).

§ 6. Experiments using X-rays

When metals are deformed unidirectionally, the crystals are distorted, so that x-ray diffraction spots become broadened and blurred. It might be thought therefore that similar techniques would be a useful tool for studying the deformations associated with fatigue; a number of investigations have indeed been made, but much more might well be attempted. The massive specimens usually employed in fatigue work demand the use of back-reflection x-ray techniques, and the usual procedure has been to use (nominally) monochromatic radiation, and to choose the illuminated area, in relation to the grain-size of the material, so that the individual diffraction spots are clearly separated from one another. For many of the investigations a 'typical' area of the specimen is illuminated; more rarely, if two or more photographs are to be taken of the same specimen at different stages of its history, the *same* area is used each time. This is a more sensitive method of detecting changes but does call for great precision in the methods of locating the specimen relative to the incident radiation. If sufficient care is not taken about this point, it may lead to erroneous conclusions. Further, it is interesting to note that, in a recent symposium, two authors independently remarked on the lack of consistency of the evidence furnished by x-ray reflections from neighbouring points of the same fatigue specimen.

Before summarizing some of the earlier work, attention may be drawn to a note by Davies (1954) which, besides being interesting in itself, is by way of being a cautionary tale. Well annealed copper specimens were tested in push–pull at 200 and 400 cycles per minute and a stress of ± 5 tons/in.^{2}. Very little blurring of the diffraction spots was produced in 1000 cycles. When, however, the testing machine was deliberately thrown out of adjustment so that a mean stress (tensile or compressive) amounting to only 2% of the alternating stress amplitude was superposed, a change of length of the test piece of the order of 1% resulted, together with a considerable blurring of the diffraction spots. It is thus particularly important in x-ray work to ensure that the mean stress really is zero when this is its nominal value. The 'frequency effect' reported by Wood and Head (1951) and by Bullen *et al.* (1953) was almost certainly really due to a variation in mean stress, and some doubt is raised about other work also.

Around 1937–39 four separate papers appeared from various sources, all concerned primarily with the possibility of determining a fatigue limit quickly by means of x-ray observations on one or two specimens. Barrett (1937) reviewed previous work and carried out a number of tests mainly on commercial steels, but including also some non-ferrous materials. He concluded that the amount of blurring of the diffraction spots increased as the stress increased, but that there was no qualitative change on passing

the stress corresponding to the fatigue limit. Spencer (1939) on the other hand, found no effect on the diffraction spots from malleable iron due to 10^7 cycles of a stress below the fatigue limit, whereas a stress which produced failure in $2{\cdot}5\times10^6$ cycles had already caused considerable changes in the x-ray pattern after only 1000 cycles. The work of Gough and Wood (1936, 1938) is more detailed. The material, a normalized mild steel (0·12% C) was tested in push–pull and the fatigue limit established at 11·6 tons/in.^{2}. A specimen tested at 11·5 tons/in.^{2} for 10^7 cycles showed little or no change in the x-ray reflections. When tested at 12 tons/in.^{2}, 1000 cycles was sufficient to produce a radical change in the nature of the spot pattern. This specimen broke after 3×10^7 cycles but even then the spots were much less blurred than if the material had been deformed unidirectionally to fracture.

Broadly similar conclusions were reached by Wever and Möller (1937) and again by Möller and Hempel (1938). The material was again a well annealed iron (0·02% C) tested in rotating bending, the surface being particularly carefully prepared to be undistorted at the beginning of the test. They record no detectable change in the x-ray reflections after 4×10^7 cycles at a stress below the fatigue limit. Some blurring of the reflections was recorded at stresses above the fatigue limit, but the changes were less dramatic than those found by Gough and Wood. Later work (e.g. Möller and Hempel 1954) has tended to confirm the general conclusion that, in mild steels and similar materials at stresses below the fatigue limit, there is little or no blurring; that above the fatigue limit, the diffraction spots do become diffuse at an early stage of a fatigue test, but the total amount of blurring is much less than that produced in a tensile test; and that at stresses very close to the fatigue limit some reflections may become diffuse and others not.

Similar experiments on materials which do not show a fatigue limit (see § 4) are less numerous. Spencer and Marshall (1941), and also Barkow (1945) report no detectable changes in the reflections from an aluminium alloy—a result that was confirmed by Louat (1953). He used an alloy of aluminium with 4% copper, and found no detectable blurring of the reflections from a specimen broken in fatigue at 1000 c.p.s., except within about 0·1 mm of the crack. Reflections from the fracture surface itself and from another similar specimen extended 1·5% in static tension were extensively blurred. Wood and Thorpe (1940) used a brass containing 70% Cu. If stressed in static tension above its 'yield point' at 4·8 tons/in.^{2}, the x-ray reflections immediately became very diffuse. A fatigue specimen, however, could be run to fracture at much higher stresses (up to 10 tons/in.^{2}) without producing more than a comparatively small blurring. Similar results were obtained later on aluminium and copper by Wood and Head (1951) and Bullen *et al.* (1953). See also Clareborough *et al.* (1957). The former paper also shows that the diffuseness of the x-ray reflections produced by a tensile strain of 2% was considerably reduced, but not completely removed, when the specimen

was compressed back to its original dimensions. This effect depended on the size of the individual step. A strain of -6% following one of $+6\%$ increased the blurring slightly, but much less than if both steps had been in the same sense. On the other hand, with strains of $\pm\frac{1}{2}\%$ several cycles could be given with almost no resultant blurring.

The effect has been demonstrated even more clearly by a recent paper of Wood and Segall (1957a) who tested specimens of copper and brass (and to a lesser extent aluminium and nickel) in torsion, using slow cycles of constant plastic strain-amplitude. The amount of blurring of the x-ray reflections increased with the number of cycles initially but eventually settled down to a steady condition in which the degree of diffuseness was greater at greater strain-amplitudes. If, however, the amplitude were small (corresponding to surface strains of the order of $0{\cdot}15\%$ or less) there was no detectable blurring of the reflections after 500 cycles. The conditions of the experiments did not permit them to be continued for numbers of cycles comparable with those used in a typical fatigue test, but it is suggested that the result would not have been very different. The plastic strains may be small, but they are not zero, and the total strain in, say, 10^7 cycles, summed without regard to sign may amount to several hundred per cent. The resultant blurring of the x-ray reflections is negligible compared to that produced by a similar unidirection strain (if this were possible).

If a metal which has been cold-worked by a unidirectional straining process is subjected to a fatigue test, the initially very diffuse x-ray reflections tend to become sharper. This effect was observed on rolled copper and silver foils in a very early paper by Dehlinger (1931) and has since been recorded by a number of workers (e.g. Clareborough *et al.* 1957). It is clearly to be related to the 'work softening' discussed on p. 107. Extensive observations on the phenomena in iron and mild steel have been made by Sander and Hempel (1952), Hempel and Houdremont (1953), and Möller and Hempel (1954). These show that the sharpening of the original diffuse reflections from cold-worked material does not take place if the fatigue stress is below the fatigue limit, and that, the higher the fatigue stress, the more effective it is in removing the initial diffuseness. There is, however, no discontinuity in the effect at the fatigue limit.

In connection with the discussion of 'coaxing' in §4.2 it is further interesting to note that if a cold-worked specimen were subject to prolonged fatigue below the fatigue limit, subsequent testing above this limit did not produce so much sharpening of the reflections and, in extreme cases, the sharpening could be almost completely inhibited. Similarly the blurring of the sharp reflections from a fully annealed specimen which was caused by stressing above the fatigue limit, could also be suppressed by previous prolonged stressing below this limit.

Experiments using the more refined x-ray techniques developed in recent years are very few. Paterson (1955) reports the appearance of Kossel lines in the radiation scattered from his single crystal specimens

after being subjected to cyclic straining. The inference is that the nett distortion of the lattice cannot have been very great. Franks and Holden (1955) have used a focusing camera to investigate the radiation scattered at small angles, and observe streaks which they attribute to the presence of minute disc-shaped cavities in the slip planes of the fatigued crystal. Later work by Atkinson and Lowde (1957), however, casts some doubt on this interpretation. Jacquesson (1955) uses the Guinier–Thenevin technique to investigate the effect of alternating stresses on the spread of orientation of sub-grains. The technique appears promising, but the published results are not sufficiently detailed for any conclusions to be drawn at this stage.

§ 7. Surface Effects

7.1. *Introduction*

In fatigue tests, the surface is the most important part of the specimen. Metallographic work shows that the cracks form at the surface: this is true even if the stress is macroscopically uniform over the whole volume. When exceptions to this rule are reported, it is usually found either that the crack has originated at some sub-surface stress raiser (e.g. slag inclusion or cavity, see Frith 1954) or else that the properties of the surface layers are considerably different from the interior, either by accident or design. An apparent exception is the observation by Haigh and Jones (1930) that fatigue cracks in lead tested in push pull had a bright lip indicating that they had originated one or two grains below the surface. There is, however, some doubt about the result as Gough and Sopwith (1935) failed to confirm it.

It follows that the preparation of the specimen surface is a particularly important factor in fatigue testing, and it is now well known that different methods of machining a specimen can produce significantly different results.

We do not propose to discuss this question except to point out that even the comparatively gentle processes of metallographic polishing can, it appears, produce sufficient effect on the surface layers to give rise to a fatigue behaviour different from that shown by an electropolished surface. This is clearly shown in a recent paper by Cina (1957) on a variety of alloy steels, and also by Hempel *et al.* (1957) on single crystals of iron.

Since cracks originate at the surface, it is possible to increase the life of specimens considerably by removing the surface layers after part of the test, when the cracks have formed but have not penetrated appreciably. When this is done the cracks reform on the new surface, indicating that fatigue 'damage' has not occurred further down. Siebel and Stähli (1942) investigated this effect on steel tested in rotating bending and found that removing as little as 0·05 mm from the surface after 50% of the life (of 2×10^6 cycles) removed the damage. The specimens were of sufficiently large diameter (8 mm) for the effects of the reduction in diameter on the stress distribution to be negligible. In these experiments the life of the

specimens after removing the surface was longer than that of new specimens—a phenomenon presumably connected with coaxing (see § 4).

Similar results were obtained by Lissner (1955) on four steels, also tested in rotating bending. The removal of 1/10 mm from the surface after one half of the expected life produced a significant increase in the residual life. In this case care was taken that both the initial surface, and the new surface after removing the thin layer were made stress-free by electropolishing. Möller and Hempel (1954) obtained similar results. All the above fatigue tests were done in bending, so that the stresses and strains were, for that reason alone, larger on the surface than in the interior. But the thickness of the layers removed was so small compared to the specimen radius, that it appears likely that the same results would have been obtained in a push–pull test. Siebel and Stähli (1942) did in fact carry out one such test, with very similar results. They also showed that by repeatedly polishing away the surface, the life could be prolonged, apparently indefinitely. One specimen, for example, was reduced in diameter by 0·1 mm after 40% of its normal life, and at about equal intervals thereafter. After 10 such treatments it was run to failure, and still gave 150% of its normal life, the total of all stress cycles being 660% of the expected normal life.

Thompson *et al.* (1956) showed that when cracks were polished off copper specimens in push–pull new cracks formed on the surface when the test was continued, and the total life was increased. At no time were cracks found in the material below the surface of either polycrystalline or single crystal specimens. It seems that the fatigue strength of the metal away from the surface must be considerably greater than that of the free surface.

7.2. *Mechanical Effects*

There are two aspects in which the surface is unique and which may be important in causing fatigue failure to start there. Firstly, the surface is the only part of the specimen which is not supported by adjoining material. This effect will be most marked on polycrystalline material, but not altogether absent in single crystals. Since the slip systems in neighbouring grains are not related to each other, the presence of surrounding grains makes slip more difficult in the bulk of the specimen: near the surface, however, the effect is less pronounced, and slip is easier. There is much evidence that the static properties of polycrystalline specimens are affected by the grain size (e.g. Feltham and Meakin 1957 on copper, and Ziegler 1930 on mild steel). There are also some papers in which the effect of grain size on fatigue has been particularly investigated (e.g. Walker and Craig 1949, and Sinclair and Craig 1952 both on brass, and Toolin 1953 on a complex Co–Cr Ni alloy). There are, however, so many other factors that might be involved, that the relevance of the results to possible effects of the free surface itself may not be very great.

With single crystals, sub-grain boundaries may play a similar role (see, for example, Ball 1957 on direct stress tests on aluminium). There are, however, other reasons why the surface layers would be expected to behave

abnormally. A dislocation line terminating on a clean surface (and the presence of etch pits shows that many of them do) may behave, on account of the imaging properties of surfaces, as a line twice as long as it really is. For these reasons plastic deformation due to the action of Frank–Read sources should begin near the surface at a lower stress than in the interior. Secondly, phenomena of extrusion from fatigue slips (see § 2.3) can hardly be imagined except at a free surface. On the other hand, the presence of coherent surface films (e.g. of oxide) may constitute an abnormal restriction on plastic deformation near the surface (see, for example, Barrett 1953 and many other references).

Evidence is not wanting that the surface shows exceptional properties, even in single crystals homogeneously stressed, although most of the observations have been made using unidirectional stressing. Suzuki *et al.* (1956) showed that the length of the easy glide region in the stress–strain relation for copper cystals increases considerably as the radius of the specimens is reduced from 1 mm to 0·1 mm. Makin (1952) on the other hand, found that the critical stress for the onset of glide in cadmium crystals increased as the diameter was reduced over about the same range. One possible explanation of this is the strengthening effect of the thin layer of hydroxide which readily forms on cadmium specimens. Graham and Maddin (1954) showed that a layer about 5×10^{-3} cm thick on the surface of an aluminium crystal provided, preferentially, nuclei for recrystallization after a tensile strain. The explanation offered was again in terms of the dislocations trapped below the surface by the oxide film. No observations comparable to any of the above seem to have been made using alternating stresses. (The so-called 'size effect' in bending fatigue tests is almost certainly of a different origin (see § 5.2).)

Considering polycrystalline specimens again, there are numerous papers which show that, after a uniform tensile stress, residual stresses remain in the surface layers which are largely compressive in character; the thickness of such a surface layer might be, for example, 1 mm on a specimen of typical laboratory size (see Bollenrath *et al.* 1939, Smith and Wood 1944, Wood 1948, Nishihara and Taira 1950). Möller and Hempel (1954) report the surprising result that, after fatigue testing, the removal of a layer only 0·03 mm thick restored the blurred x-ray reflections to their original sharpness.

We thus see that there are several lines of evidence to support the view that, in some cases at least, the amount of plastic deformation is likely to be greater near a free surface than in the interior. Two attempts have been made to treat this problem theoretically (Vitovec 1953, Nishihara and Taira 1950) but neither has led to any very convincing conclusions.

7.3. *Chemical Effects*

In addition to the freedom from mechanical constraint, the surface is unique in another respect in that it is the only part of the specimen that is exposed to chemical attack by the surrounding fluid. If this fluid is water,

acid or salt solution, the corrosion produced may be obvious. The whole subject of corrosion-fatigue (the effect of simultaneous corrosion and alternating stress) is complex and has been reviewed elsewhere (e.g. Gough 1932, Gilbert 1956). For the moment we will do no more than note that the effect of corrosion and fatigue operating together is much greater than the effect of either acting alone or of both acting consecutively.

We are here concerned only with normal fatigue tests which are usually done in air in which no obvious corrosion occurs. There is, however, considerable evidence that sufficient corrosion does occur in these tests to affect the life appreciably. Haigh and Jones (1930) showed that the life of lead specimens could be increased by a factor of 10 if the air were partially excluded by covering the specimen with oil, water or grease. (These methods are not normally very effective.) Gough and Sopwith (1935) investigated the matter further. They tested specimens in push–pull either in air or in a partial vacuum (about 10^{-3} mm Hg) and found an even larger increase in life. They also showed that it was essential to have the air present during the fatigue to get the short life. If air and fatigue stresses were applied alternately, the normal vacuum life was obtained. Gough and Sopwith (1932, 1935, 1946) also investigated copper and brass which gave smaller but significant increases in life when tested in vacuum. The ratio of endurance limit (3×10^7 cycles) in vacuum to that in air for brass was 1·26, and for various sorts of copper from 1·02 to 1·13, whereas for lead it was 2·24. Copper and brass were investigated further, and it was found that both oxygen and water vapour had to be present to reduce the life to the normal air value but that the acid impurities normally present in air had little effect. Armco iron and mild steel gave small increases in vacuum while the effect on duralumin was inconclusive, because of the large scatter. Other work on aluminium alloys, connected with corrosion fatigue proper (Gerard and Sutton 1935, Inglis and Lark 1954) has shown that the endurance limit in air of various aluminium alloys can be increased by 10–20% by suitable protective surface coatings. Similarly Brown (1955) reports an increase in the life of Mg + 5% Zn alloys when the surface was protected by a layer of rubber solution.

Thompson *et al.* (1956) showed that when oxygen was excluded from copper specimens the initial stages of crack formation occurred at the same rate as in air but that the first persistent slip bands or cracks took longer to spread, i.e. the major effect of oxygen was to speed up crack propagation, cracks still being formed at the surface. Later work by Wadsworth (unpublished) shows that there exists a clear relation between the life of copper specimens tested at a specified stress, and the degree of vacuum which constitutes their environment. Schaub and Liedtke (1955) have discussed the phenomena in general and have used a photographic technique to detect some form of activity (? chemical) at that point on the surface at which the fatigue crack forms.

It seems probable that both mechanical and chemical effects combine to give the surface its predominant role in fatigue but more work is needed

before the mechanism can be understood in detail. When interpreting fatigue tests one must always bear in mind that all normal tests are performed in air and are probably really corrosion fatigue tests, and so the results obtained may not be typical of the behaviour of the isolated metal itself.

§ 8. Annealing Experiments

If an appreciable part of the fatigue life of a specimen is occupied by the progressive hardening of critical parts of an initially soft specimen (or by softening of critical parts of a hard specimen) and if cracks form only at a later stage, then it should be possible to remove the early damage and return the specimen to its original state by a suitable annealing treatment. On the other hand if cracks have already formed, the annealing will not remove them and might even help them to spread by softening the material in their path. Thus annealing experiments should indicate at what stage in the test cracks form. A number of such observations have been made.

Laute and Sachs (1928) fatigued annealed nickel specimens under conditions giving lives of a few million cycles. They annealed some specimens at intervals during the test and found that annealing after half the life had almost no effect on the total life, while if the intervals between the anneals were reduced to about 10% of the normal life, the life was reduced slightly. Sinclair and Dolan (1951) performed similar experiments on α-brass. The specimens were divided into three groups of 10–15 each. Specimens in one group were fatigued to failure without intermediate annealing while those in the second and third group were annealed respectively every 50% and 20% of the mean life of the first group. The lives of the specimens in each group were compared statistically and no significant difference was found. Thompson *et al.* (1956) performed similar, though less detailed, experiments on copper with essentially similar results. Smith and Harries (quoted by Thompson 1956) annealed aluminium specimens once only during the fatigue test at either 75%, 42% or 8·4% of their normal life and found no statistically significant effect on their life.

These experiments are all consistent with the metallographic evidence that in pure metals cracks are formed after only a few per cent of the total life. In age hardened alloys on the other hand it appears that the first stage in fatigue is the local over-ageing and softening of slip bands before cracks form in them, and that this process takes a long time. If this is so it should be possible to undo the fatigue damage by suitable heat treatment before the cracks form. Hanstock (1954) tried this on one specimen. This specimen was fatigued for 10^7 cycles by which time energy dissipation measurements showed that considerable softening had occurred and crack formation was thought to be imminent. The specimen was then given a new solution heat treatment, and re-aged. This process returned the energy dissipation to its original value. After a further 10^7 cycles at the same stress, the energy dissipation had increased as before but the specimen was unbroken. Hanstock says that if small cracks had formed

during the first 10^7 cycles, the second 10^7 cycles would almost certainly have produced a major fatigue crack. Further work on these lines would be interesting.

Möller and Hempel (1954) made observations on iron containing 0·02%C. Specimens were tested at a stress above the fatigue limit, for about half of their estimated lives, and some of them were then annealed for one hour at 930°C. The effect of the annealing was assessed by comparing the mean lives of the two groups of specimens during a subsequent test at a stress equal to the fatigue limit. The conclusion was that the 'damage' done to the specimens in the first part of the experiment had not been undone by the subsequent annealing treatment.

Other experiments on the effect of a rest pause on the fatigue life or iron and steel specimens—which is in effect an anneal at room temperature —are described in § 4.

Apart from the question of fatigue fracture, it is also of interest to enquire into the effect of an increase of temperature on the other physical changes which are caused by fatigue stressing. The amount of work which has been done in this direction is very small.

Clarebrough *et al.* (1955, 1957) have investigated the release of the energy of deformation stored in a fatigue specimen. Earlier observations by Welber and Webeler (1953) appear to have been in error. The work has been mainly on copper, and shows that, in a specimen broken at a fairly high stress (to give a fatigue life of the order of 10^4 cycles) the amount of stored energy may be comparable with that resulting from about 50% static compression. At lower stresses the energy stored at fracture is much less. Of more interest, however, is the observation that, with a fatigue specimen, the energy is released gradually over an extended temperature range (e.g. 100°C–600°C) instead of over a range of about 50° as in a metal deformed unidirectionally. Parallel observation showed that much of the energy is released with no appreciable re-sharpening of the blurred x-ray reflections and only a small drop in the (Brinnell) hardness.

The same papers also give some information about the recrystallization of fatigued specimens on heating. The general impression is that recrystallization does not readily occur in fatigued specimens at all, but takes place more easily if failure has taken place at a higher stress. Similar results have been recorded by Jacquet (1956) on brass.

Other isolated observations include that made by Wadsworth (1955) that much of the hardening produced in a single crystal of cadmium by 10^6 cycles of stress had disappeared after annealing for 30 minutes at room temperature. The basis of the observations was the estimation of hysteresis loop area. Similarly Miles (unpublished) finds that an appreciable fraction of the hardening of aluminium crystals produced by, say, 100 slow cycles of stress at 90°K disappears if the temperature is raised to 200°K for a few minutes.

It is clear that observations of the effect of a rise in temperature on hardness, on damping on x-ray reflections and particularly on stored

energy provide a valuable method of obtaining information on the nature of the changes produced by cyclic stress, and also that much remains to be done in this field.

§ 9. The Effect of Fatigue on Diffusion

A number of instances have been reported in which metallurgical changes have been observed during a fatigue test which would not have occurred in the same time at the same temperature in the absence of the fatigue stress. The changes are similar to those produced by heating, and appear to be caused by an increase in diffusion rate. The most striking example is the apparent over-ageing of aluminium alloy specimens investigated by Hanstock and described more fully in § 3.3.2. Similar observations were made by Broom and Molineux (1955, discussion of paper by Hanstock 1954) and Broom *et al.* (1956) also on an age-hardening aluminium alloy. They make the additional point that some of their results can be explained if it is assumed that the enhanced diffusion and hence the over-ageing is suppressed when the fatigue test is carried out at 90°K. A later note (Broom and Whittaker 1956) gives metallographic evidence of the segregation of solute atoms in slip bands under the action of an alternating stress. Schenck and Schmidtmann (1954) showed that the carburizing of steel at about 900°C progressed more rapidly if the specimens were fatigued at the same time. Similarly the diffusion of carbon already in the specimen was increased by fatiguing. The higher the fatigue strain the greater was the effect.

The appearance of precipitates of cementite during a fatigue test of a mild steel, studied by Hempel, has already been described (§ 4.2) but it is not clear to what extent this can be attributed to diffusion in the usual meaning of the word. Holden (1954) showed that silica particles were precipitated in a copper–0·05% silicon alloy in an oxidizing atmosphere at 325°C if the specimens were fatigued, whereas no precipitation occurred at this temperature if the specimens were unstressed or under a static stress equal to the peak fatigue stress. A temperature of 750°–1000°C was needed to produce precipitation with no stress. A similar effect is the local recrystallization seen by Forsyth and Stubbington (1954) in cold rolled aluminium, and the growth of large soft grains in cold-worked copper found by Kenyon (1950). In these cases the diffusion entity would be a vacant lattice site or an interstitial atom, rather than a solute atom, but the mechanism is similar.

All these phenomena may be explained by assuming that fatigue produces an increase in diffusion rate near the active slip bands. There are a number of possible explanations of this. The simplest is to assume that the active slip bands are considerably hotter than the rest of the specimen but it appears that this cannot be so. All the heat released at the slip planes must leave the specimens by its ends (or from its surface). Thus, since the total area of all the slip planes in the specimen is usually greater than the area of the specimen, then the temperature gradient near the

slip planes must be comparable with the macroscopic gradient in the specimen. The mean temperature of slip bands cannot therefore be much above that of the specimen as a whole. The macroscopic temperature is measurable and in most cases, particularly in small specimens of high conductivity, is little above that of the surroundings.

While the mean temperature of the slip bands in cool specimens must be low it might be possible for it to reach high instantaneous values occasionally and over restricted areas. There are two chief sources of short pulses of heat the movement of dislocations and the annihilation of dislocations, vacancies or interstitial atoms. The movement of dislocations produces the longest heat pulse, and a number of calculations have been made (Freudenthal and Weiner 1956, Eshelby and Pratt 1956, Wadsworth 1956). The temperature rise produced by a single moving dislocation is of the order of a degree or less, the exact value depending on the stress applied and on the velocity (usually assumed to be about half that of sound, as an upper limit). If a number of dislocations move along a slip plane in a close group, the temperature reached will depend on the number of dislocations and on their spacing. The number of dislocations is limited to about 500 by observed slip step heights. Freudenthal and Weiner assumed that the dislocations were separated by about 5 atomic spacings, and so deduced a maximum temperature rise of some hundreds of degrees for a number of simultaneous avalanches on neighbouring planes. It seems impossible that the dislocations could in fact be as close together as this, as the stresses would be greater than the theoretical strength of the metal. Eshelby and Pratt assumed that the dislocations were produced by a Frank–Read source in which the rotating dislocations move with about a third of the speed of sound. This gave a wider dislocation spacing and a temperature rise of about 2°. Wadsworth took the case in which the spacing of the moving dislocations was the same as that in a stationary piled-up group and got a rise of about 10°c for one avalanche. The temperature rise, whatever its exact value, lasts about as long as the avalanche takes to pass, which is less than a microsecond at the speeds assumed; such a combination of temperature rise and time is too small to enhance diffusion appreciably. If the dislocations move more slowly the temperature rise is less, but lasts longer; the conclusion is unaffected. In all these models the thermal strain produced is much less than the elastic strain surrounding the assumed distribution of dislocations, and may be ignored.

Transient increases in local temperature can also be produced by the annihilation of vacancies, interstitials or dislocations produced during the test (Seitz 1952). This process can produce very high temperatures but only for a few atomic vibrations at most, and it seems doubtful if atoms could move more than about a hundred times during a typical fatigue test (Wadsworth 1956). Very short range diffusion by this mechanism is however possible at all temperatures.

Since the observed diffusion cannot be accounted for by thermal effects other mechanisms must be considered. The dislocations, vacancies and

interstitials which are produced during fatigue can all assist diffusion directly. Diffusion down dislocations is considerably more rapid than through the bulk of the metal (Hendrickson and Machlin 1954). That dislocations can in fact lead to enhanced ageing was demonstrated by Gayler (1946) who showed that the rate of ageing of aluminium–4% copper was greatly increased by previous cold work and that visible precipitates first occurred along the slip planes. Similarly Forsyth (1957 b) fatigued an aluminium–zinc–magnesium–copper alloy coated with pure aluminium and found that if it were annealed after fatiguing the solute diffused up the grain boundaries in the pure aluminium and then into the grains along the slip bands. Vacancies and interstitials produced during fatigue will increase the concentration in the lattice above the equilibrium value and this will increase the diffusion rate. A calculation of the magnitude of the effect needs an estimate of the lifetime of a vacancy or interstitial during a fatigue test and so is difficult, but appreciable increases could probably be produced at temperatures a little below those at which diffusion would normally occur.

It seems that the enhanced diffusion observed during fatigue tests must be caused by the dislocations, vacancies and interstitials rather than by actual local heating and since these mechanisms still need thermal activation the diffusion should be suppressed at a sufficiently low temperature as Broom and Molineux (1955) found on aluminium alloys.

PART III

Discussion

In Part II we have summarized the results of experimental work on various aspects of fatigue without making any mention of theories relating to the central problem: By what mechanism does a specimen fracture after, say, a million reversals of a stress which would have had very little effect if applied once only? There have been numerous attempts to provide an explanation: some of these are summarized by Wood (1956). It is clear from the complexity of the observations, however, that no simple theory is likely to suffice.

The observations described in § 2 show that there is a close connection between slip bands and fatigue cracks and suggest that slip is usually † an essential process in the initiation of a fatigue crack and probably also in its propagation. It is in fact true that some plastic deformation always takes place during a fatigue test. At low stresses the amount may be small, as is shown by results on damping capacity. But at a stress of the order of the endurance limit there is a considerable increase. This correlation is particularly marked for substances showing a fatigue limit. One might possibly find exceptions among very brittle materials but Fegredo's

† The formation of cracks in twin—or grain—boundaries will be considered later.

results on the hardening of zinc during fatigue at 90°K suggests that even here some irreversible changes in the crystal texture take place. Further work on brittle crystals would be interesting. On the other hand it should be pointed out that continuing cyclic plastic deformation does not necessarily lead to fracture. There are many cases on record of specimens remaining unbroken after very long lives during the whole of which considerable energy dissipation was taking place (e.g. Föppl 1936).

The extensive series of experiments by Gough and his collaborators showed that the crystallographic features of slip were the same in a fatigue test as in unidirectional slip. Wadsworth showed that the initial hardening of a hexagonal crystal in fatigue was very much slower than that of a cubic crystal—a behaviour which is analogous to that shown in unidirectional straining. Similarly the work of Paterson and of Charsley on the orientation dependence of fatigue hardening in face-centred cubic crystals runs parallel to the known results on direct stress, although further quantitive observations in this field would be valuable. Again, the few measurements that have been made show that the amount of stored energy in a broken fatigue specimen is comparable with that resulting from several percent of unidirectional strain, in spite of the fact that there is no significant change of macroscopic shape or size of the fatigue specimen.

On the other hand there are significant differences. The appearance of slip bands on the surface is different. The mode of release of the stored energy is quite different. The temperature dependence of fatigue hardening is not the same as that of unidirectional hardening. And—most striking of all—the x-ray results show that the detail of the local crystal distortions is quite different in the two cases, as has been emphasized by Wood.

A detailed description of unidirectional hardening in terms of the movement of dislocations can by no means be regarded as established beyond question, while very little attention at all has been paid to the interpretation, in terms of dislocation movements, of the observed events when the stress is first removed, and then applied in an opposite sense. Recent theoretical work on strain hardening has tended to be concerned with comparatively large strains (say 1% or more) while the strains involved on each cycle of a fatigue test are very much smaller. The cumulative plastic strains in fatigue, summed without regard to sign, are however quite large so that it might perhaps be maintained that mechanisms relevant only to large strains in unidirectional tests are also relevant to fatigue.

We have given evidence in Part II that in 'pure' metals the fatigue crack is already present quite early in the test, most of which is occupied by its growth. Figures of a few percent of the life are not uncommon, as it seems quite probable that the regions with the essential characteristics of a crack may be present even earlier. If this is so, the gap between the end of the initial hardening period, and the beginning of a crack, has shrunk to something quite small. This viewpoint removes one of the major

difficulties concerned with fatigue fracture. It has always been difficult to conceive of a mechanism which could count up to, say, 10^6 cycles, and then begin to produce a crack. Alternatively, if one had to wait for 10^6 cycles for some random event to produce a crack, the scatter of fatigue data might be expected to be even worse than it is. But if the major part of the life is occupied by the growth of a crack, the process of counting up to a million becomes more comprehensible. The *area* of cracked surface could increase by many hundreds of atoms per cycle, and still give rise to an average rate of increase of crack length which would be small compared to the observed rates of growth of small cracks. Moreover the production of the initial crack is now confined to some thousands of cycles. During this time there is other evidence that the state of the crystal is changing continuously (initial hardening period) and the production of a micro-crack at the end of the period is not unreasonable. Alternatively, if random events are to be invoked to start the crack, it would be possible to have an enormous dispersion in the number of cycles of stress to produce the crack without introducing a comparable variability on the total life.

On this viewpoint then we must first seek to set up a model for the initiation of a crack, but now the time scale of the process is to be measured in thousands rather than millions of cycles. And—whatever the mechanism of hardening may be—it is probably fair to conclude that it is the continuing to-and-fro motion of dislocations that is responsible for the crack in the first place. We may cite as supporting evidence Gough's early observation that cracks tended to form on that slip system on which the *range* of shear stress was the greatest. The form of a typical fatigue slip band should also be borne in mind. Whatever may be the explanation, it is clear that slip has taken place on many slip-planes closely spaced. The individual slip lines appear to be very fine, and are often unresolved, even under the electron microscope. This is possibly a consequence of the very small amount of slip taking place on any one slip plane per cycle or possibly due to the slip of one half-cycle being almost reversed on the next half-cycle. Some such explanation must be found for the fact, emphasized by Wood, that slip lines do not become visible for a large number of cycles, by which time the initial hardening process is well advanced.

The local lattice distortion which results from many cycles of stress is, however, considerable. This is clear from both optical and electron micrographs although it is perhaps difficult to reconcile these observations with the x-ray results. The application of some of the modern high-resolution and micro-beam x-ray techniques might prove valuable in this connection. The observation that the cracks always start on the surface should not be forgotten, although the interpretation may not be simple. It may indeed be that—for reasons outlined in § 7 of for other reasons—the crack is only initiated on the surface: but it is also a possible interpretation that although cracks may start in other places, those on the surface grow so much faster than the others that they alone need be considered.

A number of suggestions have been made from time to time to account for crack initiation, none of them completely satisfactory:

(*a*) It is known that dislocation moments can produce vacant lattice sites (Seitz 1952); as the slip bands are the seat of continuing dislocation movement, the concentration of vacancies may be high and the possibility arises of them condensing to form voids. This process would occur more readily in the interior than on the surface of a grain. But it could hardly proceed at very low temperatures since it depends essentially on diffusion.

(*b*) The accumulation of lattice defects in a fatigue slip band, if continued far enough may destroy all semblance of the original lattice: the material will then eventually recrystallize even at low temperatures. This sequence will destroy the coherence of the crystal across the slip plane, and the associated changes in volume may give rise to a crack (cf. Mott 1955).

(*c*) A film of oxide, or adsorbed gas, formed on a slip step on the surface in one half cycle, may be drawn into the crystal by the to-and-fro relative motion of the two parts of the crystal which face one another across a slip plane, provided that the transfer of foreign atoms across the slip plane can take place sufficiently rapidly (a version of this suggestion in which the foreign atoms are replaced by 'unbonded atoms' has been given by Shanley (1955)). This accounts for the importance of a free surface, but makes crack initiation depend *essentially* on the nature of the environment. The fact that fatigue takes place readily in liquid helium seems to make it an impossible hypothesis.

(*d*) Dislocations may cause cracks directly in more than one way. The tensile stress near a piled-up group of edge dislocations could become large enough to produce a crack; but Stroh (1954, 1955a) suggests that, while this may happen near a grain boundary, and does in brittle fracture, the stress would be relieved by the production of new dislocations before it could occur in the interior of a grain. If there are two such groups of opposite sign, on neighbouring glide planes, it is possible according to Fujita (1954) for them to take up a position opposite to one another, and for them to give rise to a narrow crack joining them. Fujita estimates that cracks 10 Å wide can be formed in this way and can grow by the absorption of further dislocations. Both mechanisms are independent of temperature.

(*e*) The observations on extrusions and intrusions immediately suggest a possible origin for a crack. Intrusions, in fact, are ready made cracks, and while it is clear that extrusion can occur only at the free surface, intrusion from a grain boundary might be possible. Cottrell and Hull (1957) have suggested a possible dislocation mechanism which seems to be both geometrically and energetically possible. It requires the co-operation of two Frank–Read sources on different slip systems, and produces an intrusion on one system and an extrusion on the other simultaneously. This has not been observed, while simultaneous production of extrusions and intrusions on neighbouring parts of the same slip system has been reported,

(*f*) Mott (1958) has suggested an attractive dislocation mechanism involving cross-slip by which an internal cavity can grow, and an extrusion appear on the surface. The original cavity could be formed, for example, by Fujita's mechanism. In this case the whole process could proceed at any temperature, being independent of diffusion, and in any material in which cross-slip is possible. The model requires, however, that extrusions are accompanied by corresponding cavities immediately below them. It is difficult to decide experimentally whether or not this occurs in metals, but Forsyth (1957 b) has shown that it does not happen in silver chloride at least. In addition, the mechanism cannot be reversed to produce intrusions. Like that of Cottrell and Hull it does give preference to a free surface, without relying essentially on effects of the environment. It would be an interesting check to see whether extrusions can be observed in hexagonal metals, where cross-slip is not possible†.

The initiation of fatigue cracks in grain boundaries must be considered separately. It is noteworthy that these are relatively more important at higher temperatures, higher stresses and lower speeds. At room temperature, low stresses and ordinary speeds, for example, copper shows practically no such cracks and aluminium a fair proportion, while tin is reported to fail almost entirely by grain boundary cracking. Grain boundary failures are less in aluminium at lower temperatures, and less in copper at higher speeds. This immediately suggests that diffusion, possibly assisted by extensive plastic deformation, is an essential part of the process. Perhaps the most obvious idea is that the vacancies produced by dislocation movement diffuse to the grain boundaries and condense there to form voids in a manner analogous to that proposed to account for failure in high temperature creep tests. The presence of large numbers of dislocations would enable the diffusion to occur at temperatures below that of normal vacancy diffusion, and the greatly enhanced plastic flow at higher stresses might account for the greater preponderance of grain boundary failures under such conditions. It is not clear whether twin boundary cracking should be considered as a special case of grain boundary failure or not. In face-centred cubic metals the twinning plane is the same as the slip plane and it is possible that the presence of the twin boundary merely makes slip band failure more likely. In hexagonal metals this cannot be the explanation, and the formation of cracks must be associated with the processes occurring at the twin boundary. These boundaries become black during continuous cyclic stressing indicating considerable local disturbance analogous to that in slip bands, but the restrictions on the movement of twinning dislocations make most of the mechanisms discussed for slip bands impossible.

Turning now to the question of crack propagation, perhaps the most striking feature is the success of Head's theory, based entirely on macroscopic concepts, in explaining a phenomenon which must be taking place on an atomic scale. It is perhaps worth pointing out that real cracks

† It is interesting to note that Calnan and Williams (1956) have published a photograph showing an extrusion formed in a simple tensile test on copper.

exist in a three-dimensional solid, while the theory, and most of the few observations that have been made, refer to the increase of crack *length* with time. In other words, a crack growing in length at an an average rate of one atom per cycle may, if the cracked area is already 0·01 mm^2, really be growing in area at the rate of 10^6 atoms per cycle.

Any treatment of the stresses round the tip of such a crack by methods of classical elasticity will lead to exceeding high values: and Elliott (1947) has shown that similar results are obtained if the situation is considered on an atomic basis. If it were proper to attribute normal macroscopic properties to the material around the tip, extensive plastic deformation would take place every cycle. We know however that on a sufficiently small scale the properties of a real crystal will approximate more to the high strength properties of an ideal crystal. Even so, if there is no plastic deformation at all, the local stresses may be large enough to fracture even an ideal crystal. The conclusion that *either* dislocation movements, *or* fracture must occur locally every cycle seems inevitable.

It is not impossible, however, that these events should be largely reversible and so give, to a first order, no nett rate of growth. Dislocation movements are, in principle, reversible, although if large numbers are involved it is improbable that detailed reversibility would be found in practice. Also, if the fracture surfaces remain perfectly clean, it is quite possible that they will weld together when brought into contact on the compressive half cycle. This also points to a possible mechanism for the considerable effect of the surrounding atmosphere on the rate of crack propagation. But the fact that fatigue cracks can grow even in liquid helium indicates that such a mechanism is not essential—or, alternatively, that even the loosely bound adsorbed layer is sufficient to prevent the crack re-closing once it has opened. The fact that the major part of a typical fatigue test is occupied by crack propagation, taken together with the observed form of the S–N curve, indicates that the rate of propagation is very stress-sensitive. No explanation of this, in terms of atomic mechanisms, has been suggested.

If the initial material is not a fully-annealed crystal, there will be other stages to be considered. A work-hardened pure metal is initially softened by fatigue. Such softening appears to be auto-catalytic in character, and gives rise to soft regions near the slip bands, as was originally suggested by Forsyth as an explanation of his extrusion observations. From this point the development of a crack would parallel that in an annealed specimen. Similarly the over-ageing and consequent re-softening of a precipitation hardened alloy will take place preferentially in slip bands. As before, once the material has softened and dislocation movement can proceed more easily, crack formation can result by whatever mechanism operates in a pure metal.

In conclusion, perhaps it should be said that some of the experimental results are not as simple and clear-cut, and some of the opinions not as firmly held, as a first reading of this article might suggest; the exigencies of space have led to the suppression of many ifs and buts. It is at least

clear, however, that much more experimental work will be needed before a full understanding of the mechanism of fatigue is reached; some of the more promising lines of attack have already been indicated. In the words of the authors of the official report on the Comet disaster: "Enough is now known about the fundamental physics of fatigue for engineers to be aware that there is still much to be learned. Research is continuous."

Acknowledgments

The sources of the following figures are gratefully acknowledged:

Figures 8, 9, 18, 19, 24 and 29 from the Institution of Mechanical Engineers.

Figure 28 from The Royal Society.

Figure 30. Crown copyright reserved; reproduced by permission of the Controller, H.M. Stationery Office.

References

Afanasiev, N. N., 1940, *J. tech. Phys., Moscow*, **10**, 1553; 1941, *Ibid.*, **11**, 349; 1948, *Engrs. Dig.*, **9**, 96.

Allen, N. P., and Forrest, P. G., 1956, *Int. Conf. on Fatigue of Metals* (I. Mech. Engrs.).

Atkinson, H. H., and Lowde, R. D., 1957, *Phil. Mag.*, **2**, 589.

Bairstow, L., 1910, *Phil. Trans.*, **210**, 35.

Ball, C. J., 1957, *Phil. Mag.*, **2**, 1011.

Barkow, A. G., 1945, *J. appl. Phys.*, **16**, 111.

Barrett, C. S., 1937, *Trans. Amer. Soc. Metals*, **25**, 1115; 1953, *Trans. Amer. Inst. min. (metall.) Engrs.*, **197**, 1652.

Bauschinger, J., 1886, *Mitt. mech.-tech. Lab. Münch.*, **13**, 1.

Bollenrath, F., and Cornelius, H., 1940, *Z. Ver. dstch. Ing.*, **84**, 295.

Bollenrath, F., Hauck, V., and Osswald, E., 1939, *Z. Ver. dtsch. Ing.*, **83**, 129.

Broom, T., and Ham, R. K., 1957, *Proc. roy. Soc.* A, **242**, 166.

Broom, T., and Molineux, J. H., 1955, *J. Inst. Met.*, **83**, 528.

Broom, T., Molineux, J. H., and Whittaker, V. N., 1956, *J. Inst. Met.*, **84**, 356.

Broom, T., and Whittaker, V. N., 1956, *Nature, Lond.*, **177**, 486.

Brown, D. J., 1955, *Thesis*, University of Durham.

Buckley, S. N., and Entwistle, R. M., 1956, *Acta Met.*, **4**, 352.

Bullen, F. P., 1953, *Aer. Res. Lab. Report* ARL/SM218.

Bullen, F. P., Head, A. K., and Wood, W. A., 1953, *Proc. roy. Soc.* A, **216**, 332.

Calnan, E. A., and Williams, B. E., 1956, *J. Inst. Met.*, **84**, 318.

Case, S. L., 1938, *Metal Progr.*, **33**, 54.

Charsley, P., 1957, *Thesis*, University of Bristol.

Cina, B., 1957, *Metallurgia*, **55**, 11.

Clarebrough, L. M., Hargreaves, M. E., Head, A. K., and West, G. W., 1955, *J. Metals, N.Y.*, **7**, 99.

Clarebrough, L. M., Hargreaves, M. E., West, G. W., and Head, A. K., 1957, *Proc. roy. Soc.* A, **242**, 160.

Clayton-Cave, J., Taylor, R. J., and Ineson, E., 1955, *J. Iron St. Inst.*, **180**, 161.

Coffin, L. F., and Read, J. H., 1956, *Int. Conf. on Fatique of Metals* (I. Mech. Engrs.).

Cottrell, A. H., and Hull, D., 1957, *Proc. roy. Soc.* A, **242**, 211.

Cox, H. L., 1953, *Aero. Res. Cttee.*, R. & M., 2704; 1956, *Int. Conf. on Fatigue of Metals* (I. Mech. Engrs.).

Craig, W. J., 1952, *Proc. Amer. Soc. Test. Mater.*, **52**, 877.

Daeves, K., Gerold, E., and Schultz, E. H., 1940, *Stahl u. Eisen, Düsseldorf*, **60,** 100.
Davies, R. B., 1954, *Nature, Lond.*, **174,** 980.
Davies, R. B., Mann, J. Y., and Kemsley, D. S., 1956, *Int. Conf. on Fatigue of Metals* (I. Mech. Engrs).
Dehlinger, U., 1931, *Metallwirtschaft*, **10,** 26.
Dolan, T. J., and Brown, H. F., 1952, *Proc. Amer. Soc. Test. Mater.*, **52,** 733.
Duce, A. G., 1950, *Thesis*, Cambridge University.
Edwards, E. H., and Washburn, J., 1954, *Trans. A.I.M.E.*, **200,** 1239.
Elliot, H. A., 1947, *Proc. phys. Soc., Lond.*, **59,** 208.
Epremian, E., and Mehl, R. F., 1952, *N.A.C.A. Tech. Note* 2719.
Eshelby, J. D., and Pratt, P. L., 1956, *Acta Met.*, **4,** 560.
Ewing, J. A., and Humphrey, J. C. W., 1903, *Phil. Trans.* A, **200,**, 241.
Fegredo, D. M., 1957, *Thesis*, Sheffield University.
Feltham, P., and Meakin, J. D., 1957, *Phil. Mag.*, **2,** 105.
Fenner, A. J., Owen, N. B., and Phillips, C. E., 1951, *Engineering*, **171,** 637.
Föppl, O., 1936, *J. Iron St. Inst.*, **134,** 393.
Forrest, P. G., 1956, *Engineering*, **182,** 266 ; 1957, *Proc. roy. Soc.* A, **242,** 223.
Forrest, P. G., and Tapsell, H. J., 1952 a, *Engineering*, **173,** 757 ; 1952 b, *N.P.L. Report* No. PM 112 ; 1954, *Proc. Inst. Mech. Engrs*, **168,** 763.
Forsyth, P. J. E., 1951, *J. Inst. Met.*, **80,** 181 ; 1953 a, *Ibid.*, **82,** 449 ; 1953 b, *Nature, Lond.*, **171,** 172 ; 1955, *J. Inst. Met.*, **83,** 395 ; 1956, *Int. Conf. on Fatigue of Metals* (I. Mech. Engrs) ; 1957 a, *Phil. Mag.*, **2,** 437 ; 1957 b, *Proc. roy. Soc.* A, **242,** 198.
Forsyth, P. J. E., and Stubbington, C. A., 1954, *J. Inst. Met.*, **83,** 173 ; 1955, *Nature, Lond.*, **175,** 767 ; 1957, *J. Inst. Met.*, **85,** 339.
Franks, A., and Holden, J., 1955, *Nature, Lond.*, **176,** 1022.
Freudenthal, A. M., 1946, *Proc. roy. Soc.* A, **187,** 416.
Freudenthal, A. M., and Weiner, J. H., 1956, *J. appl. Phys.*, **27,** 44.
Frith, P. H., 1954, *Spec. Rep.* No. 50, Iron and Steel Inst.
Frost, N. E., 1955, *The Engineer*, **200,** 464, 501 ; 1956, *M.E.R.L.* Rep. No. P.M. 184.
Frost, N. E., and Dugdale, D. S., 1957, *J. Mech. Phys. Solids*, **5,** 182.
Frost, N. E., and Phillips, C. E., 1957, *Proc. roy. Soc.* A, **242,** 216.
Fujita, F. E., 1954, *Sci. Rep. Res. Inst. Tohoku Univ.*, **6,** 565.
Gayler, M. V. L., 1946, *J. Inst. Met.*, **72,** 543.
Gerard, I. J., and Sutton, H. J., 1935, *J. Inst. Met.*, **56,** 29.
Gilbert, P. T., 1956, *Met. Revs.*, **1,** 379.
Gibbs, P., 1957, *Univ. of Utah, Tech. Rep.* 3.
Gough, H. J., 1922, *Engineering*, **114,** 291 ; 1926, *The Fatigue of Metals* (London : Benn) ; 1928 a, *Trans. Faraday Soc.*, **24,** 137 ; 1928 b, *Proc. roy. Soc.* A, **118,** 498 ; 1932, *J. Inst. Met.*, **49,** 17 ; 1933, *Proc. Amer. Soc. Test. Mater.*, **33,** 3 ; 1938, *Trans. Faraday Soc.*, **24,** 137.
Gough, H. J., and Cox, H. L., 1929, *Proc. roy. Soc.* A, **123,** 143 ; 1930 a, *Ibid.*, **127,** 431 ; 1930 b, *Ibid.*, **127,** 453 ; 1931, *J. Inst. Met.*, **45,** 71.
Gough, H. J., and Hanson, D., 1923, *Proc. roy. Soc.* A, **104,** 538.
Gough, H. J., Hanson, D., and Wright, S. J., 1927, *Phil. Trans.* A, **226,** 1.
Gough, H. J., and Sopwith, D. G., 1932, *J. Inst. Met.*, **49,** 93 ; 1935, *Ibid.*, **56,** 55 ; 1946, *Ibid.*, **72,** 415.
Gough, H. J., Wright, S. J., and Hanson, D., 1926, *J. Inst. Met.*, **36,** 173.
Gough, H. J., and Wood, W. A., 1936, *Proc. roy. Soc.* A, **154,** 510 ; 1938, *Ibid.*, **165,** 358.
Graham, C. D., and Maddin, R., 1954, *J. Inst. Met.*, **83,** 169.
Guest, J. J., and Lee, F. C., 1916, *Proc. roy. Soc.*, **93,** 313.
Haigh, B. P., 1928, *Trans. Faraday Soc.*, **24,** 125.

Haigh, B. P., and Jones, B., 1930, *J. Inst. Met.*, **43**, 271.
Hanstock, R. F., 1947, *Proc. phys. Soc., Lond.*, **59**, 279 ; 1948, *J. Inst. Met.*, **74**, 469 ; 1954, *Ibid.*, **83**, 11 ; 1956, *Int. Conf. on Fatigue of Metals* (I. Mech. Engrs).
Hanstock, R. F., and Murray, A. J., 1946, *J. Inst. Met.*, **72**, 97.
Harper, S., 1951, *Phys. Rev.*, **83**, 709.
Head, A. K., 1953, *Phil. Mag.*, **44**, 925 ; 1956, *J. appl. Mech.*, **78**, 407.
Held, H., 1940, *Z. Metallk.*, **32**, 201.
Hempel, M., 1956 a, *Fatigue in Aircraft Structures* (New York : Academic Press) ; 1956 b, *Int. Conf. on Fatigue of Metals* (I. Mech. Engrs).
Hempel, M., and Houdremont, E., 1953, *Stahl u. Eisen, Düsseldorf*, **73**, 1503.
Hempel, M., Kochendörfer, A., and Hillnhagen, E., 1957, *Arch. Eisenhüttenw.*, **28**, 417.
Hempel, M., Sander, H. R., and Möller, H. M., 1952, *Stahl u. Eisen, Düsseldorf*, **72**, 1076.
Hendrickson, A. A., and Machlin, E. S., 1954, *J. Metals, N.Y.*, **6**, 1035.
Henry, O. H., and Coyne, T. D., 1942, *Welding J., Lond.*, **21**, 249.
Heywood, R. B., 1947, *Aircr. Engng*, **19**, 87.
Holden, J., 1954, *N.P.L.* Report HT75/54.
Hunter, M. S., and Fricke, W. G., 1954, *Proc. Amer. Soc. Test. Mater.*, **54**, 717 ; 1955, *Ibid.*, **55**, 942.
Hyler, W. S., Lewis, R. A., and Grover, H. J., 1954, *N.A.C.A. Tech. Note* 3291.
Inglis, E. C., and Lark, E. C., 1954, *J. Inst. Met.*, **83**, 117.
Jacquesson, R., 1955, *Colloquium on Fatigue* (Berlin : Springer-Verlag).
Jacquet, P. A., 1956, *Int. Conf. on Fatigue of Metals* (I. Mech. Engrs).
Jenkin, C. F., and Lehman, G. D., 1929, *Proc. roy. Soc.* A, **125**, 83.
Karry, R. W., and Dolan, T. J., 1953, *Proc. Amer. Soc. Test. Mater.*, **53**, 789.
Kemsley, D. S., 1956, *Nature, Lond.*, **178**, 653 ; 1957 a, *Phil. Mag.*, **2**, 131 ; 1957 b, *J. Inst. Met.*, **85**, 417 ; 1957 c, *Ibid.*, **85**, 420.
Kennedy, A. J., 1956, *Int. Conf. on Fatigue of Metals* (I. Mech. Engrs).
Kenyon, J. N., 1950, *Proc. Amer. Soc. Test. Mater.*, **50**, 1073.
Kommers, J. B., 1943, *Proc. Amer. Soc. Test. Mater.*, **43**, 749.
Kuhlmann-Wilsdorf, D., Van der Merwe, J. H., and Wilsdorf, H., 1952, *Phil. Mag.*, **43**, 632.
Kuhlmann-Wilsdorf, D., and Wilsdorf, H., 1953, *Acta Met.*, **1**, 394.
Laute, von K., and Sachs, G., 1928, *Z. Ver. dtsch. Ing.*, **72**, 1188.
Lazan, B. J., 1954, *Fatigue* (American Society for Metals).
Lazan, B. J., and Demer, L. J., 1951, *Proc. Amer. Soc. Test. Mater.*, **51**, 611.
Lazan, B. J., and Wu, T., 1951, *Proc. Amer. Soc. Test. Mater.*, **51**, 639.
Lea, F. C., 1923, *Engineering*, **115**, 217, 252.
Levy, J. C., and Sinclair, G. M., 1955, *Proc. Amer. Soc. Test. Mater.*, **55**, 866.
Lipsitt, H. A., *et al.*, 1955, *N.A.C.A. Tech. Note* 3380.
Lipsitt, H. A., and Horne, G. T., 1956 a, *Carnegie Inst. of Tech. Res. Rep.* ; 1956 b, *Int. Conf. on Fatigue of Metals* (I. Mech. Engrs).
Lissner, O., 1955, *Colloquium on Fatigue* (Berlin : Springer-Verlag).
Lomas, T. W., Ward, J. O., Rait, J. R., and Colbeck, E. W., 1956, *Int. Conf. on Fatigue of Metals* (I. Mech. Engrs).
Louat, N., 1953, *Thesis*, University of Bristol.
Louat, N., and Hatherley, M., 1954, *Proc. phys. Soc. Lond.* B, **67**, 260.
Love, W. J., 1952, *Tech. Rep.* 33, Dept. of Theor. and Appl. Mech., Univ. of Illinois.
Makin, M. J., 1952, *Thesis*, University of London.
Mann, J. Y., 1953, (Aust.) *Aero. Res. Lab. Rep.* SM 217.
Masing, G., 1923, *Wiss. Veröff. Siemens*, **3**, 231 ; 1926, *Ibid.*, **5**, 135.

Masing, G., and Mausch, W., 1925 a, *Wiss. Veröff. Siemens*, **4**, 74 ; 1925 b, *Ibid.*, **4**, 244 ; 1926, *Ibid.*, **5**, 142.
McCammon, R. D., and Rosenberg, H. M., 1957, *Proc. roy. Soc.* A, **242**, 203.
McClintock, F. A., 1952 a, *Proc. 1st U.S. Nat. Congress appl. Mech.*, 653 ; 1952 b, *J. appl. Mech.*, **19**, 54 ; 1955, *Ibid.*, **22**, 427.
McClintock, F. A., and Ryan, F. J., 1954, *J. appl. Mech.*, **21**, 296.
Memmler, K., and Laute, K., 1930, *Forschungsarbeiten auf den Gebiete des Ingenieurwesens*, 329.
Möller, H., and Hempel, M., 1938, *Mitt. K.-Wilh.-Inst. Eisenforsch.*, **20**, 15, 229 ; 1954, *Arch. Eisenhüttenw.*, **25**, 39.
Moore, H. F., and Alleman, N. J., 1931, *Proc. Amer. Soc. Test. Mater.*, **31**, 114.
Moore, H. F., and Ver, T., 1930, *Bull. Eng. Exp. Station, Univ. of Illinois*, 208.
Morkovin, D., and Moore, H. F., 1944, *Proc. Amer. Soc. Test. Mater.*, **44**, 137.
Morrison, J. L. M., Crossland, B., and Parry, J. S., 1956, *Proc. Inst. Mech. Engrs*, **21**, 170.
Mott, N. F., 1955, *Deformation and Flow of Solids* (Berlin : Springer-Verlag) ; 1958, *Acta Metallurgica* (in the press).
Neuber, H., 1937, *Kerbspannungslehre* (Berlin : Springer).
Nishihara, T., and Taira, S., 1950, *Mem. Fac. Engng. Kyoto*, **12**, 90.
Orowan, E., 1939, *Proc. roy. Soc.* A, **171**, 79.
Paterson, M. S., 1946, *The Failure of Metals by Fatigue* (Melbourne : University Press) ; 1955, *Acta Met.*, **3**, 491.
Peterson, R. E., 1930, *Proc. Amer. Soc. for steel treating*, **18**, 1041 ; 1933, *Trans. Amer. Soc. mech. Engrs*, APM **55**, 19 ; 1938, *Stephen Timoshenko 60th Anniversary Volume* (New York : Macmillan), p. 179 ; 1953, *Stress Concentration Design factors* (New York : John Wiley).
Petch, N. J., 1953, *J. Iron St. Inst.*, **174**, 25.
Phillips, C. E., and Heywood, R. B., 1951, *Proc. Inst. mech. Engrs*, **165**, 113.
Phillips, V. A., Swain, A. J., and Eborall, R., 1952, *J. Inst. Met.*, **81**, 625.
Polakowski, N. H., 1951, *J. Iron St. Inst.*, **169**, 337 ; 1952, *Proc. Amer. Soc. Test. Mater.*, **52**, 1086.
Polakowski, N. H., and Palchoudhuri, A., 1954, *Proc. Amer. Soc. Test. Mater.*, **54**, 701.
Rahlfs, P., and Masing, G., 1950, *Z. Metallk.*, **41**, 454.
Rally, F. C., and Sinclair, G. M., 1955, Univ. of Illinois. Dept. of Theor. and Appl. Mech., Report 87.
Rider, J. G., 1953, *Thesis*, University of Bristol.
Sachs, G., and Shoji, H., 1927, *Z. Phys.*, **45**, 776.
Sander, H. R., and Hempel, M., 1952, *Arch. Eisenhüttenw.*, **23**, 383.
Schaub, C., and Liedtke, W., 1955, *Colloquium on Fatigue* (Berlin : Springer-Verlag), p. 244.
Schenck, H., and Schmidtmann, E., 1954, *Arch. Eisenhüttenw.*, **25**, 579.
Scholl, H., 1957, *Z. Metallk.*, **48**, 258.
Seeger, A., 1954, *Z. Naturf.*, **9**, 758, 856, 870.
Seeger, A., Diehl, J., Mader, S., and Rebstock, H., 1957, *Phil. Mag.*, **2**, 323.
Seitz, F., 1952, *Advanc. Phys.*, **1**, 43.
Shanley, F. R., 1955, *Colloquium on Fatigue* (Berlin : Springer-Verlag), p. 251.
Siebel, E., and Stähli, G., 1942, *Arch. Eisenhüttenw.*, **15**, 519.
Sinclair, G. M., 1952, *Proc. Amer. Soc. Test. Mater.*, **52**, 743.
Sinclair, G. M., and Craig, W. J., 1952, *Trans. Amer. Soc. Metals*, **44**, 929.
Sinclair, G. M., and Dolan, T. J., 1951, *Proc. 1st U.S. Nat. Congress of Appl. Mech.*, 647.
Smith, G. C., 1957, *Proc. roy. Soc.* A, **242**, 189.
Smith, S. L., and Wood, W. A., 1944, *Proc. roy. Soc.* A, **182**, 404.
Spencer, R. G., 1939, *Phys. Rev.*, **55**, 991.

Spencer, R. G., and Marshall, S. W., 1941, *J. appl. Phys.*, **12,** 191.
Stroh, A. N., 1954, *Proc. roy. Soc.* A, **223,** 404 ; 1955 a, *Ibid.*, **232,** 548 ; 1955 b, *Phil. Mag.*, **46,** 198.
Stromeyer, C. E., 1914, *Proc. roy. Soc.*, **90,** 411.
Stubbington, C. A., and Forsyth, P. J. E., 1957, *J. Inst. Met.*, **86,** 90.
Suzuki, H., Ikeda, S., and Teleuchi, S., 1956, *Proc. phys. Soc. Japan*, **11,** 382.
Swift, H. W., 1944, *Metallurgia*, **31,** 61.
Thompson, N., 1956, *Fatigue in Aircraft Structures* (New York : Academic Press Inc.).
Thompson, N., Coogan, C. K., and Rider, J. R., 1955, *J. Inst. Met.*, **84,** 75.
Thompson, N., and Wadsworth, N. J., 1957, *Brit. J. appl. Phys. Suppl.*, **6,** 51.
Thompson, N., Wadsworth, N. J., and Louat, N., 1956, *Phil. Mag.*, **1,** 113.
Toolin, P. R., 1953, *Amer. Soc. Test. Mater., Special Tech. Pub.*, **128,** 142.
Vitovec, F. H., 1953, *W.A.D.C. Tech. Rep.* 53–167.
Wade, A. R., and Grootenhuis, P., 1956, *Int. Conf. on Fatigue of Metals* (I. Mech. Engrs).
Wadsworth, N. J., 1955, *Thesis*, University of Bristol ; 1956, unpublished M.O.S. report ; 1957 a, *J. appl. Mech.*, **24,** 161 ; 1957 b, *Dislocations and Mechanical Properties of Crystals* (New York : John Wiley).
Wållgren, G., 1953, *F.F.A. Report*, No. 48.
Walker, H. L., and Craig, W. J., 1949, *Trans. Amer. Inst. min.* (*metall.*) *Engrs*, **180,** 42.
Weibull, W., 1949, *Trans. Roy. Inst. Tech.* (Stockholm) No. 27 ; 1952, *Appl. Mech. Rev.*, **5,** 449 ; 1954, *SAAB Aircraft Co.*, Tech. Note 30 ; 1955, *Aero. Res. Inst. Sweden*, Report No. 58.
Weinberg, E. H., 1953, *J. appl. Phys.*, **24,** 734.
Welber, B., and Webeler, R., 1953, *J. Metals, N.Y.*, **5,** 1558.
Wever, von F., Hempel, M., and Schrader, A., 1955, *Arch. Eisenhüttenw.*, **26,** 739.
Wever, F., and Möller, H., 1937, *Naturwissenschaften.*, **25,** 449.
Woolley, R. L., 1953, *Phil. Mag.*, **44,** 597.
Wood, W. A., 1948, *Proc. roy. Soc.* A, **192,** 218 ; 1956, *Fatigue of Aircraft Structures* (New York : Academic Press Inc.).
Wood, W. A., and Davies, R. B., 1953, *Proc. roy. Soc.* A, **220,** 255.
Wood, W. A., and Head, A. K., 1951, *J. Inst. Met.*, **79,** 89.
Wood, W. A., and Thorpe, P. L., 1940, *Proc. roy. Soc.* A, **174,** 310.
Wood, W. A., and Segall, R. L., 1957 a, *Proc. roy. Soc.* A, **242,** 180 ; 1957 b, *Bull. Instn Metall.*, **3,** 160.
Yen, C. S., and Dolan, T. J., 1952, *Illinois Bull.*, No. 398.
Ziegler, N. A., 1930, *Trans. Amer. Inst. min.* (*metall.*) *Engrs*, **90,** 209.

ERRATA

Palaeomagnetic Collections from Britain and South Africa Illustrating Two Problems of Weathering, by A. E. M. Nairn, 1957, *Advanc. Phys.*, **6**, 162.

p. 163. Delete " Bk1, Bk2, Bk3, flows from Bulawayo ; 1, 2, 3, 4, flows from Victoria Falls ; M.C., flows from quarries near Victoria Falls " from the caption of fig. 1.

p. 167. Delete " 1, 2, Lias limestones, Skye ; 3, 4, 5, Gt. Estuarine Series, Skye ; 6, Brorabrensceans Series, Sandstone, Sutherland ; 7, 8, 9, 10, 11, 12, Estuarine Series, Sandstone, Yorkshire " from the caption of fig. 4.

Fig. 2

(*a*)

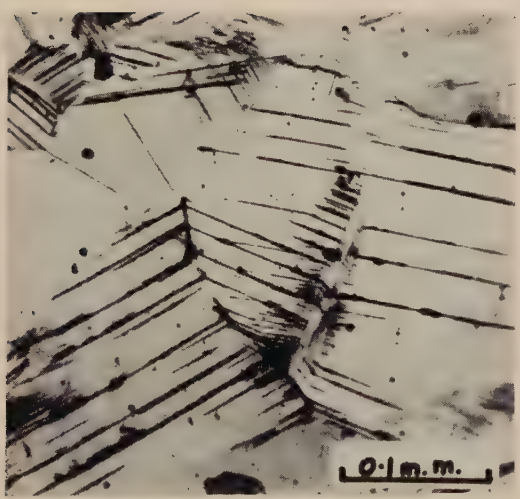

(*b*)

Typical slip lines (*a*) unidirectional strain, (*b*) fatigue strain. Both copper (×200) (from Bullen, Head and Wood, 1953).

Figs. 3–6

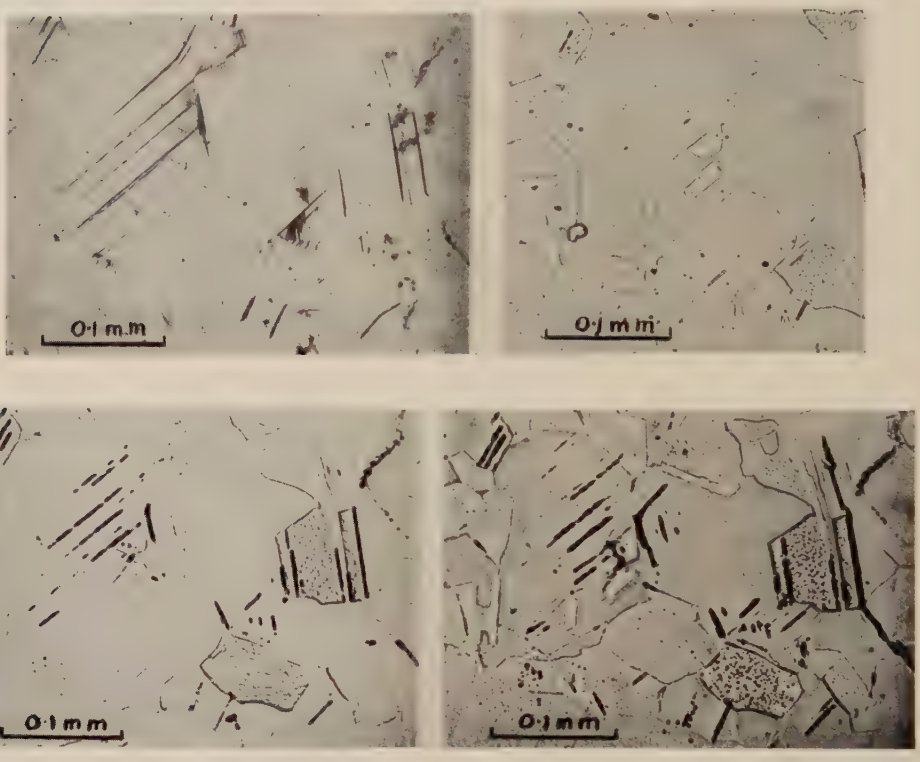

Development of a fatigue crack in copper. (3) after $7\frac{1}{2}\%$ of life; (4) as (3) electropolished; (5) after 42% of life, electropolished; (6) after 77% of life, electropolished; (from Thompson, Wadsworth and Louat 1956).

Fig. 7

Early stages of fatal fatigue crack in copper (same specimen as figs. 3–6); after 42% of life, electropolished.

Fig. 8

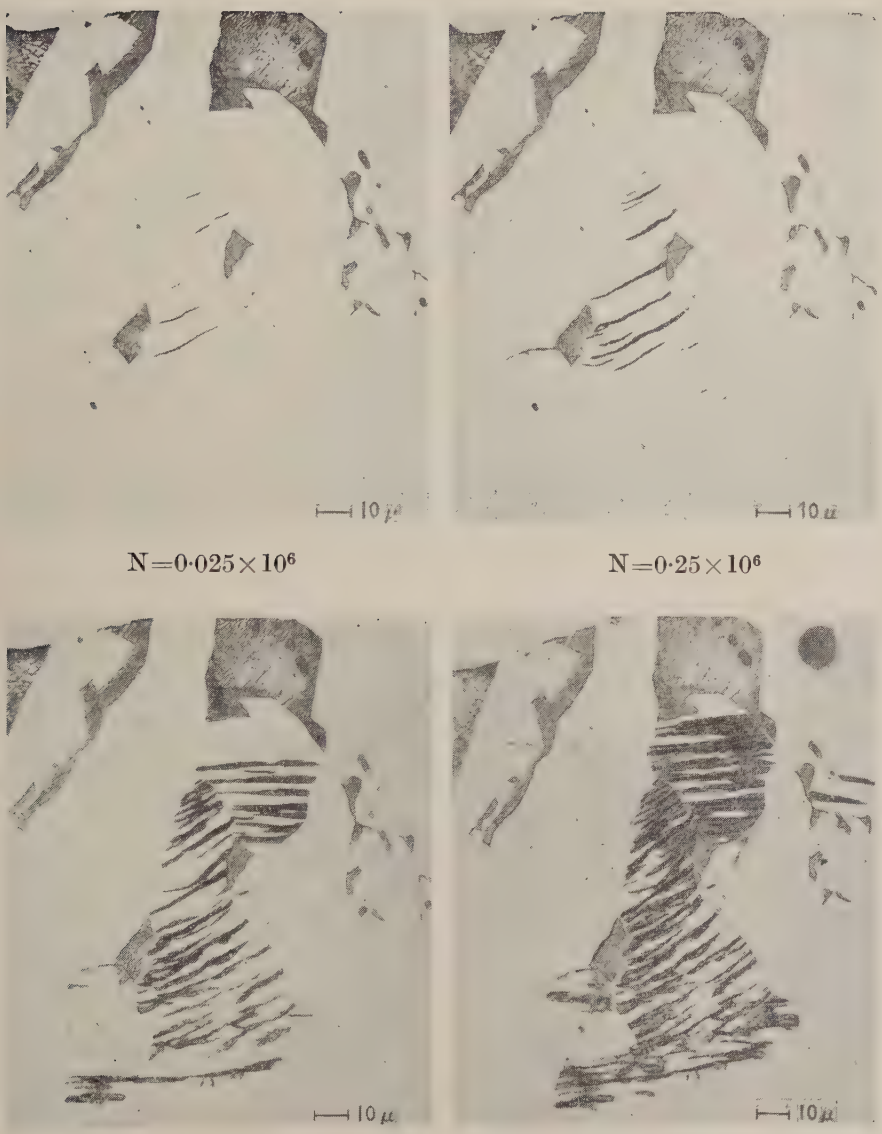

$N = 0{\cdot}025 \times 10^6$ $N = 0{\cdot}25 \times 10^6$

$N = 6{\cdot}5 \times 10^6$ $N = 46{\cdot}0 \times 10^6$

Slip lines forming on iron stressed below its fatigue limit. (Hempel 1956 b.)

Fig. 9

Electron micrograph of slip bands in iron stressed below its fatigue limit. (Hempel 1956 b.)

Fig. 10

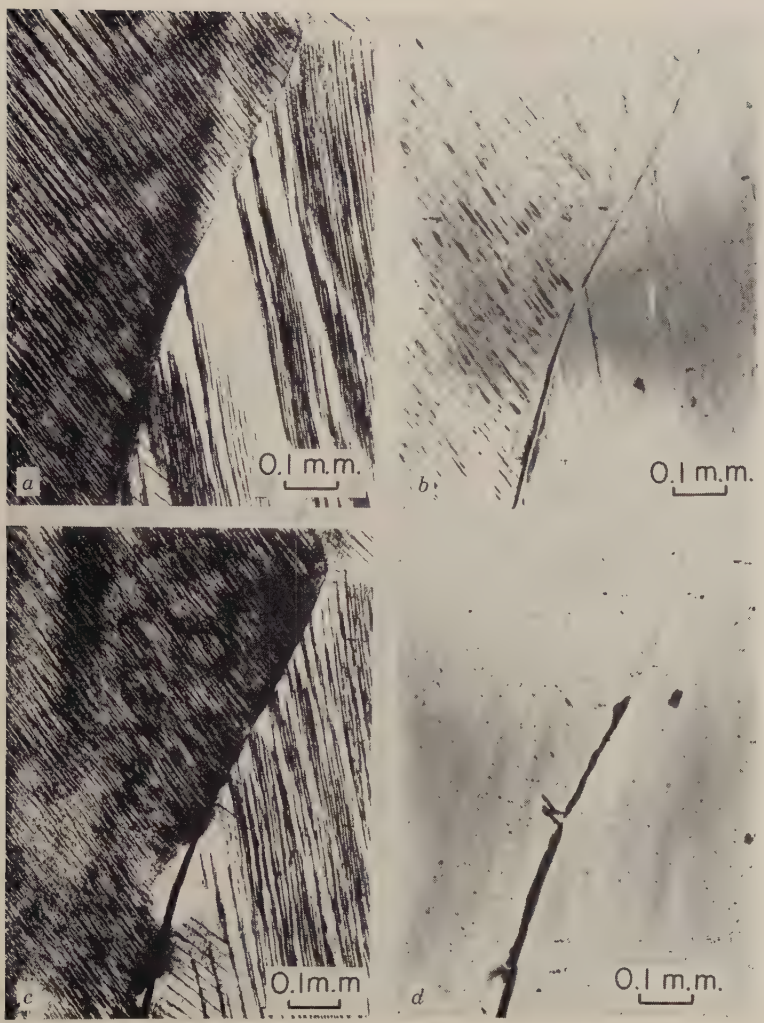

Stages in the development of a fatigue crack in aluminium (*a*) after 11% of life : (*b*) as (*a*) electropolished ; (*c*) after 33% of life ; (*d*) as (*c*) electropolished. (Observations by Smith and Harries, quoted by Thompson 1956.)

Fig. 11

Aluminium after 5×10^6 cycles at very low stress, electropolished and lightly etched. Electron micrograph; oxide replica. (Smith and Harries, quoted by Thompson 1956.)

Fig. 12

Aluminium after 5×10^6 cycles at very low stress. No further treatment. Electron micrograph; oxide replica. (Smith and Harries, quoted by Thompson 1956.)

Fig. 13

Pure aluminium fatigued at room temperature and electropolished. (Forsyth and Stubbington 1955.)

Fig. 14

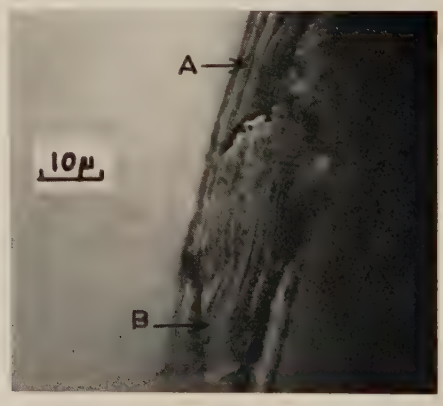

A section of a fatigued aluminium–7·5% Zn–2·5% Mg alloy, aged before fatiguing. (Forsyth 1957 a.)

Fig. 15

Polygonized regions along slip bands in fatigued aluminium–$\frac{1}{2}$% Ag revealed by etching. (Forsyth 1951.)

Fig. 16

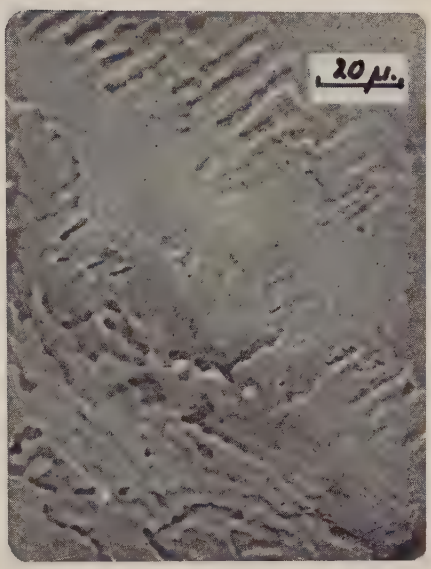

General polygonization of fatigued aluminium–$\frac{1}{2}$% Ag revealed by etching. (Forsyth 1951.)

Fig. 17

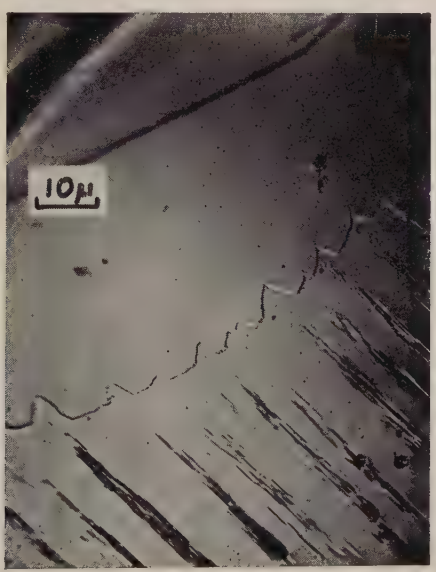

Grain boundary movements at the ends of slip bands in fatigued aluminium. (Forsyth 1953a.)

Fig. 18

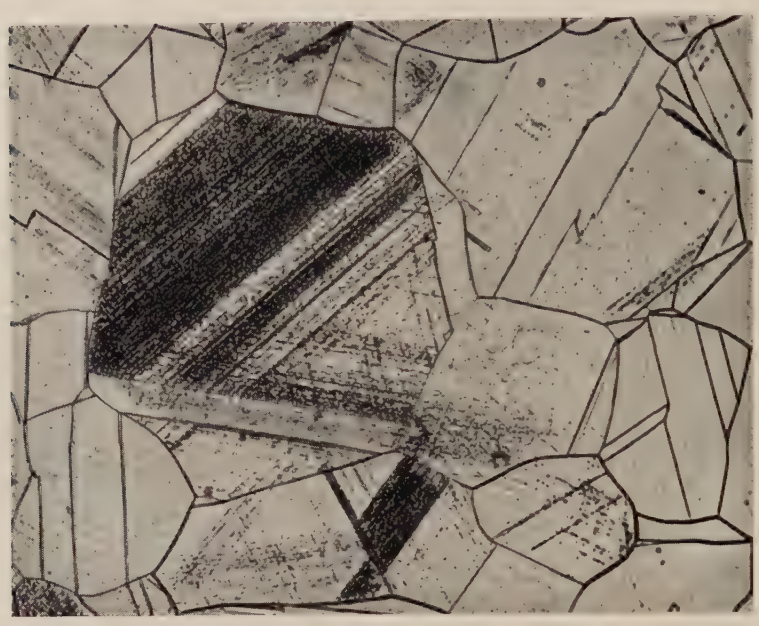

Slip bands revealed by etching below the surface of α-brass after fatigue. (×400.) (Jacquet 1956.)

Fig. 19

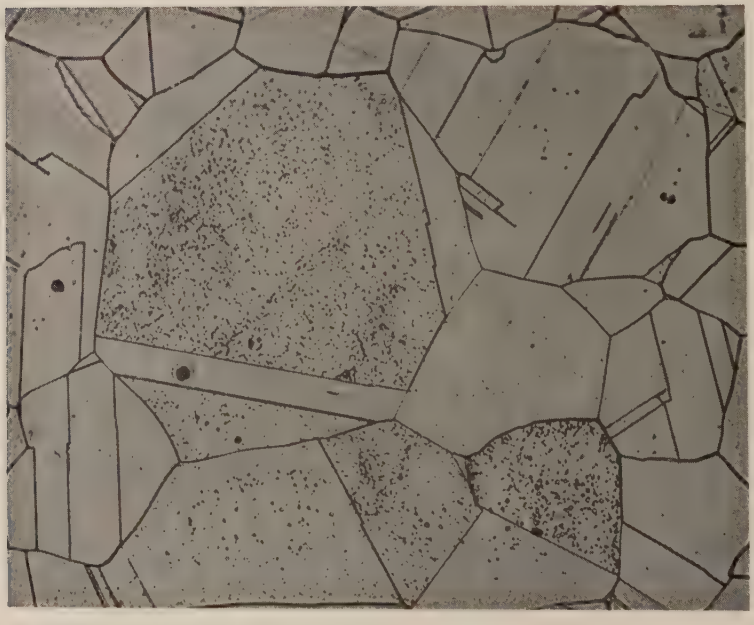

The same field as fig. 18 after annealing for 1 hour at 550°c and re-etching. (×400.) (Jacquet 1956.)

Fig. 20

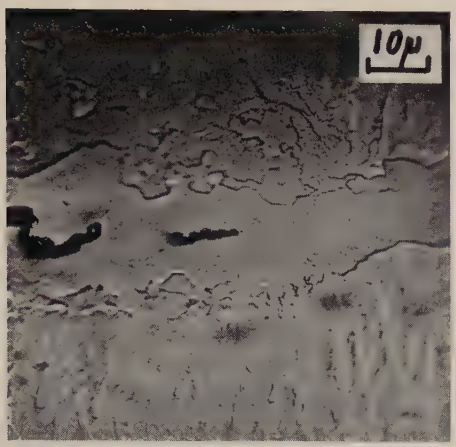

Recrystallized regions and cracks in pure aluminium, cold rolled before fatigue. (Forsyth and Stubbington 1954.)

Fig. 21

Slip bands and extrusions in aluminium –4% Cu after fatigue. (Forsyth 1955.)

Fig. 22

Slip bands similar to those shown in fig. 21 after repolishing and etching. (Forsyth 1955.)

Fig. 23

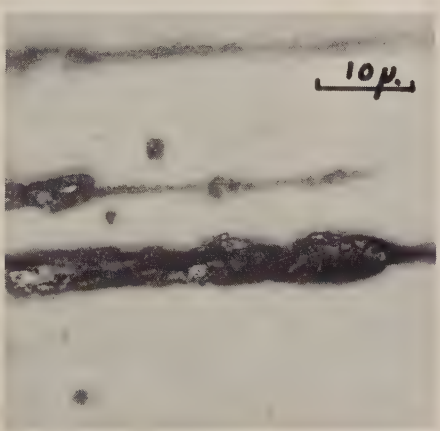

Slip band extrusion from aluminium–4% Cu fatigued at 250°c. (Forsyth and Stubbington 1957.)

Fig. 24

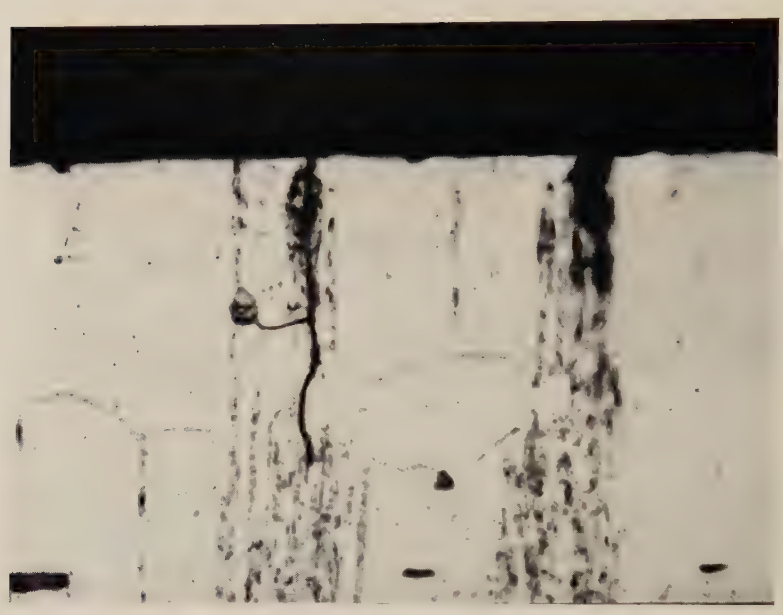

Section showing precipitation bands and cracks formed in DTD 683 during fatigue. (×1500.) (Hanstock 1956.)

Fig. 25

Slip band extrusion from pure aluminium lightly cold rolled before fatigue. (Forsyth and Stubbington 1955.)

Fig. 26

Aluminium–$\frac{1}{2}$% Ag after fatigue, showing varying displacements on the active slip planes. Compare the ringed regions. (Forsyth 1951.)

Fig. 27

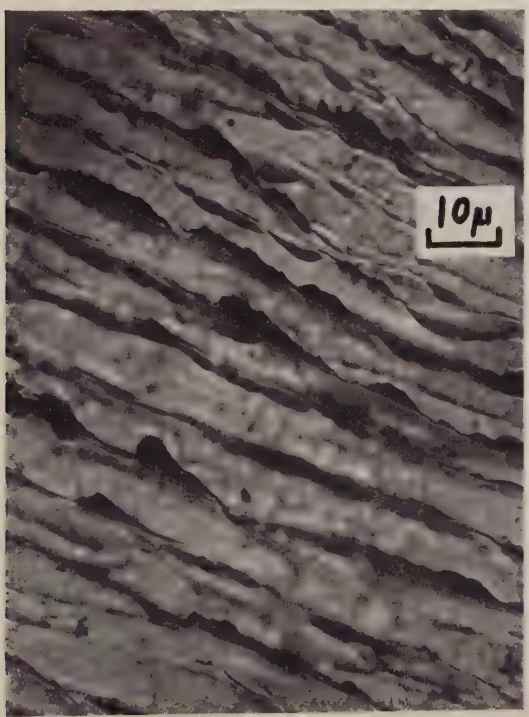

Intrusions in silver chloride after fatigue. (Forsyth 1957 b.)

Fig. 28

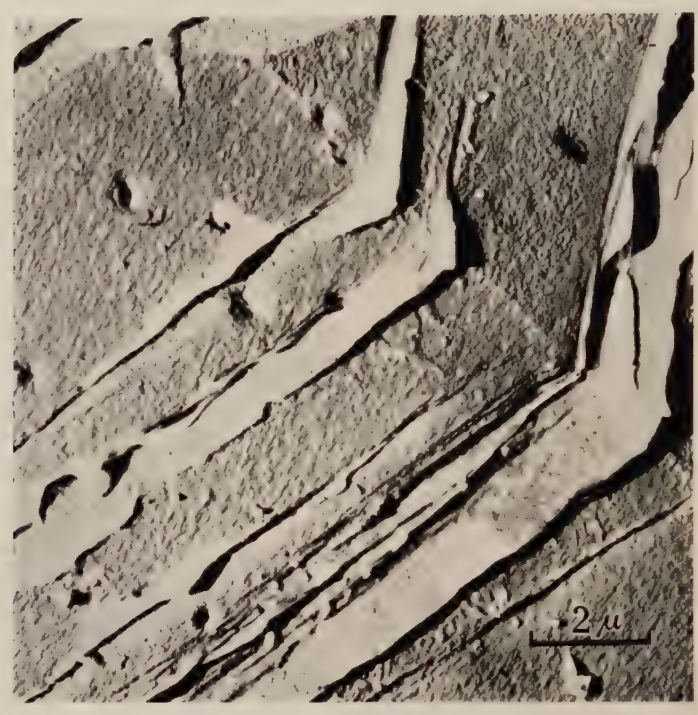

Intrusions in copper fatigued at 90°K (shadowed carbon replica). (Cottrell and Hull 1957.)

Fig. 29

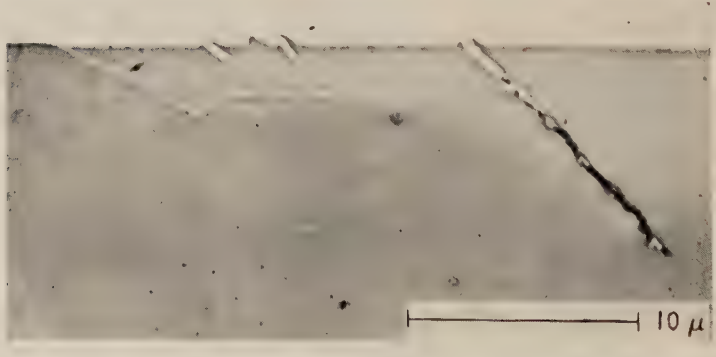

A section of a fatigued iron specimen showing incipient cracks. (Wever, Hempel and Schrader 1955.)

Fig. 30

Extrusions and intrusions in fatigued copper (double shadowed carbon replica). The black regions, A, represent extrusions or intrusions. Extrusions cast shadows, (white on print) to the left as at B while intrusions cast shadows to the right as at C.

Contents of January, 1958

Editorial

Nuclear Magnetic Resonance and Rotational Isomerism in Substituted Ethanes. By J. A Pople, Department of Theoretical Chemistry, University of Cambridge

Some considerations on the Dipole Moments of Azines. By H. F. Hameka and A. M. Liquori, Instituto di Chimica Farmaceutica Centro di Strutturistica Chimica del C.N.R., University of Rome, Italy

The Pressure-Induced Rotational Absorption Spectrum of Hydrogen : I. By J. P. Colpa and J. A. A. Ketelaar, Laboratory for General and Inorganic Chemistry of the University of Amsterdam, The Netherlands

Kritische Opaleszenz fester Lösungen. Von A. Münster und K. Sagel, Metall-Laboratorium der Metallgesellschaft A. G., Frankfurt/M

Electron–Electron Separation in Molecular Hydrogen. By M. P. Barnett, I.B.M. United Kingdom Limited, 101 Wigmore Street, London, W.1, F. W. Birss and C. A. Coulson, Mathematical Institute, Oxford

On Irreversible Process in Quantum Mechanics. By I. Prigogine and M. Toda, Faculté des Sciences, Université Libre de Bruxelles

Transport of Energy and Momentum in a Dense Fluid of Rough Spheres. By J. P. Valleau, Department of Theoretical Chemistry, University of Cambridge

Constant Pressure Ensembles in Statistical Mechanics. By W. Byers Brown, Department of Chemistry, University of Manchester

One-dimensional multicomponent mixtures. By H. C. Longuet-Higgins, Department of Theoretical Chemistry, University of Cambridge

Thermodynamic Properties of Gas Hydrates. By J. C. Platteeuw and J. H. van der Waals, Koninklijke/Shell-Laboratorium, Amsterdam (N.V. De Bataafsche Petroleum Maatschappij)

Dielectric Properties of Iodine in Aromatic Solvents at 9000 Mc/sec. By G. W. Nederbragt and J. Pelle, Koninklijke/Shell-Laboratorium, Amsterdam (N.V. De Bataafsche Petroleum Maatschappij)

Price per part £1 5s. 0d. plus postage

Subscription per volume (4 issues) £4 15s. 0d. post free, payable in advance

Printed and Published by

TAYLOR & FRANCIS LTD

RED LION COURT, FLEET STREET, LONDON, E.C.4

Orders originating in U.S.A. and Canada should be sent to the Academic Press Inc., 111 Fifth Avenue, New York, 3, N.Y., U.S.A.